ACADEMIE UNIVERSITAIRE WALLONIE-EUROPE
UNIVERSITE DE LIEGE
FACULTE DE MEDECINE VETERINAIRE
DEPARTEMENT CLINIQUE DES ANIMAUX DE COMPAGNIE ET DES EQUIDES
SERVICE DE PATHOLOGIE MEDICALE DES PETITS ANIMAUX

# LA FIBROSE PULMONAIRE IDIOPATHIQUE CANINE: AMELIORATION DE LA CARACTERISATION CLINIQUE, RECHERCHE DE BIOMARQUEURS, ET D'AGENTS ETIOLOGIQUES

# CANINE IDIOPATHIC PULMONARY FIBROSIS: IMPROVEMENT OF THE PHENOTYPE CHARACTERIZATION, AND SEARCH FOR BIOMARKERS AND FOR ETIOLOGIC AGENTS

**Elodie ROELS**

**THESE PRESENTEE EN VUE DE L'OBTENTION DU GRADE DE DOCTEUR EN SCIENCES VETERINAIRES**

**ANNEE ACADEMIQUE 2015-2016**

# REMERCIEMENTS

Je tiens à adresser toute ma gratitude et mes remerciements les plus sincères à ma promotrice de thèse, le Professeur Cécile Clercx, qui a su me guider et m'encourager tout au long de ces 4 années de doctorat. Dans les couloirs de la clinique vétérinaire des petits animaux, il a été souvent entendu que j'étais votre portrait tout craché. C'est un compliment qui me va droit au cœur car j'admire votre énergie, votre enthousiasme, votre gentillesse, votre sens de l'écoute et votre capacité à nous pousser au meilleur de nous-même. Merci à vous, Cécile, de m'avoir toujours soutenue et d'avoir supporté mon caractère parfois un peu rebelle. Votre disponibilité et votre optimisme ont été pour moi des bouffées d'oxygène lors des moments plus difficiles et c'est à vous que je dois l'accomplissement de ce travail.

Je tiens également à remercier tout particulièrement ma co-promotrice, le Professeur Kathleen Mc Entee, qui a su m'aiguiller tout le long de ce parcours avec beaucoup de bienveillance et d'encouragements. Merci de m'avoir donné gout à cette magnifique discipline qu'est la cardiologie. Merci également d'avoir passé tant d'heures à faire des mesures sur un échocardiographe pas toujours conciliant !

Merci aux membres de mon comité de thèse, les Professeurs Géraldine Bolen et Fabrice Bureau, pour leur collaboration, leur aide précieuse et le temps consacré à l'évaluation de ce travail. Merci Gégé d'avoir ouvert les portes de la radio à ma horde de Westies et d'avoir toujours été disponible pour les échographier, scanner et radiographier. Merci pour ta bonne humeur à toute épreuve et pour le temps que tu as passé à lire et relire les images récoltées toute au long de ce travail. Merci Fabrice pour ta disponibilité et pour m'avoir accueillie dans ton laboratoire où je me suis directement sentie acceptée et intégrée.

Merci aux membres de mon jury de thèse, les Professeurs Tania Art, Didier Cataldo, Benoit Nemery, Paul De Vuyst et Mutien-Marie Garigliany, et le Docteur Thomas Marichal d'avoir accepté de juger ce travail. Merci au Professeur Laurent Gillet d'avoir accepté de présider ce jury de thèse.

Je souhaite également remercier de tout cœur toutes les personnes qui ont contribué de près ou de loin à l'accomplissement de ce travail et qui m'ont aidé à m'épanouir tant sur le plan professionnel que sur le plan personnel. La liste est longue et j'espère n'avoir oublié personne… !

Merci à l'équipe vétérinaire finlandaise composée de Lisa, Saila, Henna et Minna pour leur précieuse collaboration au fil des années et leurs encouragements lors de mes présentations

en congrès internationaux. Merci Saila d'avoir toujours répondu présente pour l'échange d'informations et de matériels biologiques nécessaire à la réalisation de ce travail.

Merci aux collaborateurs vétérinaires extérieurs à l'université de Liège pour leur participation dans la récolte de nouveaux cas et leur implication dans notre projet. Merci aux Docteurs Fergus Allerton, Ghita Benchekroun, Éric Bomassi, Domingo Casamian, Cécile Damoiseau, Aleksandra Domanjko, Andrea Fischer, Reinhart Hirt, Rachel Lavoué, Davide Delorenzi, Frederic Mergenthal, Nina Müller, Viktor Szatmari, Benoit Vanbrugghe, Nicole Van Israël, Audrey Vrancken et Hans Von Euler.

Merci à tous les membres du laboratoire de physiologie cellulaire et moléculaire du GIGA pour leur accueil chaleureux, leur aide technique et leurs excellents conseils. Merci Dimitri pour ta patience, ton calme et ta disponibilité. Grace à toi, j'ai appris à gérer un qRT-PCR du début à la fin et à remplir correctement une plaque 384 puits en un temps record. Merci Claire pour ton aide en cytométrie en flux même si on n'a pas eu beaucoup de chance sur ce coup-là ! Merci Coraline et Joey d'avoir été des partenaires de chants idéaux (à quand l'établissement d'une chorale ?) et merci Thibaut et Pierre pour vos petites blagues qui m'ont fait beaucoup rire. Merci Cédric d'avoir été mon fournisseur officiel de carboglace !

Merci au laboratoire d'immunologie et de vaccinologie de la FMV de m'avoir initiée à la recherche en virologie. Merci au Professeur Laurent Gillet de m'avoir si gentiment accueillie, conseillée et guidée tant dans la démarche scientifique que dans la rédaction qui s'en est suivie. Merci Mickael pour ton calme et ta rigueur dans les manips ainsi que pour ta gentillesse et ton optimisme, ce fut un plaisir de travailler avec toi. Merci également au Professeur Berhard Ehlers du Robert-Koch Institute d'avoir accepté de collaborer sur notre projet et de s'être investi à 100% dans notre travail malgré la distance entre nos institutions.

Merci au laboratoire d'histologie de la FMV de m'avoir épaulé dans la réalisation des immunohistochimies et des ELISA. Merci au Professeur Nadine Antoine d'avoir été disponible pour les lectures des immuno-marquages et pour les rédactions scientifiques associées. Merci Joëlle d'avoir toujours répondu présente pour m'assister dans les manips. Ta patience, ta bonne-humeur, ton calme et ta précision font de toi une technicienne en or avec laquelle j'ai eu la chance de pouvoir à travailler.

Merci au Professeur Frédéric Farnir pour son aide précieuse en statistiques mais également pour son réconfort et son soutien dans les moments plus difficiles. Merci d'avoir toujours trouvé les mots justes quand mon moral n'était pas au beau fixe.

Merci au Professeur Michael Day pour son aide dans la lecture des coupes histopathologiques de poumon ainsi que dans la rédaction d'abstract et d'articles scientifiques.

Merci à la team Olson (Amy et Patricia) d'avoir pris le temps de relire et de corriger entièrement ce manuscrit en un temps record. Thank you ☺

Merci à toute l'équipe du service de médecine interne de la CVU pour m'avoir supporté pendant ces 4 années de doctorat. Merci d'avoir partagé mes joies et mes réussites tout comme mes doutes, mes angoisses et mes peines. Merci aux chefs, Fred, Dominique et Kris pour leur confiance, leur soutien et leur côté taquin. Merci Kiki d'avoir toujours accepté (presque sans broncher) d'échocardiographier mes Westies. Merci également pour tes conseils quant à mon futur et à la rédaction de ma thèse. Merci aux copines, Chachou, MiniMi, Maudinette, Elo, Morganette et Cécile d'avoir été toujours présente à mes côtés et de m'avoir fait rire aux éclats tellement de fois. Chaque moment passé avec vous a été un cadeau, que ce soit au boulot ou en dehors. Vous êtes des filles géniales et le MIPA power restera gravé à tout jamais. Merci Val, Isabelle, Charlotte et Iris pour votre écoute attentive et vos conseils. Merci Jacques et Jérôme pour votre bonne-humeur et votre sens de l'humour. Merci également à François pour qui rapidité et efficacité sont les principaux mots d'ordre (bang-bang !), atouts indispensables quand il s'agit de faire face à une personne aussi impatiente que moi ! Merci Sylvain d'avoir été tellement méticuleux et ordonné avec la tonne de prélèvements que je t'ai demandés de ranger et répertorier. Merci de t'être gelé les mains dans le -80°C autant de fois pour moi. Enfin merci aux Nadines, à Audrey, Patricia et Dominique pour leur dévouement à toute épreuve et leur gentillesse hors du commun.

Merci également à toute l'équipe du service d'imagerie de la CVU pour leur aide dans l'acquisition et l'interprétation des examens d'imagerie et pour l'accueil irréprochable qu'ils ont réservés à mes petits Westies. Mercis particuliers à Anne-Laure et Annalisa ainsi qu'à Philippe et Laurie pour vous être particulièrement investis dans le bon déroulement des opérations. Merci également au Professeur Johny Verschakelen et au Docteur Thierry Couvreur pour leurs collaborations et le partage de leur expertise dans la lecture et l'interprétation des images.

Merci à toute l'équipe du service d'anesthésie de la CVU pour avoir gérer avec succès toutes les anesthésies des Westies réalisées pendant ce travail. Merci Olivia et Véro pour votre délicatesse et votre efficacité ainsi que pour vos qualités humaines irréprochables. Merci Alexandru pour ta zen-attitude à toute épreuve.

Merci également à tous les autres membres de la CVU avec qui j'ai eu l'occasion de partager et d'échanger sur ma thèse, ma vie, le travail, la fac ou encore la météo. Ceux qui me connaissent diront en effet que j'ai la langue bien pendue !!! Merci Mikou, Oli, Martinos, Bart et Fabinou = la team des chirurgiens (DP ne soit pas jaloux) de m'avoir accompagné mainte et mainte fois à la cafèt et de m'avoir diverti avec vos sujets de conversation plus que variés (et souvent graveleux avouons-le). Merci aux fées de l'ICU, Céline et Catherine, pour leur simplicité et leur joie de vivre (et aussi pour leur talents de coiffeuse !). Merci aux filles de la compta, Catherine, Fred et Antonella pour avoir géré mes commandes, débours et autres paperasseries à la perfection. Merci à Maurizio pour ton dévouement aux beagles du chenil et tes qualités d'électricien ! Et enfin merci aux internes (en particulier Caroline et Fabienne) et aux étudiants pour leur disponibilité sans faille.

Je tenais également à remercier tous les propriétaires et éleveurs de Westies qui ont cru en notre projet et ont été d'accord d'y participer avec leurs chiens. Un merci tout particulier à Madame Véronique Desramé, présidente du club français des Westies, qui nous soutient dans nos recherches depuis plusieurs années et est toujours motivée pour organiser des évènements et rencontres afin d'améliorer la communication et les avancées sur la maladie.

Je terminerai en adressant un énorme merci à mes amies proches, Ana, Mapi, Sam, Céline, Steph L., Steph D. et Aurélie, ainsi qu'à mes parents, à mes grands-parents, à ma sœur et à mon frère pour leur soutien, leurs encouragements et leur présence dans ma vie. A mes amies, merci d'être toujours là pour moi, même si la distance et nos vies bien remplies nous empêchent de nous voir aussi souvent qu'on en aurait envie. A ma famille, merci pour la fierté que je peux lire sur vos visages à chaque fois que vous évoquez mon parcours. Merci de m'avoir guidé jusqu'ici. Vous êtes un exemple de courage, de volonté, de simplicité, de respect et d'amour.

# LIST OF ABBREVIATIONS

| | |
|---|---|
| 5-HT | 5-hydroxytryptamine, serotonin |
| 5-HTR | 5-hydroxytryptamine receptor |
| 5-HTT | 5-hydroxytryptamine transporter |
| 6MWD | 6-minutes walked distance |
| 6MWT | 6-minute walking test |
| AE | Acute exacerbation |
| AEC | Alveolar epithelial cell |
| AHV | Asinine herpesvirus |
| ALP | Alkaline phosphatase |
| Ao | Aorta |
| AT | Acceleration time of the pulmonary artery flow |
| AT:ET | Acceleration to ejection time ratio of the pulmonary artery flow |
| ATS | American thoracic society |
| ARDS | Acute respiratory distress syndrome |
| BALF | Bronchoalveolar lavage fluid |
| CB | Chronic bronchitis |
| CCL2 | Chemokine (CC-motif) ligand 2 |
| CHF | Congestive heart failure |
| CIPF | Canine idiopathic pulmonary fibrosis |
| CPFE | Combined pulmonary fibrosis and emphysema |
| CXCL8 | Chemokine (CXC-motif) ligand 8 |
| DAD | Diffuse alveolar damage |
| DLCO | Diffusion lung capacity for carbon monoxide |
| DMVD | Degenerative mitral valve disease |
| EBP | Eosinophilic bronchopneumopathy |
| EBV | Epstein-Barr virus |
| EHV | Equine herpesvirus |

| | |
|---|---|
| ELF | Epithelial lining fluid |
| ELISA | Enzyme-linked immunosorbent assay |
| EMPF | Equine multinodular pulmonary fibrosis |
| EMT | Epithelial to mesenchymal transition |
| ERS | European respiratory society |
| ET-1 | Endothelin-1 |
| EVG | Elastic Von Gieson |
| FGF | Fibroblast growth factor |
| FVC | Forced vital capacity |
| GGO | Ground-glass opacity |
| GOR | Gastro-oesophageal reflux |
| GWAS | Genome wide association study |
| HHV | Human herpesvirus |
| HP | Hypersensitivity pneumonitis |
| ILD | Interstitial lung disease |
| IPF | Idiopathic pulmonary fibrosis |
| MPA | Main pulmonary artery |
| MPA/Ao | Main pulmonary artery to aortic diameters ratio |
| MUC5B | Mucin 5B |
| NSIP | Non-specific interstitial pneumonia |
| NT-proBNP | N-terminal pro-brain natriuretic peptide |
| LTBP | Latent TGF-β binding protein |
| p(A-a)O2 | Alveolar to arterial oxygen gradient |
| PAP | Pulmonary arterial pressure |
| pCO2 | Partial pressure of carbon dioxide |
| PDGF | Platelet-derived growth factor |
| PH | Pulmonary hypertension |
| PIIINP | Procollagen type III amino terminal propeptide |

| | |
|---|---|
| pO2 | Partial pressure of oxygen |
| PPFE | Pleuroparenchymal fibroelastosis |
| PR | Pulmonary regurgitation |
| PV/PA | Pulmonary vein to pulmonary artery ratio |
| qRT-PCR | Quantitative reverse-transcription polymerase chain reaction |
| RPAD Index | Right pulmonary artery distensibility index |
| Se | Sensitivity |
| Sp | Specificity |
| TBB | Trans-bronchial biopsy |
| TGF-β | Transforming growth factor-beta |
| T-HRCT | Thoracic high-resolution computed tomography |
| TR | Tricuspid regurgitation |
| UIP | Usual interstitial pneumonia |
| VEGF | Vascular endothelial growth factor |
| VmaxTR | Tricuspid regurgitant jet maximal velocity |
| WHWTs | West Highland white terriers |

# TABLE OF CONTENTS

# SUMMARY

Canine idiopathic pulmonary fibrosis (CIPF) is a progressive parenchymal lung disease of unknown origin, mainly described in old-aged West Highland white terriers (WHWTs). It is characterized by exercise intolerance, cough and dyspnoea/tachypnea with a progressive deterioration until death from respiratory insufficiency. CIPF shares clinical features with human idiopathic pulmonary fibrosis (IPF), while tomodensitometric and histopathological findings do not appear to be exactly the same. Over the past 10 years, several studies have been performed to improve our knowledge about CIPF. However, this disease is still misunderstood and clinicians are dealing with several challenges including the absence of clinical or biological markers for estimating the presence, severity or progression of the disease and related co-morbidities such as pulmonary hypertension, the absence of etiologic agent, and the absence of targeted therapy. Consequently, the aims of the present project were (1) to investigate whether high-resolution computed tomography (HRCT) of the lungs obtained under sedation can be used for the diagnosis and for the follow-up of the disease, (2) to study a new echocardiographic parameter for the diagnosis of precapillary pulmonary hypertension induced by CIPF, (3) to study the potential roles of 2 chemokines of interest, CCL2 and CXCL8, as biomarkers of fibrosis and as actors in the pathogenesis of the disease, (4) to determine breed variation of basal blood concentrations of the same chemokines, vascular endothelial growth factor (VEGF), and serotonin, and (5) to search for the presence of herpesvirus as a possible etiologic agent.

To meet objective (1), lung HRCT findings found in WHWTs affected with CIPF, as well as unaffected WHWTs matched for age were described. The effect of the sedation vs. anaesthesia on the identification and gradation of the lung lesions was studied in order to determine the utility of the sedation for the diagnosis of CIPF, given that anaesthesia is a potential risk in pulmonary-diseased dogs, particularly in the presence of pulmonary hypertension. Results showed that both sedation and general anaesthesia allowed identification of ground-glass opacities (GGO), the classical HRCT features described in CIPF. This suggests that sedation may be a good alternative for the CIPF HRCT diagnosis when general anaesthesia is not recommended. GGO was also observed in some control dogs, essentially localised to the cranial lung lobes, which may correspond to methodological artefact or to sub-clinical early CIPF lesions. Differences between sedation and general anaesthesia were found in the identification of consolidation and in the gradation of the GGO and mosaic attenuation pattern extent, more probably related to the different breathing pattern of the dogs between the two examinations: spontaneous breathing under sedation vs. end-expiratory pause following hyperventilation under general anaesthesia, inducing a variable content of air within the alveoli

and influencing the interpretation of lung lesions on HRCT images. However, the differences in lesion gradation extent did not prevent the establishment of the CIPF diagnosis, given that GGO was observed in all CIPF dogs in a greater extent than in controls or in association with other CIPF features not present in controls.

Objective (2) was to study a novel echocardiographic index, the pulmonary vein to pulmonary artery ratio (PV/PA) in correlation with other non-invasive echocardiographic indices of pulmonary hypertension (PH): the maximal velocity of tricuspid regurgitation (VmaxTR), the acceleration to ejection time ratio of the pulmonary flow (AT:ET), the main pulmonary artery to aorta diameter ratio (MPA/Ao), and the right pulmonary artery distensibility index (RPAD Index). Echocardiographic measures were performed in WHWTs affected with CIPF and control WHWTs matched for age. Correlations were calculated with the partial pressure of oxygen (pO2), the distance walked in the 6-minute walking test (6MWD), and serum concentrations of NT-proBNP. A tricuspid regurgitant jet allowing the estimation of pulmonary pressure gradient was found in 50% WHWTs affected with CIPF and 12.5% controls. In CIPF WHWTs with concomitant PH (VmaxTR above 2.8 m/s) significantly lower PV/PA values were found in comparison with control WHWTs. This decrease in PV/PA was due to an increase in the pulmonary artery diameter and a decrease in pulmonary vein diameter. A trend for a decrease of AT:ET and RPAD Index and an increase of MPA/Ao was observed in CIPF WHWTs affected with PH in comparison with controls. Significant moderate correlations were found between PV/PA and all of the other echocardiographic parameters of PH, as well as with 6MWD. There was no correlation between PV/PA and serum NT-proBNP concentrations or arterial pO2 values. Those results suggest the potential benefit of the PV/PA ratio for the non-invasive diagnosis of precapillary PH in WHWTs affected with CIPF. Further investigations in a larger cohort of dogs with precapillary PH, and with a measurable tricuspid regurgitant jet, are needed to validate this finding.

In 2013, Krafft and collaborators highlighted an overexpression of chemokines CCL2 and CXCL8 in the lung parenchyma of WHWTs affected with CIPF in comparison with controls. The objective (3) of the present work was therefore to investigate serum and bronchoalveolar lavage fluid (BALF) concentrations of CCL2 and CXCL8 in CIPF and control WHWTs, and to study the lung signalling pathways of those molecules via qRT-PCR (CCL2, CXCL8, CCR2, CXCR2) and immunohistochemistry (CCL2 and CXCL8). Such tests might lead to determining the potential role of the chemokines as biomarkers of the disease and as actors in the pathogenesis. Higher serum CCL2 concentrations were found in WHWTs affected with CIPF in comparison with controls; serum CCL2 concentrations above 700 pg/mL were associated with a shorter survival time in CIPF WHWTs. Conversely, there was no significant

difference between CIPF and control WHWTs for serum CXCL8 concentrations. For BALF concentrations, both CCL2 and CXCL8 chemokines were significantly increased in WHWTs affected with CIPF. Relative CCL2, CXCL8, and their respective receptors CCR2 and CXCR2 gene expression was not significantly different between the lungs of WHWT with CIPF and control dogs of various breeds, while an immunolabelling for CCL2 and CXCL8 was found in the lung parenchyma of CIPF WHWTs at the level of bronchial epithelial cells. Those results tend to indicate that chemokines CCL2 and CXCL8 are potentially involved in the fibroproliferative process associated with CIPF. Whether the modifications observed are a cause of, or a consequence of, the disease remain unknown.

To test our hypothesis that higher circulating basal blood concentrations of profibrotic molecules could serve as predisposing factors for CIPF development in the WHWT breed, serum concentrations of CCL2, CXCL8, vascular endothelial growth factor (VEGF) and serotonin (5-HT) were measured in healthy dogs from various breeds variably predisposed to CIPF. In addition to the WHWT breed, 6 other breeds of dogs were included: Scottish terrier and Jack Russel terrier considered as potentially predisposed for CIPF, Maltese and King Charles spaniel considered as non-predisposed breeds sharing similarities in weight and size with the WHWT breed, and Labrador Retriever and Malinois Belgian Shepherd considered as non-predisposed breeds not-matched for size and weight with the WHWT breed. Increased serum CXCL8 concentrations were found in healthy dogs from the WHWT breed in comparison with all other breeds less or not predisposed to CIPF. Serum CCL2 concentrations were significantly increased in healthy WHWTs, but also in Maltese, a non CIPF-predisposed breed, compared with King Charles spaniel and Malinois Belgian Shepherd. No relevant interbreed differences were observed for 5-HT with regard to CIPF predisposition. Breed-related differences in VEGF blood concentrations could not be investigated since most of the results obtained were below the kit detection limit.

Finally, to meet objective (5), a study was performed to search for the presence of gammaherpesvirus in the lung parenchyma of WHWTs affected with CIPF, given that an association between Epstein-Barr virus and human IPF has been proposed. A panherpesvirus nested PCR targeting the DPOL gene was applied on both lung and blood samples, but herpesvirus DPOL sequences were not identified in any of the samples tested.

# RESUME

La fibrose pulmonaire idiopathique canine (FPIC) est une affection fibrosante chronique du parenchyme pulmonaire, majoritairement rencontrée chez le chien de race West Highland White Terrier (WHWT) d'âge avancé. Elle se traduit par une intolérance à l'effort, de la toux et de la dyspnée/tachypnée avec aggravation progressive jusqu'au décès de l'animal par insuffisance respiratoire. La FPIC partage de nombreuses similitudes cliniques et pathogéniques avec la fibrose idiopathique pulmonaire (FIP) décrite chez l'homme, bien que les lésions tomodensitométriques et histologiques ne soient pas strictement superposables entre les 2 espèces. Au cours de ces 10 dernières années, plusieurs études ont été menées afin d'améliorer les connaissances sur la FPIC. Toutefois, cette maladie reste encore mal comprise à l'heure actuelle et le clinicien doit faire face à plusieurs challenges incluant l'absence de marqueur clinique ou biologique permettant d'estimer la présence, la sévérité ou la progression de la maladie ainsi que la présence de comorbidités relatives dont l'hypertension pulmonaire, l'absence d'agent étiologique, et l'absence de thérapie ciblée. Le présent travail a donc été entrepris afin de répondre au moins partiellement à ces différents challenges. Les objectifs ont été (1) d'investiguer l'intérêt de l'examen tomodensitométrique à haute résolution obtenu sous sédation pour le diagnostic et le suivi de la maladie, (2) d'étudier un nouveau paramètre échocardiographique pour le diagnostic de l'hypertension pulmonaire associé à la FPIC, (3) d'élucider les rôles potentiels de 2 chémokines d'intérêt, CCL2 et CXCL8, en tant que biomarqueurs de fibrose et d'agents de pathogénèse, (4) de déterminer les variations raciales des concentrations sanguines basales en ces mêmes chémokines ainsi qu'en VEGF et en sérotonine, et (5) de rechercher la présence d'herpesvirus comme agent étiologique.

Pour répondre à l'objectif (1), les lésions tomodensitométriques pulmonaires ont été décrites chez des WHWTs atteints de FPIC, ainsi que chez des chiens sains de même race matchés pour l'âge (chiens âgés). L'impact d'une sédation versus une anesthésie sur l'identification et la gradation des lésions tomodensitométriques a été étudié, afin de déterminer l'intérêt de l'examen obtenu sous sédation pour le diagnostic de FPIC dans les cas où l'anesthésie est risquée, ce qui est particulièrement le cas chez les chiens sévèrement atteints de fibrose et d'hypertension pulmonaire concomitante. Les résultats ont montré que la sédation et l'anesthésie permettaient tous deux d'observer les images en verre dépoli classiquement décrites en cas de FPIC, suggérant l'utilisation préférentielle de la sédation pour le diagnostic de FPIC en cas d'anesthésie risquée. Des images en verre dépoli ont également été observées chez certains chiens sains, essentiellement dans les lobes pulmonaires crâniaux, suggérant un artéfact lié à la méthode ou la présence de lésions sub-cliniques de FPIC. Des différences entre sédation et anesthésie ont été observées pour l'identification des consolidations et pour la

gradation des images en mosaïque et en verre dépoli. Ces différences sont attribuables à la phase respiratoire différente entre sédation (respiration spontanée) et anesthésie (pause expiratoire induite par une hyperventilation préalable) induisant une quantité variable d'air dans les alvéoles et une apparence variable des lésions pulmonaires sur les images tomodensitométriques. Cependant, ces différences ne semblent pas interférer avec le diagnostic de FPIC étant donné que les images en verre dépoli ont été retrouvées chez tous les WHWTs atteints de FIPC dans une étendue plus importante en comparaison aux contrôles et/ou en association avec d'autres caractéristiques tomodensitométriques de fibrose.

Dans le cadre de l'objectif (2), un nouveau paramètre échocardiographique (pulmonary vein to pulmonary artery ratio : PV/PA) a été étudié en corrélation à d'autres indices échocardiographiques susceptibles d'identifier de manière non-invasive l'hypertension pulmonaire : la vitesse maximale du reflux tricuspide (VmaxTR), le rapport entre l'accélération et l'éjection du flux pulmonaire (AT:ET), le rapport entre le diamètre de l'artère pulmonaire principale et le diamètre de l'aorte (MPA/Ao), et la distensibilité de l'artère pulmonaire (RPAD Index). Les mesures ont été faites chez des WHWTs atteints de FPIC et chez des WHWTs contrôles matchés pour l'âge. Des corrélations avec la pression partielle artérielle en oxygène (pO2), la distance marchée en 6 minutes (6MWD) et les concentrations sériques en NT-proBNP ont également été calculées. Un reflux tricuspide permettant d'estimer le gradient de pression dans les artères pulmonaires n'était présent que chez 50% WHWTs atteint de FPIC et 12,5% des contrôles. Des valeurs significativement plus basses en PV/PA ont été observées chez les WHWTs atteints de FPIC avec hypertension pulmonaire (VmaxTR supérieur à 2,8 m/s) en comparaison aux contrôles suite à une augmentation du diamètre de l'artère pulmonaire et à une diminution du diamètre de la veine pulmonaire. Une tendance pour une diminution des paramètres AT:ET et RPAD et pour une augmentation du paramètre MPA/Ao a été observée chez les WHWTs atteints de FPIC et d'hypertension pulmonaire. Des corrélations modérées significatives ont été observées entre PV/PA et tous les autres paramètres échocardiographies d'hypertension pulmonaire étudiés, de même qu'avec la 6MWD mais pas avec la pO2 artérielle. Il n'y avait pas de différence entre les groupes pour les concentrations sériques en NT-proBNP ni de corrélation avec le paramètre PV/PA. Ces résultats suggèrent que le paramètre PV/PA peut être utilisé comme indicateur d'hypertension pulmonaire d'origine pré-capillaire et encourage la réalisation de recherches ultérieures dans ce domaine dans une plus large population de chien pour lesquels un reflux tricuspide est présent.

Suite à la mise en évidence par Krafft et collaborateurs (2013) d'une surexpression relative des chémokines CCL2 et CXCL8 au sein du parenchyme pulmonaire des WHWTs atteints de FPIC, l'objectif (3) du présent travail a été d'investiguer les concentrations en CCL2

et CXCL8 retrouvées dans le sérum et dans le liquide de lavage bronchoalvéolaire (BALF) de WHWTs avec CIPF et de WHWTs contrôles sains, ainsi que d'étudier la signalisation de ces chémokines au sein du parenchyme pulmonaire par qRT-PCR (CCL2, CXCL8, CCR2, CXCR2) et par immunohistochimie (CCL2 et CXCL8) ; le but étant de déterminer le rôle de ces chémokines en tant que biomarqueur de la maladie et en tant qu'acteur potentiel dans la pathogénèse. Des concentrations sériques en CCL2 significativement augmentées ont été observées chez les WHWTs atteints de FPIC en comparaison aux contrôles ; les WHWTs atteints de FPIC avec des concentrations sériques supérieurs à 700 pg/mL ayant une espérance de survie significativement raccourcie. A l'inverse, aucune différence significative n'a été mise en évidence pour les concentrations sériques en CXCL8 entre les WHWTs atteint de FPIC et les WHWTs sains. Concernant les concentrations mesurées dans le BALF, les WHWTs atteints de FPIC présentaient des concentrations en CXCL8 et en CCL2 significativement augmentées en comparaison aux individus contrôles. Aucune différence significative n'a été mise en évidence par qRT-PCR pour l'expression relative des gènes codant les chémokines CCL2 et CXCL8 et leurs récepteurs associés CCR2 et CXCR2, bien qu'un immunomarquage fût présent au sein des poumons de WHWTs atteints de FPIC essentiellement à hauteur des cellules épithéliales bronchiques. Ces résultats indiquent une implication potentielle des chémokines CCL2 et CXCL8 dans le processus fibroprolifératif de la FPIC. Cependant, savoir si les modifications observées représentent une cause ou une conséquence de la maladie reste encore à déterminer.

Les concentrations sériques en CCL2, CXCL8, VEGF (vascular endothelial growth factor) et 5-HT (sérotonine) ont également été analysés dans le sérum d'autres races de chiens sains peu ou pas prédisposées à développer la maladie, afin de tester notre hypothèse selon laquelle la présence de concentrations basales élevées en molécules profibrotiques chez le WHWT pourrait expliquer la plus grande susceptibilité de cette race pour la maladie. En plus du WHWT, 6 races de chiens ont été inclues : le Scottish terrier et le Jack Russell terrier considérées comme potentiellement prédisposée à la FPIC, le Bichon Maltais et le Cavalier King Charles considérées comme non-prédisposées à la FPIC mais de taille et de poids similaires à la race WHWT, et enfin le Labrador et le Berger Malinois considérées comme non-prédisposées à la FPIC et non-matchés pour la taille et le poids avec la race WHWT. Les concentrations en CXCL8 étaient significativement plus élevées dans le sérum de WHWTs sains en comparaison à toutes les autres races de chiens sains inclues peu ou pas prédisposées à la fibrose. Les concentrations en CCL2 étaient significativement augmentées chez le WHWT et le Bichon Maltais en comparaison au Cavalier King Charles et Berger Malinois. Aucune différence significative remarquable n'a été observée pour les concentrations sériques en sérotonine. La comparaison des concentrations sériques en VEGF entre les races n'a pas pu être

objectivée étant donné que la plupart des échantillons ont donné des valeurs inférieures au seuil de détection du kit.

Enfin, pour répondre à l'objectif (5), une étude s'est portée sur la recherche de la présence potentielle de gammaherpesvirus dans le parenchyme pulmonaire de WHWTs atteints de CIPF, au vu de l'association décrite entre l'Epstein-Barr virus et l'IPF chez l'homme. Une PCR panherpes (gène DPOL) a été appliquée mais n'a pas permis d'identifier la présence de gammaherpesvirus dans le parenchyme pulmonaire de WHWTs atteints de CIPF.

# INTRODUCTION

Fibrosis is defined as any pathological condition where fibrous connective tissue invades any organ, usually as a consequence of inflammatory or other injury (MeSH PubMed, year introduced 1987). In the particular case of pulmonary fibrosis, the normal lung tissue is progressively replaced by fibroblasts and collagen causing an irreversible loss of organ function resulting in death (MeSH PubMed). The present work will focus on pulmonary fibrosis in a specific dog breed, the West Highland white terrier (WHWT). In this introductory section, we will review what is already known about this disease in dogs, and then report what was discovered about pulmonary fibrosis in other animal species and in human medicine with the help of experimental murine models of the disease. General aspects of pulmonary fibrosis in each species will be addressed, in addition to more advanced literature review in link with the objectives of the present work.

## 1. Canine idiopathic pulmonary fibrosis: an update

Canine idiopathic pulmonary fibrosis (CIPF) is a chronic and progressive lung disease of unknown aetiology affecting mainly old-aged WHWTs. Since its first description in 1999, several studies have been conducted to improve the clinical characterisation of the disease, expand our understanding about the pathophysiology and identify biomarkers of the disease. At the present time, however, several aspects of CIPF remain unknown and will be addressed at the end of this section.

### 1.1. Description of CIPF - History

Corcoran and associates initially described, in 1999a, a chronic clinical pulmonary condition in a cohort of 29 WHWTs characterized by marked inspiratory crackles audible on auscultation of the thorax in association with radiographic interstitial changes. Additional case reports and case series were thereafter published allowing a better characterization of this clinical entity in relation with knowledge available from idiopathic pulmonary fibrosis (IPF) in humans (Corcoran et al., 2011; Heikkila et al., 2011; Norris et al., 2005; Webb and Armstrong, 2002).

The term ‘canine idiopathic pulmonary fibrosis’ was firstly introduced in 2005 by Johnson and collaborators and used by our team and Finland partners since 2011 to refer to this chronic pulmonary disease affecting the WHWT breed. This nomenclature was chosen because the disease affects the dog, is characterized by the presence of fibrosis on lung histopathology, and because no etiologic agents have been reported so far. This clinical syndrome has previously been referred, depending on the authors, as chronic pulmonary disease (Corcoran et

al., 1999a; Schober and Baade, 2006), chronic idiopathic pulmonary fibrosis (Lobetti et al., 2001; Webb and Armstrong, 2002), idiopathic pulmonary fibrosis (Norris et al., 2002), or interstitial lung disease (Norris et al., 2005; Reinero and Cohn, 2007). It is important to point out that the term CIPF should be used cautiously, as it may suggest a complete resemblance with human IPF, but as we will discuss in this introduction section, CIPF is not the same disease than IPF in humans even though some clinical and pathological features are shared.

## 1.2. Clinical characterization of CIPF

### *1.2.1. Clinical presentation*

CIPF affects mainly middle-aged to old WHWTs, with a mean age at diagnosis ranging from 9 to 13 years (Corcoran et al., 1999a; Heikkila et al., 2011). Symptoms may appear earlier in rare cases with an onset at 3 years of age described in the literature (Johnson et al., 2005; Schober and Baade, 2006). No sex predisposition has been reported (Heikkila-Laurila and Rajamaki, 2014). Rare cases of pulmonary fibrosis have also been described in other terrier breeds, such as the American Staffordshire terrier, the Bull terrier, the Cairn terrier and the Scottish terrier (Corcoran et al., 1999b; Johnson et al., 2005; Krafft et al., 2013; Lobetti et al., 2001; Norris et al., 2002). However, only limited data are available in those breeds and it is not known if pulmonary fibrosis is exactly the same as in the WHWT breed.

Clinical signs of CIPF in WHWTs vary among individuals, but generally develop slowly and deteriorate progressively over time (Corcoran et al., 1999a). Symptomatology is often attributed by the owners to normal aging process (Corcoran et al., 1999a). History in the majority of cases revealed exercise intolerance alone or in association with chronic cough in an otherwise alert and bright dog; more pronounced respiratory symptoms may be reported such as tachypnea, excessive panting, dyspnoea, cyanosis or syncope (Heikkila-Laurila and Rajamaki, 2014). The duration of clinical signs at diagnosis also varies between individuals and ranges from few weeks to several months (Heikkila-Laurila and Rajamaki, 2014). The major clinical feature is the presence of inspiratory crackles on thoracic auscultation. In some dogs, crackles can even be heard without stethoscope when the dog is breathing with an open mouth (Heikkila-Laurila and Rajamaki, 2014). Other common clinical examination findings include positive laryngo-tracheal reflex, tachypnea and excessive abdominal breathing (Heikkila-Laurila and Rajamaki, 2014). The presence of wheezes on thoracic auscultation, tachypnea, dyspnoea and cyanosis have also been reported (Corcoran et al., 1999a).

### *1.2.2. Blood haematological and biochemical analyses*

Blood haematological and biochemical analyses are generally unremarkable in WHWTs affected with CIPF, but are useful in the diagnostic approach to rule out other causes responsible for the exercise intolerance (Heikkila-Laurila and Rajamaki, 2014). Interestingly, the alkaline phosphatase (ALP) concentration and platelet count are frequently increased in WHWTs affected with CIPF, but are also observed in age-matched unaffected WHWTs, suggesting that those blood characteristics are more likely related to the breed than to the underlying pathological condition (Heikkila et al., 2011). Such an increase in ALP concentration has also been reported in healthy dogs of the Scottish terrier breed (Gallagher et al., 2006; Nestor et al., 2006), and has been speculated to be due to benign subclinical hyperadrenocorticism in this breed (Zimmerman et al., 2010). Whether such phenomenon also exists in the WHWT breed has not been investigated to date.

### *1.2.3. Cardiopulmonary function testing*

Diagnostic tools allowing the investigation of the cardiopulmonary function are limited in dogs in comparison with those available in human medicine given that conscious manoeuvres are not possible in dogs. The only two tests that have been investigated for the overall assessment of the cardiopulmonary function in WHWTs affected with CIPF are the arterial blood gas analysis and the 6-minute walking test (6MWT). Hypoxemia is a common finding in WHWTs affected with CIPF, arterial partial pressure of oxygen (pO2) comprised between 80 and 60 mmHg (mild hypoxemia) or below 60 mmHg (severe hypoxemia) being respectively noticed in 45% and 45% of affected WHWTs (Heikkila-Laurila and Rajamaki, 2014). In comparison with control WHWTs, WHWTs affected with CIPF displayed reduced arterial pO2 values and increased alveolar to arterial oxygen gradient (p(A-a)O2), while there was no difference between groups for the arterial partial pressure of carbon dioxide (pCO2) (Table 1) (Heikkila-Laurila and Rajamaki, 2014).

Table 1: Arterial blood gas analysis in WHWTs affected with CIPF and controls. (Heikkila-Laurila and Rajamaki, 2014)

**Arterial blood gas analysis in WHWTs with CIPF (9 dogs) and healthy control WHWTs (11 dogs)**

| | WHWTs with CIPF | Healthy WHWTs |
|---|---|---|
| $PaO_2$[a] | 65.5 ± 15.4 (33.5–87.4) mm Hg | 99.1 ± 7.8 (89.6–113.0) mm Hg |
| $P(A\text{-}a)O_2$[a] | 50.1 ± 17.3 (28.0–84.7) mm Hg | 17.5 ± 4.9 (10.7–26.8) mm Hg |
| $PaCO_2$ | 29.3 ± 3.8 (25.0–35.7) mm Hg | 28.7 ± 3.8 (20.5–34.6) mm Hg |

Results are given as mean ± SD and range.
[a] Statistically significant difference, $P<.001$.

It is important to note that arterial blood gas analysis modifications are not specific of CIPF and may also be observed in ventilation-perfusion mismatch due to any pulmonary parenchymal disease (e.g. pneumonia, acute respiratory distress syndrome, pulmonary thromboembolism) or in case of right-to-left shunting (Balakrishnan and King, 2014). Consequently, arterial blood gas analysis in WHWTs affected with CIPF are generally used to quantify the severity of the cardiorespiratory system dysfunction, rather than to confirm the diagnosis (Balakrishnan and King, 2014). Interestingly, despite such low oxygen levels, most of the WHWTs affected with CIPF were bright and alert, and not in respiratory distress, suggesting that the slow progression rate of the disease enables the dogs to adapt to progressive lower oxygen levels (Heikkila-Laurila and Rajamaki, 2014). This adaptation is apparently independent of an enhanced erythropoiesis as polycythaemia is not commonly observed in WHWTs affected with CIPF (Heikkila-Laurila and Rajamaki, 2014).

The 6MWT is a submaximal exercise test that measures the distance an individual is able to walk over 6 minutes (6MWD) (Lilja-Maula et al., 2014b). This test is widely used in human clinical practice to assess disease progression and response to treatment, as well as in therapeutic trials to serve as a primary end-point, as it is inexpensive, easily applicable and well-tolerated (Demir and Kucukoglu, 2015). In WHWTs affected with CIPF, the 6MWT is an easy and well-tolerated test (Lilja-Maula et al., 2014b). The 6MWD is significantly decreased in WHWTs affected with CIPF compared with controls and seems to correlate positively with arterial pO2 values, suggesting that the test can serve as a non-invasive means of monitoring lung function and exercise tolerance in WHWTs affected with CIPF (Lilja-Maula et al., 2014b).

### *1.2.4. Echocardiography*

Echocardiography is an essential complementary examination in the diagnostic approach of CIPF, allowing the non-invasive diagnosis of pulmonary hypertension (PH) and ensuring the absence of any concomitant primary cardiac diseases. PH is frequently present in WHWTs affected with CIPF (Schober and Baade, 2006). Right-sided cardiac enlargement suggestive of PH has been described in 15 out of 29 (51.7%) WHWTs affected with CIPF in the study of Corcoran and collaborators (1999a) and in 6 out of 10 (60%) WHWTs affected with CIPF in the study of Heikkila and collaborators (2011). However, this subjective assessment of the right heart does not allow to quantify pulmonary arterial pressures (PAP), which is needed for definitive diagnosis of PH and therapeutic decisions.

Right heart catheterization (RHC) is considered as the gold standard technique for quantitative determination of PAP, but its invasive nature and the concomitant risk of complications preclude its routine use in clinical practice (Kellihan and Stepien, 2010; McGoon

and Kane, 2009). Consequently, echocardiography is classically used for the non-invasive diagnosis of PH in veterinary medicine. Doppler flow interrogations of tricuspid or pulmonary insufficiency jets are the current echocardiographic gold standard for the diagnosis of PH as they provide estimates of systolic or diastolic PAP by applying the Bernoulli equation (pressure gradient = 4 * [peak flow velocity]²) (Currie et al., 1985; Kellihan and Stepien, 2010). In absence of right ventricular outflow tract obstruction, right ventricular and pulmonary artery pressures are equivalent during systole and quantitative assessment of tricuspid regurgitation (TR) jet velocity provides an estimate of systolic PAP (Table 2) (Kellihan and Stepien, 2010). Pulmonic regurgitation (PR) occurs in diastole and the measurement of its peak velocity allows the quantitative assessment of estimated diastolic PAP; a PR velocity ≥ 2.2m/s (corresponding to a gradient of ≥ 19 mmHg) being suggestive of PH (Kellihan and Stepien, 2010).

Table 2: PH severity grading system based on peak TR velocity and associated TR gradient. (Kellihan and Stepien, 2010)

| | Mild | Moderate | Severe |
|---|---|---|---|
| TR peak systolic velocity (m/s) | ≥ 2.8 to < 3.5 | 3.5–4.3 | >4.3 |
| TR systolic gradient (mm Hg) | ≥ 31.4 to < 50 | 50–75 | >75 |

Obtaining an optimal peak TR or PR measurement may be challenging due to several factors such as poor patient compliance, poor image quality secondary to pulmonary disease/dyspnoea, or poor jet alignment with Doppler interrogation beam (Kellihan and Stepien, 2010). Furthermore, some patients do not have identifiable TR or PR (Schober and Baade, 2006), and, in case of right ventricular function failure, TR jet velocity may be reduced due to the inability of the right ventricular myocardium to generate high pressures leading to a significant underestimation of the severity of PH (Kellihan and Stepien, 2010). On the other hand, increased cardiac contractility (due to medication) or volume overload may be associated with increased TR jet velocity and can lead to an overestimation of the severity of PH (Bonagura and Twedt, 2014). To illustrate this challenge, a recent study in dogs, including healthy beagles with experimentally induced PH, compared non-invasive estimates of PAP obtained via echocardiography with invasive measurements of PAP obtained during RHC (Soydan et al., 2015). They demonstrated that using peak TR gradient as surrogate for invasive PAP measurement is prone to inaccuracy as the correlation between the 2 methods was moderate with wide confidence intervals (Soydan et al., 2015).

The limitations related to the use TR jet velocity for estimation of PAP greatly encourage the development of new echocardiographic measures for a non-invasive diagnostic approach of PH. The use of multiple echocardiographic imaging modalities - allowing the identification of a maximum number of supportive findings of PH in patients in whom direct estimation of PAP

via Doppler flow interrogation is not possible - is highly encouraged in dogs (Kellihan and Stepien, 2010). Consequently, several authors investigated two-dimensional and Doppler echocardiographic indices that may help to predict PH. Among them, Schober and associates (2006) investigated whether systolic time intervals of the pulmonary flow (Fig. 1) may be predictive of PH in a cohort of 41 healthy WHWTs and 45 WHWTs affected with CIPF. Among the diseased WHWTs, 7 (15.5%) of them had no evidence of Doppler-derived systolic PH (tricuspid regurgitant jet maximal velocity VmaxTR < 3.1 m/s), 18 (40%) were of unknown status with regard to PAP given the absence of any measurable tricuspid regurgitant jet, and 20 (44.4%) had systolic PH (VmaxTR ≥ 3.1 m/s). A shortening of the acceleration time (AT) and a decrease of the acceleration to ejection time (AT:ET) of the pulmonary flow was identified in CIPF WHWTs with PH in comparison with healthy WHWTs. They also determined cut-off values for both measurements to predict the presence of PH (estimated systolic PAP ≥ 45 mmHg) as ≤ 0.31 for AT:ET (Se 73%, Sp 87%) and ≤ 58 ms for AT (Se 88%, Sp 80%).

Fig. 1: Normal Doppler flow pattern of pulmonary artery to demonstrate measurement of acceleration time (AT) and ejection time (ET).
(Schober and Baade, 2006)

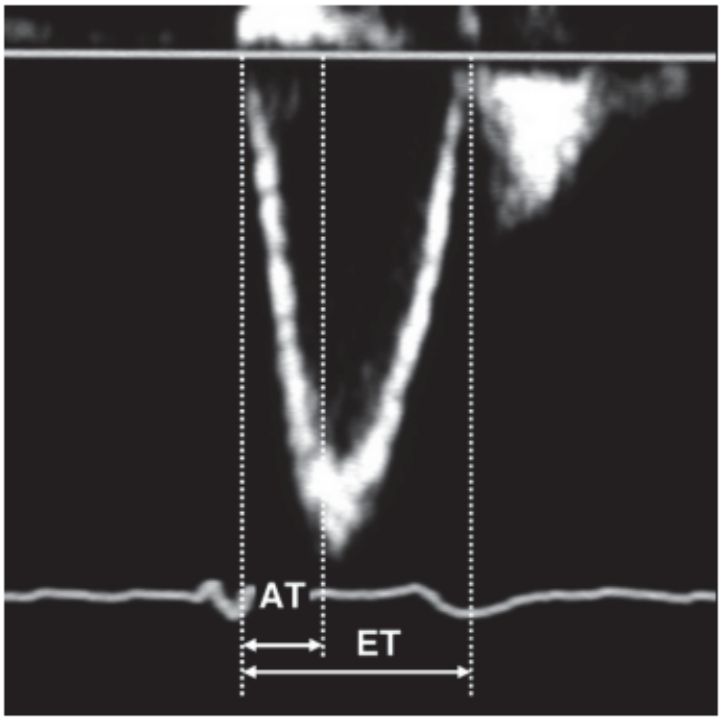


Other indirect non-invasive echocardiographic indices that may help to predict PH have been described in dogs suffering from PH from other origins (mainly left heart disease and various respiratory disorders). These include the diameter of the main pulmonary artery in relation with the diameter of the aorta (MPA/Ao) (Serres et al., 2007), the Tei index representative of global right ventricular function (Baumwart et al., 2005; Paradies et al., 2014),

tissue Doppler imaging assessment of systolic and diastolic right ventricular function (Serres et al., 2007; Visser et al., 2014), tricuspid annular plane systolic excursion (Pariaut et al., 2012), and the right pulmonary artery distensibility index (RPAD Index) (Venco et al., 2014; Visser et al., 2016). However, none of these measures have already been studied specifically in WHWTs affected with CIPF, and their diagnostic utility for PH determination in that particular case is presently unknown.

MPA/Ao is classically measured in the right parasternal basilar short axis view; values exceeding 0.98 being indicative of MPA enlargement suggestive of PH (systolic PAP ≥ 30mmHg) with sensitivity and specificity of 73% and 76%, respectively (Serres et al., 2007). The RPAD Index has been most recently studied in both heartworm infected dogs and dogs with PH from different origins. Reportedly, in heartworm infected dogs, the RPAD index, calculated as the systolic diameter minus diastolic diameter, divided by systolic diameter of the pulmonary artery imaged in M-mode (Fig. 2), can predict the presence of PH (systolic PAP ≥ 30mmHg) at a value < 35% and was strongly correlated with the PAP obtained invasively by RHC (Fig. 3) (Venco et al., 2014).

Fig. 2: M-mode echocardiography of the pulmonary artery. Systolic size is measured at the maximum diameter (usually at the T wave) and diastolic size is measured at its smallest diameter (usually at the Q wave).
(Venco et al., 2014)

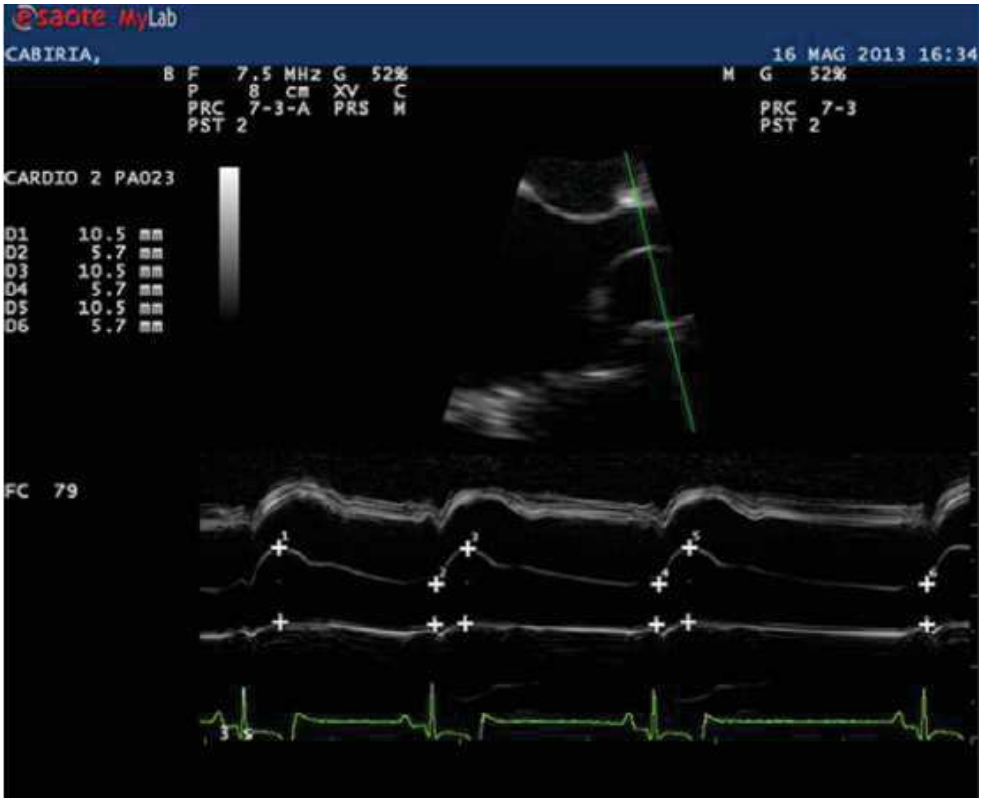

Fig. 3: Correlation between RPAD Index and systolic PAP obtained by RHC.
(Venco et al., 2014)

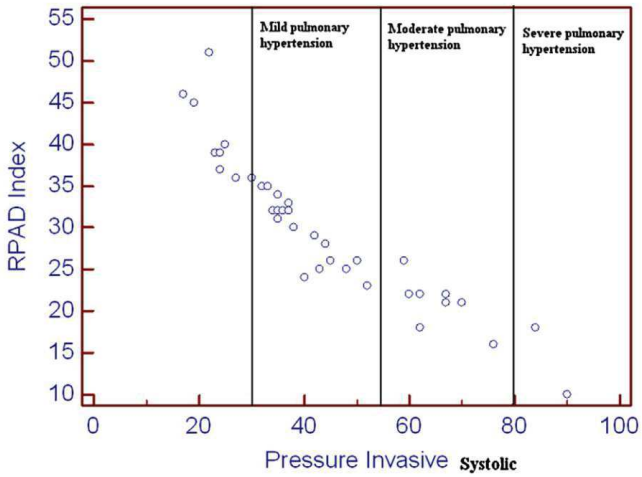


The RPAD Index has also been recently investigated by Visser and collaborators (2016) in a different echocardiographic view than previously described (Fig. 4) in dogs with PH of different origins. They demonstrated that the RPAD Index displayed the strongest correlation with TR pressure gradient ($r = -0.90$, $P < 0.001$) in comparison with AT ($r = -0.69$, $P < 0.001$), AT:ET ($r = -0.68$, $P < 0.001$) and MPA/Ao ($r = 0.78$, $P < 0.001$) and may predict a TR pressure gradient > 50 mmHg at a cut-off value of < 29.5% with a sensitivity and specificity of 84% and 95% respectively (Visser et al., 2016).

Fig. 4: Representative measurement and calculation of RPAD Index.
(Visser et al., 2016)

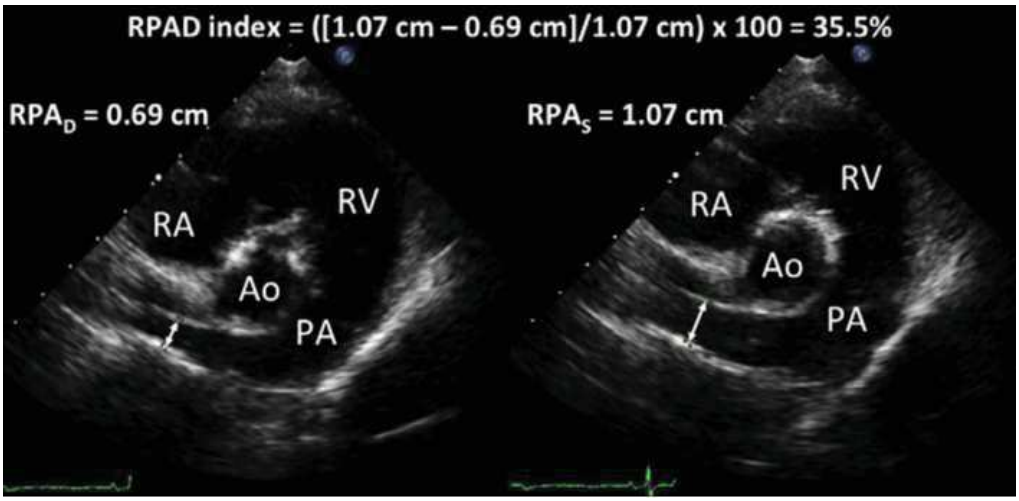


Some authors were also interested in the use of blood biomarkers in predicting the presence of PH in dogs. N-terminal pro-brain natriuretic peptide (NT-proBNP) concentration was studied in a canine model of chronic embolic PH (Hori et al., 2012) and in dogs with

precapillary PH (Kellihan et al., 2011). Both studies yielded the same conclusions that NT-proBNP increases in case of severe PH, but lack sensitivity in cases of mild to moderate PH.

### *1.2.5. Diagnostic imaging*

Thoracic X-rays findings described in WHWTs affected with CIPF are not specific and varied from generalised bronchointerstitial pattern (Fig. 5) to only interstitial, predominantly bronchial or patchy alveolar opacities, findings that might be observed in a diversity of other pulmonary diseases (Heikkila-Laurila and Rajamaki, 2014). The main reason for taking thoracic radiographs is to rule out other lung diseases such as neoplasia (Heikkila-Laurila and Rajamaki, 2014). An increased size of the heart shadow, especially in the dorso-ventral view resulting in a reverse-D shaped cardiac silhouette and an enlarged main pulmonary artery, may indicate the presence of PH and further encourages the realisation of a Doppler echocardiography (Heikkila-Laurila and Rajamaki, 2014).

Fig. 5: Right lateral (A) and ventro-dorsal (B) thoracic radiographs of a 10-year-old WHWT showing redundant tracheal membrane and a severe generalised bronchointerstitial pattern with main pulmonary artery enlargement (<) and pleural fissure line (v) between right lung lobes.
(Roels and Clercx, 2015)

A 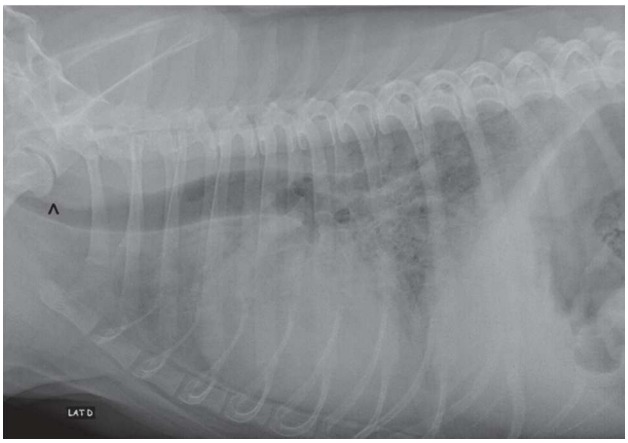

B 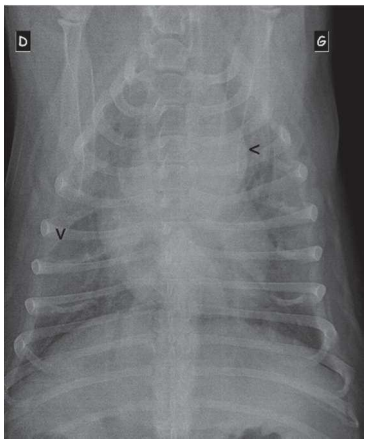


More precise information about the lung parenchyma is obtained with the use of thoracic high-resolution computed tomography (T-HRCT), a diagnostic imaging device which become widely available in veterinary practice. T-HRCT appears to be the complementary examination of choice in the diagnostic approach of CIPF as it allows for the investigation of the lung in a better spatial resolution. The only negative point is that T-HRCT classically requires general anaesthesia, which might not be suitable in severely affected dogs due to the increased anaesthetic risk (Heikkila-Laurila and Rajamaki, 2014). The initial description of T-HRCT features of CIPF was made in 2005 in a cohort of 10 dogs (8 WHWTs and 2 Cairn terriers) using a classification scheme adapted from the human literature (Johnson et al., 2005). In their

study, CIPF dogs were arbitrary classified as having mild (1 dog), moderate (7 dogs) or severe (2 dogs) disease based on clinical signs and thoracic radiographs appearance. They described patchily distributed abnormalities throughout the lung fields with ground-glass opacities (GGO) observed in all dogs, linear and reticular opacities in moderately and severely affected dogs, and bronchiectasis and honeycombing in severe cases. In 2011, two other descriptive studies were published independently using the same classification system. The first study described lesions observed in 6 WHWTs affected with CIPF and 12 controls (Heikkila et al., 2011). The dorso-caudal lung lobes were reported as predilection sites for the lesions, with GGO described in all affected dogs; parenchymal bands, consolidations and traction bronchiectasis in 4 dogs; and honeycombing in 1 dog. In the control population, 8 dogs had 1 or 2 focal lesions of unspecified origin. The second study published in 2011 cited succinctly T-HRCT changes observed in 22 WHWTs affected with CIPF. Bronchial changes were present in the half of the study population (Corcoran et al., 2011). Those 3 studies, collectively, suggest that T-HRCT findings observed in WHWTs affected with CIPF include GGO, parenchymal bands, subpleural bands, subpleural interstitial thickening, peribronchovascular interstitial thickening, consolidation, bronchial thickening, bronchiectasis and honeycombing (Corcoran et al., 2011; Heikkila et al., 2011; Johnson et al., 2005). Imaging findings in an individual dog are typically a combination of one or more of the above mentioned features with distribution of the lesions varying from patchily distributed (Johnson et al., 2005) to predominantly localised in the dorso-caudal lung lobes (Heikkila et al., 2011).

### *1.2.6. Bronchoscopy and bronchoalveolar lavage fluid analysis*

Bronchial abnormalities have been reported in a high proportion of WHWTs affected with CIPF (Corcoran et al., 2011; Heikkila et al., 2011). However, whether those bronchial abnormalities occur secondary to the underlying interstitial lung disease or are an independent phenomenon remains to be elucidated. Age may partially contribute to abnormalities encountered given that some bronchial changes such as irregular bronchial mucosa, prominent mucosal vessels and bronchiectasis have been described in old dogs (Mercier et al., 2011). Common bronchoscopic findings detected in WHWTs affected with CIPF include tracheal collapse, bronchial mucosal irregularity, increased amount of bronchial mucus, bronchomalacia, dynamic airways collapse and bronchiectasis (Heikkila-Laurila and Rajamaki, 2014). Those bronchial changes are not specific for CIPF as they are frequently observed in other pathological respiratory conditions (Heikkila-Laurila and Rajamaki, 2014). Analysis of the bronchoalveolar lavage fluid (BALF) usually shows a moderate increase in the total cellular count due to increased numbers of macrophages, neutrophils, and mast cells (Heikkila-Laurila

and Rajamaki, 2014). The major goal to perform a bronchoalveolar lavage is therefore to exclude a parasitic or a bacterial infection from the differential diagnosis.

### *1.2.7. Histopathological features*

Histopathological examination of parenchymal lung tissue provides a definitive diagnosis of CIPF in the majority of cases, but lung biopsies are seldom taken due to expense and the need for invasive surgery (Heikkila and Rajamäki, 2014). Consequently, the diagnosis of CIPF is classically based on anamnestic information, findings in clinical examination and diagnostic imaging, and exclusion of other respiratory diseases. The first description of histopathological characteristics of CIPF was made in 1999a by Corcoran and collaborators in 4 WHWTs affected with CIPF. They described a multifocal to regional deposition of interstitial extracellular matrix, multifocal epithelial squamous metaplasia, and an increased number of alveolar and circulating macrophages as well as occasional lymphocytes and plasma cells. In 2005, Norris and collaborators attempted to compare histopathological characteristics of CIPF with those described in humans, such as a usual interstitial pneumonia (UIP) pattern, typical histological pattern of IPF in humans. Collagen and elastin stains were used in concert with immunohistochemical characterisation of collagen subtypes and smooth muscle actin-positive cells in 6 WHWTs affected with CIPF. Histopathological lesions observed in their study ranged from generalised deposition of septal collagen with a scant inflammatory cell infiltrate in some cases, to marked septal thickening by collagen, a more abundant cellular infiltrate of predominantly macrophages and lymphocytes and hyperplasia of alveolar-lining type II pneumocytes in more severely affected dogs. Based on results of Mason's trichrome and immunohistochemical stains, the extracellular matrix was shown to be composed of a mixture of type-I and –III collagens with type-III collagen being the most prominent type. Elastin does not appear to be altered in CIPF. Fibroblastic foci were not observed, and smooth muscle actin immunoreactivity was limited to individual cells in the septa, a feature which differs from fibrosis in human UIP. Recent work by Syrja and collaborators (2013) further characterised CIPF histopathological lesions and compared them systematically to the human UIP and non-specific interstitial pneumonia (NSIP) histopathological patterns. All 18 WHWTs affected with CIPF included in their study were displaying a mild to moderate diffuse mature fibrosis of the alveolar walls, in addition to concentric collagen deposition around pre- and post-capillary small vessels (Fig. 6). Multifocal subpleural or peribronchiolar areas of more severe and less mature interstitial fibrosis accompanied by a diffuse presence of myofibroblasts was also observed in 60% of affected dogs. Fibroblastic foci were not observed. Hyperplastic type II pneumocytes were observed in the majority of dogs, as well as epithelial pseudostratification and squamous metaplasia in areas of more severe fibrosis (Fig. 6). Alveolar macrophage

accumulations were also observed in areas of severe interstitial fibrotic changes, while alveolar proteinosis (alveolar luminal homogenous dense eosinophilic material) was randomly distributed throughout the lungs in a multifocal pattern and not co-localised with areas of more severe interstitial lesions. The inflammatory changes in lungs of WHWTs affected with CIPF consisted of mild to moderate lymphoplasmacytic inflammation with few macrophages. In humans, the UIP pattern is characterised by areas of marked interstitial pulmonary fibrosis and honeycombing, distortion of the alveolar architecture in a patchy, often subpleural and paraseptal pattern (Raghu et al., 2011). On the other hand, the NSIP pattern, encountered in collagen vascular disease, hypersensitivity pneumonitis, drug-induced pneumonia and pulmonary infection, is characterised by a relative diffuse and uniform fibrosing interstitial disease with no or minimal honeycombing and rare or absent fibroblastic foci (Katzenstein et al., 2008). Consequently, Syrja and collaborators (2013) concluded that CIPF in WHWTs shares features of both human NSIP and UIP patterns, given that the diffuse interstitial lesions present in all affected dogs is in favour of NSIP, while the presence of more severely affected areas of progressive fibrosis tend to correlate with the UIP pattern (Table 3).

Fig. 6: Histopathological characteristics of CIPF in WHWTs: transition from mild diffuse fibrosis on the left, to a focus of accentuated disease, with severe interstitial fibrosis on the right. HE .Bar, 200µm. Inset: type-II pneumocytes hyperplasia and squamous metaplasia of the alveolar epithelium.
(Syrja et al., 2013)

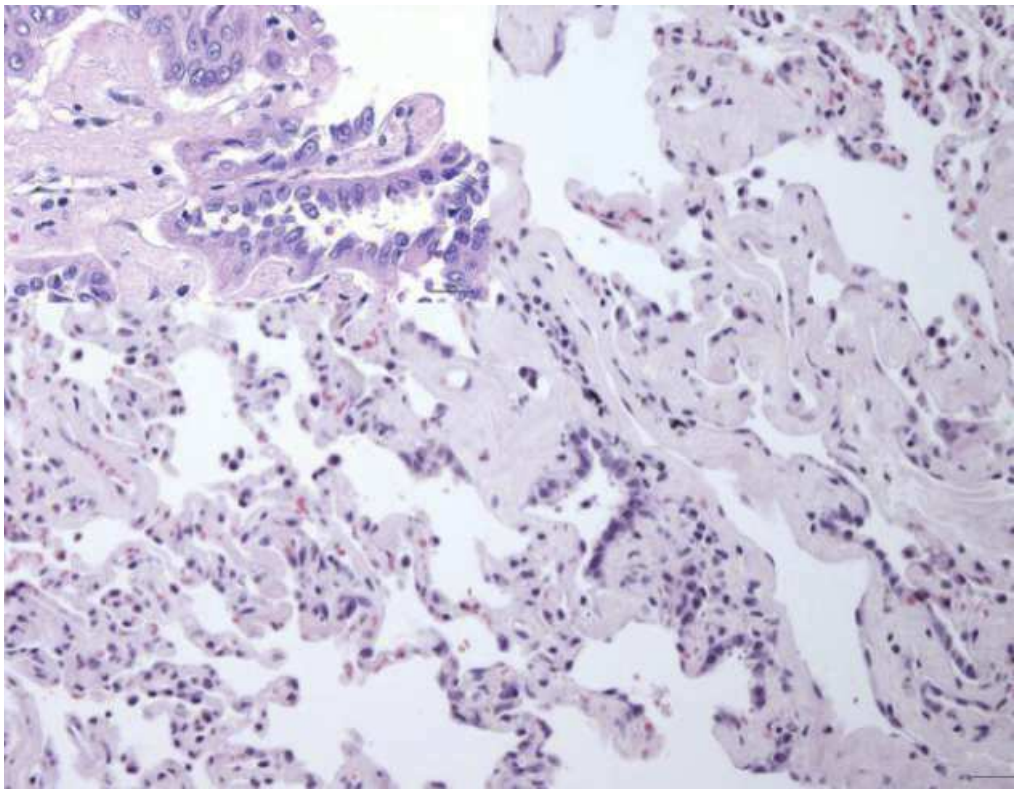

Table 3: Comparison between the main histological criteria required for the diagnoses UIP or NSIP in man and the findings in CIPF in WHWTs.
(Syrja et al., 2013)

| *Criteria* | *UIP* | *IPF in WHWT* | *NSIP (fibrosing)* |
|---|---|---|---|
| Pattern | Patchy, subpleural or paraseptal | Diffuse with subpleural/peribronchiolar accentuation | Relatively diffuse |
| Interstitial fibrosis | Marked, distorting, replacing alveolar tissue | Mild to marked, not obliterating alveolar architecture | Variable degree |
| Honeycombing | Yes | Yes | Not characteristic |
| Fibroblastic foci | Yes | No | Absent or inconspicuous |
| Interstitial inflammation | Minimal, mild | Mild to moderate | Mild to moderate |
| SM hyperplasia | Yes | Yes | Not characteristic |
| PCII | Hyperplasia | Hyperplasia, atypia | Hyperplasia in areas of inflammation |
| Bronchiolar epithelium | Bronchial metaplasia of alveolar epithelium | Bronchial metaplasia of alveolar epithelium | Not recorded |

### *1.2.8. Long-term outcome and prognostic indicators*

The clinical course, long-term outcomes and prognostic factors of CIPF were assessed by Lilja-Maula and collaborators (2014b) in a cohort of 15 WHWTs affected with CIPF and 10 healthy WHWTs. WHWTs affected with CIPF were prospectively followed every 3- to 6-months until death or study end-point, while the majority of the control WHWT were followed by phone calls to the owners. The causes of death were divided into CIPF-related (defined as euthanasia because of acute dyspnoea or severe progression of respiratory symptoms) or non-CIPF-related. They showed that CIPF has significant negative impact on life expectancy in WHWTs (Fig. 7). They found a survival time from onset of clinical signs in the CIPF-related death group ranging from 2 months to 4.3 years with a median of 2.7 years, indicating that CIPF in WHWTs may have a rapid or slow disease progression. No significant prognostic factors at diagnostic were identified among the chosen variables including arterial pO2, arterial pCO2, p(A-a)O2, serum endothelin-1 concentrations, severity of changes in thoracic X-rays and HRCT Hounsfield unit values. However, a slight indication of high arterial pO2 values having a protective effect on survival and high p(A-a)O2 being a risk factor were noted (statistical significance set at P=0.10 rather than P=0.05). A decline in arterial pO2 values between the first and the last measurement was noted in WHWTs that died of CIPF-related causes. However, in some dogs, temporary increases in arterial oxygenation were recorded, and some owners described a temporal improvement in clinical signs. Consequently, whether repeated measurements of arterial blood gas values over time may serve as a useful tool for evaluating disease progression requires further investigations.

Fig. 7: Kaplan-Meier survival curves for all-cause survival of WHWTs with CIPF (dotted line) and control WHWTs (solid line) from study inclusion. Censored animals (WHWTs alive at study endpoint) are presented as circles.
(Lilja-Maula et al., 2014b)

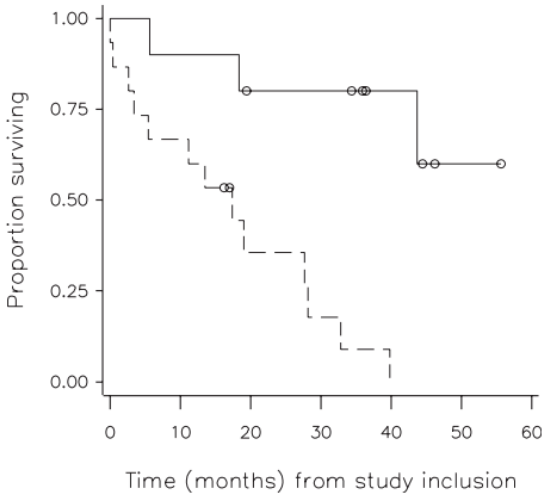


## 1.3. Understanding the pathogenesis

The pathogenic mechanisms behind CIPF are not yet understood. The strong predisposition of the WHWT breed to CIPF raises suspicion for a genetic background (Heikkila-Laurila and Rajamaki, 2014). However, other triggering events are probably involved in the course of the disease given that not all dogs from the WHWT breed develop the disease at an advanced age. CIPF probably results from a complex dialogue between genetic and environmental factors (Heikkila-Laurila and Rajamaki, 2014). Unfortunately, no epidemiologic studies have been performed until now and investigation of the genetic background has just started at the University of Helsinki. Nevertheless, several studies, briefly reported in the next sections, were conducted to provide clues on underlying fibrotic mechanisms while others researched the use of biomarkers to differentiate CIPF from other chronic lower respiratory diseases.

### *1.3.1. Surfactant protein C mutation*

In humans, mutations in the gene encoding surfactant protein-C was associated with rare family cases of pulmonary fibrosis (Devine and Garcia, 2012). In 2009, Eriksson and collaborators analysed by Western blots immunoreactivity the presence of surfactant proteins-B and –C in the BALF from 3 dogs affected with CIPF (2 WHWTs and 1 Tibetan terrier) and 5 controls of various breeds including 1 WHWT. In the Tibetan terrier CIPF dog, no surfactant protein-C was found in the BALF, although immunoreactivity for surfactant protein-B was detected. In the 2 WHWTs affected with CIPF and the 5 controls both surfactant proteins-B

and –C were detected in the BALF. Amplification and sequencing of the surfactant protein-C and its exon for 2 CIPF cases, including the Tibetan terrier, and for 1 control revealed no mutations that influence the expression of surfactant protein-C. Consequently, the absence of surfactant protein-C in the BALF of the Tibetan terrier remains unexplained and requires further investigations in a larger group of dogs with breed-matched controls.

### *1.3.2. Endothelin-1*

Endothelin-1 (ET-1), a vasoactive peptide with pro-inflammatory and pro-fibrotic properties, has been identified as a mediator of IPF in humans through its contribution in fibroblasts activation, proliferation and differentiation into myofibroblasts (Ross et al., 2010; Swigris and Brown, 2010). Higher concentrations of ET-1 have been detected in lung tissue, blood and BALF from people with IPF (Ross et al., 2010; Swigris and Brown, 2010). In 2011, Krafft and collaborators investigated whether concentrations of serum and BALF ET-1 would be higher in dogs affected with CIPF compared with healthy dogs and dogs affected with other chronic lower respiratory diseases, namely eosinophilic bronchopneumopathy (EBP) and chronic bronchitis (CB). They included 2 groups of control dogs (13 healthy WHWTs and 9 healthy experimental Beagle dogs) and 3 groups of dogs with chronic lower respiratory disease (12 dogs affected with CIPF including 11 WHWTs and 1 Scottish terrier, 10 dogs of various breeds affected with CB, and 6 dogs of various breeds affected with EBP). They found that serum ET-1 concentrations were significantly higher in dogs affected with CIPF compared with healthy Beagles, healthy WHWTs, dogs affected with EBP, and dogs affected with CB (Fig. 8A). BALF ET-1 concentrations were only measurable in dogs affected with CIPF, whereas they were below the kit detection limit in healthy WHWTs and in dogs affected with CB (Fig. 8B). Dogs in the CIPF group were all from the WHWT breed expect for one dog, a Scottish terrier, while dogs in the EBP and CB groups were from various breed but non-WHWT breeds. Therefore, differences observed between pathological groups were potentially due to a physiological breed variation. However, the absence of difference between healthy Beagles and healthy WHWTs suggested that this breed effect is null or minimal and that the differences observed between CIPF, EBP and CB are related to the disease process. Elevated ET-1 may potentially relate to the presence of PH. Indeed, in human IPF patients, higher plasma ET-1 concentrations were found to be associated with higher pulmonary arterial pressures (Ventetuolo et al., 2012). However, the study in dogs showed no difference in serum ET-1 concentrations between dogs affected with CIPF that had or did not have indirect signs of PH on echocardiography (right-sided cardiac hypertrophy, septal flattening or dilatation of pulmonary trunk), and highest serum ET-1 concentrations were found in dogs with normal

echocardiographic examination; both arguments that are not in favour of this hypothesis in dogs.

Fig. 8: Serum (A) and BALF (B) ET-1 concentration in dogs affected with CIPF, healthy WHWTs, healthy Beagles, dogs affected with EBP, and dogs affected with CB. Statistically significant differences: *P<0.0001, †P=0.001, ‡P=0.005
(Krafft et al., 2011)

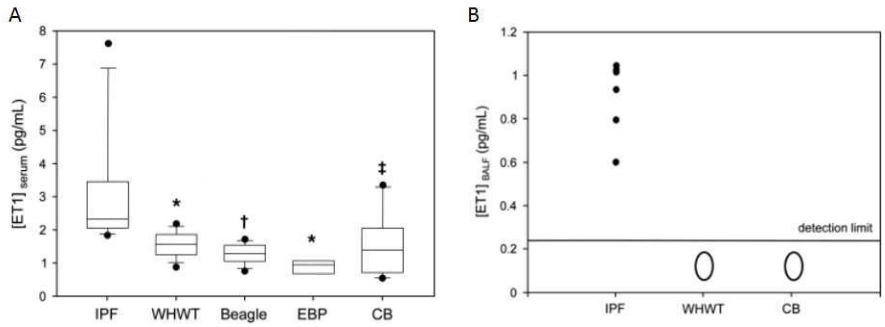


### *1.3.3. Procollagen type III amino terminal propeptide*

Procollagen type III amino terminal propeptide (PIIINP) is a marker of fibroblast activity and enhanced collagen type III turnover in humans. During synthesis of collagen type III, an amino terminal propeptide is cleaved from the procollagen molecule. This propeptide is then released into extracellular fluid and the circulation in proportion to the amount of collagen produced (Prockop et al., 1979). On histopathology of CIPF lungs, the extracellular matrix was shown to be composed of a mixture of type-I and –III collagens with type-III collagen being the most prominent type (Norris et al., 2005). Therefore, Heikkilä and collaborators (2012) decided to investigate by radioimmunoassay whether measurement of PIIINP in serum and BALF is useful in differentiation CIPF from other chronic lower respiratory diseases. Their study design was the same as in the above described study from Krafft and collaborators (2011). They did not found significant differences between groups for serum PIIINP concentrations (Fig. 9A). BALF PIINP concentrations were significantly higher in dogs affected with CIPF compared with healthy dogs and dogs affected with CB, but were also elevated in dogs affected with EBP (Fig. 9B). Those results demonstrated that measurement of PIIINP in BALF may provide a more accurate indication of lung disease compared with its measurement in the serum where PIINP concentrations are more likely influenced by processes unrelated to pulmonary pathology. However, the fact that BALF PIIINP concentrations were also increased in EBP indicated that this marker may lack specificity to indicate CIPF and can therefore not be used for diagnostic purposes. They attributed the elevation of BALF PIIINP concentrations in dogs affected with EBP to secondary fibrotic changes and active collagen type III synthesis caused by chronic and intense eosinophilic inflammation.

Fig. 9: Serum (A) and BALF (B) PIIINP concentrations in dogs affected with CIPF, CB and EBP and in healthy dogs. Values more than 1.5 times IQ are labelled as outliers and represented as dots. Statistically significant differences: *P<0.05, **P<0.01, ***P<0.001 (Heikkila et al., 2012)

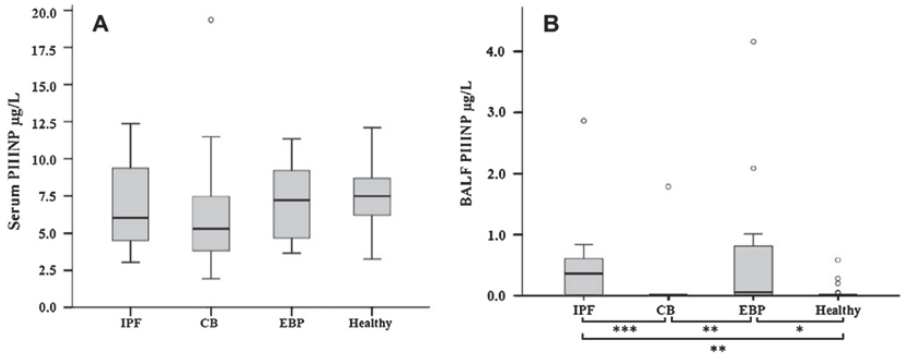


### *1.3.4. Proteomic analysis of bronchoalveolar lavage fluid*

Proteomics, defined as a large-scale characterisation of proteins expressed by a genome, can be used to identify biomarkers and reveal disease-specific mechanism. Lilja-Maula and collaborators (2013) employed 2-D differential gel electrophoresis and liquid chromatography-tandem mass spectrometry for proteomic analysis and protein identification to evaluate protein expression in BALF obtained from dogs affected with CIPF (n=6) and dogs affected with CB (n=5). They also compared those results with findings obtained from healthy control dogs (n=4) in order to identify potential biomarkers for CIPF. Unfortunately, the quantitative comparison of proteomes revealed similar changes for the dogs affected with CIPF and CB compared with healthy dogs, which suggests a common response to disease processes in different lung diseases. Upregulated proteins in dogs affected with CIPF or CB compared with healthy controls were complement C3, α-1-antitrypsin, apolipoprotein A-1, haptoglobin, transketolase and β-actin. Lysosyme C was identified as a downregulated protein in CIPF and CB dogs compared with controls. The study was limited by a small number of dogs and did not allow for specific biomarkers of CIPF to be identified. The upregulated proteins represent different aspects of cellular responses and interplay, allowing for the speculation that CIPF and CB share a variety of cellular changes and molecular pathways for their pathogenic processes.

### *1.3.5. Microarray analysis of pulmonary gene expression*

Tissue-wide gene expression analysis using microarrays is a powerful instrument to study disease pathways, with the help of bioinformatics tools that allow for the analysis of gene expression changes by grouping relevant genes into biological functions or by filtering genes encoding potential biomarkers (Thomas and Bonchev, 2010). In 2013, Krafft and collaborators examined pulmonary gene expression in CIPF by microarray analysis in an attempt to gain new

insights into the pathogenesis of the disease and found upregulated genes encoding proteins with biomarker potential. For this purpose, they extracted RNA from lung tissue samples of 12 dogs affected with CIPF (10 WHWTs, 1 Scottish terrier and 1 Lhasa-Apso) and 14 controls dogs of various breeds. Gene expression was analysed via hybridisation of the Affymetrix GeneChip Canine Genome 2.0 Array on pooled RNA aliquots (5 dogs from each group) to form 2 experimental sets (CIPF vs. healthy). Results were confirmed by quantitative reverse-transription polymerase chain reaction (qRT-PCR) for 10 genes selected on the basis of their fold changes in gene expression and their potential role in immunological processes and/or fibrosis and/or potential interest as biomarkers. RNA samples from all dogs included in the study were used for the qRT-PCR experiments. Results of the microarray study demonstrated that a total of 789 probes sets fulfilled the criteria for differential expression between lung tissues from the CIPF and controls groups. Those criteria were: (1) there must be at least a two-fold difference in expression of the gene between CIPF and control lung tissues, (2) the gene should be known to be expressed in the lungs, and (3) the corresponding protein should be detectable in the blood and/or in BALF. Among these 798 transcripts, 249 were up-regulated, whilst 549 were down-regulated (Table 4).

Table 4: Selected up- and down-regulated genes in CIPF vs. controls.
(Krafft et al., 2013)

| Probe identification | Gene symbol | Fold-change | Gene name |
|---|---|---|---|
| Cfa.16337.1.S1_s_at | CCL7 | 6.8 | Chemokine (C–C motif) ligand 7 |
| Cfa.16041.1.S1_at | ANKRD1 | 6.1 | Ankyrin repeat domain 1 |
| Cfa.3745.1.S1_s_at | HTR2B | 5.2 | 5-Hydroxytryptamine (serotonin) receptor 2B |
| CfaAffx.16581.1.S1_at | ELF3 | 5.1 | E74-like factor 3 (ets domain transcription factor, epithelial-specific) |
| CfaAffx.11223.1.S1_s_at | SLC1A2 | 5.0 | Solute carrier family 1 (glial high affinity glutamate transporter), member 2 |
| Cfa.3851.1.S1_s_at | CCL2 | 4.9 | Chemokine (C–C motif) ligand 2 |
| CfaAffx.16274.1.S1_at | FAP | 4.7 | Fibroblast activation protein, α |
| CfaAffx.29216.1.S1_at | HMGB3 | 4.5 | High-mobility group box 3 |
| Cfa.3173.2.A1_at | SAA1 | 4.4 | Serum amyloid A1 |
| Cfa.3510.1.S1_s_at | IL8 | 4.3 | Interleukin 8 |
| CfaAffx.19822.1.S1_at | MUC20 | 4.3 | Mucin 20, cell surface associated |
| Cfa.15713.1.A1_s_at | MARCO | 4.0 | Macrophage receptor with collagenous structure |
| CfaAffx.23602.1.S1_s_at | GLDN | 3.9 | Gliomedin |
| CfaAffx.2003.1.S1_at | TRHR | 3.9 | Thyrotropin-releasing hormone receptor |
| CfaAffx.15427.1.S1_at | PRMT3 | 3.8 | Protein arginine methyltransferase 3 |
| CfaAffx.1882.1.S1_s_at | HSP70 | 3.8 | Heat shock protein 70 |
| CfaAffx.6312.1.S1_at | LOC612714 | 3.7 | Similar to Complement C5 precursor |
| CfaAffx.19116.1.S1_at | ANXA9 | 3.7 | Annexin A9 |
| Cfa.12375.1.A1_at | FKBP5 | 3.6 | FK506 binding protein 5 |
| Cfa.7839.1.S1_at | KRT8 | 3.6 | Keratin 8 |
| Cfa.21149.1.S1_at | CXCL14 | 3.4 | Chemokine (C–X–C motif) ligand 14 |
| CfaAffx.360.1.S1_s_at | ADAMDEC1 | 3.3 | ADAM-like, decysin 1 |
| CfaAffx.28187.1.S1_at | ITGA2 | 3.2 | Integrin, α 2 (CD49B, α 2 subunit of VLA-2 receptor) |
| CfaAffx.23498.1.S1_at | FGFBP1 | 3.0 | Fibroblast growth factor binding protein 1 |
| Cfa.182.1.S2_at | DLA-DQA1 | 2.7 | Major histocompatibility complex, class II, DQ α 1 |
| CfaAffx.6329.1.S1_s_at | C5 | 2.6 | Complement component 5 |
| Cfa.280.1.S1_at | dla88 | −462.4 | MHC class I DLA-88 |
| CfaAffx.11921.1.S1_s_at | PLUNC | −25.0 | Palate, lung and nasal epithelium associated |
| CfaAffx.23201.1.S1_at | MMP7 | −17.6 | Matrix metallopeptidase 7 (matrilysin, uterine) |
| Cfa.6128.1.A1_at | SLPI | −13.7 | Secretory leukocyte peptidase inhibitor |
| Cfa.19619.1.A1_at | FBN2 | −11.3 | Fibrillin 2 |
| Cfa.21324.1.S1_at | PIP | −8.1 | Prolactin-induced protein |
| CfaAffx.26848.1.S1_at | MYH2 | −5.2 | Myosin, heavy chain 2, skeletal muscle, adult |
| Cfa.1262.1.S2_at | COL1A2 | −3.3 | Collagen, type I, α 2 |
| Cfa.100.1.S1_at | COL1A1 | −2.2 | Collagen, type I, α1 |
| Cfa.6009.2.A1_at | FBLN1 | −2.0 | Fibulin 1 |

The significant biological functions associated with these genes were related to cellular growth and proliferation, developmental processes, cellular movements, cell to cell signalling and interaction, and antigen presentation. Altered levels of expression were confirmed by qRT-

PCR for genes encoding CCL2, CCL7, CXCL8, CXCL14, fibroblast activation protein, and the palate, lung and nasal associated protein, identifying them as possible diagnostic or prognostic biomarkers. Because the study was limited by the fact that control dogs were not age- and breed-matched with the CIPF group part of the differences observed between groups may result from age or breed effects.

### *1.3.6. TGF-beta 1*

In human IPF, transforming growth factor beta 1 (TGF-β1) is considered as a key profibrotic agent in the pathogenesis of the disease (Coward et al., 2010). In dogs, 2 complementary studies were published in 2014 to investigate how this molecule may also be involved in CIPF. The first one, published by Lilja-Maula and collaborators (2014a), aimed to investigate the expression of known extracellular matrix protein regulators of TGF-β1 storage and activation, namely the latent TGF-β binding protein-1 (LTBP-1) and fibrillin-2, and of phosphorylated signalling protein Smad2 (P-Smad2) in lung tissue sections from WHWTs affected with CIPF (n=14), control WHWTs (n=3), humans with UIP (n=5), and humans with NSIP (n=6), using immunohistochemistry (Lilja-Maula et al., 2014a). They found that P-Smad2 immunoreactivity, an indicator of TGF-β signalling activity, was increased in WHWTs affected with CIPF in comparison with control WHWTs and localised predominantly in the altered alveolar epithelium, as seen in both UIP and NSIP. This suggested an enhanced TGF-β signalling in CIPF as part of the pathophysiological mechanisms of the disease and pointed out the central role of the alveolar epithelium in the fibrogenic mechanisms. LTBP-1 and fibrillin-2 immunolabelling were localised to bronchial epithelial cells and smooth muscle cells of the bronchiolar and vascular walls, as well as in the altered alveolar epithelium in both CIPF and control WHWTs. A significant increase in LTBP-1 immunoreactivity in WHWTs affected with CIPF compared with controls was noted for peribronchial and perivascular areas, while there was no difference in expression of alveolar LTBP-1 and fibrillin-2 immunoreactivity between groups. The authors attributed this lack of significant difference to the small number of dogs included. Despite this, they concluded that the presence of those extracellular matrix proteins in the lungs of WHWTs affected with CIPF may potentially participate in the pathogenesis of the disease by contributing to the storage and activation of TGF-β1. The second study assessing TGF-β1 in CIPF was published by Krafft and collaborators (2014a) and aimed to evaluate TGF-β1 biochemical pathways in healthy dogs and dogs with CIPF. For this purpose, they employed immunohistochemistry to evaluate expression and localisation of TGF-β1 protein and proteins involved in TGF-β1 signalling (TGF-β receptor type I and P-Smad2/3). Additionally, qRT-PCR was used to measure expression of TGF-β1 and molecules involved in its storage (LTBP-1, -2 and -4), activation (αvβ6 and αvβ8 integrins, thrombospondin-1) and signal inhibition (Smad7).

Circulating TGF-β1 concentrations were measured by enzyme-linked immunosorbent assay (ELISA) in WHWTs affected with CIPF and control WHWTs, in addition to healthy dogs from other breeds variably predisposed to the disease. By immunohistochemistry, high levels of TGF-β1 protein were found in areas of fibrosis in CIPF lungs, while there was only a trend toward increase gene expression of TGF-β1 compared with controls. Altered alveolar epithelial cells displayed strong intracellular expression of TGF-β receptor type I and intra-nuclear expression of P-Smad2/3, suggesting enhanced TGF-β1 signalling at the level of activated alveolar epithelial cells, such as proposed by Lilja-Maula (2014a). Gene expression was decreased for LTBP-4 and αvβ8 integrin, and increased for thrombospondin-1, while no difference was observed for Smad7, LTBP-1 and LTBP-2. Therefore, results suggested that part of the activating, storage and signalling pathways of TGF-β1 are modified in WHWTs affected with CIPF and may play a role in the pathophysiology of the disease. This study showed no difference in serum TGF-β1 concentration between WHWTs affected with CIPF and control WHWTs. However, serum TGF-β1 concentrations were higher in predisposed compared with non-predisposed breeds (Fig. 10), which suggests a potential cause-effect relationship between high circulating TGF-β1 and subsequent development of CIPF.

Fig. 10: Serum TGF-β1 concentrations measured by ELISA in healthy dogs from breeds with variable predisposition for CIPF, including the highly predisposed WHWT (n=13), 2 breeds reported to be mildly predisposed: the Scottish terrier (ST, n=12) and the Bichon Frisé (B, n=13), and 3 breeds considered to be non-predisposed: the Whippet (W, n=10), the Belgian shepherd (BS, n=10) and the Labrador (L, n=8).
(Krafft et al., 2014a)

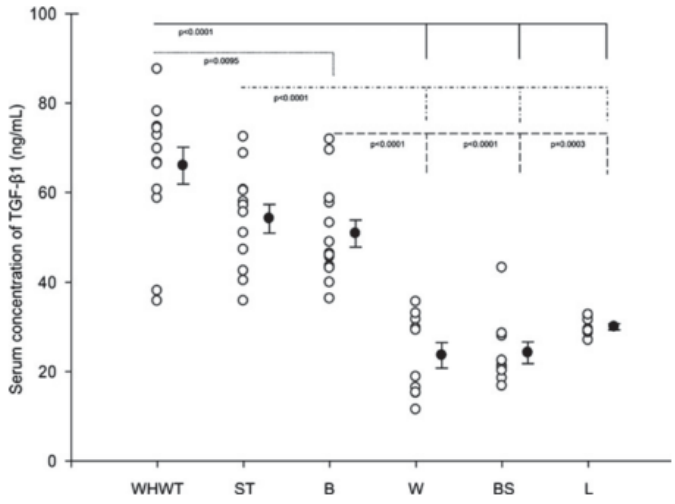


### *1.3.7. Activin A and B*

Activins are cytokines belonging to the TGF-β superfamily and have been shown to be involved in a variety of inflammatory, repair and fibrotic processes (Mayer et al., 2012). Activin

A has been suggested to participate in the pathophysiology of human IPF by promoting proliferation of airway smooth muscle cells and lung fibroblasts, but studies on the role of activin B are sparse (Matsuse et al., 1996). In 2015, Lilja-Maula and collaborators investigated, by immunohistochemistry, activins A and B expression in normal canine lung tissue (n=8), lung tissue from WHWTs affected with CIPF with or without concurrent histopathological signs of diffuse alveolar damage (DAD) (n=4 and n=6 respectively), and lung tissue from dogs with acute respiratory distress syndrome (ARDS) (n=4). Western blot analysis of activin B from BALF from WHWTs affected with CIPF (n=5) and healthy WHWTs (n=3) was also evaluated. In the lungs from both WHWTs affected with CIPF and dogs with ARDS, activin B was strongly expressed in the altered alveolar epithelium and in bronchial epithelial cells. In controls, intense activin B immunoreactivity was only observed in the bronchial epithelium, while the alveolar surface remained negative, suggesting that the cellular origin of activin B in the normal canine lung tissue is the bronchial epithelium. Activin A, in contrast, was not significantly expressed by canine lung tissue in either normal or disease state. Activin B was detected in the BALF of WHWTs affected with CIPF, most notably in samples from WHWTs with concurrent DAD, but not in healthy WHWTs. Based on the results, activin B was suggested to play a role in fibrosis and in pathological alteration of the alveolar epithelium.

### *1.3.8. Serotonin*

Serotonin, or 5-hydroxytryptamine (5-HT), exhibits several regulatory functions in multiple physiological systems, including the neurological, cardiac and hepatic systems (Fidalgo et al., 2013; Frishman and Grewall, 2000). In human IPF, a marked upregulation of the expression of serotonin receptors 5-HTR1A/B and 5-HTR2A/B and a dramatic downregulation of the serotonin transporter (5-HTT) were observed, suggesting a role of the 5-HT signalling in lung fibrosis (Konigshoff et al., 2010). In dogs, preliminary results about the potential implication of the serotonin pathway in CIPF were presented at the 17th ICLAF colloquium (2014b) by Krafft and collaborators. They investigated the expression of genes involved in 5-HT signalling (5-HTR2A, 5-HTR2B, and 5-HTT) by qRT-PCR after RNA extraction from affected (n=14) and control (n=11) lung tissues. They also measured circulating 5-HT levels by ELISA in sera from affected WHWT (n=14) and healthy WHWT (n=18). They found that the expression of 5-HTR2A and 5-HTR2B was not statistically different between CIPF and control lung tissues, while the expression of 5HTT was significantly decreased in dogs with CIPF compared with controls, which partially confirmed observations made in human medicine. They also observed that serum 5-HT concentrations in WHWTs affected with CIPF were significantly lower compared with healthy WHWTs. Since 5-HTT has been shown to participate in the uptake and clearance of the serotonin from the lung, it may be suggested

that the downregulation of 5-HTT observed in CIPF lungs leads to increased 5-HT levels in lung tissue, potentially contributing to the fibrogenesis. Such speculations require further investigations to conclude to an involvement of the serotonin pathway in CIPF.

## 1.4. Unexplored fields

### *1.4.1. Prevalence rate*

The prevalence rate of CIPF is currently unknown and difficult to estimate. Reasons for this reside in the incapacity to properly estimate the exact number of WHWTs affected with CIPF given the diagnostic constraints associated with the disease, and to the impossibility to determine the size of the general WHWT population in a given area due to the absence of inventory database. Early recognition of CIPF in a dog may be difficult for owners because the slow progressive clinical signs may be confused with physiological expressions of aging. Additionally, some veterinarians are not familiar with CIPF in dogs and may miss the diagnosis by interpreting the presence of pulmonary crackles as congestive heart failure rather than CIPF. Besides, the diagnosis of CIPF requires a thorough examination including T-HRCT, and finally relies on histopathological examination of pulmonary tissue. T-HRCT is not routinely available in clinical practice and pulmonary biopsies are not currently performed due anaesthetic considerations and concomitant risk of complications. The definitive diagnosis may not be obtained until death, and only when owners consent to necropsy. Furthermore, histopathological examinations of CIPF-suspected lungs are not always conclusive, probably due to the fact that the localized information obtained from biopsies does not necessarily reflect the phenomenon ongoing as a whole, particularly in the case of a heterogeneous disease such as CIPF.

### *1.4.2. Genetic background*

As explained above, the strong predisposition of the WHWT breed to CIPF raises suspicion for a genetic background (Heikkila-Laurila and Rajamaki, 2014). A genome-wide association study was recently initiated at the University of Helsinki to explore this field in both a global and targeted approach based on the discoveries made in human IPF (e.g. genes associated with telomere length, with alveolar stability, and with immunity and inflammation) (Zhou and Wang, 2016). However, obtaining a sufficient number of unaffected WHWTs matched for the age with the CIPF population is extremely difficult, because it is not certain that healthy WHWTs at the time of blood sampling will remain free of the disease in subsequent following years. To date, no significant results have been published from these ongoing genetic studies, and the recruitment of well-phenotyped CIPF and control WHWTs is still in progress

to increase the number of dogs in the analysis. In humans, IPF may be sporadic or familial. The familial pulmonary fibrosis accounts for up to 20% of all cases and is clinically and histopathologically indistinguishable from sporadic IPF expect that the age of onset tend to be earlier (Wallis and Spinks, 2015; Zhou and Wang, 2016). In dogs, the potential familial component of the disease is presently investigated at the University of Helsinki through detailed analysis of pedigrees, but no communication has already been done about this subject. As the disease was never described before 1999, a spontaneous mutation in a common ancestor intensively used in breeding programs could potentially explain the spreading of the disease over the past years. However, this hypothesis need to be confirmed and is balanced by the fact that CIPF cases are described in several continent (USA, Europe and recently in Asia – Japan).

### *1.4.3. Etiologic agents*

To date, no etiologic agent has been investigated in CIPF. In human IPF, predisposing factors such as environmental exposures, cigarette smoking, gastroesophageal reflux and chronic viral infections have been speculated as potential risk factors for IPF development (Raghu et al., 2011). Chronic exposure to avian proteins, chemicals, or even spores of macroscopic fungi have been related to the development of chronic hypersensitivity pneumonitis, a major differential diagnosis for IPF in humans (Lacasse Y et al., 2012). Whether those risk factors or others are involved in CIPF is presently unknown and merits considerations as dietary habits, grooming or special care dedicated to the WHWTs may predispose this breed for the disease. Considerations about the respiratory health of the CIPF dog's owners has neither been investigated to date but could represent an interesting alternative to study the epidemiologic aspects of CIPF given that both the dog and its owner share the same environment. It is also important to note that some etiologic agents cause damage years before CIPF is eventually diagnosed. Thus, correlating potential etiological agents with CIPF is a challenging endeavour.

### *1.4.4. Treatments*

At the present time, no effective treatments for CIPF have been described and no clinical trials have been performed. The current therapy specifically aims at reducing clinical signs on an individual basis, and alleviating possible complications that can develop during the course of the disease, such as pulmonary arterial hypertension (Heikkila-Laurila and Rajamaki, 2014). Oral or inhaled corticosteroids seem to relieve cough in many dogs, particularly in the presence of concurrent bronchial changes (Corcoran et al., 1999b; Heikkila-Laurila and Rajamaki, 2014). Antitussives can be used if cough is irritating. Bronchodilators, such as theophylline may be used to promote bronchodilation, enhance mucociliary clearance, and increase the contractility

of the diaphragm muscle. When concomitant pulmonary hypertension is present, treatment with sildenafil may be indicated. Although evidence regarding sildenafil benefit in dogs with pre-capillary PH is limited to few small retrospective studies, improvement of clinical signs and a decrease in PAP after treatment has been reported (Bach et al., 2006; Kellihan et al., 2015; Kellum and Stepien, 2007).

### *1.4.5. Follow-up tools*

As explained above, CIPF in WHWTs may have a rapid or slow disease progression (Lilja-Maula et al., 2014b) and some dogs can experience acute worsening of their respiratory function during the course of the disease (Heikkila-Laurila and Rajamaki, 2014). Response to specific anti-fibrotic treatment has not yet been investigated in WHWTs affected with CIPF. Moreover, accurate tools allowing the monitoring of CIPF progression and, consequently, treatment efficacy have not been described to date. Arterial blood gas analysis and the 6MWT can be used for the evaluation of lung function in WHWTs affected with CIPF, but these tests seemingly lack sensitivity (Lilja-Maula et al., 2014b). Therefore, surrogate markers of fibrosis that could help in the quantification of disease severity and progression are needed.

## 2. Pulmonary fibrosis in other animal species

Pulmonary fibrosis has been specifically described in donkeys, horses and cats and will be briefly developed in the present section. Note that progressive pneumonia leading *in fine* to a certain degree of fibrosis have also been described in sheep and cattle. In sheep, a lentivirus infection causing a disease called Maedi-visna or ovine progressive pneumonia has been shown to cause respiratory failure in susceptible individuals (Straub, 2004; Larruskain and Jugo, 2013). In cattle, causes of chronic interstitial pneumonia are wide and range from parasitic (e.g. *Dictyocaulus viviparous*), viral (e.g. bovine respiratory syncytial virus, parainfluenza-3 virus) and bacterial (e.g. *Mannheimia haemolyticia*, *Pasteurella multocida*) to toxic (e.g. L-tryptophan in lush pasture grasses, perilla mint, moldy potatoes) (Kerr and Linnabary, 1989). Hypersensitivity pneumonitis secondary to chronic exposure to insecticides, dead ascarid larvae, or dust from moldy hay containing spores of *Micropolyspora faeni* have also been described (Pearson, 1984).

### 2.1. Pleuropulmonary fibrosis and elastosis in donkeys

Pulmonary fibrosis in donkeys is a relatively common finding within the lungs of elderly donkeys, reported to occur at a prevalence of 35% in necropsies in a UK cohort (Morrow et al., 2011). Clinical data have not been described so far and solely one recent study made by Miele and collaborators (2014) aimed at determining the similarities between pulmonary fibrosis in donkeys and recognized patterns of human pulmonary fibrosis. For this purpose, they collected whole lungs from 32 aged donkeys during routine necropsy. Nineteen of the lungs were selected because of grossly visible fibrosis, whereas 13 grossly unaffected control lungs were selected at random. Eighteen whole inflated ex vivo lungs (11 with fibrosis and 7 controls) were imaged by HRCT, and 8 lung samples (4 with fibrosis and 4 controls) served for herpesvirus PCR after DNA extraction. Among the 19 fibrotic lungs included, 10 were categorized as being pleuroparenchymal fibroelastosis (PPFE)-like based on imaging and histopathological findings. Gross examination revealed visceral pleural fibrosis on the dorsal/costal surface with no involvement of the parietal pleura. On histopathology, the fibrosis was located dorsal and subpleural with evidence of subpleural intra-alveolar fibrosis and elastosis (Fig. 11).

Spatial heterogeneity was a consistent feature, often with a sharp interface between fibrotic and adjacent normal tissue. Other common features included septal and bronchiolocentric fibrosis, lymphoplasmacytic bronchiolitis, granulomatous inflammation, and vascular remodelling within areas of fibrosis. Honeycombing and fibroblastic foci were not detected, although myofibroblasts were demonstrated within fibrotic lesions through α-smooth muscle actin immunohistochemistry. The remaining 9 fibrotic lungs included were classified

as inconsistent with PPFE on histology because of the lack of intra-alveolar fibrosis. However, seven of those had intra-alveolar mononuclear infiltrates with organizing intra-alveolar fibrin, which likely precludes intra-alveolar fibrosis and may consequently represent an earlier stage of PPFE-like disease.

Fig. 11: Lung sections from donkey lungs with a PPFE-like condition. (A) Pleural and subpleural fibrosis with alveolar septal elastosis and intra-alveolar fibrosis. Elastic Van Gieson (EVG) staining. (B) Spatial heterogeneity. EVG staining.
(Miele et al., 2014)

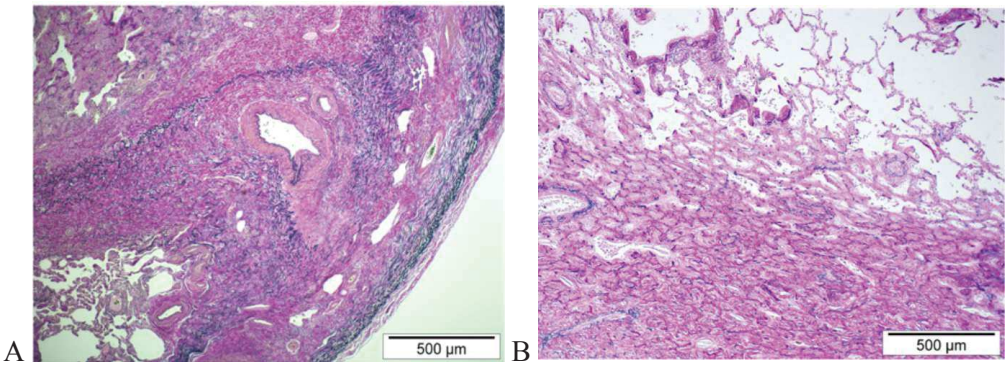


Seven PPFE-like lungs were imaged by HRCT, revealing pleuroparenchymal thickening of the dorsal lung lobes and associated subpleural consolidation consistent with established fibrosis. The consolidation extended from the subpleural region along parenchymal bands into mid and ventral zones that often radiated out to surround adjacent bronchi (Fig. 12). Traction bronchiectasis and ground glass opacity were present to varying degrees in all 7 and 4 cases respectively.

Fig. 12: Craniocaudal HRCT image of PPFE-like inflated ex vivo donkey lung. Note the thickened rinds of pleural fibrosis encasing the dorsal surface of the lung, with traction bronchiectasis (large arrow) and bronchocentric fibrosis (small arrow).
(Miele et al., 2014)

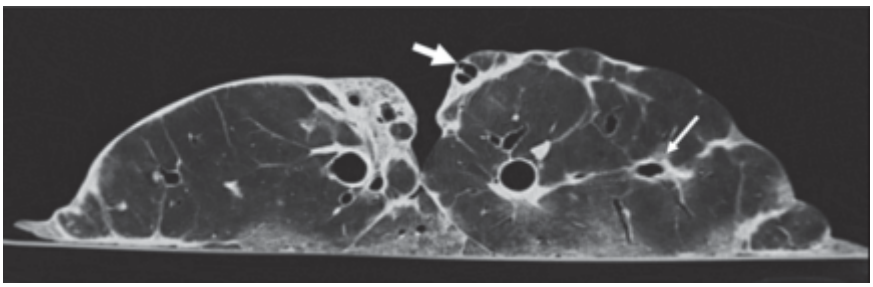

Herpesviral sequences were identified in six of eight lung homogenates, with five mapping to asinine herpesvirus (AHV)-5 and one to AHV-4. Those two gammaherpesviruses were discovered in 2002 by Kleiboeker and collaborators in lung tissues (n=17) from donkeys in which the histopathology was characterised by interstitial pneumonia and marked syncytial

cell formation. In their study, Kleiboeker and collaborators also included lung tissues from 6 control donkeys which were all negative for the viruses, which lead them to conclude to an association between gammaherpesvirus and interstitial pneumonia in donkeys. However, the ubiquitous presence of gammaherpesvirus in lungs from both control and PPFE-like affected donkeys in the study of Miele and collaborators (2014) discords with previous results and warrants further investigation regarding the potential role of herpesvirus in the aetiology of pulmonary fibrosis in donkeys.

## 2.2. Equine multinodular pulmonary fibrosis

The first description of the gross pathology, histopathology and virology findings of 24 horses with equine multinodular pulmonary fibrosis (EMPF) was provided by Williams and collaborators in 2007. All horses included in their study underwent euthanasia after a period of severe respiratory disease that did not respond to therapy, but the exact clinical presentation and duration of symptoms were not reported in the study. On gross examination, numerous coalescing pale and moderately firm nodules of diameters ranging from <1 to 5cm were observed interposed with normal unaffected lung. On histopathology, the lung lesions were largely confined to the alveolar parenchyma. Nodules were sharply demarcated from adjacent less affected lung and consisted of marked interstitial expansion of well-organised mature collagen. The interstitium was infiltrated by variable numbers of mixed inflammatory cells, consisting primarily of lymphocytes, with smaller numbers of macrophages and neutrophils. There was a preservation of an “alveolar-like” architecture, with the lumen of the spaces lines by cuboidal cells (Fig. 13).

Fig. 13: Lung sections from horses lungs with EMPF. (A) Discrete border between the foci of interstitial fibrosis and the relatively unaffected lung (arrow). HE. Bar = 200µm. (B) Higher magnification of interstitial fibrosis with inflammatory cells, primarily neutrophils and macrophages, within lumen of the airspaces. HE. Bar = 50µm.
(Williams et al., 2007)

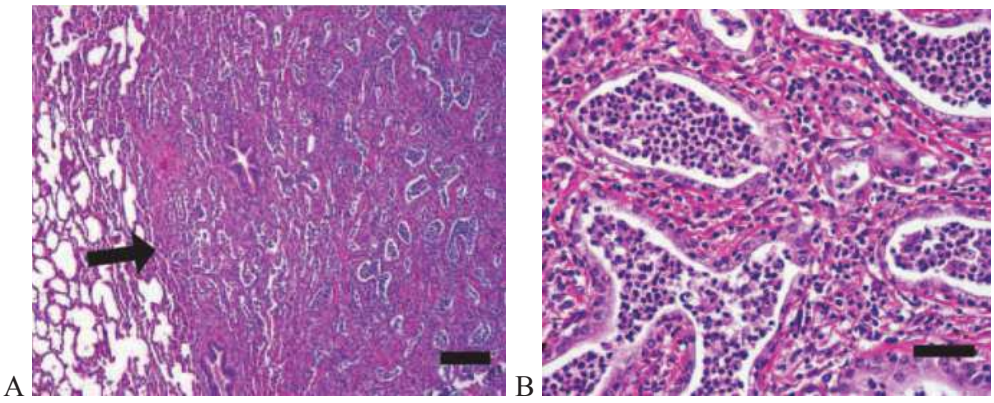

All of the affected horses were positive for equine herpesvirus 5 (EHV-5) and 8/24 (33%) for EHV-2, while EHV-5 and EHV-2 were found in 0 and 1, respectively, in the 23 control horses included. EHV-5 and EHV-2 were isolated from 2 and 1/7 EMPF horses, respectively. In addition, in situ hybridization demonstrated viral genome within the pulmonary lesions but not in adjacent unaffected lung or within the lungs of control horses. Those findings were the first to suggest an association between fibrotic lung disease and viral infection with EHV-5 in veterinary medicine. Since then, several case reports have been published confirming the association of EHV-5 and EMPF (the virus being consistently amplified from lung of affected horses), and describing the clinical symptoms of the disease. The clinical signs includes tachypnea, coughing, lethargy, weight loss, low-grade fever and nodular interstitial pattern on thoracic radiographs (Back et al., 2012; Dunowska et al., 2014; Marenzoni et al., 2011; Niedermaier et al., 2010; Soare et al., 2011; Spelta et al., 2013). Treatments with corticosteroids and/or anti-viral drugs does not improve the clinical signs and euthanasia is generally performed within weeks following the first apparition of the symptoms (Dunowska et al., 2014; Marenzoni et al., 2011; Spelta et al., 2013). Recently, a study was published to address to ability of EHV-5 to experimentally induce EMPF in normal horses. For this purpose, isolates of EHV-5 obtained from spontaneous cases of EMPF were inoculated into the accessory lung lobe of 6 normal old horses. Two horses were used as sham-inoculated control animals. After inoculation, none of the experimentally infected horses exhibited clinical signs of disease that could be associated with a viral infection. Viruses were not isolated from any blood sample obtained during the study. A modest rise in neutralizing antibody titer was observed trough day 49 post-inoculation in all EHV-5 inoculated horses, indicating infection with EHV-5 had occurred. Horses were euthanized between 98 and 108 days port virus inoculation. On gross pathology, lesions were found in 3/6 experimentally inoculated horses and shared similarities to horses naturally affected with spontaneous EMPF. On histopathology, multiple nodules of fibrosis with the alveolar parenchyma were observed in 5/6 EHV-5 inoculated horses, with the severity of the histologic lesions varying with the length of time that had lapsed between infection and euthanasia. Myofibroblasts, characterized by a positive α-smooth muscle actin immunolabelling, were detected within the alveolar walls of all experimentally infected horses, but not in controls. Virus was not isolated nor detected from any tissues collected post-mortem from the control or experimentally inoculated horses. However, using immunohistochemistry, EHV-5 antigen was observed widely within the lungs of infected horses, including in bronchiolar airway epithelial cells, macrophages, and interstitial fibroblasts. Because of the difficulty to detect EHV-5 by PCR or reisolate the virus in inoculated horses, the authors hypothesized that the antigens detected by immunohistochemistry represent latency-associated proteins expressed by latent virus, and that this latent virus is driving the resultant lung fibrosis. They concluded that EHV-5-induced lung fibrosis can occur, and may begin, during viral

latency, without additional known stimuli. They also hypothesized that the clinical form of the disease displayed spontaneously affected EMPF horses correspond to a transition into a lytic productive infection coincident with progression of the disease.

## 2.3. Pulmonary fibrosis in cats

Pulmonary fibrosis in cats is a rare and poorly described clinical condition. Indeed, only few reports have been published about this pathological entity and mainly aimed at describing the clinical presentation, the radiographic characterisation, and the histopathological findings. The first two studies were published by the same team in 2004 and described the clinical and pathologic features of pulmonary fibrosis in a cohort of 23 cats (Cohn et al., 2004; Williams et al., 2004). No obvious sex or breed predilection was noted and most cats were middle aged or older with a median age of 8.3 years. The major clinical signs were laboured or rapid respiration (n=18) and cough (n=13). The duration of signs before clinical presentation was short, and even for cats with longer histories there was a recent exacerbation of symptoms. Signs not specifically referable to the respiratory tract (e.g., lethargy and anorexia) were common, of short duration, and most often noted in the cats with severe respiratory distress. Thoracic auscultation was abnormal in all but 2 cats examined, with wheezes described as commonly as crackles. All cats had abnormal thoracic radiographs with alveolar, bronchiolar, and interstitial patterns being described in nearly equal numbers of cats and often in combination. The distribution of the lung infiltrates was usually patchy or diffuse. Radiographic evidence of bronchial disease was common, which suggested the concurrence of bronchial disease in some of the cats. No consistent hematologic or biochemical alterations were detected. On BALF analysis, inflammation was an inconsistent finding and, when noted, was mild with no evidence of causation. Culture of lavage fluid was usually negative. Although the risks inherent to airway lavage are generally considered minimal, 4 of the 7 cats that underwent bronchoscopic evaluation deteriorated afterwards and died or were euthanized within 24h. Only 7 cats survived for more than 1 year after the first respiratory signs became and the remaining cats died or were euthanized within weeks of the initial onset of symptoms. Histological changes of the lungs included interstitial fibrosis in a subpleural and temporal heterogeneity distribution with fibroblast and myofibroblast foci, honeycomb formation with abundant metaplasia of the alveolar epithelium, and interstitial smooth muscle metaplasia and hyperplasia (Fig. 14).

Concurrent pulmonary neoplasia (generally in areas of marked fibrosis) was noticed in 6 of 23 cats. The neoplastic foci were limited in extent, whereas the histologic changes compatible with fibrosis were widely distributed.

Fig. 14: Lung sections from a cat with an IPF-like condition. (A) Low magnification of feline IPF showing heterogeneity of the lesions. The lung remodelling is patchy, with adjacent affected and unaffected areas present. HE. Bar = 200µm. (B) Honeycomb epithelial metaplasia in feline IPF. Note the enlarged airspaces lined by cuboidal to columnar epithelial cells with intervening interstitial fibrosis. HE. Bar = 50µm.
(Williams et al., 2004)

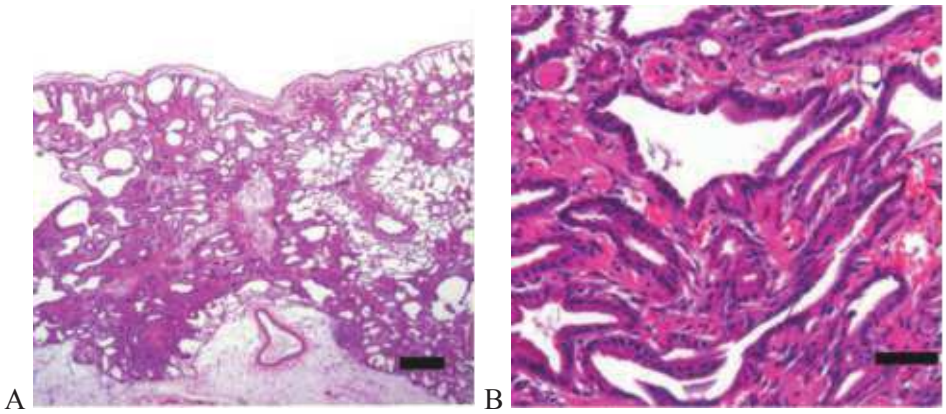

A B

A more recent work about pulmonary fibrosis in cats was published in 2014 by Evola and collaborators in a cohort of 9 cats. They confirmed results previously obtained by Cohn and collaborators (2004). Cats included in their study had a median age at diagnosis of 13 years and a survival time from diagnosis ranging from 1 to 226 days with a median of 15 days. Radiographic findings were highly variable between cats, with 2 cats having focal soft tissue masses seen on radiographs and confirmed on thoracic CT-scan images. Echocardiography was performed in 3 cats and revealed indirect signs of pulmonary arterial hypertension in all of them. On histopathology, all cats were showing type II pneumocytes hyperplasia and smooth muscle hypertrophy/hyperplasia. Histiocytic interstitial pneumonia was seen in 8 cats and all of these had either diffuse or multifocal lesions. Increased foamy or epithelioid macrophages within alveoli and terminal bronchioles were also observed in most section of lung examined, both features which indicates a more pronounced inflammation of the lungs in comparison with previous reports of feline pulmonary fibrosis made by Cohn and collaborators (2004).

## 3. Idiopathic pulmonary fibrosis in humans

Idiopathic pulmonary fibrosis (IPF) is a chronic and progressive lung disorder characterized by the aberrant and excessive deposition of extracellular matrix leading to extensive lung remodelling and obliteration of functional alveolar units, resulting in respiratory failure (Datta et al., 2011; Sgalla et al., 2015). It accounts for approximately 20% of all cases of interstitial lung disease (ILD) (Sgalla et al., 2015). ILD encompass a large heterogeneous group of diseases with a wide range of aetiologies, and a variety of tissue reactions within the lung (Popper, 2013) (Fig. 15, next page). These different entities are associated with varying prognoses and clinical behaviours (Wallis and Spinks, 2015). Among the ILDs, idiopathic NSIP and chronic hypersensitivity pneumonitis (HP) are the two main differential diagnosis of IPF (Neurohr and Behr, 2015) and will be further discussed in the next section.

The number of publications about IPF has been increasing for several years (Fig. 16). The exact causes and the underlying pathophysiology behind this disease remain largely unknown and no curative treatments other than transplant have still been discovered. The two new medications approved for IPF – nintedanib and pirfenidone – appear modestly effective in slowing loss of lung function in some patients, letting the field open for further research.

Fig. 16: Numbers of publications listed per year with the search [Idiopathic pulmonary fibrosis] in MEDLINE (PubMed) database.

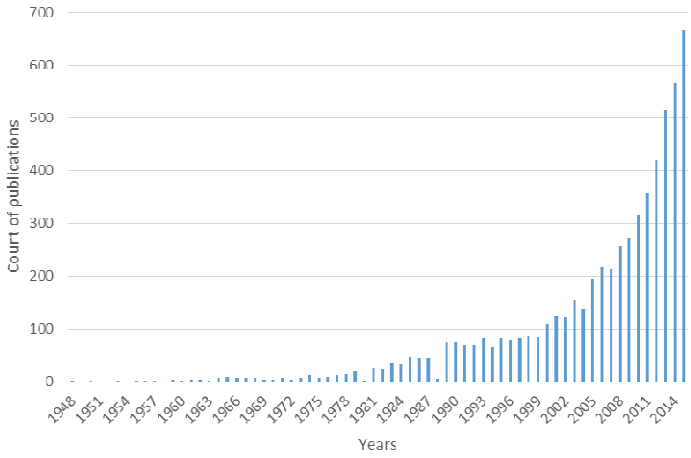


The diagnostic approach of IPF and the understanding of the underlying pathogenesis have greatly evolved over time, notably due to the introduction of novel imaging and molecular techniques. This section will focus on the most recently updated information regarding this disease.

Fig. 15: Classification algorithm for ILD adapted from (Antoniou et al., 2014; Neurohr and Behr, 2015; Popper, 2013; Sverzellati et al., 2015; Wallis and Spinks, 2015)

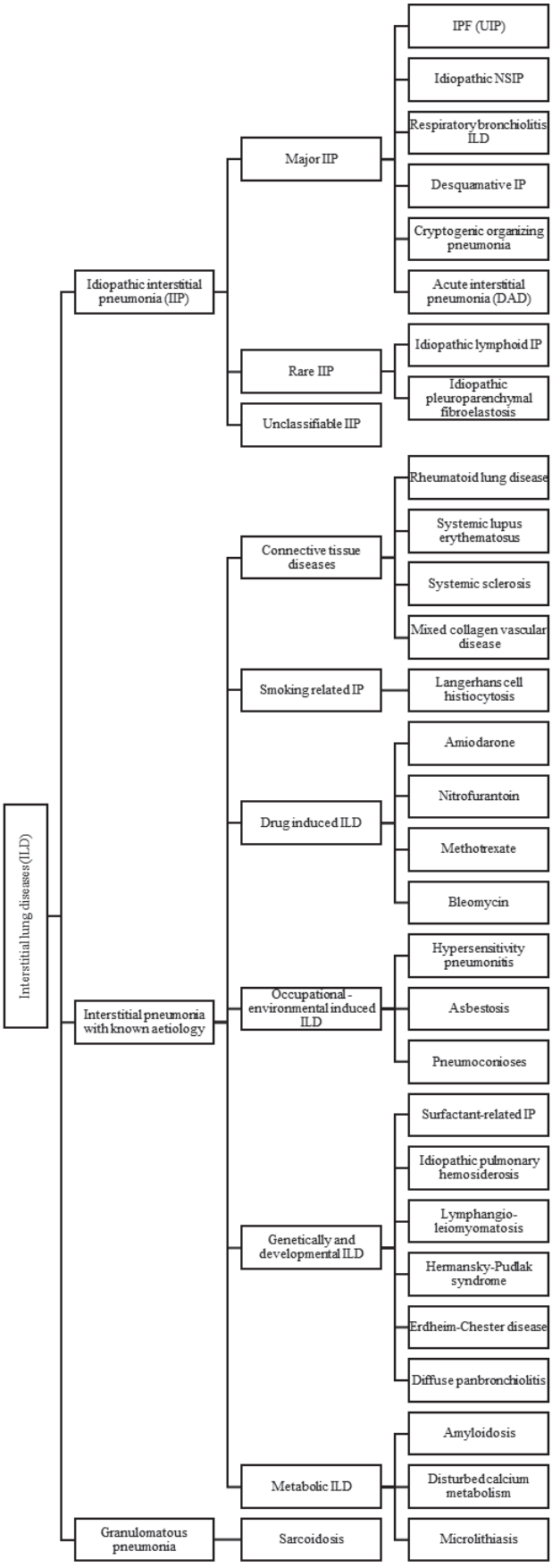

## 3.1. Incidence and prevalence rates

The true incidence and prevalence rates of IPF are difficult to establish. Caminati and collaborators (2015) listed three main reasons for the lack of epidemiologic parameters for IPF. Firstly, the diagnostic criteria or disease definition of IPF have changed over time. Secondly, the coding system for IPF in administrative database has been modified in the past few years; and lastly, the methodology and the population selected among epidemiologic studies vary greatly making comparison difficult. Generally, it seems that the prevalence and incidence of IPF are higher in American studies than in European and Asian studies. Although, it is unclear whether this is due to true differences in geographic and ethnic aspects or due to methodological differences in the way the studies were conducted (Caminati et al., 2015). By taking all the studies published between 2000 and 2012, Kaunisto and collaborators (2013) found that the prevalence and annual incidence of IPF varied among studies from 0.5-27.9/100,000 and 0.22-8.8/100,000, respectively (Kaunisto et al., 2013). Some studies suggest that the prevalence and incidence appear to be increasing over the last decades, while prior diagnostic uncertainty of IPF may have contributed to previous lower rates (Sgalla et al., 2015).

## 3.2. Clinical presentation

IPF generally occurs at a median age of 66 years (range 55 – 75) and is more prevalent in men (King et al., 2011b; Sgalla et al., 2015). Clinical signs are non-specific and include chronic and progressive dyspnoea on exertion combined with dry cough, which significantly impact patients' health-related quality of life (Kim et al., 2015; Kishaba, 2015; Sgalla et al., 2015). Bibasilar inspiratory Velcro-type crackles are consistently heard on chest auscultation and appear early in the disease (Sgalla et al., 2015). Finger clubbing is present in 25-50% of cases, whereas fatigue, weight loss, malaise, fever, and alteration of the general status are not common (Kim et al., 2015).

## 3.3. Diagnostic approach

In 2011, the American Thoracic Society (ATS), the European Respiratory Society (ERS), the Japanese Respiratory Society, and the Latin-America Thoracic Society jointly published an evidence-based statement providing recommendation for the diagnosis and management of IPF (Raghu et al., 2011). They recommended a multidisciplinary discussion approach involving ILD specialists, radiologists and pathologists to reach a consensus diagnosis of IPF based on the following criteria: (1) exclusion of other known causes of ILD (mainly domestic and occupational environmental exposures, connective-tissue disease and drug toxicity), (2) presence of an UIP pattern on HRCT of the chest in individuals where surgical lung biopsies

are not indicated or available, and (3) specific combinations of HRCT and a histological UIP pattern in individuals undergoing surgical lung biopsies. Since then, it has been shown that, in an appropriate clinical setting, the presence of a classical UIP pattern on HRCT has a high positive predictive value for histopathological diagnosis of UIP, and considered sufficient for a diagnosis of IPF (Fulton and Ryerson, 2015; Olson and Swigris, 2012; Prasad et al., 2015). However, HRCT scanning can provide a confident, highly specific diagnosis of IPF based on the presence of a classical UIP pattern in solely 50-60% of patients (Tomassetti et al., 2015). In the remaining 40-50% of patients with suspected IPF, transbronchial lung cryobiopsy (Tomassetti et al., 2015) or more invasive surgical lung biopsies are still required to make a definitive diagnosis (Olson and Swigris, 2012). An alternative to those invasive procedure may also be to observe the clinical development of the disease over a follow-up period when the patient's condition permits (Poletti et al., 2016).

### *3.3.2. Blood analyses*

Laboratory haematological and biochemical findings are usually non-specific in IPF patients (Sgalla et al., 2015). A few IPF patients have mildly positive anti-nuclear antibody titer and/or rheumatoid factor levels without any other clinical features of connective tissue disease (Prasad et al., 2015; Sgalla et al., 2015); the prevalence of positive autoantibodies having been shown to increase with advancing age (Meyer et al., 2015). Serial serologic and clinical evaluation monitoring is essential in those patients for subsequential confirming or infirming the development of a connective tissue disease associated ILD and refine the diagnosis if needed (Prasad et al., 2015).

### *3.3.3. Cardiopulmonary function testing*

Several cardiopulmonary function testing are available in human medicine and may help to ascertain the degree of lung impairment, which is needed to evaluate the severity and progression of the disease as well as the response to specific treatments (Sgalla et al., 2015). A restrictive pattern is usually observed at spirometry with reduced forced vital capacity (FVC) and total lung capacity (Sgalla et al., 2015). An impairment of gas exchange reflected by a reduction of the diffusion lung capacity for carbon monoxide (DLCO), a low arterial pO2 at rest and an oxygen desaturation during 6MWT is also classically observed and may represent the only functional abnormality in mild diseases (Sgalla et al., 2015; Wallaert et al., 2012). Cardiopulmonary function testing may suggest the presence of comorbidities such as PH or emphysema (see below).

### *3.3.4. Diagnostic imaging*

Chest radiography is generally the first radiological investigation performed in the diagnostic approach of any suspicion of ILD, although neither sensitive nor specific (Wallis and Spinks, 2015). It may help to exclude oedema or infection and can screen for malignancies (Wallis and Spinks, 2015). Typical IPF-UIP findings include reticulations with a peripheral and basal predominance and reduced lung volume (Fig. 17) (Kadoch et al., 2015; Wallis and Spinks, 2015).

Fig. 17: Chest radiograph demonstrating peripheral reticulations and volume loss. (Kadoch et al., 2015)

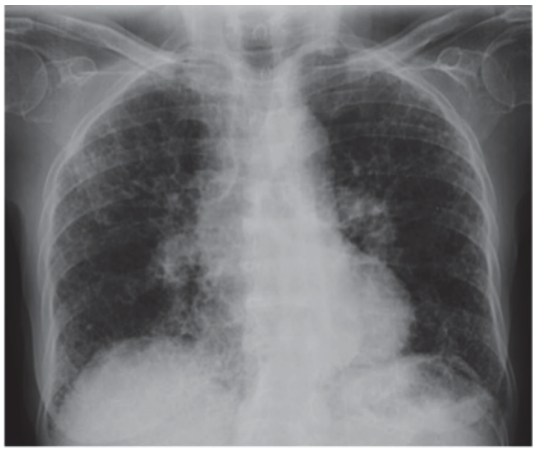

Transthoracic ultrasonography findings of IPF have also been described and include fragmented and irregular thickening of the pleura, subpleural cysts, reduction or absence of the physiological "gliding sign", and increased number of horizontal (and to a lesser extent vertical) reverberations artefacts in a severity which correlate with the degree of fibrosis (Sperandeao et al., 2009). This imaging technique provides good visualisation of the peripheral lung tissue (where most interstitial lesions are found), as well as real-time imaging of respiratory movements (Sperandeo et al., 2009). However, such as for chest radiography, lesions observed are neither sensitive nor specific of IPF as they can be observed in other ILD (Sperandeo et al., 2009).

Thoracic HRCT is pivotal for the diagnosis and evaluation of IPF and other ILD (Sverzellati et al., 2015). On HRCT, the IPF hallmarks are reticular opacities and honeycombing, often associated with traction bronchiectasis, in a peripheral/subpleural and basal distribution corresponding to the 'classical' UIP pattern (Fig. 18) (Kadoch et al., 2015; Sverzellati et al., 2015). The 'possible' UIP pattern shows all of these features except for honeycombing (Sverzellati et al., 2015). Honeycombing is manifested on HCRT as clustered well-defined cystic airspaces, typically of comparable diameters on the order of 3-10 mm but

occasionally as large as 2.5cm (Raghu et al., 2011). In some cases, GGO may be present but in a less extensive distribution than reticular and honeycombing patterns (Hansell et al., 2008). Both the classical and possible UIP patterns on HRCT have been shown to have a very high positive predictive value for histologic UIP pattern, eliminating the need for surgical lung biopsies in carefully selected cases (Kadoch et al., 2015; Sverzellati et al., 2015). However, in 40-50% of IPF cases, atypical HRCT appearance is found and is mainly characterized by concomitant presence of extensive areas of GGO, whereas consolidation, nodules, or extensive areas of decreased attenuation can be seen less frequently (Sverzellati et al., 2015). In those cases, histopathological confirmation of the diagnosis is still required. It is important to emphasise that, even among experienced thoracic radiologists, agreement on the presence or absence of honeycombing is highly variable (Hansell et al., 2015). Reasons for these differing opinions are due to an overlap in the CT appearances of honeycombing, traction bronchiectasis, and paraseptal emphysema (Hansell et al., 2015).

Fig. 18: Classical HRCT UIP pattern characterized by subpleural basal honeycombing with traction bronchiectasis, as well as reticular opacities and GGO.
(Sverzellati et al., 2015)

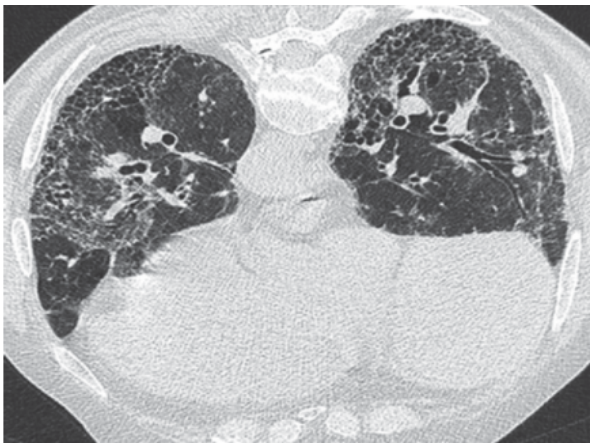

### *3.3.5. Bronchoscopy and bronchoalveolar lavage fluid analysis*

The most important application of bronchoscopy and BALF analysis in patients with suspected IPF is to exclude alternative disorders such as chronic HP or idiopathic NSIP characterised by a BAL lymphocytosis (Kishaba, 2015; Poletti et al., 2016; Prasad et al., 2015). However, current guidelines recommends that BALF analysis should not be performed routinely in the diagnostic approach of IPF as there is unclear evidence regarding diagnostic usefulness (Prasad et al., 2015; Raghu et al., 2011). This recommendation has been challenged when atypical clinical and radiological features predominant, alternative diagnoses need to be considered and BAL could contribute to the collection of useful information with lower risk to the patients (Poletti et al., 2016).

### *3.3.6. Histopathological features*

Different techniques are available to obtain lung samples for histopathological analysis in cases of ILD: trans-bronchial biopsy (TBB), transbronchial cryobiopsy, and surgical lung biopsy. Each technique has its advantages and inconvenients and should be chosen in view of the individual patient's risk/benefice. TBB often contains lung parenchyma which may allow the identification of IPF histopathological hallmarks, but with an inherent low sensitivity due to the small specimen size (Poletti et al., 2016). More recently, cryoprobes have been developed to obtained larger pieces of lung tissue (40-50 $mm^2$) to encounter this limitation. However, studies on the standardization of the procedure are still absent (size of the probe, freezing time, use of bronchial blockers) and the rate of pneumothorax following the procedure may reach 28% compared with the 8% obtained with classical TBB (Poletti et al., 2016). Consequently and according to the current guidelines, surgical lung biopsies remains the recommended technique for patients suspected of IPF with atypical HRCT pattern (Raghu et al., 2011). However, the procedure is more invasive and has been associated with a significant mortality rate within 30-90 days of the procedure, mainly related to acute exacerbation of IPF (Poletti et al., 2016).

Classical histopathological features of IPF include: fibroblastic foci, spatial heterogeneity (normal lung tissue adjacent to affected fibrotic lung), cystic and fibrotic destruction resulting in honeycombing, and the absence of inflammatory infiltrates in areas of fibroblastic foci, absence of granulomas, or features of other interstitial inflammation (Fig. 19) (Popper, 2013). These histopathological changes often affect the subpleural and paraseptal parenchyma most severely (Raghu et al., 2011). The fibroblastic focus lies within the walls of alveolar and interlobular septa, as well as bronchioles, but do not project into the alveolar lumen. The fibroblastic foci composed of fibroblasts and myofibroblasts in a dense collagen matrix (Popper, 2013). Areas of honeycomb changes are composed of cystic lesion covered by a cuboidal and cylindrical epithelium, with mucus and inflammatory cells accumulation within the lumen (Popper, 2013). Smooth muscle metaplasia in the interstitium is commonly seen in areas of fibrosis and honeycomb changes (Raghu et al., 2011).

## 3.4. Risk factors

Although IPF, is by definition, a disease of unknown aetiology, several risk factors have been associated with its development and progression, while their exact roles in the pathogenesis of the disease remains unclear for much of them.

Fig. 19: Histopathological UIP pattern characteristics of IPF include (A) a subpleural distribution of fibrosis (20x, H&E), (B) fibroblastic foci (arrows) with a relative absence of inflammatory cell infiltrate (400x, H&E), (C) smooth muscle proliferation in the subpleural scars (asterisk) (40x, H&E), and (D) honeycomb remodelling (20x, H&E).
(Smith et al., 2013b)

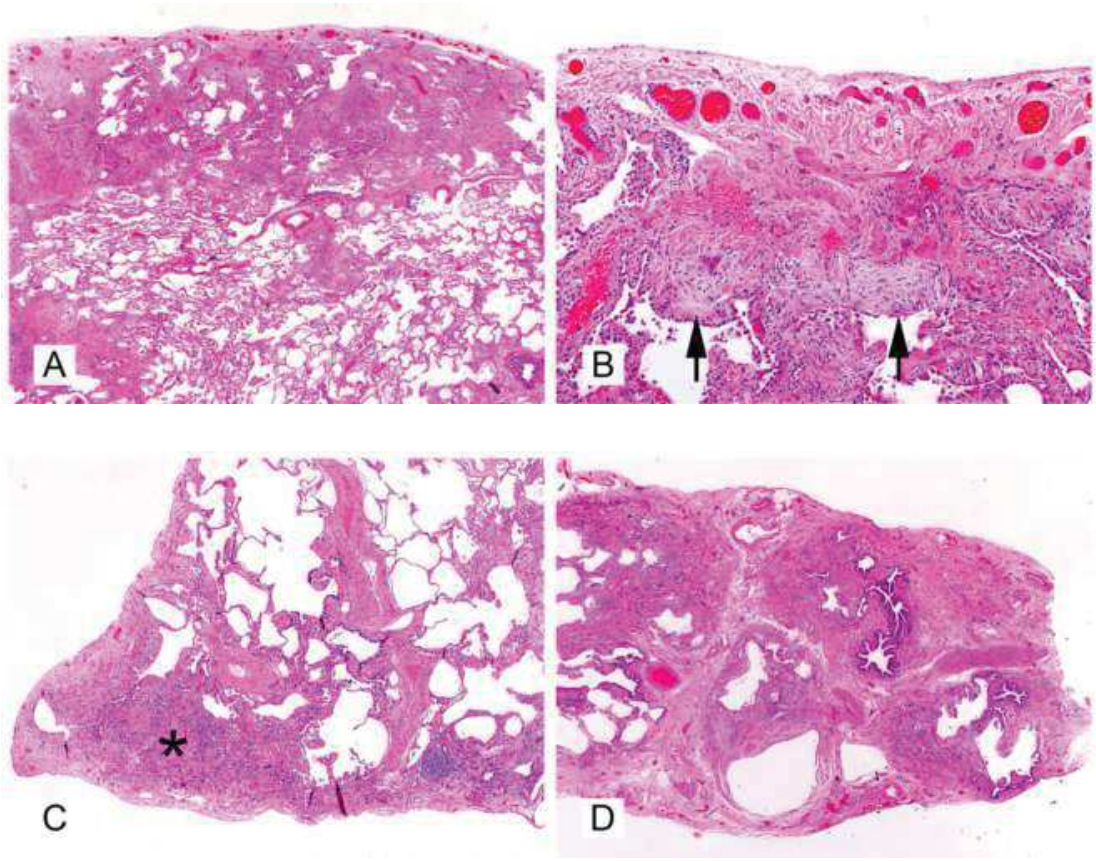


### *3.4.1. Cigarette smoking*

A smoking history is common in patients affected with IPF (Olson and Swigris, 2012), particularly in individuals with a smoking history of more than 20 pack-years (Raghu et al., 2011).

### *3.4.2. Environmental exposures*

Several studies have investigated whether environmental or occupational exposures may increase the risk for developing IPF. Metal (brass, leas, and steel) and wood (pine) dust exposures, exposures to sand, stone or silica, and agriculture/farming/livestock-related exposures have all been found to be associated with IPF (Olson and Swigris, 2012; Raghu et al., 2011).

### *3.4.3. Gastro-oesophageal reflux*

The exact implication of gastro-oesophageal reflux (GOR) in the pathogenesis of IPF is still debated. Indeed, two hypothesis have been proposed. The first hypothesis states that the reduced compliance of the lung in case of IPF may lead to an increased negative intra-thoracic pressure, increased respiratory workload and altered oesophageal tone thereby promoting reflux; while the second hypothesis speculates that GOR acts as a causal agent for IPF development and exacerbation by promoting micro-aspiration causing repetitive injuries to the lung parenchyma (Minnis et al., 2016). At the present time, there is a lack of data to illuminate the precise relationship between GOR and IPF, but it might be speculated that both hypotheses may act in a vicious circle. The prevalence of GOR in IPF patients is estimated between 60 – 90% depending on the diagnostic criteria used, with around 50-75% of patients being asymptomatic (Minnis et al., 2016). Proximal reflux events have been shown to be more common in patients suffering from IPF compared with those suffering from other interstitial lung diseases. It has also been reported that both pepsin and bile salts were found in increased concentrations in saliva and BALF from IPF patients in comparison with non-IPF ILD patients, as well as in IPF patients suffering from acute exacerbation (AE) of the disease (Minnis et al., 2016). Concerning the use of anti-reflux medication (anti-secretory + prokinetics agents), data are controversial but some studies indicated a longer survival time and a slower decline in FVC in patients undergoing an aggressive anti-reflux treatment (Minnis et al., 2016).

### *3.4.4. Infectious agents*

Infectious agents, including both viruses and bacteria, have been associated with IPF development (Antoniou et al., 2014; Molyneaux and Maher, 2013). Among viruses, most researches have focused on human herpesviruses (HHVs) and particularly on Epstein-Barr virus (EBV) (Raghu et al., 2011). Several studies have reported an increased identification of EBV, but also of other HHV genomes in lung biopsies and BAL specimens from IPF patients compared with controls, suggesting a strong association of HHVs with IPF (Molyneaux and Maher, 2013). Those data in addition to the ones available from the murine model of the disease, lead to the theory that HHVs may participate in the initiation and progression of pulmonary fibrosis by latently infecting alveolar epithelial cells causing repetitive injuries to the lung and subsequent cell apoptosis (Molyneaux and Maher, 2013; Williams, 2014). The development of modern microbiological techniques has allowed the composition of the lung bacterial microbiome in IPF patients to be studied. Molyneaux and collaborators (2014) found that patients with IPF have a higher bacterial load in BALF with significant differences in the composition and diversity of microbiota in comparison to controls, with the presence of more abundant Haemophilus, Streptococcus, Neisseria and Veillonella spp. (Molyneaux et al., 2014). However, whether the modifications observed in the respiratory microbiome in IPF are causal

in nature or simply result from the destruction of the normal lung architecture is presently unknown.

### *3.4.5. Genetic background*

Several genome-wide association studies have identified several common and rare genetic variants in more than a dozen loci on different chromosomes that appears to contribute to the risk of developing IPF (Fingerlin et al., 2013; Sgalla et al., 2015). Among them, a single nucleotide polymorphism in the promoter of the gene encoding for mucin 5B (MUC5B) located on the chromosome 11 has been found to be the strongest and the most replicated genetic risk factor for IPF, with an 6 to 8-fold increased risk for IPF (Yang et al., 2015). MUC5B is an evolutionary conserved gene that encodes mucin glycoprotein a principal macromolecules in airway mucus (Zhou and Wang, 2016). The presence of the common variant rs35705950 in the promoter of the MUC5B gene was associated with excess production of MUB5B protein in IPF patients which is thought to impair mucus clearance and alveolar repair consequently contributing to the development of the disease (Zhou and Wang, 2016). Other mutations involved in a higher risk of IPF development are mutation of the alveolar stability-associated genes (surfactant protein C, surfactant protein A2, and ATP-binding cassette member A3) and of the genes involved in the control of telomere length (e.g., telomerase reverse transcriptase and telomerase RNA component) (Raghu et al., 2011; Yang et al., 2015; Zhou and Wang, 2016).

## 3.5. Disease progression

Despite the discovery of two agents effective in reducing the decline of pulmonary function, IPF remains a progressive disease with unfavourable prognosis, with a median survival time from diagnosis ranging from 3-5 years (Kim et al., 2015; Sgalla et al., 2015). The rate of progression of IPF is highly variable between individuals and is difficult to predict at the time of the diagnosis (Kim et al., 2015; Sgalla et al., 2015). Many patients have a slow but progressive clinical course over a period of years, while in 10-15% of patients the course of the disease is much more rapid, leading to death from respiratory failure in few months (Sgalla et al., 2015). A minority of patients remain relatively stable over long periods punctuated by episodes of acute deterioration, which may be due to a known cause such as infection, or to an unknown cause. Deteriorations associated with unknown causes are defined as acute exacerbations (AE) (Kim et al., 2015). AE leads to death in approximately 40-50% of cases during hospitalization, or to a step down in pulmonary function in surviving individuals (Sgalla et al., 2015). AE represents an acceleration of the underlying fibrotic process without identifiable cause, while viral infection, exposure to ozone and nitrogen dioxide, or aspiration

of gastric content have been suggested as causative agents for disease worsening (Sgalla et al., 2015). AE is estimated to occur in 5-10% of IPF patients annually (Kim et al., 2015).

## 3.6. Prognostic factors

Many clinical and physiological parameters have been proposed as predictors of poor outcome in IPF patients and were summarized in the recent review of Sgalla and collaborators (2015) (Table 5). Among them, older age and male sex seem to be correlated with a poorer prognosis, whereas there are contrasting data about smoking status (Meyer et al., 2015; Sgalla et al., 2015). Dyspnoea scores, oxygen levels, FVC, DLCO, 6MWD, and the extent of fibrosis on HRCT images at baseline and their longitudinal changes have also been shown to predict survival (Kim et al., 2015; Sgalla et al., 2015). Several risk models, including a combination of those demographic, clinical, physiological and radiological data, have also been developed to stage IPF and predict survival by several authors, but their application in clinical practice has not yet been evaluated (Sgalla et al., 2015). Whereas, identifying clinical characteristics that may help to predict disease progression and survival would be useful for making treatment decisions and indications for lung transplantation (Kim et al., 2015).

Table 5: Proposed prognostic predictors of IPF.
(Sgalla et al., 2015)

| Category | Parameter | Evidence |
|---|---|---|
| Demographic/clinical | Age | Older age[27] |
| | Sex | Male[42] |
| | Dyspnoea and oxygen level | • Baseline[68]<br>• Changes at 6 months[67] |
| | Comorbidities | • Pulmonary hypertension[48]<br>• Pulmonary emphysema[48]<br>• GERD[51]<br>• Lung cancer[50] |
| Physiological | FVC | • Baseline FVC < 55%[45]<br>• 6 months' decline > 10% or 5–10%[69] |
| | $DL_{CO}$ | • Baseline[45]<br>• 6 or 12 months' decline >15%[67,69] |
| | 6MWD | • Baseline <250 m[71]<br>• 24-week decline >50 m[71] |
| Radiological | Fibrosis score | Baseline and changes at follow-up[14,72,73] |
| | Traction bronchiectasis | Extent of traction bronchiectasis[18] |
| Biomarkers | Serum and plasma biomarkers | Baseline levels of: SPA, SPD, KL6/MUC1, alfa1 defensins, CCL18, YKL40, CXCL13, anti-HSP70 IgG, MMP7, MMP1, osteopontin, periostin[75] |
| | MMP collagen fragments (neoepitopes) | Baseline levels and changes at 3 months[81] |
| | Fibrocytes | >5% (Total leucocytes)[82] |
| | αvβ6 integrin | Extent of immunostaining on lung IPF tissue[86] |
| Microbiome | Members of Staphylococcus and Streptococcus genera | Higher concentration in BAL at diagnosis[87] |
| | Bacterial burden | Higher bacterial burden in BAL at diagnosis[88] |
| Genetic | MUC5B promoter polymorphism rs35705950 | Minor 'risk' allele (improved survival)[84] |
| | TOLLIP polymorphism rs5743890 | Major 'risk' allele (improved survival)[85] |

6MWD, 6-min walking test distance; $DL_{CO}$, diffusion lung capacity for carbon monoxide; FVC, forced vital capacity; GERD, gastro-oesophageal reflux disease; IPF, idiopathic pulmonary fibrosis; MMP, matrix metalloproteinases; MUC5B, mucin 5B; TOLLIP, Toll-interacting protein.

Additionally, large number of peripheral blood proteins and cytokines have been studied in IPF as potential biomarkers of disease progression and survival (Kim et al., 2015; Sgalla et al., 2015). However, most data come from retrospective studies with biomarkers not yet validated for use in the clinical practice. In their recent review, Kim and collaborators compiled the most studied biomarkers (Table 6) and pointed out that the potential applicability of these biomarkers is presently hampered by the lack of their routine availability in practice.

Table 6: Peripheral blood biomarkers in IPF.
(Kim et al., 2015)

| Serum biomarker | Differences between IPF and other ILDs | Correlates with | | | Study lead author and year | Study population | |
|---|---|---|---|---|---|---|---|
| | | Baseline parameter of disease severity | Disease progression/ longitudinal change in parameter | Mortality | | Number of subjects | Number of IPF subjects |
| KL-6 | N | — | — | Y | Satoh et al., 2006 | 219 | Not specified: 152 IIP |
| | N | — | — | — | Ohnishi et al., 2002 | 115 | 21 |
| | Y | — | — | — | Ishii et al., 2003 | 66 | 19 |
| Surfactant proteins | | | | | | | |
| SP-A | N | — | — | — | Ohnishi et al., 2002 | 115 | 21 |
| | Y | — | — | — | Ishii et al., 2003 | 66 | 19 |
| | — | N | — | Y | Kinder et al., 2009 | 82 | 82 |
| | — | N | [a] | Y | Greene et al., 2002 | 543 | 210 |
| | — | N | N | Y | Takahashi et al., 2000 | 160 | 52 |
| SP-D | Y | — | — | — | Ohnishi et al., 2002 | 115 | 21 |
| | Y | — | — | — | Ishii et al., 2003 | 66 | 19 |
| | — | — | — | — | Kinder et al., 2009 | 82 | 82 |
| | — | N | [a] | Y | Greene et al., 2002 | 543 | 210 |
| | — | N | Δ%VC/yr, Δ%TLC/yr | Y | Takahashi et al., 2000 | 160 | 52 |
| Matrix metalloproteinases | | | | | | | |
| MMP1 | Y | N | — | — | Rosas et al., 2008 | 322 (D) 33 (V) | 74 (D) 9 (V) |
| MMP7 | Y | FVC, DLCO | — | — | Rosas et al., 2008 | 322 (D) 33 (V) | 74 (D) 9 (V) |
| | — | — | — | [b] | Richards et al., 2011 | 140 (D) 101 (V) | 140 (D) 101 (V) |
| CCL18 | — | TLC, DLCO | ΔTLC | — | Prasse et al., 2007 | 78 (D) 40 (V) | 16 (D) 17 (V) |
| | — | — | ΔTLC, ΔFVC | Y | Prasse et al., 2009 | 72 | 72 |
| VEGF | — | N | ΔVC (subset) | — | Ando et al., 2010 | 98 | 41 |
| YKL-40 | — | N | — | Y | Korthagen et al., 2011 | 211 | 85 |
| | — | DLCO, $AaDO_2$, $PaO_2$ | — | — | Furuhashi et al., 2010 | 63 | 41 |
| Osteopontin | N | $PaO_2$ | — | — | Kadota et al., 2005 | 46 | Not specified: 17 ILD |
| Periostin | Y | Not reported | ΔTLC, ΔFVC | — | Okamoto et al., 2011 | 105 | 51 |
| Fibrocytes | — | N | — | Y | Moeller et al., 2009 | 75 | 58 |
| T cells | | | | | | | |
| CD4:CD28% | — | FVC | ΔFVC, ΔFVC rate | Y | Gilani et al., 2010 | 89 | 89 |
| Tregs | Y | FVC, DLCO | TLC, FVC | — | Kotsianidis et al., 2009 | 84 | 21 |

Abbreviations: Y, yes; N, no; —, not studied; $AaDO_2$, alveolar-arterial oxygen difference; D, derivation cohort; DLCO, diffusing capacity for carbon monoxide; FVC, forced vital capacity; IIP, idiopathic interstitial pneumonia; ILD, interstitial lung disease; IPF, idiopathic pulmonary fibrosis; TLC, total lung capacity; Tregs, regulatory T cells; V, validation cohort; IPF, idiopathic pulmonary fibrosis.
[a] Longitudinal data available for a subset of 19 subjects. No significant changes over time, although patients were relatively stable.
[b] MMP7 levels were associated with mortality in derivation cohort, but not validation cohort.

Finally, the prompt establishment of the diagnosis and referral to a tertiary care centre is of importance for the prognosis; delayed access to a tertiary care centre has been associated with a higher risk of death in IPF patients independent of disease severity (Lamas et al., 2011).

## 3.7. Co-morbidities

Co-morbidities are frequent in IPF patients and are generally associated with poor survival. Consequently, they should be timely evaluated and treated whenever possible in order to improve morbidity and potentially impact on mortality (Antoniou et al., 2014; Sgalla et al., 2015).

### *3.7.1. Pulmonary hypertension*

Pulmonary hypertension (PH) is present in up to one third of patients with IPF at the time of referral for lung transplantation and is associated with increased risk of mortality (Fulton and Ryerson, 2015; Smith et al., 2013a). IPF patients with suspected pulmonary hypertension, based on findings such as the presence of severe dyspnoea, impaired cardiopulmonary testing performance disproportionate to fibrosis severity, or clinical findings of right heart dysfunction (tricuspid murmur, jugular distention) typically undergo screening with a transthoracic echocardiogram (Fulton and Ryerson, 2015; Glaser et al., 2013; Patel et al., 2007; Smith et al., 2013a). However, due to the poor accuracy of echocardiographic findings of PH, right heart catheterization may be indicated in patients with a great likelihood of PH even in the presence of negative echocardiographic results (Arcasoy et al., 2003; Nathan et al., 2008). Indeed, in the specific context of IPF, it has been shown that solely half of the patients have a measurable TR for echocardiographic estimation of PAP, which was found accurate for reflecting PAP measured by RHC in only 40% of cases (Nathan et al., 2008). Another study in IPF patients confirmed that the non-invasive estimation of PAP by echocardiography is not reliably accurate in comparison with RHC as the mean bias between the 2 methods was 7.75 mmHg with limits of agreements ranging from -35 to 20 mmHg (Swanson et al., 2008).

Pathophysiology of PH associated with lung disease is still poorly understood and is thought to result from an interaction between fibrotic destruction of the vasculature, reflex hypoxic pulmonary vasoconstriction, imbalance between vasodilator and vasoconstrictor mediators, and aberrant vascular remodelling (Patel et al., 2007; Singh et al., 2015; Smith et al., 2013a). PH is associated with a higher risk of death in IPF patients, suggesting a potential benefit of pulmonary vasodilators in these patients. Several small studies have been performed to evaluate the impact of sildenafil, a 5-phosphodiestare inhibitor, on exercise performance in IPF. Although some studies displayed contrasting results, sildenafil treatment appears to

improve arterial oxygenation, degree of dyspnoea and quality of life, suggesting a potential benefit of this treatment in IPF patients, particularly if they are concomitantly suffering from PH (Collard et al., 2007; Han et al., 2013; Jackson et al., 2010; Zimmermann et al., 2014; Zisman et al., 2010). Clinical trials have also be done to evaluate the safety and efficacy of endothelin receptor antagonists (bosentan, macitentan, and ambrisentan) to decrease time to disease progression (defined as death, respiratory hospitalisation or decline in lung function parameters), but results were less encouraging than those obtained for sildenafil, with no advantage of endothelin receptor antagonists over placebo (King et al., 2008; King et al., 2011a; Raghu et al., 2013a; Raghu et al., 2013b).

### *3.7.2. Emphysema*

Emphysema frequently coexists with IPF under the terminology of CPFE for combined pulmonary fibrosis and emphysema, a clinical syndrome that is characterized by upper lobe emphysema and lower lobe fibrosis (Fulton and Ryerson, 2015). CPFE has been described in 8% to 30% of patients with IPF (Antoniou et al., 2014; Meyer et al., 2015). Patients with CPFE have less lung restriction on spirometry and worse gas exchange compared to IPF patients without emphysema (Antoniou et al., 2014). The higher FVC found in CPFE patients is explained by the fact that emphysema is mitigating the impact of the fibrosis on ventilator physiology, while both fibrosis and emphysema have a similar and cumulative effects on gas exchange, resulting in a disproportionate oxygen requirement and low DLCO in CPFE patients (Antoniou et al., 2014; Ciccarese et al., 2016). Patients with CPFE showed a poorer prognosis than patients with IPF alone as they are more prone to develop comorbidities (Ciccarese et al., 2016).

### *3.7.3. Neoplasia*

The risk of developing lung neoplasia is approximately 7 times higher in patients with IPF compared to a control population and shortens survival by around 2 years (Fulton and Ryerson, 2015). Those IPF patients suffering from lung cancer are frequently poor candidates for curative oncologic therapy given the low functional capacity and decreased ability to tolerate cancer therapies (Sgalla et al., 2015). Furthermore, acute IPF worsening has been reported following tumour resection, radiation therapy, or chemotherapy (Kreuter et al., 2015).

### *3.7.4. Thromboembolic disease*

Patients affected with IPF are at increased risk for thromboembolic disease due to decreased mobility causing venous stasis, and potential involvement of the coagulation cascade in the pathogenesis of IPF (Crooks and Hart, 2015; Fulton and Ryerson, 2015). Indeed, it has

been shown that IPF patients are more than 4 times more likely than age- and sex-matched controls to have a pro-thrombotic state favouring venous thromboembolism (Antoniou et al., 2014). However, pulmonary thromboembolism can be difficult to identify in patients with IPF given its nonspecific presentation in a patient already diagnosed with a chronic and progressive lung disease, prompting evaluation with contrast CT in patients with acute respiratory worsening (Fulton and Ryerson, 2015). Due to their predilection to develop thromboembolism, anticoagulation treatment have been investigated with the idea to disrupt the contribution of the coagulation cascade to the fibrotic process. However, warfarin therapy has been shown to provide no benefit and was associated with increased risk of significant adverse events and premature death, which does not favour its use in IPF treatment (Noth et al., 2012).

## 3.8. Overview of the pathogenesis

It was long been believed that lung fibrosis was preceded and provoked by a chronic inflammation process that injures the lung and modulates fibrogenesis, leading to end-stage fibrotic scarring (Borensztajn et al., 2013). However, inflammation is never a prominent histopathological finding in UIP pattern, and clinical trials using combination of corticosteroids and immunosuppressive agents revealed increased risks of death and hospitalisation in treated patients compared with placebo arm of the study (Borensztajn et al., 2013; Raghu et al., 2012) Consequently, this model of inflammation-driven fibrogenesis was shifted to another pathogenic paradigm suggesting that IPF arises as a result of repetitive epithelial injury and subsequent highly aberrant wound healing response in genetically susceptible individuals under the influence of environmental risk factors (Chambers and Mercer, 2015). The abnormal wound healing response in IPF is felt to be perpetuated by an aberrant epithelial-mesenchymal cross-talk that drives the excessive activation of fibroblasts and myofibroblasts leading to increased production of extracellular matrix (Chambers and Mercer, 2015). Mechanisms underlying this deregulated epithelial-mesenchymal crosstalk are multifactorial with current evidence suggesting critical roles for diverse fibrogenic factors acting through both autocrine and paracrine mechanisms (Chambers and Mercer, 2015).

Major cellular contributors acting in the pathogenesis of IPF will be briefly addressed in this chapter. Besides, among the myriad of molecules that have already been investigated in the context of IPF, we will focus specifically on the potential role of chemokine (CC-motif) ligand 2 (CCL2), chemokines (CXC-motif) ligand 8 (CXCL8), vascular endothelial growth factor (VEGF) and 5-HT in the pathogenesis of the disease.

### *3.8.1. Cellular mechanisms of pulmonary fibrosis*

Alveolar epithelial cells (AECs), fibroblasts, myofibroblasts, pericytes, bronchial cells, pleural cells, endothelial cells, macrophages, lymphocytes and polymorphonuclear cells have all been incriminated in the pathogenesis of IPF (Bagnato and Harari, 2015). Dysregulated cross talk between epithelial and mesenchymal cells is thought to be one of the most important mechanisms involved in the development of fibrosis. Thus, we will focus on the interaction between AECs, fibroblasts and myofibroblast in this section (Fig. 20). Repetitive injuries to the lungs is thought to occur mainly to type 1 AECs that line the majority of the alveolar surface (Bagnato and Harari, 2015; Camelo et al., 2014). In response to cellular loss and exposure of the basement membranes following injury, type 2 AECs generally undergo hyperplastic proliferation to regenerate type 1 AECs in normal repair conditions (Barkauskas and Noble, 2014; Camelo et al., 2014). Under pathological conditions, chronically damaged epithelial cells release a variety of profibrotic mediators that favour the migration and proliferation of resident fibroblasts into the injured areas as well as their differentiation into myofibroblasts, which initiates the fibrotic process (Barkauskas and Noble, 2014). Furthermore, rather than to differentiate in type 1 AECs, type 2 AECs may undergo a transdifferentiation into fibroblasts through a process called epithelial-mesenchymal transition (EMT), which further contributes to the fibrotic perpetuation (Kage and Borok, 2012). Additionally, it has been demonstrated that AECs are prone to apoptosis in IPF lungs, in contrast with fibroblasts and myofibroblasts which become resistant to this programmed cellular death, a phenomenon called “apoptosis paradox” favouring abnormal healing and excessive collagen production leading to scar formation (Thannickal and Horowitz, 2006). Triggers that stimulate the apoptotic cascade of AECs are still under scrutiny, but premature aging, genetic mutations, and environmental factors have all been suggested as causal factors (Barkauskas and Noble, 2014; Camelo et al., 2014; Renzoni et al., 2014). Myofibroblasts are the key effector cells responsible for excessive matrix synthesis and deposition in IPF (Chambers and Mercer, 2015). These spindle-shaped cells combine the synthesising features of fibroblasts with cytoskeletal contractile characteristics of smooth-muscle cells conferring them contractile properties and the capability of producing extracellular matrix components (Bagnato and Harari, 2015; Barkauskas and Noble, 2014). They are mainly derived from the local recruitment, proliferation, and differentiation of resident lung fibroblasts, but other sources are also implicated including circulating bone marrow-derived fibrocytes, epithelial cells (via EMT), pleural mesothelial cells (via mesothelial to mesenchymal transition), and endothelial cells (via endothelial to mesenchymal transition) (Bagnato and Harari, 2015; Chambers and Mercer, 2015; Kendall and Feghali-Bostwick, 2014). Myofibroblasts cause the exaggerated accumulation of extracellular

matrix and contribute to further basement membrane destruction and epithelial cell death, favouring the establishment of a fibrotic self-perpetuating circle (King et al., 2011b).

Fig. 20: Schematic illustration of the dysregulated cross talk between the epithelium and the mesenchyme in the IPF context.
(Barkauskas and Noble, 2014)

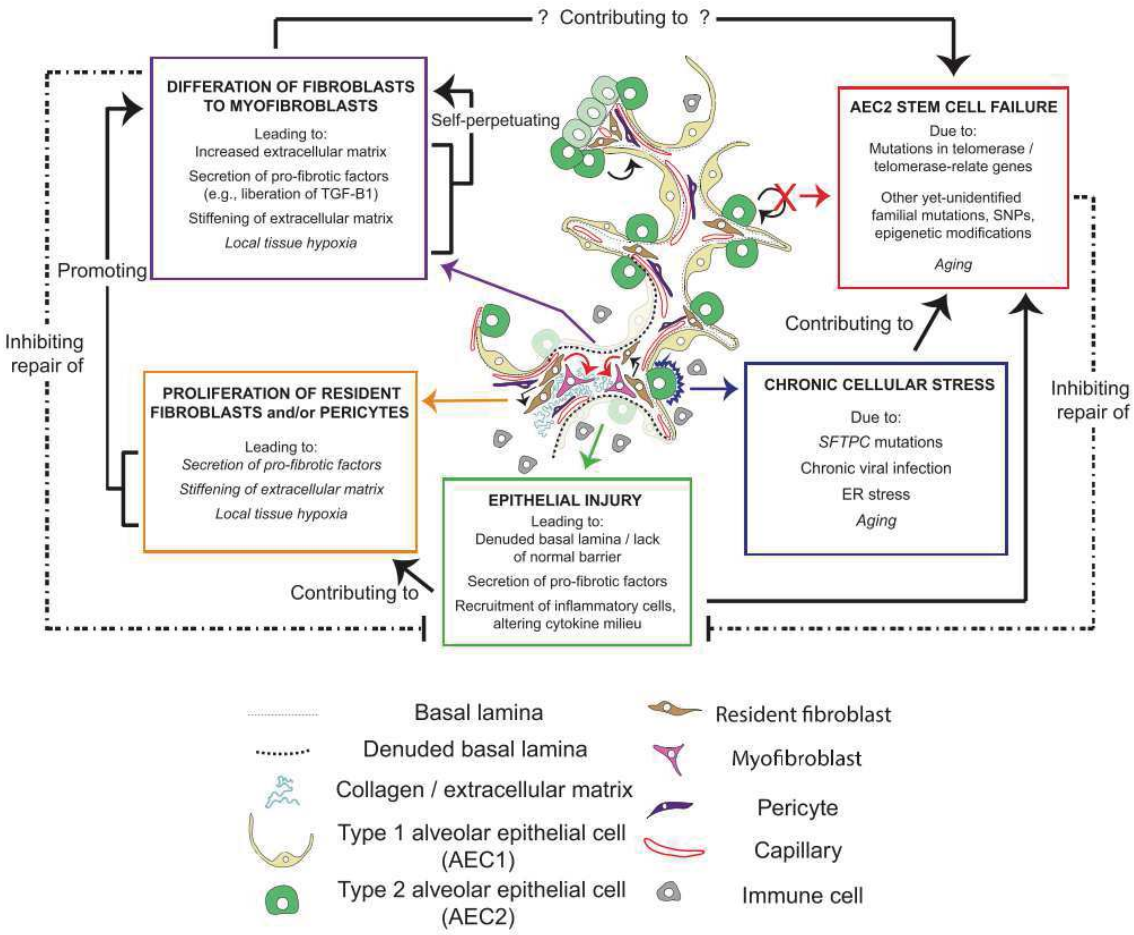


### *3.8.2. Molecular mechanisms of pulmonary fibrosis*

More than 20 years of extensive research has established an undeniable central role of TGF-β signalling in pulmonary fibrosis (Chambers and Mercer, 2015). TGF-β acts as a major pro-fibrotic cytokine by inducing fibroblast recruitment, proliferation and differentiation to myofibroblast, by promoting fibroblasts and myofibroblasts survival, and by inhibiting extracellular matrix degradation (Camelo et al., 2014; Chambers and Mercer, 2015). Production, activation and signalling pathways of TGF-β are complex, such as the mechanisms by which it exerts its pro-fibrotic properties. Those aspects were particularly well reviewed in a recent doctoral thesis (Krafft, 2015) and will not be addressed here. Instead, we will focus

specifically on the potential implication of chemokines CCL2 and CXCL8, VEGF and 5-HT in the pathogenesis of IPF.

Chemokines are chemotactic cytokines classically defined by their ability to induce directional migration and activation of leukocytes into inflammatory sites. They are classified on the basis of their structural features in two main categories, the CC and CXC-chemokines (Bonecchi et al., 2009). Among the CC-chemokines group, CCL2, also known as monocyte chemotactic protein-1, is able to attract and activate cells of the monocyte lineage through G-protein-coupled CCR2 receptor. CXCL8, a CXC-chemokine also known as interleukin-8, mediates neutrophil chemotaxis and degranulation through G-protein-coupled CXCR2 receptor (Bonecchi et al., 2009). CXCL8 also binds to CXCR1 receptor, which is believed to mediate activation of the neutrophil respiratory burst and release of myeloperoxidase (Rose et al., 2003). In addition to their chemotactic roles, CCL2 and CXCL8 act on different ways in the pathogenesis of a variety of human diseases ranging from infectious and inflammatory diseases to cancer (Locati et al., 2005). In the particular context of IPF, CCL2 overexpression was found in fibrotic areas of the lungs (Antoniades et al., 1992; Mercer et al., 2009) and the CCL2/CCR2 axis was reported to promote fibrosis notably through fibrocytes recruitment and M2 macrophage activation (Moore et al., 2005; Sun et al., 2011). CCR2 knockout mice were protected from bleomycin- and fluorescein isothiocyanate-induced lung fibrosis, and anti-CCL2 gene therapy attenuated bleomycin-induced fibrosis in the murine IPF model (Gharaee-Kermani et al., 2003; Inoshima et al., 2004; Moore et al., 2001). Elevated concentrations of CCL2 were found in BALF and serum of IPF patients and were correlated with clinical parameters of lung function and with outcome (Baran et al., 2007; Capelli et al., 2005; Emad and Emad, 2007; Shinoda et al., 2009; Suga et al., 1999). A recent study also showed that pirfenidone significantly improved bleomycin-induced lung fibrosis in mice through attenuation of CCL2 production and concomitant fibrocytes recruitment (Inomata et al., 2014).

Although the exact role of angiogenesis in the pathogenesis of IPF remains presently unclear, aberrant vascular remodelling occurs in IPF lungs, with areas at the interface to normal parenchyma displaying increased vascularisation in contrast with affected fibrotic areas where vascularisation is found minimal or absent (Barratt and Millar, 2014). A balance disturbance between angiogenic and angiostatic mediators has been proposed to explain this phenomenon. In this respect, Keane and collaborators (1997) were the first to introduce the potential implication of CXCL8 in the pathogenesis of IPF as an angiogenic factor promoting aberrant vascular remodelling (Keane et al., 1997). They demonstrated an imbalance in the expression of angiogenic chemokines (CXCL8 and CXCL5) vs. angiostatic factors (CXCL10) in favour of a net angiogenesis in IPF lungs. They also found that the fibroblasts were the predominant

source of CXCL8, supporting a role for fibroblasts in mediating angiogenic activity in IPF. Consistent with these findings, Russo and collaborators (2009) demonstrated that the inhibition of CXCR2 attenuated bleomycin-induced pulmonary fibrosis through an inhibitory effect on angiogenesis rather than on neutrophils recruitment and subsequent inflammation (Russo et al., 2009). Furthermore, as for CCL2, CXCL8 concentrations were found to be increased in BALF and serum of IPF patients and correlated with lung function parameters and with the extent of fibrosis (Antoniou et al., 2006; Martina et al., 2009; Totani et al., 2002; Vasakova et al., 2009; Ziegenhagen et al., 1998). CXCL8 was also proved to be one of the strongest predictors of IPF survival when taken in combination with clinical characteristics (Richards et al., 2012). A single nucleotide polymorphism (rs4073T>A) located in the promoter of the CXCL8 gene was also found to be significantly associated with an increased risk of IPF development in homozygous patients due to overexpression of the CXCL8 gene reflected by higher concentrations of CXCL8 in BALF (Ahn et al., 2011).

VEGF is a highly specific mitogen for vascular endothelial cells (Neufeld et al., 1999). In vivo, VEGF induces angiogenesis as well as permeabilisation of blood vessels, and plays a central role in the regulation of vasculogenesis (Neufeld et al., 1999). The role of VEGF in IPF pathogenesis is controversial (Barratt and Millar, 2014). Contrasting reports either suggest that VEGF may be protective against formation of pulmonary fibrosis, or instead promote fibrogenesis (Barratt and Millar, 2014; Yan et al., 2014). Increased expression of both VEGF and CXCL8 was observed by immunohistochemistry in the capillary endothelial cells and type 2 AECs of the highly vascularised alveolar septa found in preserved areas of the IPF lungs, while minimal expression of VEGF was found in fibroblastic foci (Ebina et al., 2004). This observation suggested that fibrosis development does not require neovascularisation and that VEGF may contribute to locally increased vascularity in non-affected lung areas as a secondary adaptive change following the fibrotic process (Ebina et al., 2004). Conversely, VEGF receptor blockade was reported to result in the attenuation of bleomycin-induced pulmonary fibrosis (Ou et al., 2009), and treatment with nintedanib (a triple tyrosine kinase inhibitor) demonstrated positive results in slowing-down the progression of the disease in IPF patients (Richeldi et al., 2016) (see below), suggesting that VEGF may be involved in the fibrogenic mechanisms of IPF. Serum VEGF concentrations were increased in IPF patients and tended to be associated with survival; patients having VEGF concentration above the median tended to have a shorter survival time in comparison with patients having VEGF concentration below the median (Ando et al., 2010). On the contrary, two studies reported surprisingly reductions in VEGF concentrations in the BALF of IPF patients in comparison with non-smoking healthy individuals (Koyama et al., 2002; Meyer et al., 2000). Epithelial cell apoptosis and cellular injury observed in case of IPF have been proposed as a mechanism to explain the decrease of

VEGF concentrations in BALF, knowing that VEGF cellular localisation in the lung was primarily the AECs (Koyama et al., 2002).

Finally, the serotonin signalling has been recently proposed as a novel pathway that controls fibroblast activation, while evidence currently available remains sparse (Fernandez and Eickelberg, 2012). The main role of serotonin is to act as a neurotransmitter in the central nervous system, controlling integrative functions, such as mood, anxiety, stress, feeding and cognition (Olivier, 2015). Outside the central nervous system, serotonin is synthetized from tryptophan by gastro-intestinal enterochromaffin cells and then pooled in platelets, which store and release serotonin by its transporter 5-HTT to prevent its degradation by the monoamine oxidase A (Fabre and Crestani, 2010). Serotonin exerts its action on different cellular type and tissue through 7 different receptors (Fabre and Crestani, 2010). In the lung, serotonin may result from different sources including platelets, neuroendocrine cells, mast cells and endothelial cells (Fabre and Crestani, 2010). Increased expression of receptors 5-HTR1A, -1B, -2A, and -2B and decreased expression of 5-HTT were detected by RT-PCR in lung biopsies obtained from patients with IPF in comparison with transplant donors (Konigshoff et al., 2010). By immunohistochemistry, 5-HTR2A was shown to be largely localised to lung fibroblasts, whereas epithelial cells largely express 5-HTR2B (Konigshoff et al., 2010). Treatment with 5-HTR2A and -2B inhibitors in bleomycin injured mice resulted in improvement in lung function, fibrotic score, and a decrease in collagen content (Fabre et al., 2008; Konigshoff et al., 2010). Furthermore, in vitro inhibition of 5-HTR2A and -2B was shown to prevent TGFβ induced collagen production by fibroblasts (Konigshoff et al., 2010). Those results suggest that targeting serotonin pathways could be a therapeutic option in IPF, whereas no clinical trials have already been published in this perspective.

## 3.9. Therapeutic options

In the past decade several multicentre, randomised, placebo-controlled trials have been conducted to investigate agents with different mechanisms of action that may help to slow-down IPF progression (Antoniou et al., 2014). Among them, solely two compounds with antifibrotic properties, pirfenidone (Esbriet®) and nintedanib (Ofev®), have been consistently proven to be effective in reducing functional lung decline and disease progression with acceptable safety profiles in IPF patients with mild to moderate functional impairment (Kreuter et al., 2015). These two therapeutic options have been approved by the US food and drug administration for IPF (Kreuter et al., 2015). Pirfenidone is thought to exert antifibrotic, anti-inflammatory, and antioxidant actions in IPF lungs through downregulation of several key profibrotic growth factors including TGF-β, whereas its exact mechanism of action is not yet fully understood (Kreuter et al., 2015; Puglisi et al., 2016). A pooled analysis of three large

randomised control trials (CAPACITY-PIPF 004, CAPACITY-PIPF 006, and ASCEND) including a total of 1334 patients demonstrated the benefit of pirfenidone in IPF patients by slowing-down the decline in FVC and 6MWD over time, and by increasing the progression free-survival in comparison with placebo (Nathan et al., 2016). Nintedanib is a tyrosine kinase inhibitor that targets VEGF receptors, fibroblast growth factor (FGF) receptors, and platelet-derived growth factor (PDGF) receptors; VEGF, FGF and PDGF having all been implicated in the pathogenesis of IPF through their fibrogenic or angiogenic actions (Bonella et al., 2015; Inomata et al., 2015; Kreuter et al., 2015). The efficacy of nintedanib in IPF patients has been evaluated in a pooled analysis of three randomised control trials (INPULSIS-1 and -2 and TOMORROW) including a total of 1231 patients that demonstrated that nintedanib significantly reduced the rate of decline in FVC over time and the change from baseline in the St. George's Respiratory Questionnaire, and increased to time to first AE in comparison with placebo (Richeldi et al., 2016). A trend was also observed favouring nintedanib in all-cause mortality or death from a respiratory cause (Richeldi et al., 2016).

Beside targeted antifibrotic treatments, comprehensive care of patients with IPF, including management of comorbidities/complications, pulmonary rehabilitation, oxygen therapy, and timely referral for palliative care or, in small number of highly selected patients, for lung transplantation, remains essential (Bonella et al., 2015; Kreuter et al., 2015). As explained above, treating GOR with aggressive anti-acid therapy and PH with sildenafil may be beneficial for the IPF patient. Pulmonary rehabilitation may improve functional exercise capacity, quality of life and level of perceived dyspnoea, and has also been associated with positive psychosocial outcomes including reduced symptoms of anxiety and depression (Egan, 2011; Kenn et al., 2013). However, there is currently no standardisation about the type, the duration, or the intensity of exercise to advise a patient (Kenn et al., 2013; Puglisi et al., 2016). The role of oxygen supplementation has received strong recommendation for patients with significant resting hypoxemia in IPF-specific guidelines, albeit with very low-quality evidence (Douglas et al., 2000; Raghu et al., 2011). Despite this lack of evidence, it is easily understandable that providing sufficient compensation of oxygen deficiencies may be an important key for increasing the ability of IPF patients to perform and to sustain any kind of daily activity (Kenn et al., 2013). Finally, lung transplantation represents opportunity for IPF patients to obtain survival benefit, with survival at 5-years post-transplantation around 50% (Meyer, 2014; Puglisi et al., 2016).

# 4. Other pulmonary fibrotic disorders in humans

Chronic HP and fibrosing NSIP are the two main differential diagnoses for IPF (Neurohr and Behr, 2015). These pathological entities share similar clinical presentation with IPF, and have overlapping imaging and histopathological findings. In this section, we will briefly overview the clinical, radiological and histopathological characteristics of those 2 interstitial lung diseases.

## 4.1. Chronic hypersensitivity pneumonitis

Chronic HP is a complex pulmonary syndrome resulting from a prolonged diffuse inflammation of lung parenchyma and airways in response to the repeated inhalation and sensitization to aerosolized antigens or low-molecular-weight inorganic molecules (Jeong et al., 2014; Spagnolo et al., 2015). HP-inducing antigens are commonly classified in 5 broad categories including bacteria, fungi and yeast, mycobacteria, animal proteins and chemicals; avian antigens and microbial agents being the most common causes of HP (Spagnolo et al., 2015). Clinical signs of chronic HP appear insidiously over a period of months to years with a slowly progressive cough, exertional dyspnoea, fatigue, malaise, chest tightness and weight loss (Selman and Buendia-Roldan, 2012; Spagnolo et al., 2015). Physical examination usually reveals diffuse fine crackles or wheezes and digital clubbing (Smith et al., 2013b; Spagnolo et al., 2015). Pulmonary function testing is characterized by a restrictive or mixed (obstructive and restrictive) ventilator defect accompanied by a reduced DLCO (Spagnolo et al., 2015). Serum precipitating antibodies against a selection of antigens can be useful as supportive evidence for the diagnosis of HP in case of positive result, but does not allow for rule out the diagnosis of HP in case of negative result due to a high proportion of false negative (Lacasse et al., 2012; Spagnolo et al., 2015). On BALF analysis, the total cell yield is usually very high with a marked lymphocytosis (> 20% and often > 50% of the total cells recovered) (Selman et al., 2012; Spagnolo et al., 2015). On HRCT, fibrotic changes include traction bronchiectasis and honeycombing in a mid to upper lung zone predominance surimposed on extensive GGO, centrilobular nodules, and air trapping that is exaggerated on expiration CT due to underlying cellular bronchiolitis (Hodnett and Naidich, 2013; Spagnolo et al., 2015). The HRCT feature that best differentiate chronic HP from UIP and fibrosing NSIP are the presence of lobular areas of mosaic attenuation pattern (present in 80% of patients with chronic HP), centrilobular small nodules (present in 56% of cases) and the lack or lower zone predominance (Jeong et al., 2014; Silva et al., 2008) (Fig. 21).

Fig. 21: Chronic HP HRCT findings. (A) Patchy areas of subpleural GGO with centrilobular small nodules (arrows). (B) Lobular areas of mosaic attenuation (open arrows) and subpleural GGO. (C) Patchy areas of subpleural GGO and reticulation.
(Jeong et al., 2014)

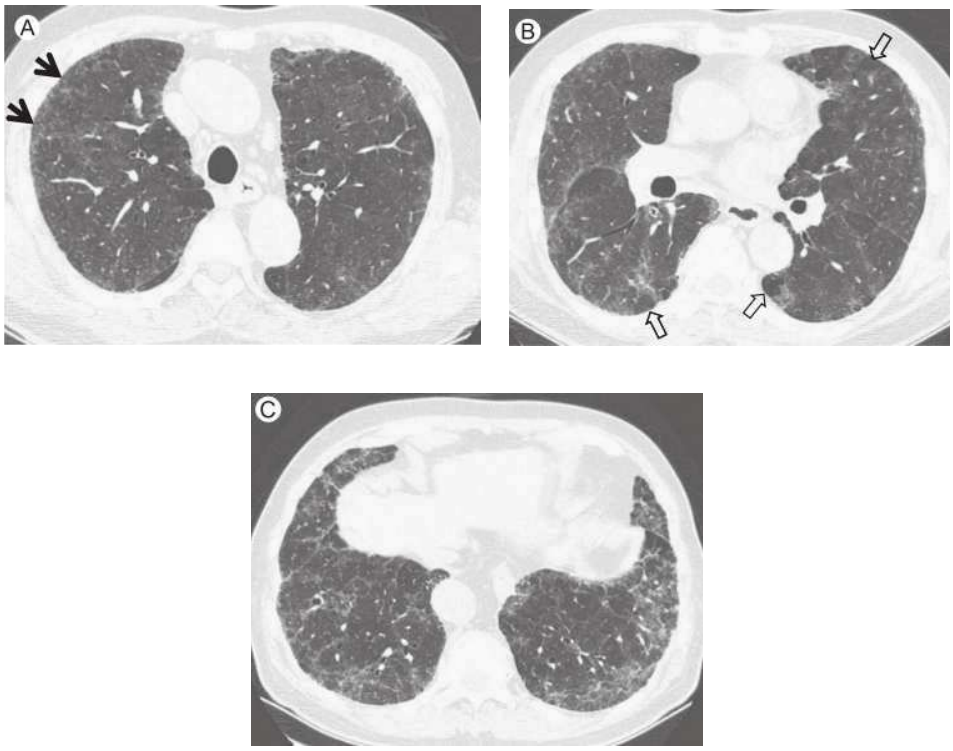


Histological findings of chronic HP share similarities with those of fibrosing NSIP and UIP and are characterized by patchy fibrotic changes with preferential centrilobular distribution, fibroblastic foci (typically present at the edge of the fibrosis in peribronchiolar areas), honeycombing, bronchiolar epithelial hyperplasia, lymphoid/plasmacytic infiltrates (particularly outside the fibrotic areas), and small granulomatous or multinucleated giant cells (Selman et al., 2012; Smith et al., 2013b; Spagnolo et al., 2015). Bridging fibrosis is frequently identified and is represented as linear fibrotic connection between centrilobular and perilobular areas (subpleural or/and paraseptal) or between centrilobular and adjacent centrilobular areas (Smith et al., 2013b). Avoidance of exposure to the suspected or confirmed causative agent is the cornerstone of HP management along with prolonged corticosteroids therapy (Selman et al., 2012; Spagnolo et al., 2015). However, chronic HP with extensive lung scarring has no effective therapy, and oxygen therapy and lung transplantation are often recommended (Jeong et al., 2014; Selman et al., 2012).

## 4.2. Fibrosing non-specific interstitial pneumonia

The radiological and histological features of the NSIP pattern were introduced for the first time in 2002 in the ERS/ATS classification of idiopathic interstitial pneumonias as a

distinct pattern, while previously considered as a "wastebasket" category. As the name implies, NSIP displays many "nonspecific" features from a clinical, radiologic, and pathologic view (Travis et al., 2008). Accordingly, the NSIP pattern occurs not only as an idiopathic condition, but also in a variety of settings including connective tissue diseases, HP, and drug toxicity, and in some patients with familial pulmonary fibrosis (Travis et al., 2013). The clinical presentation of idiopathic NSIP includes dyspnoea and cough of usually 6 to 7 months duration, predominantly in women, never-smokers, and in the sixth decade of life (Glaspole and Goh, 2010; Travis et al., 2008). Inspiratory crackles are commonly noticed, but digital clubbing is rarely present (8% in NSIP compared with 25-50% in IPF) (Glaspole and Goh, 2010). The most common HRCT abnormalities are bilateral and symmetrical GGO in a peripheral and lower lobes distribution surimposed on reticular opacities with traction bronchiectasis; honeycombing being sparse or absent (ATS/ERS, 2002; Travis et al., 2013). At HRCT longitudinal examination, most patients with NSIP have persistent abnormalities, with the extent of GGO classically decreasing with time while the extent of reticular abnormality persists or increases, leading to a pattern suggestive of UIP (Sverzellati et al., 2015). The histologic NSIP features include interstitial thickening by uniform fibrosis usually preserving the alveolar architecture, with varying amounts of cellular inflammation (Travis et al., 2008). The inflammatory infiltrate consists of lymphocytes and variable numbers of plasma cells, while neutrophils, eosinophils and histiocytes are relatively inconspicuous (Glaspole and Goh, 2010). Honeycombing is not present, but areas of interstitial fibrosis with enlarged airspaces may be seen with preservation of the lung architecture (Travis et al., 2008). The prognosis is variable: some patients improve, others remain stable or improve on treatment, while others evolve to end stage fibrosis and eventually die of the disease (Travis et al., 2013), but globally NSIP carries a far better prognosis than IPF/UIP with a 5-year survival of 82.3% (Travis et al., 2008).

# OBJECTIVES

As detailed in the introduction section, CIPF is a rare spontaneous progressive fibrotic lung disease of unknown origin affecting mainly older WHWTs, and unresponsive to currently available therapies. CIPF shares clinical and pathogenic features with human IPF, while imaging and histopathological characteristics are not identical. The identification of targeted therapies for CIPF or transposition of therapies available in human medicine would require an improvement of the phenotypic characterization of the disease and a better understanding of the mechanism leading to pulmonary fibrosis in dogs. Given that pulmonary function testings are limited in dogs and lack sensitivity (Lilja-Maula et al., 2014b), the discovery of biomarkers to ascertain the presence and severity of fibrosis seems crucial before undertaking clinical therapeutic trials in dogs. The search for etiologic agents of the disease is also of interest for targeted therapies.

## 1. Case – control recruitment

Recruitment of well-phenotyped CIPF cases and controls is an essential preliminary step to obtain clinical information and materials needed for clinical and experimental studies. Thanks to a collaboration between our group and our Finnish veterinary partners from the University of Helsinki who have been working on CIPF for several years, biological material (serum, BALF and lung tissue samples) issued from CIPF and age-matched control WHWTs was already available at the beginning of this work. To increase the size of the study populations, obtain detailed clinical information about the disease, and collect additional specific samples, our objective was to continue to prospectively recruit WHWTs affected with CIPF, as well as healthy age-matched WHWTs.

## 2. Improvement of the phenotypic characterization

### 2.1. T-HRCT interpretation: sedation vs. general anaesthesia

In human medicine, the potential use of serial CT as an effective endpoint for drug trials is increasingly considered. Indeed, for chronic progressive diseases, mortality may not be an adequate endpoint and many surrogate markers that have been explored, ranging from pulmonary function decline to biomarkers, are not entirely reliable (Hansell et al., 2015). Therefore, combinations of endpoints, including change in disease extent on CT, are being investigated in human medicine (Hansell et al., 2015). In dogs, whether serial CT may be a useful tool for monitor disease progression or evaluate a response to a therapy remains to be determined. In veterinary medicine, T-HRCT classically requires general anaesthesia, which

might be not suitable in a follow-up approach particularly in severely cardio-pulmonary affected dogs. Obtaining images under sedation may therefore be an alternative as it is safer, easier and quicker. However, it is presently not know whether the variation of the breathing pattern under sedation and general anaesthesia may influence images interpretation and quality. Therefore, our aim was to investigate whether differences exist between images obtained under sedation and general anaesthesia for the identification and gradation of major lung lesions, in order to known if sedation can be used for the diagnosis and the follow-up of CIPF.

## 2.2. Echocardiographic investigation of pulmonary hypertension: PV/PA

As explained in the introduction section, non-invasive diagnosis of PH by echocardiography is challenging due to several limitations related to the use TR jet velocity for estimation of PAP. Consequently, we aimed at investigating whether the new echocardiographic index "pulmonary vein to pulmonary artery diameters ratio (PV/PA)" (Fig. 22) can be used to indicate the presence of PH by considering the WHWTs population affected with CIPF as a model of pre-capillary PH.

Fig. 22: Illustration of pulmonary vein diameter (●) and pulmonary artery diameter (●●) measurements in two-dimensional (A) and M-mode (B) using the inner edge to inner edge method at the end of the T-wave.
(Merveille et al., 2015)

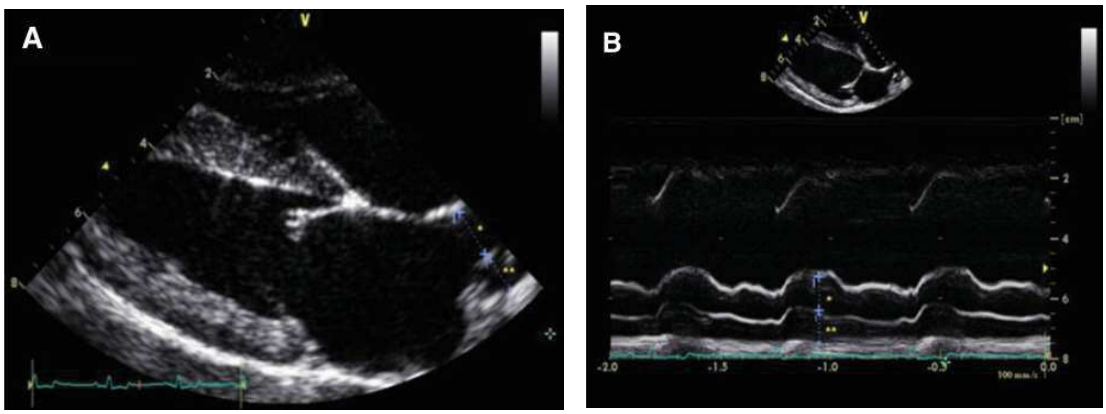


The PV/PA ratio was firstly described at the 20th annual ECVIM congress by Birettoni and collaborators (2010). They found a PV/PA value of 1.00 +/- 0.11 in heathy dogs and hypothesized that this value would increase in case of uncomplicated left-sided congestive heart failure (CHF) and decrease in case of pre-capillary PH. Later, Merveille and collaborators (2015) confirmed a PV/PA value of 1 in healthy dogs and demonstrated a gradual increase of PV/PA proportionally to the stage of heart failure in dogs suffering from degenerative mitral valve disease (DMVD). They also reported that a cut-off value of 1.7 in 2D-mode, PV/PA may help to discriminate dogs in CHF from asymptomatic dogs with DMVD with a sensitivity and

specificity of 96 and 91% respectively, using thoracic radiographs as the gold standard. Based on those encouraging data, we decided to investigate PV/PA in WHWTs affected with CIPF hypothesizing that this ratio would decrease proportionally to the presence and the severity of pre-capillary PH. We aimed to compare PV/PA obtained in WHWTs affected with CIPF and unaffected controls (sub-grouped according to the presence and maximal velocity of a tricuspid regurgitant jet) in correlation with two-dimensional and Doppler-echocardiographic indices of PH, namely VmaxTR, MPA/Ao, AT:ET and RPAD Index. Additional study objectives were to correlate PV/PA with clinically available indices of cardiopulmonary function, arterial pO2 and the 6MWD, and with serum NT-proBNP concentrations, given that those complementary tools have shown to be helpful in the diagnostic approach of PH in humans and/or dogs.

## 3. Investigation of biomarkers

Biomarkers refer to any objectively quantifiable substance that can be measured in biological tissue or fluids to inform the underlying biological mechanism involved in a disease (Ley et al., 2014). In IPF, it seems straightforward that epithelial cell damage, as well as aberrant scar formation, will lead to the liberation and/or exposure of molecules in the lung tissues, BALF or even in peripheral blood, which can reflect the presence of the disease (Borensztajn et al., 2013). An ideal biomarker should be reliable, valid, responsive to changes in disease status, able to show a clinically meaningful difference, predictive of clinical outcome and responsive to the treatment effect of a given intervention (Borensztajn et al., 2013). In CIPF, the response to specific anti-fibrotic treatments has not yet been determined and few sensitive clinical markers are currently available for monitoring disease progression and, consequently, treatment efficacy. Molecules that may serve as surrogate markers for fibrosis are therefore needed in order to permit a better characterisation of disease severity and progression and to evaluate response to any specific anti-fibrotic treatment in the future. The pulmonary gene expression analysis performed on samples from CIPF cases demonstrated increased expression of several genes, including those encoding CCL2 and CXCL8 chemokines (Krafft et al., 2013). Consequently, we aimed at further investigate the possible use of those two chemokines as CIPF biomarkers by comparing their serum and BALF concentrations between WHWTs affected with CIPF and healthy controls. We also aimed at investigating their potential role in the pathogenesis of the disease by using immunohistochemistry and qRT-PCR. Furthermore, Krafft and collaborators demonstrated higher serum TGF-β1 concentrations in healthy dogs from the WHWT breed in comparison with breeds not predisposed to the disease (Krafft et al., 2014a). Hypothesizing that higher circulating concentrations of pro-fibrotic molecules in dogs from the WHWT breed may serve as predisposing factors for CIPF

development, we aimed at comparing basal circulating blood concentrations of CCL2, CXCL8, VEGF and 5-HT obtained in healthy dogs from seven breeds differently predisposed to CIPF.

## 4. Search for etiologic agents

To date, no etiologic agent has been investigated in CIPF. In humans, horses and rodents, a strong association between pulmonary fibrotic disorders and gammaherpesvirus infection has been suggested as a cause of repetitive epithelial cells injuries and subsequent deregulated tissue repair. Therefore, our aim was to search for the presence of gammaherpesvirus in lung tissue and blood samples form WHWTs affected with CIPF in comparison with controls; although the actual existence of such viruses in dogs is still under debate. Few contrasting publications have been published so far regarding the potential existence of gammaherpesvirus in dogs. In 2005, Chiou and collaborators were the first to report the presence of antibodies against EBV antigens in 32 of 36 healthy domestic dogs in Taiwan, confirmed by a PCR assay based on the EBV BamHI W sequence in 15 of 21 blood samples. Serological evidence of EBV or EBV-like virus exposure was thereafter confirmed in three other studies (Huang et al., 2012; Milman et al., 2011; Waugh et al., 2015), while molecular data displayed varying results according to studies and methods employed. Milman and collaborators (2011) found no evidence of gammaherpesvirus DNA in 50 blood, 33 lymphoma tissue, and 104 palatine tonsil samples, such as Waugh and collaborators (2015) who failed to detect herpesviral sequences in 111 canine tumour samples. On the contrary, Huang and collaborators (2012) detected herpesviral genome in 2 of 3 B-cell lymphoma, and Chiu and collaborators (2013) found EBV BamHI W sequence in 10 of 12 canine tumour specimens (mainly oral tumours) (Chiu et al., 2013).

# RESULTS SECTION

## 1. Case – control recruitment

Thanks to the long lasting collaboration between our group and our Finnish veterinary partners from the University of Helsinki (Prof. Rajamäki Minna and collaborators), significant clinical information from WHWTs affected with CIPF and unaffected WHWT were available at the beginning of this work and consequent biological material (blood, BALF, and lung tissue samples) had been banked. Part of the samples were selectively used for the studies detailed here. In the framework of present work, the prospective recruitment of CIPF and unaffected WHWTs was continued at both Liege and Finland universities and is still in progression. In order to facilitate the recruitment, we created a website containing essential information about the disease and about the research project (www.caninepulmonaryfibrosis.ulg.ac.be). The major aim of this website was to inform the breeders about the existence of such a disease and to encourage owners with WHWTs suspected of CIPF to present their dogs to the academic faculty. Owners of WHWTs above 8 years of age with no respiratory clinical signs were also encouraged to come at the faculty for a complete work-up of their dog to serve as a control group. Furthermore, to improve the communication around our project, we participated annually in the Brussels dog shows where we meet the WHWTs breeders and informed them about our research. We also organised meeting days at the University of Lyon (March 2012), Maison-Alfort (April 2013), and Liège (March 2015) in collaboration with the French WHWT breed club. Additionally, through direct email contacts, oral communications in congresses or publications in veterinary journals, we also informed veterinarians from other universities and private practices in Belgium and other European countries. We encouraged them to refer cases when possible, or to submit biological material (blood, BALF, lung tissue) according to standardized procedures described in details in our website.

At the University of Liège, owners of each affected or unaffected recruited WHWT dog were asked to sign an informed consent form. Each dog was then subjected to a complete clinical examination which included physical examination, complete blood work, 6MWT, arterial blood gas analysis, echocardiography, thoracic HRCT, endoscopy + BALF analysis, and post-mortem lung biopsy for histopathology. Blood, BALF, and lung tissue samples obtained were stored in a biobank at -80°C until further analysis and clinical information was recorded in an Access database. Details about WHWTs affected with CIPF and unaffected WHWTs examined at the faculty of Liège during the 3.5 years period of the present work are summarized in Table 1 and Table 2.

Table 1: Clinical information of CIPF WHWTs recruited at the small animal clinic of the University of Liège between September 2012 and March 2016.

| Nb | Dog Name | Age (years) | Sex | First visit | Nb of follow-up | Survival (months) | Cause of death | Cardiac US | Thoracic CT | Blood | BAL | Lung |
|---|---|---|---|---|---|---|---|---|---|---|---|---|
| 1 | Vicky | 12,1 | F | 28-03-2015 | - | 1,3 | Unknown | + | + | + | - | - |
| 2 | Youngman | 13,6 | M | 23-01-2013 | - | 1,2 | Unknown | - | - | + | - | - |
| 3 | Brian | 13,9 | M | 28-11-2013 | - | 11,6 | Unknown | + | + | + | + | + |
| 4 | Gaston | 11,6 | M | 20-12-2013 | 1 | 5,7 | IPF-related | + | + | + | + | + |
| 5 | Rubykub | 13,4 | M | 17-01-2014 | 2 | 10,1 | IPF-related | + | + | + | + | + |
| 6 | Arthus | 10,4 | M | 22-10-2015 | - | 3,8 | IPF-related | + | - | + | - | - |
| 7 | Titus | 10,4 | M | 08-06-2013 | 6 | 26,3 | IPF-related | + | + | + | - | + |
| 8 | Tom | 14,5 | M | 26-03-2013 | 3 | 17,8 | Non-IPF related | + | + | + | + | + |
| 9 | West | 13,1 | M | 04-07-2014 | 2 | 18,3 | Non-IPF related | + | + | + | + | + |
| 10 | Juul | 10,8 | M | 10-04-2014 | 7 | 23,7 | Alive | + | + | + | + | - |
| 11 | Ginger | 13,0 | F | 23-05-2014 | 3 | 22,3 | Alive | + | - | + | - | - |
| 12 | Casper | 12,1 | M | 12-12-2014 | 1 | 15,6 | Alive | + | + | + | + | - |
| 13 | Shana | 7,4 | F | 21-08-2015 | 3 | 7,3 | Alive | + | + | + | + | - |
| 14 | Cepia | 8,5 | F | 10-03-2016 | - | 0,7 | Alive | + | + | + | + | - |
| 15 | Vickie | 10,6 | F | 13-08-2014 | - | 20,2 | Alive | + | + | + | + | - |
| 16 | Rosy | 5,2 | F | 09-09-2013 | - | *Lost to follow-up* | | + | + | + | + | - |

Table 2: Clinical information of control WHWTs recruited at the small animal clinic of the University of Liège between September 2012 and March 2016.

| Nb | Dog name | Age (years) | Sex | Visit date | Concurrent disease status | Cardiac US | Thoracic CT | Blood | BAL | Lung |
|---|---|---|---|---|---|---|---|---|---|---|
| 1 | Ermine | 4,0 | F | 23/01/2013 | | - | - | + | - | - |
| 2 | Just for you | 2,5 | F | 23/01/2013 | | - | - | + | - | - |
| 3 | Just for me | 2,6 | F | 23/01/2013 | | - | - | + | - | - |
| 4 | Hubble | 4,1 | M | 23/01/2013 | | - | - | + | - | - |
| 5 | Chelsea | 5,9 | F | 23/01/2013 | Spleen haemangioma | - | - | + | - | - |
| 6 | Tess | 10,5 | F | 06/04/2013 | | + | - | + | - | - |
| 7 | Djack | 4,9 | M | 06/04/2013 | | + | + | + | - | - |
| 8 | Vulkain | 9,0 | M | 06/04/2013 | Chronic diarrhoea | + | + | + | - | - |
| 9 | Crocus | 6,2 | M | 06/04/2013 | | + | - | + | - | - |
| 10 | Framboise | 3,2 | F | 06/04/2013 | | - | - | + | - | - |
| 11 | Happy White | 9,2 | M | 06/04/2013 | | + | - | + | - | - |
| 12 | Butterfly Kisses | 7,0 | F | 06/04/2013 | | + | + | + | - | - |
| 13 | Tea for Two | 10,4 | F | 06/04/2013 | | + | + | + | - | - |
| 14 | Delight forever | 4,6 | F | 06/04/2013 | | - | - | + | - | - |
| 15 | Diane | 7,6 | F | 21/05/2013 | Chronic diarrhoea | - | - | + | - | - |
| 16 | Upper trooper | 9,6 | M | 24/05/2013 | | - | - | + | - | - |
| 17 | Juka | 3,1 | F | 27/05/2013 | | + | - | + | - | - |
| 18 | Sue | 10,8 | F | 27/05/2013 | Cruciate ligament rupture | + | + | + | + | - |

| | | | | | | | | | | |
|---|---|---|---|---|---|---|---|---|---|---|
| 19 | Blandine | 3,9 | F | 26/07/2013 | Bilateral renal polykystosis | + | - | + | - | - |
| 20 | Chivas | 6,5 | M | 03/12/2013 | | + | + | + | + | - |
| 21 | Bouchon | 11,1 | F | 23/01/2014 | Bilateral otitis | + | + | + | + | - |
| 22 | Athena | 9,5 | F | 20/06/2014 | Atopic dermatitis | + | + | + | + | - |
| 23 | Deimon | 5,8 | M | 20/06/2014 | | + | + | + | + | - |
| 24 | Eliot | 11,3 | M | 20/06/2014 | Bilateral otitis | + | + | + | + | - |
| 25 | Dandy | 5,8 | M | 20/06/2014 | | + | + | + | - | - |
| 26 | Amy | 10,4 | F | 09/07/2014 | Bilateral hip luxation | + | + | + | - | - |
| 27 | Benji | 10,6 | M | 16/10/2014 | Rectal adenocarcinoma | + | + | + | - | - |
| 28 | Caesar | 12,5 | M | 21/10/2014 | Urinary incontinency | + | + | + | - | - |
| 29 | Cannelle | 15,0 | F | 11/12/2014 | Nasal adenocarcinoma | + | + | + | + | + |
| 30 | Lola | 14,0 | F | 12/12/2014 | | + | - | + | - | - |
| 31 | Napitia | 5,7 | F | 05/01/2015 | | - | + | + | - | - |
| 32 | Casper | 11,4 | M | 28/03/2015 | | + | + | + | - | - |
| 33 | Tomy | 8,8 | M | 28/03/2015 | | + | + | + | - | - |
| 34 | Collin | 9,0 | M | 28/03/2015 | Atopic dermatitis | + | + | + | - | - |
| 35 | Jerome | 12,7 | M | 14/07/2015 | Keratoconjunctivitis | + | + | + | - | - |
| 36 | Misstache | 12,7 | F | 14/07/2015 | Pulmonary mass | + | + | + | - | - |
| 37 | Simba | 9,2 | M | 14/01/2016 | | + | + | + | + | - |

# 2. Improvement of the phenotypic characterization

Results obtained for T-HRCT interpretation (sedation vs. general anaesthesia) and echocardiographic investigation of pre-capillary PH in WHWTs affected with CIPF have not yet been published. However, the redaction of 2 distinct manuscripts presently under review in the *Journal of Veterinary Radiology and Ultrasound* and the *Journal of Veterinary Cardiology*, respectively, has been permitted. To improve the readability of the present work, we included in the present result section a slightly adapted version of the manuscripts submitted in each journal.

## 2.1. T-HRCT interpretation: sedation vs. general anaesthesia

### *2.1.1. Title & authors*

**Comparative study of thoracic high resolution computed tomography under sedation and under general anaesthesia in West Highland white terriers with canine idiopathic pulmonary fibrosis and control dogs**

Elodie Roels[a], Thierry Couvreur[b], Frederic Farnir[a], Cécile Clercx[a], Johny Verschakelen[c], Geraldine Bolen[a]

[a]Department of Clinical Sciences, FARAH, Faculty of Veterinary Medicine, University of Liege, Belgium; [b]Department of Radiology, Christian Hospital Center Liège, Belgium, [c]Department of Radiology, Faculty of Medicine, University Clinic Leuven, Belgium

### *2.1.2. Abstract*

Canine idiopathic pulmonary fibrosis (CIPF) is a progressive interstitial lung disease mainly affecting West Highland white terriers (WHWTs). Thoracic high-resolution computed tomographic (T-HRCT) findings of CIPF acquired under general anesthesia (T-HRCT$^{GA}$) have been described previously. T-HRCT can also be performed under sedation (T-HRCT$^{S}$) with potential for improved speed and safety. However, it is not known whether T-HRCT$^{S}$ provides similar results in terms of the identification and grading of CIPF lesions in a diagnostic setting. The aim of the present prospective observational study was to compare T-HRCT$^{S}$ and T-HRCT$^{GA}$ images obtained from WHWTs affected with CIPF (n=11) and age-matched controls (n=9) using the glossary of terms of the Fleischner Society and a novel scoring system. A permutation test was used for statistical analysis, $P \leq 0.05$ was considered significant. Ground-glass opacity (GGO) was identified in all CIPF WHWTs on both T-HRCT$^{S}$ and T-HRCT$^{GA}$ images, although the GGO extent varied significantly between the two acquisitions ($P<0.001$).

GGO was the sole lesion observed in control dogs (n=6), but was less extensive compared with CIPF WHWTs. Identification and grading of mosaic attenuation pattern differed significantly between T-HRCT$^{S}$ and T-HRCT$^{GA}$ ($P$<0.001). Difference was also noted for the identification of consolidations ($P$=0.121), but not for other CIPF features including nodules, parenchymal and subpleural bands, bronchial wall thickening, or bronchiectasis. The present study demonstrates that T-HRCT may provide similar diagnostic information, identifying the major CIPF features, when performed under sedation or general anesthesia. Nevertheless, there were some differences in the grading of lesions extent between the two approaches.

### *2.1.3. Introduction*

Canine idiopathic pulmonary fibrosis (CIPF) is a progressive interstitial pulmonary disease affecting mainly old West Highland white terriers (WHWTs). (Heikkila-Laurila and Rajamaki, 2014). Clinical signs include cough, exercise intolerance, progressive dyspnoea and inspiratory crackles on lung auscultation (Corcoran et al., 1999a; Heikkila et al., 2011). Definitive diagnosis of CIPF relies on histopathology (Syrja et al., 2013). However, ante-mortem lung biopsies are not routinely performed in veterinary practice due to the invasiveness of the procedure (Lobetti et al., 2001; Norris et al., 2005). To further complicate matters, information obtained from focal biopsies may not be representative of the organ as a whole. The present lack of effective therapy for CIPF is also a poor incentive for such aggressive intervention. Consequently, thoracic high resolution computed tomography (T-HRCT) has become the key modality for the diagnosis of CIPF (Heikkila-Laurila and Rajamaki, 2014; Johnson et al., 2005). T-HRCT findings have previously been described in CIPF dogs under general anaesthesia (T-HRCT$^{GA}$) (Corcoran et al., 2011; Heikkila et al., 2011; Johnson et al., 2005). T-HRCT has not yet been investigated in WHWTs affected with CIPF under sedation (T-HRCT$^{S}$). The diagnosis of CIPF based on T-HRCT$^{S}$ images could avoid the need for general anaesthesia in patients considered at high risk (e.g. pulmonary-diseased patients with concurrent pulmonary hypertension). Furthermore, the opportunity to easily, rapidly, and safely repeat T-HRCT examination of WHWTs affected with CIPF at multiple time-points may help improve knowledge about the progression of this disease and assess the effects of potential treatments.

It is presently unknown whether T-HRCT$^{S}$ can be interpreted with the same confidence as T-HRCT$^{GA}$ for the identification and grading of CIPF lesions. We speculated that the different breathing patterns seen with sedation (spontaneous breathing) and general anesthesia (induced apnea following hyperventilation) would provoke differences in the CIPF lung on T-HRCT due to the variable content of air present in the alveoli. However, we also hypothesized that this would not prevent the diagnosis of CIPF. The objective of the present study was thus

to compare T-HRCT$^{S}$ with T-HRCT$^{GA}$ images obtained from CIPF and control WHWTs. A scoring system was employed to describe CIPF lesions in a standardized manner using the glossary of terms of the Fleischner Society (Hansell et al., 2008).

### *2.1.4. Materials and Methods*

**Study population -** WHWTs affected with CIPF and control WHWTs were prospectively enrolled at the Veterinary Teaching Hospital of the University of Liège during a three-year period from March 2013 to March 2016. All dogs that underwent successively both T-HRCT$^{S}$ and T-HRCT$^{GA}$ were included in the present observational study. The study protocol was approved by the Committee of Experimental Animals of the University of Liège, Belgium (permit number: 1435, date of approval: 14 March 2013). All examinations were performed with the owner's informed consent. The control group included WHWTs unaffected with CIPF age-matched with the CIPF population. Control dogs were included if they had no history of cardiovascular or pulmonary clinical signs, and a normal cardiopulmonary physical examination. Furthermore, echocardiography was performed in all control dogs to exclude primary cardiac disease. The CIPF groups included WHWTs with evidence of CIPF. Inclusion criteria comprised history of cough, exercise intolerance and/or dyspnea, the presence of marked inspiratory crackles on lung auscultation, and the exclusion of primary cardiac disease through echocardiography. Additional examinations, including arterial blood gas analysis, 6-minute walking test and endoscopy with bronchoalveolar lavage were performed in the majority of CIPF dogs. Results of these tests supported the diagnosis of CIPF in dogs where histopathologic examination of pulmonary tissue was not available.

**T-HRCT acquisition** – T-HRCT$^{S}$ and T-HRCT$^{GA}$ were performed successively on each dog at a single occasion. Dogs were maintained in sternal recumbency following premedication and throughout both sets of T-HRCT acquisitions. Sedative agents and dosages were adjusted for each dog according to the recommendations of the anesthetist. Sedated dogs were not provided with supplemental oxygen. After T-HRCT$^{S}$, general anesthesia was induced using intravenous propofol. Following endotracheal intubation, dogs were maintained on isoflurane gas with 100% oxygen. Several gentle lung inflations were performed prior to T-HRCT$^{GA}$ image acquisition, in order to induce apnea and minimize motion artefact. A 16 multi-slice CT scanner (Siemens, Somatom 16, Erlangen, Germany) was used to obtain scans covering the entire thorax, sequenced cranially to caudally. Acquisition parameters used were as follows: tube voltage 120 kV, reference tube current 130 mA, and pitch 0.7 – 1.15. Scan tube current was modulated by automatic exposure control (Care Dose, Siemens Medical Solutions, International). Image data sets were reconstructed using parameters of 200 – 300 mm field of view, 512 x 512 matrix, 1mm slice thickness and B-60 Sharp reconstruction algorithm.

**T-HRCT interpretation** - T-HRCT$^{S}$ and T-HRCT$^{GA}$ images were reviewed on lung window settings (WW 1500 – WL -500) by one veterinary (GB) and two medical (TC and JV) radiologists at the same time to obtain a consensus opinion for each case. Observers were blinded to the dog's CIPF status (CIPF or control) but not the anesthetic status (sedation or general anesthesia) as the endotracheal tube was visible in dogs under general anesthesia. Overall T-HRCT quality was subjectively graded as good (thoracic walls perfectly sharp and well-defined), moderate (thoracic walls partially blurred, with artefacts present only at the periphery of the lung field) or poor (thoracic walls blurred with artefacts extending significantly into the lung field). Motion artefacts were graded as absent, mild (artefacts affecting the diaphragm and/or heart without impacting evaluation of the lung fields), moderate (artefacts inducing blurred margins of the diaphragm and/or the heart that extended slightly over the periphery of the lung fields) or severe (artefacts inducing blurred margins of the diaphragm and/or the heart that extended extensively over the lung fields with several artefactual sequential images of the diaphragm and/or the heart). The nature of the T-HRCT changes were defined using the glossary of terms established by the Fleischner Society (Hansell et al., 2008). Four major groupings were used: increased attenuation, decreased attenuation, nodular opacities and linear opacities. Each category was divided into sub-groups corresponding to specific features (Table 1). Each specific feature was assessed independently for each lung lobe. For ground glass opacity (GGO), consolidation and mosaic attenuation pattern features, the following scoring system was applied for each lung lobe: 0 = absent, 1 = present in < 1/3 of the lobe, 2 = present in 1/3 to 2/3 of the lobe, and 3 = present in > 2/3 of the lobe. This grading system was qualitative and was applied following detailed review of the available images. Delimitation of each lung lobe was determined in relation to the main bronchial division (right cranial, middle and caudal lung lobes, accessory lung lobe, and left cranial and caudal lung lobes). An overall cumulative score was calculated by adding the individual lobe scores together (0 to 18). The presence or absence of cysts, emphysema, nodules, honeycombing, reticulations, parenchymal and subpleural bands was assessed for each lung lobe. Trachea, bronchi, pleura, blood vessels and lymph nodes were also evaluated. Tracheal shape was subjectively assessed at the level of the 6$^{th}$ cervical vertebrae and was classified as round with a normal or flattened dorsal membrane (no collapse), oval with a flattened dorsal membrane (mild to moderate collapse) or oval with an invaginated dorsal membrane or with a loss of > 50% of the tracheal lumen (severe collapse).

Table 1: Definitions of T-HRCT specific lung features studied according to the Fleischner Society. (Hansell et al., 2008)

| Major groups | Specific features | Definitions |
|---|---|---|
| Increased attenuation | Ground glass opacity | Area of hazy increased lung opacity with preservation of bronchial and vascular margins |
| | Consolidation | Homogeneous increase in pulmonary parenchymal attenuation that obscures the margins of vessels and airway walls |
| Decreased attenuation | Mosaic attenuation pattern | Patchwork of regions of differing attenuation |
| | Cyst | Round parenchymal lucency or low-attenuating area with a well-defined interface with normal lung |
| | Emphysema | Focal areas or regions of low attenuation, usually without visible walls |
| Nodular opacities | Nodules | Rounded or irregular opacity, well or poorly defined |
| Linear opacities | Reticulation | Collection of small linear opacities that produce an appearance resembling a net |
| | Parenchymal band | Linear opacity that usually extends to the visceral pleura |
| | Subpleural band | Linear opacity from and parallel to the pleural surface |
| | Honeycombing | Clustered cystic air spaces, typically of comparable diameters, usually subpleural and characterized by well-defined walls |

**Statistics** - Statistical analyses were performed using Excel (Microsoft Office) and XLStat software (Addinsoft SARL, International). Continuous variables were reported as median and range (minimum and maximum), and categorical data as proportions. Proportions were compared using the Fisher's exact test. Differences between T-HRCT$^{S}$ and T-HRCT$^{GA}$ for identification or grading of GGO, consolidation and mosaic attenuation patterns in CIPF dogs were assessed using a permutation test, which allowed us to test the following null-hypothesis: H0 = no difference between T-HRCT$^{S}$ and T-HRCT$^{GA}$ for the allocation of lung lobe scores. To test this hypothesis we generated permutated datasets by randomly allocating scores to either method (T-HRCT$^{S}$ or T-HRCT$^{GA}$) for each lung lobe and for each dog. We summed the absolute differences between the two methods over the whole lung for each dog to obtain a hypothetical value of the overall absolute difference for each individual (|d|). Note that

absolute values were employed as differences between the 2 methods may vary positively or negatively. Summing individual |d| allowed the calculation of a hypothetical overall difference D between the two methods over the entire sample. By repeating this procedure 1000 times (random allocation of a score for each lung lobe, calculation of |d| and then D) we obtained a distribution of overall differences D for the null hypothesis. By comparing results for the real observed overall difference (Dr) with this generated distribution we could estimate a *P*-value. The percentage of D ≥ to Dr in the distribution allows calculation of the *P*-value associated to the observed Dr. Values of $P \leq 0.05$ were considered statistically significant.

### *2.1.5. Results*

**Study population** - Eleven CIPF-affected WHWTs were included. There were six males and five females. They were aged from 5.2 to 14.5 years (median 11.6 years) and weighed between 7.3 to 16.6 kg (median 9.5 kg). Seven of them had a history of both exercise intolerance and cough, one presented for exercise intolerance alone, and three dogs exhibited only a cough. The duration of clinical signs at diagnosis ranged from 1 month to 3.5 years with a median of 3 months. Crackles were noticed on lung auscultation in all dogs, a mild restrictive dyspnea was present in six dogs and cyanosis was observed in one dog. Echocardiography was performed in all WHWTs affected with CIPF to confirm the absence of primary cardiac disease. Doppler-echocardiographic evidence of mild pulmonary hypertension was present in two CIPF dogs, with pulmonary systolic pressure gradients estimated at 37.4 and 40.7 mmHg (reference < 31.4) (Kellihan and Stepien, 2010). Arterial blood gas analysis was performed in ten WHWTs affected with CIPF and revealed hypoxemia in all dogs with a median of 58.9 mmHg (range 50.6 – 65.0) (laboratory reference range: 80 – 100mmHg). The 6-minute walking test was performed in ten affected WHWTs and a decreased walked distance was recorded in seven dogs (median 350m, range 232 – 488) (reference: > 420) (Lilja-Maula et al., 2014b). Bronchoscopy was performed in ten dogs and identified tracheal collapse (ten dogs), bronchi mucosal irregularity (nine dogs), bronchomalacia (four dogs), bronchiectasis (two dogs), and the presence of a moderate amount of mucus (seven dogs). Bronchoalveolar lavage fluid analysis revealed a moderate increase in the total cell count (median 2305 cells/mm³, range 420 – 9520) (reference: < 500) (Nelson et al., 2014). In six dogs a moderate increase in the percentage of neutrophils was observed (median 16%, range 2 – 76) (reference range: 0 – 10) (Nelson et al., 2014). Angiostrongylus infection was considered unlikely in all CIPF WHWTs, based on a negative Bearmann faecal analysis (three dogs), documentation of the absence of improvement of clinical signs following anti-parasitic treatment (five dogs) or a negative antigen test (Idexx Angio Detect, Idexx Laboratories) (three dogs). At the end of the study period, five WHWTs affected with CIPF were still alive, one dog was lost to follow-up and five had died or been

euthanized for respiratory failure. Lung tissue samples were available in four of these dogs and allowed the histopathologic confirmation of CIPF. Nine WHWTs were included as a control group. There were four males and five females aged from 5.7 to 15.0 years (median 10.4 years) and weighing between 6.6 to 11.0 kg (median 8.4 kg). Five of the nine control dogs were clinically healthy; the remaining four dogs had presented to the University for unrelated conditions including one dog with bilateral hip luxation surgery, one with a nasal tumor and two for postoperative check-ups following right ear conduct ablation (one dog), or rectal polyp resection (one dog). Control dogs did not have any signs or findings indicating cardiopulmonary disease. Echocardiography was performed to exclude the presence of primary cardiac disease in all control dogs.

**T-HRCT acquisition** - Butorphanol (0.2 – 0.35 mg/kg IV) was used as a sedative agent in all included dogs in combination with medetomidine (1 – 5 µg/kg IV) (four of the control dogs) or acepromazine (10 µg/kg IV) (one of the control dogs). The use of butorphanol alone in the CIPF WHWTs and four of the controls did not induce sufficient immobilization of the dogs, which required the use of additional gentle restraint (e.g. sand bags and Velcro straps) during T-HRCT$^{S}$ acquisition. Dogs were induced with a combination of diazepam (0.2 mg/kg IV) (one dog) or midazolam (0.2 – 0.3 mg/kg IV) (16 dogs) immediately followed by propofol (1.5 – 5 mg/kg IV) (all dogs). Anaesthesia was maintained by inhalation of isoflurane gas (1.5 - 2%) with 100% oxygen (all dogs). The median time between T-HRCT$^{S}$ and T-HRCT$^{GA}$ images acquisition was 6 minutes (range 3 – 23) (Table 2).

**T-HRCT interpretation** - ***Overall T-HRCT quality and motion artefacts*** **-** The overall T-HRCT$^{S}$ quality was graded as good in 11/20 examinations compared with 16/20 for T-HRCT$^{GA}$ (P = 0.176). Poor overall T-HRCT$^{S}$ quality was only observed in two WHWTs affected with CIPF owing to severe respiratory dyspnoea-related artefacts. Motion artefacts due to cardiac and/or respiratory movements were present in 18/20 T-HRCT$^{S}$ examinations compared with 7/20 for T-HRCT$^{GA}$ (P = 0.001). T-HRCT$^{S}$ motion artefacts were most frequently graded as mild (12/18) rather than moderate (4/18) or severe (2/18). T-HRCT$^{GA}$ motion artefacts were graded as mild (5/7) or moderate (2/7).

Table 2: Specific T-HRCT features obtained under sedation and general anaesthesia for each dog included in the study

| Status | Dog number. | Time between acquisitions (min) | Overall GGO score | Overall consolidation score | Overall mosaic attenuation pattern score | Cyst | Nodules | Reticulations | Subpleural bands | Parenchymal bands | Bronchial wall thickening | Bronchiectasis | Tracheal collapse |
|---|---|---|---|---|---|---|---|---|---|---|---|---|---|
| CIPF | 1 | 9 | 9 | 0 / 1 | 10 | - | - | - | - | - | + | - | + |
| | 2 | 14 | 6 / 2 | 0 | 4 / 0 | - | - | - | - | + | - | - | - |
| | 3 | 4 | 6 / 12 | 0 | 2 / 6 | - | + | - | + | - | + | + | ++ |
| | 4 | 6 | 16 | 0 / 6 | 0 / 4 | - | - | - | - | - | - | - | ++ |
| | 5 | 7 | 13 / 4 | 1 | 9 / 0 | - | - | - | - | + | + | - | - |
| | 6 | 5 | 18 | 0 | 18 | - | - | - | - | - | + | - | + |
| | 7 | 23 | 18 | 0 | 18 | - | - | - | - | - | - | - | + / - |
| | 8 | 6 | 12 | 2 / 0 | 0 | - | + | - | - | - | - | - | - |
| | 9 | 4 | 18 | 0 | 12 / 10 | - | + | - | - | - | - | - | - |
| | 10 | 4 | 6 | 0 | 6 | - | - | - | - | + | + | - | - |
| | 11 | 5 | 6 | 0 | 0 | - | - | - | - | - | - | - | - / + |
| Control | 12 | 9 | 6 | 0 | 0 | - | - | - | - | - | - | - | - |
| | 13 | 6 | 0 | 0 | 0 | + | - | - | - | - | - | - | + / - |
| | 14 | 8 | 2 | 0 | 0 | - | - | - | - | - | - | - | + / - |
| | 15 | 3 | 1 / 0 | 0 | 0 | - | - | - | - | - | - | - | + |
| | 16 | 7 | 0 | 0 | 0 | - | - | - | - | - | - | - | + / - |
| | 17 | 4 | 1 | 0 | 0 | - | - | - | - | - | - | - | - / + |
| | 18 | 10 | 0 | 0 | 0 | - | - | - | - | - | - | - | - |
| | 19 | 9 | 2 | 0 | 0 | - | - | - | - | - | - | - | - / + |
| | 20 | 5 | 2 | 0 | 0 | - | - | - | - | - | - | - | - |

+ indicates presence, and - indicates absence. Note that when two numbers or symbols are present in a box, the first one correspond to the result obtained under sedation and the second one to the result obtained under general anesthesia. If there is only one number or symbol in a box, it means that both sedation and general anesthesia yield the same result.

**T-HRCT interpretation** - ***Increased attenuation*** – Both T-HRCT$^{S}$ and T-HRCT$^{GA}$ images allowed the identification of GGO (Fig. 1) in all WHWTs affected with CIPF. Overall GGO score calculated on T-HRCT$^{S}$ images was the same as T-HRCT$^{GA}$ images (eight dogs), was greater in one dog and was lower in two dogs (Table 2). The difference in GGO grading between the two methods was statistically significant ($P < 0.001$). GGO was observed in every lung lobe in all dogs on T-HRCT$^{S}$ images, except for two of the CIPF WHWTs on T-HRCT$^{GA}$ images. In these two dogs, GGO was only observed in the cranial and accessory lung lobes. GGO was also present in six of the control WHWTs. In control dogs, GGO was scored identically in 5 dogs by T-HRCT$^{S}$ and T-HRCT$^{GA}$ (range 1 to 6) (Table 2). One control dog had an overall score of 1 on T-HRCT$^{S}$ images only (Table 2). In controls, GGO was visualized in the right and/or left cranial lung lobes (three dogs), the accessory lobe (two dog), the right caudal lung lobe (one dog), or in all lung lobes (one dog). Consolidations (Fig. 2) were observed in four of 11 WHWTs affected with CIPF but in no control dogs. Consolidations were observed by T-HRCT$^{S}$, T-HRCT$^{GA}$ or by both examinations in one, two and one WHWTs affected with CIPF respectively ($P = 0.121$). Overall consolidation score was low and ranged from 1 to 6 (Table 2). There was no lobe predilection for consolidations, which were found either in cranial or caudal lung lobes.

**T-HRCT interpretation** - ***Mosaic attenuation pattern and decreased attenuation*** - A mosaic attenuation pattern (Fig. 3) was observed in nine of 11 WHWTs affected with CIPF but not in any control dogs. The mosaic attenuation pattern was identified on T-HRCT$^{S}$, T-HRCT$^{GA}$ or in both examinations in two, one and six WHWTs affected with CIPF respectively. The overall scores were identical, higher or lower in four, three and two dogs respectively when T-HRCT$^{S}$ images were compared with T-HRCT$^{GA}$ (Table 2). Those differences in identification and grade of the mosaic attenuation pattern were statistically significant between the two examinations ($P < 0.001$). Both T-HRCT$^{S}$ and T-HRCT$^{GA}$ images allowed the identification of a cyst in the caudal left lung lobe (Fig. 4) in one control WHWT. Emphysema was not observed in CIPF or control dogs.

Fig. 1: Transverse thoracic HRCT image (lung window) of a CIPF WHWT CIPF (dog 4) under general anaesthesia at the level of the caudal lung lobes showing a generalized GGO of the lungs.

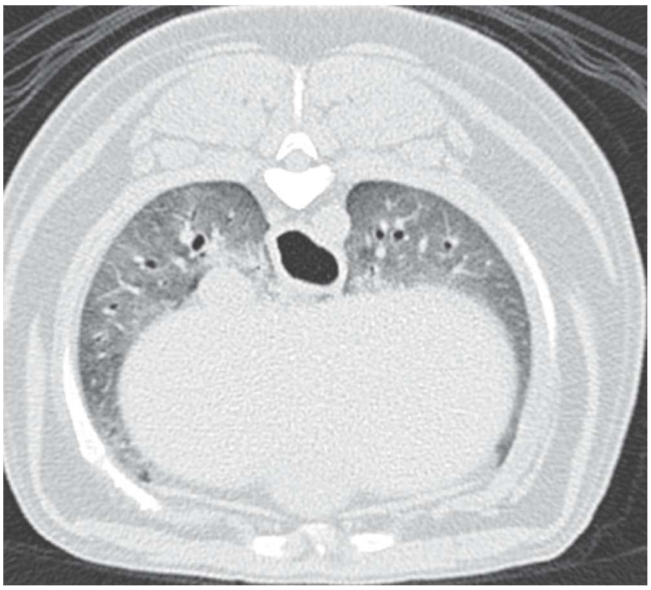

Fig. 2: Transverse thoracic HRCT image (lung window) of a CIPF WHWT (dog 4) under general anaesthesia at the level of the cranial lung lobes showing consolidations of the ventral part of the right and left cranial lung lobes in addition to ground-glass opacity in the dorsal part of the lobes.

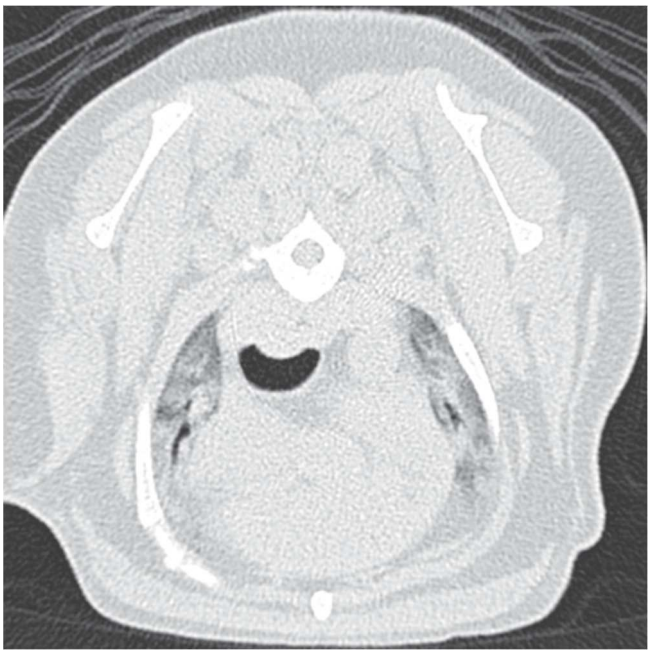

Fig. 3: Transverse thoracic HRCT image (lung window) of a CIPF WHWT (dog 6) under sedation at the level of the caudal lung lobes showing bilateral areas of higher (GGO) and lower lung attenuation (normal lung parenchyma or air trapping) resulting in a mosaic attenuation pattern.

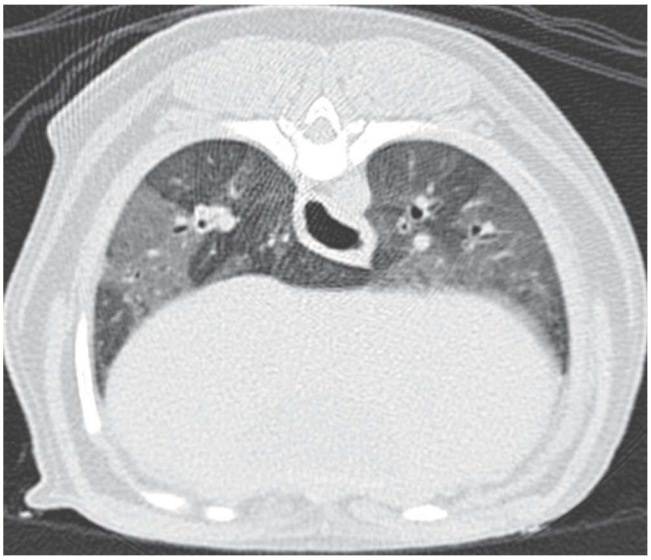

Fig. 4: Transverse thoracic HRCT image (lung window) of a control WHWT (dog 11) under sedation at the level of the caudal lung lobes showing a cyst (arrow head in the dorsal part of the left caudal lung lobe. Note the normal appearance of the remaining lung parenchyma.

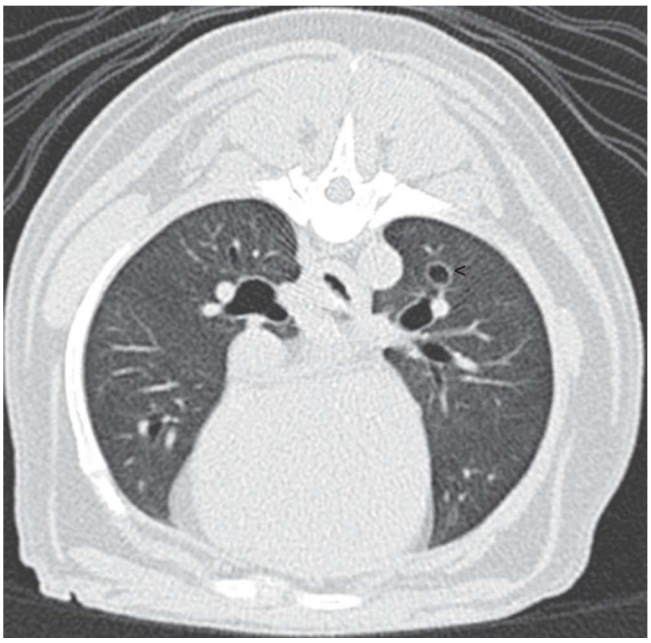

**T-HRCT interpretation** - ***Nodular opacities*** - Single or multiple nodules (Fig. 5) were noticed in two and one of 11 WHWTs affected with CIPF respectively but in no control dogs (Table 2). Nodules were localized to the right and/or left caudal lung lobes and had a median size of 4.6 mm (range 3.8 – 7.8). Nodules were identified on both T-HRCT$^{S}$ and T-HRCT$^{GA}$ images.

Fig. 5: Transverse thoracic HRCT image (lung window) of a CIPF WHWT (dog 3) under general anaesthesia at the level of the caudal lung lobes showing a nodule (arrow head) in periphery of the left lung lobe. GGO and mosaic attenuation pattern are also visible.

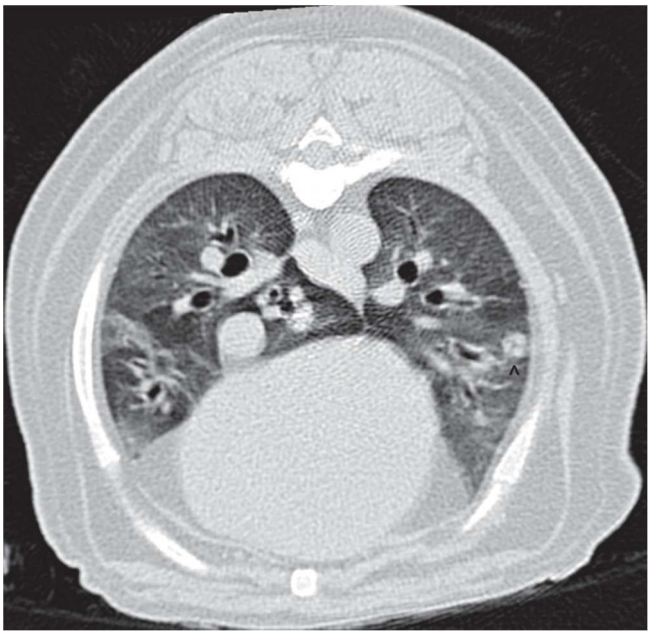

**T-HRCT interpretation** - ***Linear opacities*** - Reticulations were not seen in either CIPF or control dogs. One CIPF dog had evidence of subpleural bands, and parenchymal bands were seen in three CIPF WHWTs (Table 2). There was no difference between T-HRCT$^{S}$ and T-HRCT$^{GA}$ images in the identification of linear opacities. The subpleural bands were observed in the cranial right lung lobe and the parenchymal bands in right and/or left cranial lung lobes. Honeycombing was not observed in any dogs in this study.

**T-HRCT interpretation** - ***Other features*** - Bronchial wall thickening (Fig. 8) was recognized in five of 11 WHWTs affected with CIPF and no control dogs. Bronchial wall thickening was observed in all lung lobes in four dogs and in just the cranial lobes in one dog. Varicose bronchiectasis (Fig. 9), defined as an irregular bronchial dilatation, was observed in the right middle lobe of one CIPF WHWT (Table 2). These features were identifiable at both T-HRCT$^{S}$ and T-HRCT$^{GA}$. Tracheal collapse was observed in six of 11 WHWTs affected with CIPF and in six of nine control dogs (Table 2). In five dogs, the tracheal collapse was visible on both T-HRCT$^{S}$ and T-HRCT$^{GA}$ images, but was only visible on T-HRCT$^{S}$ in four dogs and T-HRCT$^{GA}$ in three dogs (Table 2). The tracheal collapse was considered severe in two WHWTs affected with CIPF. Neither pleural effusion nor pleural thickening were observed. Blood vessel caliber and interface with pulmonary parenchyma were within normal limits in all dogs. Lymph nodes were within normal limits in all dogs, except in one WHWT affected with CIPF in which a left cranial mediastinal lymph node appeared slightly enlarged.

Fig. 6: Transverse thoracic HRCT image (lung window) of a CIPF WHWT (dog 3) under sedation at the level of the cranial lung lobes showing a sub-pleural band (arrow heads) in the dorsal part of the right cranial lung lobe in addition to thickening of the bronchial walls and GGO.

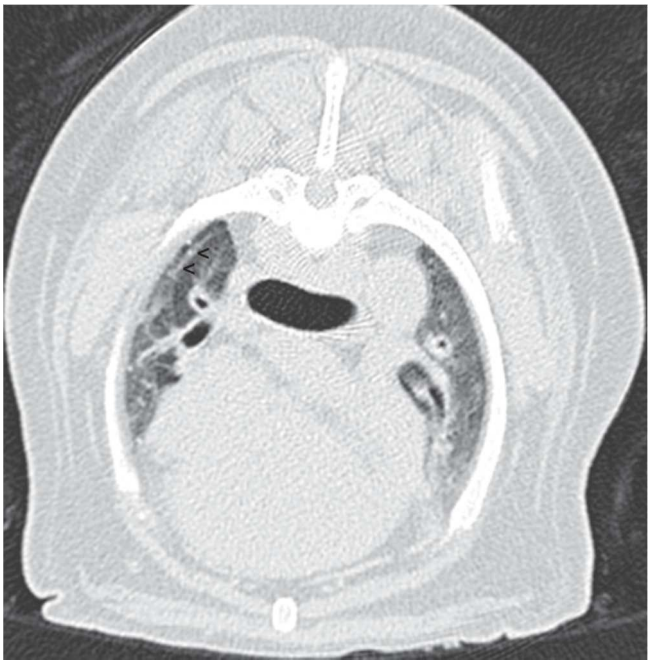

Fig. 7: Transverse thoracic HRCT image (lung window) of a CIPF WHWT (dog 2) under general anaesthesia at the level of the cranial lung lobes showing a parenchymal band (arrow heads) which extend from the visceral pleura into the lung parenchyma in the left cranial lung lobe in addition to GGO.

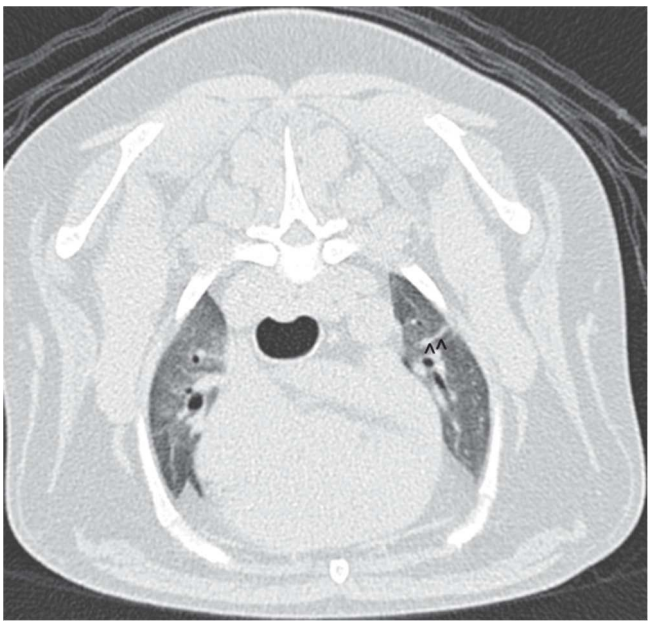

Fig. 8: Transverse thoracic HRCT image (lung window) of a CIPF WHWT (dog 9) under general anaesthesia at the level of the caudal lung lobes showing a thickening of the bronchial walls (arrow heads) and GGO, in addition to mosaic attenuation pattern in the right caudal lung lobe.

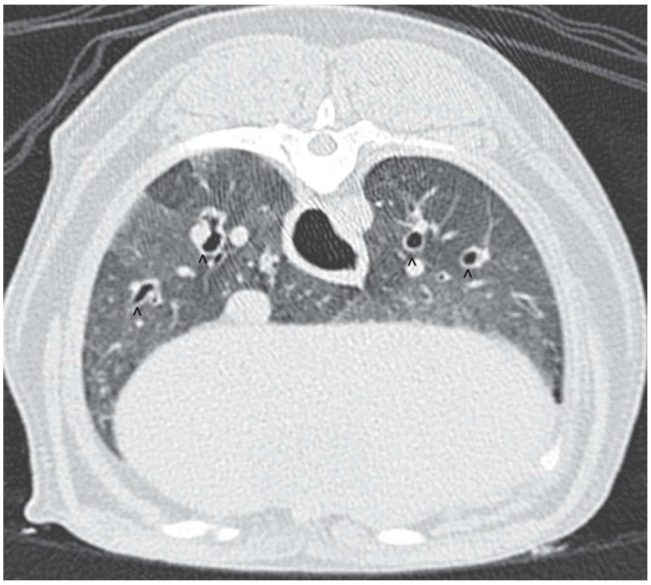

Fig. 9: Transverse thoracic HRCT image (lung window) of a CIPF WHWT (dog 3) under general anaesthesia at the level of the right middle lung lobes showing bronchiectasis (arrow heads) and GGO, in addition to mosaic attenuation pattern in the left cranial lung lobe.

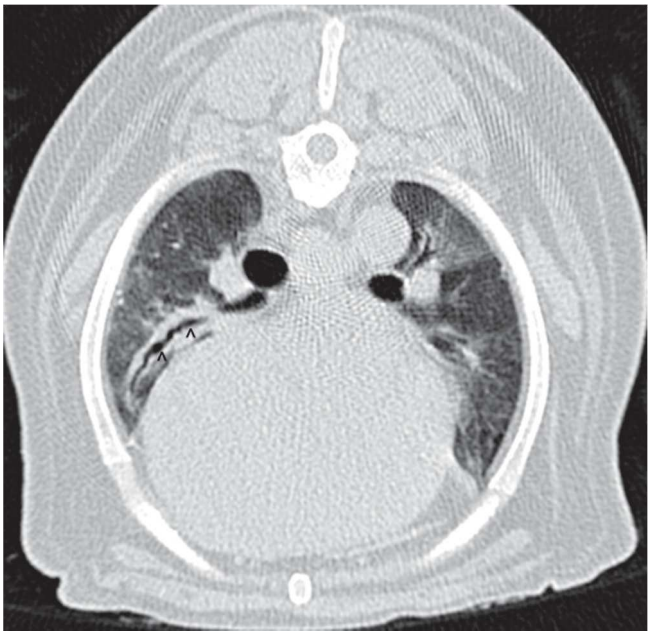

### *2.1.6. Discussion*

The present study demonstrated that T-HRCT$^{S}$ images are more frequently affected by motion artefacts than T-HRCT$^{GA}$ images, but are of sufficient quality to permit the identification of specific pulmonary features of CIPF. This finding justifies the use of sedation for CT in dogs suspected to have CIPF when general anaesthesia is contraindicated. The aim of the present study was to determine if T-HRCT$^{S}$ can be used with the same confidence as T-HRCT$^{GA}$ for the identification and grading of CIPF lesions in a diagnostic setting. Significant differences were found between T-HRCT$^{S}$ and T-HRCT$^{GA}$ examinations for grading of GGO and of mosaic attenuation pattern findings, suggesting that these examinations lack precision when determining lesion extent. However, the differences did not seem to impact the diagnostic potential of T-HRCT$^{S}$, since GGO was observed in all CIPF WHWTs on T-HRCT$^{S}$ images, with a wider distribution than seen in the control dogs and/or in association with other CIPF features not identified in control dogs. Among the features studied, GGO, mosaic attenuation pattern, and bronchial wall thickening were found to be the main T-HRCT features observed in WHWTs affected with CIPF, although they were not necessarily simultaneously present in all affected dogs. Honeycombing, the major feature of IPF in humans (Jacob and Hansell, 2015), was not observed in dogs in this study.

The differences observed between T-HRCT$^{S}$ and T-HRCT$^{GA}$ images are more likely related to the different respiratory pattern of the dogs under each condition. During sedation, dogs breathed spontaneously; CT acquisition was consequently obtained either during inspiration or expiration phases or during both phases. During general anaesthesia, an end-expiratory pause was artificially induced by providing several lung inflations to induce a transient apnoea. Such differences may have on impact on the evaluation of mosaic attenuation pattern, GGO or consolidations, since all may be influenced by the breathing pattern and the subsequent amount of air remaining in the alveoli. According to the Fleischner society, GGO may occur secondary to a reduction of air in the alveolar airspaces, although other interpretations include a partial filling of the alveolar airspaces by cells, fluids or amorphous material, a thickening of the parenchymal interstitium and alveolar walls, a relative increase in perfusion, or a combination of these (El-Sherief et al., 2014; Hansell et al., 2008). The mosaic attenuation pattern may appear in cases of patchy interstitial disease, obliterative small airway disease, or occlusive vascular disease, alone or in combination (Hansell et al., 2008). In the case of interstitial lung disease, the mosaic attenuation pattern results from hyperattenuated areas of GGO interposed with hypoattenuated areas of normal lung tissue (Hansell et al., 2008; Kligerman et al., 2015). In the case of bronchial or bronchiolar obstruction, the mosaic attenuation pattern consists of regions of hypoattenuation where air trapping has occurred,

interspersed with regions of hyperattenuation representing normal ventilation (El-Sherief et al., 2014; Kligerman et al., 2015; Ridge et al., 2011). Finally, in the case of occlusive vascular disease, regions of hypoattenuation reflect decreased blood flow and reduced vessel caliber in comparison to regions of hyperattenuation representing normal or excessive vascularization (Kligerman et al., 2015; Ridge et al., 2011). In WHWTs affected with CIPF, both underlying patchy interstitial disease and concomitant airway involvement may explain the appearance of a mosaic attenuation pattern on CT images. In human medicine, the presence of abnormalities of bronchi has proved to be a good indicator that the underlying mosaic attenuation pattern is related to small airway disease and concurrent air trapping (Kligerman et al., 2015). In humans, air trapping is generally accentuated at end-expiration, depends on the respiratory efforts of the patient at the time of image acquisition and may not be reproducible, particularly in dyspnoeic patients. This may explain why this feature was not present in all CIPF dogs included in this study (Ridge et al., 2011). Two WHWTs affected with CIPF showed signs of pulmonary hypertension on echocardiography, which may also have contributed to the appearance of a mosaic attenuation pattern, despite the absence of difference in the caliber of the vessels between the lucent and the dense part of the lung (Ridge et al., 2011). Consolidations were observed in four WHWTs affected with CIPF, but their identification varied greatly between T-HRCT$^{S}$ and T-HRCT$^{GA}$ images suggesting that this feature depends more on the ventilation pattern and the subsequent development of atelectasis, rather than on the underlying lung disease. Finally, another indication that the differences observed between sedation and general anaesthesia were more likely due to the different respiratory patterns is the fact that tracheal shape and the appearance of tracheal collapse were discordant in seven dogs. Changes in tracheal dimension during respiratory movements have previously been shown to occur in up to 24% in dogs. (Leonard et al., 2009).

Similar to previously published data about T-HRCT features of CIPF, the present study confirmed the presence of GGO in all WHWTs affected with CIPF and bronchial changes in 50% (Corcoran et al., 2011; Heikkila et al., 2011; Johnson et al., 2005). However, we described for the first time the existence of a mosaic attenuation pattern in WHWTs affected with CIPF and GGO in control WHWTs. Linear opacities were observed only in a minor proportion of CIPF dogs and honeycombing was not present in any dogs. The main explanation for the discrepancies observed between previous studies and the present one is the introduction of a new nomenclature, the glossary of terms of the Fleischner Society, which has not been employed in veterinary literature until now. Explanations for the presence of GGO in control WHWTs may relate to a reduction of air in the alveoli due to the modification of the respiratory pattern secondary to sedation or general anaesthesia. Another explanation could be that those control WHWTs were suffering from subclinical or early CIPF lesions. However, the

distribution of GGO in controls was less extensive than in CIPF WHWTs, except in one dog in which GGO was present in all lung lobes. Follow-up imaging at regular intervals and lung histopathology would be needed to confirm the presence of early CIPF lesions but neither was available. Unlike previous studies, reticulations and honeycombing were not observed in our population of WHWTs affected with CIPF and parenchymal and subpleural bands were only occasionally found in a minority of affected dogs. Beyond the different nomenclature employed, a different degree of disease severity among studied populations may be an explanation. WHWTs from our population may have been less severely affected than dogs included in previous studies. However, in the majority of the affected dogs included clinical signs had been present for several months and five WHWTs died during the study period from respiratory failure (within a median time of 8 months) suggesting that the disease was well established at the time of T-HRCT acquisition. Consequently, the absence of honeycombing in our population of CIPF dogs likely indicates a different pathophysiology or disease severity between CIPF in dogs and IPF in humans. This is an important issue that merits further investigation. Nodules were observed in three WHWTs affected with CIPF and may represent either neoplasia or granulomas. Given that an association has been already described between pulmonary carcinoma and pulmonary fibrosis in humans and cats (Aubry et al., 2002; Cohn et al., 2004), the hypothesis of neoplasia should not be discounted, but would require histopathologic confirmation.

The main limitation of the present study was the small number of dogs included. A second limitation was that histopathologic confirmation of CIPF was only available in four dogs. However, we are confident that CIPF WHWTs were suffering from the disease given that strict inclusion criteria were applied (Heikkila and Rajamäki, 2014). A third limitation was that radiologists were not blinded as to the dog's anaesthetic status. Further anaesthetic protocols for sedation were not standardized among dogs potentially influencing image interpretation. It would also have been interesting to use a positive ventilation protocol to maintain the dogs in forced full inspiration during CT acquisition under anaesthesia. However, we preferred to induce apnoea by providing several lung inflations. This technique is considered safer (less risks of barotrauma), easier and more applicable in a daily clinical practice. Streaking artefacts extending from outside the lungs onto the lung field were present on some T-HRCT images caused by photon starvation when crossing the spine and the ribs. The reconstruction process (sharp reconstruction algorithm), the thin slice thickness (1mm) and the data recording have probably magnified this noise. However, none of the radiologists found that these streaking artefacts interfered with evaluation of CIPF findings.

In conclusion, the present study demonstrated that T-HRCT$^S$ images were of sufficient quality to permit the identification of specific pulmonary features of CIPF. This justifies its use for the investigation of CIPF when general anesthesia is contraindicated. Ground-glass opacities, mosaic attenuation pattern and bronchial wall thickening were found to be the main T-HRCT features of CIPF in WHWTs. Honeycombing, the major feature of IPF in humans, was not observed in our cohort of CIPF dogs, which tends to suggest a different disease severity or pathophysiology. Further work comparing T-HRCT features of CIPF with other interstitial lung diseases in humans is warranted to improve our knowledge in comparative medicine.

## 2.2. Echocardiographic investigation of pulmonary hypertension: PV/PA

### *2.2.1. Title & authors*

**Pulmonary vein to pulmonary artery ratio in West Highland white terriers with idiopathic pulmonary fibrosis**

Elodie Roels[a], Anne-Christine Merveille[a], Emilie Krafft[a], Frederic Farnir[a], Samantha Gomart[b], Cecile Clercx[a,1], Kathleen Mc Entee[a,b,1]

[a]Department of Clinical Sciences, FARAH, Faculty of Veterinary Medicine, University of Liege, Belgium; [b]Laboratory of Physiology and Pharmacology, Faculty of Medicine, Université Libre de Bruxelles, Belgium

[1] These authors contributed equally to the elaboration and supervision of the work.

### *2.2.2. Abstract*

**Objectives**: To investigate the right pulmonary vein-to-pulmonary artery ratio (PV/PA) in West Highland white terriers (WHWTs) affected with canine idiopathic pulmonary fibrosis (CIPF) and controls, in correlation with non-invasive echocardiographic parameters of pulmonary hypertension (PH) and clinical cardiopulmonary function indices. **Animals**: Sixteen WHWTs affected with CIPF and 24 age-matched unaffected WHWTs sub-grouped according to the presence and maximal velocity of tricuspid regurgitation jet (VmaxTR). **Methods**: PV/PA, VmaxTR, acceleration time to ejection time ratio of the pulmonary artery flow (AT:ET), main pulmonary artery diameter to aortic diameter ratio (MPA/Ao) and right pulmonary artery distensibility index (RPAD Index) were retrospectively measured on saved echocardiographic images. Overall cardiopulmonary performance data, namely the arterial partial pressure of oxygen ($pO_2$) and the distance walked in 6 minute-walking test (6MWD), were recorded. Serum NT-proBNP concentrations were measured. **Results**: TR was found in

50% of CIPF-WHWTs and 25% of controls. PV/PA in both two-dimensional (2D) and M-modes (MM), was significantly lower in CIPF-WHWTs affected with PH compared with controls due to an increase in PA and a decrease in PV diameters. PV/PA was correlated with VmaxTR, AT/ET, MPA/Ao and RPAD Index, and with the 6MWD, but not with arterial $pO_2$ values nor with serum NT-proBNP concentrations. **Conclusions**: Results of the present study suggest that PV/PA can be used as a non-invasive complementary parameter for pre-capillary PH investigation in WHWTs affected with CIPF particularly if TR is absent or difficult to measure.

### *2.2.3. Introduction*

Canine idiopathic pulmonary fibrosis (CIPF) is a chronic parenchymal lung disease of unknown origin affecting mainly old West Highland white terriers (WHWTs) and sharing clinical and pathogenic features with human idiopathic pulmonary fibrosis (IPF) (Heikkila-Laurila and Rajamaki, 2014; Syrja et al., 2013). Pulmonary hypertension (PH) is a frequent co-morbidity in CIPF WHWTs, affecting more than 44% of dogs (Schober and Baade, 2006). In humans, PH occurs in up to one third of IPF patients, has a negative impact on the quality of life and is associated with a poor outcome (Hyldgaard et al., 2014; Smith et al., 2013a). Medical treatment of PH with phosphodiesterase-5 inhibitors may improve clinical signs and quality of life in patients suffering from IPF (Collard et al., 2007; Han et al., 2013; Zisman et al., 2010). Clinical improvement has also been reported in dogs with PH secondary to cardiac or pulmonary diseases treated with sildenafil (Bach et al., 2006; Kellihan et al., 2015; Kellum and Stepien, 2007). Consequently, early and accurate diagnosis of PH in CIPF WHWTs is needed for an optimal management of the disease. However, diagnosis of PH in veterinary medicine is challenging as right heart catheterization is not routinely performed in clinical situations due to the invasiveness of the procedure. Doppler-echocardiography can be used to non-invasively assess pulmonary arterial pressures (PAP) in the presence of tricuspid or pulmonic regurgitation by applying the Bernoulli principle (Currie et al., 1985). However, in the absence of a tricuspid regurgitant jet, or in situations of poor Doppler alignment, this measure may be not feasible or inaccurate (Rich et al., 2011; Soydan et al., 2015). Those diagnostic constraints enhance the need to develop new reliable non-invasive surrogate parameters for the detection of PH.

A novel echocardiographic index, the pulmonary vein to pulmonary artery ratio (PV/PA) was recently described in healthy dogs, and has been showed to be useful in the detection of congestive heart failure in dogs affected with degenerative mitral valve disease (Merveille et al., 2015). Whether this echocardiographic parameter can be used to indicate the presence of pre-capillary PH has not been investigated to our knowledge.

We hypothesized that the PV/PA ratio would decrease in WHWTs affected with CIPF due to the concomitant presence of pre-capillary PH. The study objectives were thus to compare PV/PA obtained in WHWTs affected with CIPF and unaffected controls (sub-grouped according to Doppler-echocardiographic evidence of PH), in correlation with other echocardiographic indices of PH, namely the maximal velocity of tricuspid regurgitation (VmaxTR), the acceleration time to ejection time ratio of the pulmonary artery flow (AT/ET) (Schober and Baade, 2006), the main pulmonary artery diameter to aortic diameter ratio (MPA/Ao) (Serres et al., 2007) and the right pulmonary artery distensibility index (RPAD Index) (Venco et al., 2014). Additional study objectives were to correlate PV/PA with clinically available indices of cardiopulmonary function, arterial partial pressure of oxygen ($pO_2$) and the 6-minute walked distance (6MWD), and with serum N-terminal pro-brain natriuretic peptide (NT-proBNP) concentrations, given that those complementary tools have shown to be helpful in the diagnostic approach of PH in humans and/or dogs (Andersen et al., 2012a; Hori et al., 2012; Kellihan et al., 2011; Papakosta et al., 2011).

### *2.2.4. Materials and Methods*

**Study population** - Medical records from the teaching Small Animal Veterinary Clinic of the University of Liège were reviewed for canine patients enrolled in the CIPF project between April 2013 and March 2016. The study protocol was approved by the Experimental Animals Committee of the University of Liège, Belgium (permit number: 1435, date of approval: 14 March 2013). Owner consent was obtained for all dogs enrolled. The control group included age matched-WHWTs unaffected with CIPF (Group I). Inclusion criteria for group I were: (1) absence of history of cardiovascular or pulmonary disease, and (2) normal cardiopulmonary physical examination. The CIPF groups included WHWTs with evidence of CIPF (Group II). Inclusion criteria for group II were: (1) history of cough, exercise intolerance and/or dyspnoea, (2) presence of marked inspiratory crackles on lung auscultation, and (3) imaging findings compatible with CIPF (thoracic X-rays or thoracic high resolution computed tomography - HRCT). Exclusion criteria for both groups was the presence of post-capillary PH due to left-sided cardiac disease. Both groups of dogs were subdivided into 3 separate sub-groups according to Doppler-echocardiographic evidence of PH. Subgroups IA and IIA consisted of dogs with normal VmaxTR (< 2.8 m/s), suggesting absence of systolic PH (Kellihan and Stepien, 2010). Subgroups IB and IIB included dogs with no detectable TR representing unknown status in terms of systolic PAP. Subgroups IC and IIC consisted of dogs with VmaxTR suggestive of systolic PH (≥ 2.8 m/s) (Kellihan and Stepien, 2010).

**Echocardiographic examination** - Transthoracic two-dimensional (2D), M-mode (MM) echocardiography and conventional Doppler-echocardiography were performed by three

trained observers (KME, ACM and EK) using an ultrasound unit (Vivid I, General Electric Medical System) equipped with 2.2–3.5 and 5.5–7.5 MHz phased-array transducers. Dogs were placed in right and left lateral recumbency and a simultaneous one-lead ECG was recorded. Standard right parasternal (long and short axis) and left apical parasternal views were used for data acquisition. All measurements were performed off-line by a single trained investigator (KME). Heart rate was calculated by averaging at least ten RR intervals obtained on different echocardiographic views. Right ventricle hypertrophy, right ventricle dilatation and septal flattening were subjectively assessed and recorded when present. The right and left atrial diameters were measured in the 2D right parasternal four-chamber view long axis view at the end of the T-wave. The right atrium was considered to be dilated if the diameter was greater than or equal to the diameter of the left atrium (Serres et al., 2006). A right parasternal long axis four-chamber view was optimized to simultaneously see the medial pulmonary vein (PV) in longitudinal section and the right pulmonary artery (PA) in cross-section. Measurements of PV and PA diameters were taken in MM and 2D as previously described (Merveille et al., 2015). Dimensions of both vessels were obtained by tracing a line perpendicular to the medial PV and passing through the centre of the adjacent right PA. For both measurements, the inner edge to inner edge method was used at the end of the T wave (systole). Fig. 1 illustrates 2D and MM images of PV and PA obtained in one CIPF WHWT and in one control.

Fig.1: Echocardiographic images of PV/PA in CIPF and controls. (A) PV/PA (2D) obtained in a control WHWT; (B) PV/PA (2D) obtained in a WHWT affected with CIPF; (C) PV/PA (MM) obtained in a control WHWT; (D) PV/PA (MM) obtained in a WHWT affected with CIPF.

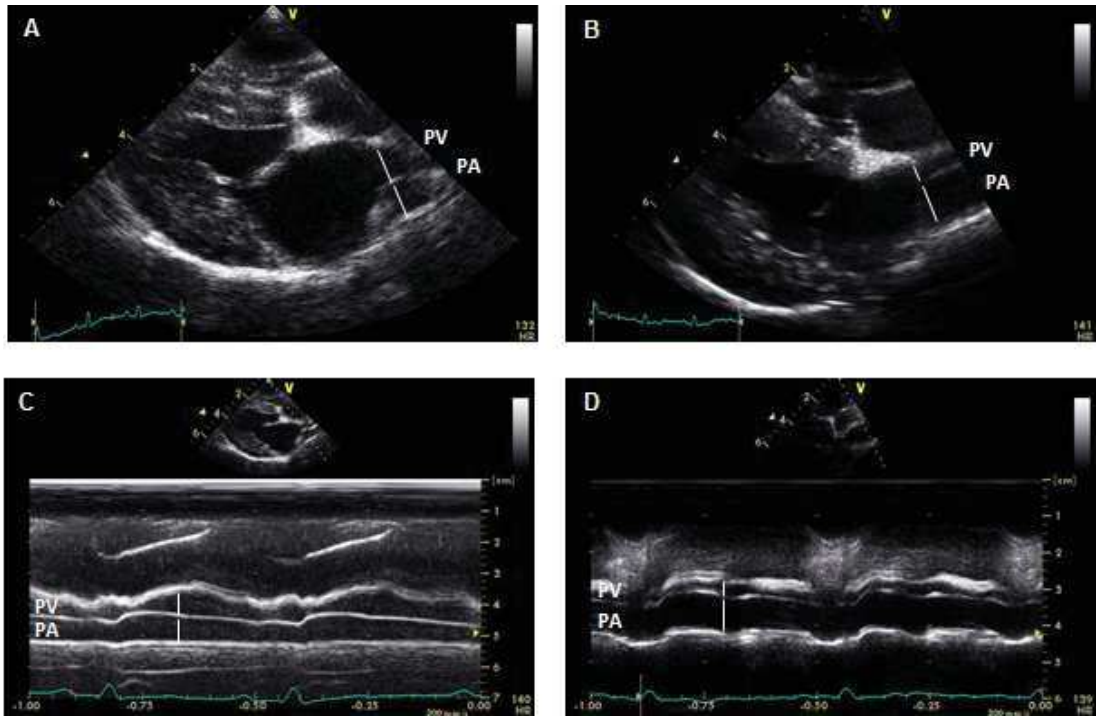

The right PA diameter was also measured at the end of the Q wave (diastole) in MM to calculate the RPAD Index following the formula: [(systolic diameter – diastolic diameter)/systolic diameter] (Venco et al., 2014). Aorta and main pulmonary artery diameters were measured in 2D from the right parasternal short axis view optimized on the right ventricular outflow tract to calculate their ratio (MPA/Ao) (Serres et al., 2007). Pulmonary flow was recorded on the same view with the pulsed wave Doppler sample positioned centrally in the flow stream between the opened pulmonic valve leaflets. The acceleration time and ejection time were measured to calculate the AT:ET ratio (Schober and Baade, 2006). Similar technique was used to record pulmonary regurgitation and measure peak regurgitation velocity (VmaxPR). A VmaxPR higher than or equal to 2.2 m/s was considered abnormal and indicative of PH (Kellihan and Stepien, 2010). The tricuspid valve was systematically evaluated for evidence of regurgitation. If a tricuspid regurgitant jet was visible, its maximal velocity (VmaxTR) was recorded. A VmaxTR higher than or equal to 2.8 m/s was considered abnormal and indicative of PH (Kellihan and Stepien, 2010). Post-capillary PH was excluded based on normal left atrial and ventricular dimensions, the absence of significant mitral regurgitation and normal left ventricular systolic function.

**6-minute walking test** - 6-minute walking test was performed as previously described (Manens et al., 2014). Dogs were walked on a leash along a 53m L-shaped corridor at their own pace for 6 minutes and the distance covered (6MWD) was measured in meters.

**Arterial blood gas analysis** - Arterial blood gas analyses was performed as previously described (Roels et al., 2016). Arterial blood was drawn from the metatarsal artery with a 25G needle in 2ml-heparinised syringe after subcutaneous injection of local anaesthetic for analgesia. Immediately after blood sampling, air bubbles were removed from the syringe and the syringe closed with an airtight lid before being gently mixed by repeated inversion. Blood gas analysis was then performed immediately on a point-of-care blood gas analysers available in the clinic (Cobas b-123 POC system, Roche diagnostics). The patient's rectal temperature was recorded to allow correction of measurements according to body temperature.

**NT-proBNP measurement** - Blood samples were drawn from the jugular vein and collected in plain tubes. Thirty minutes after blood collection, tubes were centrifuged at 4 °C for 15 min at 1300 x g. Serum was transferred into 1.5 mL plastic cryotubes and stored at -80 °C until analysis. Batched serum samples for NT-proBNP concentration measurement were shipped to assay laboratory (Cardiopet NT-proBNP, IDEXX Laboratories, Vet Med Labor GmbH) on dry ice according to manufacturer's guidelines.

**Statistical analysis** - Statistical analyses were performed using commercially available software (XLstat software, Addinsoft SARL). Continuous variables were reported as median and range (minimum and maximum), and categorical data as percentage. The Shapiro-Wilk test was applied to assess the distribution of continuous variables. Differences in continuous variables between groups I and II were performed using Student t-test for normally distributed variables with equal variance or Mann-Whitney test for variables that were not normally distributed or with unequal variance. Kruskal-Wallis test with subsequent pairwise comparisons using the Dunn test with Bonferroni correction was employed to compare continuous results obtained in the different subgroups. Results of statistical procedures with regard to PV/PA and other echocardiographic indices of PH were also depicted graphically by means of scatter plots and box plots respectively. Proportions were compared using the Fisher exact test. Correlations between PV/PA and other echocardiographic parameters studied (VmaxTR, AT/ET, MPA/Ao, RPAD Index), clinical parameters of disease severity (arterial $pO_2$ and 6MWD) or serum NT-proBNP concentrations were performed using Pearson or Spearman correlations according to variable distribution. For all analyses, P-value $\leq 0.05$ was considered statistically significant.

### *2.2.5. Results*

**Study population** - Forty WHWTs were included in the study: 24 unaffected control WHWTs (Group I) and 16 WHWTs affected with CIPF (Group II). No statistical difference in age, body weight, gender repartition and heart rate was noted between groups I and II. Detailed features of the study population according to subgroups division are summarized in Table 1. Tricuspid valve regurgitation was found in 8 CIPF WHWTs (50%) and 6 controls (25%) (P = 0.196). Five (31%) WHWTs affected with CIPF and 3 (12.5%) controls had TR peak velocity above 2.8m/s, suggestive of systolic PH. Pulmonary valve regurgitation was found in 3 (12.5%) control WHWTs and 3 (19%) WHWTs affected with CIPF (P = 0.669). Peak PR velocity was ≤ 1.48 m/s in control WHWTs. In CIPF WHWTs, peak PR velocity was above 2.2m/s in 1 dog from subgroup IIB, suggesting increased diastolic PA pressure in this dog.

Table 1. Characteristics of the study population.

| | Control WHWTs (n = 24) (Group I) | | | CIPF WHWTs (n = 16) (Group II) | | |
|---|---|---|---|---|---|---|
| | Normal PAP (IA) (n = 3) | Unknown PAP (IB) (n = 18) | PH (IC) (n = 3) | Normal PAP (IIA) (n= 3) | Unknown PAP (IIB) (n = 8) | PH (IIC) (n = 5) |
| Sex, F/M | 0/3 | 9/9 | 0/3 | 2/2 | 4/4 | 1/3 |
| Age, yr. | 8.8 (6.2 – 9.3) | 9.4 (3.1 – 15.2) | 11.6 (11.0 – 12.6) | 11.6 (5.2 – 14.5) | 11.3 (5.7 – 13.4) | 10.7 (9.9 – 13.9) |
| Body weight, kg | 9.6 (9.2 – 10.8) | 8.4 (6.6 – 10.5) | 10.4 (6.8 – 11.0) | 9.7 (8.4 – 10.0) | 9.1 (6.8 – 16.6) | 9.3 (6.3 – 14.4) |
| Heart rate, bpm | 119 (96 – 138) | 111 (79 – 153) | 114 (98 – 121) | 109 (86 – 119) | 109 (77 – 133) | 106 (88- 141) |
| TR, n | 3 | 0 | 3 | 3 | 0 | 5 |
| VmaxTR, m/s | 1.73 (1.53 – 2.61) | n.d. | 3.12 (3.08 – 3.30) | 2.22 (1.99 – 2.66) | n.d. | 3.18 (2.85 – 4.34) |
| PR, n | 0 | 2 | 1 | 0 | 3 | 0 |
| VmaxPR, m/s | n.d. | 1.45 (1.41 – 1.48) | 0.94 (n.d.) | n.d. | 1.79 (1.67 – 2.64) | n.d. |

From the 24 control WHWTs included in the study, 17 were clinically healthy at the time of echocardiography. The remaining 7 dogs enrolled in the study were presented for bilateral hip luxation surgery, postoperative recheck following rectal polyp resection, postoperative recheck after right ear canal ablation, demodicosis, urinary incontinence, bilateral otitis extern and with a unilateral nasal tumor. Control dogs did not have any signs or findings indicating pulmonary or cardiovascular disease, and had serum biochemical and haematological results within laboratory reference ranges or only mildly increased (for alkaline phosphatase and platelet count). At the time of echocardiography, 2 control dogs were treated with amoxicillin-clavulanic acid (20mg/kg q12h PO), 2 dogs with prednisolone (0.5mg/kg q24h PO), 1 dog with piroxicam (0.3mg/kg q24h PO) and 1 dog with moxidectin (0.2mg/kg q24h PO). Thoracic HRCT was performed in 18 out of 24 control WHWTs and did not reveal significant abnormalities, except localized ground-glass opacity (GGO) in cranial lung lobes in 11 of them (2 dogs from sub-group IA, 7 from sub-group IB, and 2 from sub-group IC). Among the 16 WHWTs affected with CIPF included, 8 of them had a history of both exercise intolerance and cough, 3 had exercise intolerance alone and 5 dogs exhibited cough. Crackles were noticed on lung auscultation in all CIPF WHWTs, mild restrictive dyspnoea was present in 10 dogs and

cyanosis was observed in 4 dogs. At the time of echocardiographic examination, treatments started by the referring veterinarian included prednisolone in 6 dogs (0.25 – 0.7 mg/kg q12-24h PO), furosemide in 2 dogs (2 mg/kg q12h PO), pimobendan in 2 dogs (0.2 mg/kg q12h PO), benazepril in 1 dog (0.5 mg/kg q 24h PO), theophylline in 1 dog (11 mg/kg q12h PO) and codeine in 1 dog (1 mg/kg q12h PO). Thoracic HRCT was performed in 13 out of 16 WHWTs affected with CIPF and revealed GGO in all of them in a more extensive distribution than in controls WHWTs. Other HRCT findings included a combination of bronchial wall thickening, consolidation, parenchymal and subpleural bands, nodules and bronchiectasis. Thoracic X-rays images were available in the remaining 3 WHWTs affected with CIPF and displayed a diffuse bronchointerstitial pattern consistent with the CIPF diagnosis. WHWTs affected with CIPF had significantly lower arterial $pO_2$ values and 6MWD in comparison with controls (Table 2). At the end of the study period, 6 WHWTs affected with CIPF were still alive, 1 dog was lost of follow-up and 9 died or were euthanized for respiratory failure. Lung tissue samples were available in 6 of these dogs and allowed the histopathological confirmation of the CIPF diagnosis.

Table 2: Results of cardiopulmonary function tests.

| Parameters | n | CIPF dogs | n | Control dogs | *P*-value |
|---|---|---|---|---|---|
| pO2 (mmHg) | 6 | 86.0 (61.0 – 101.6) | 14 | 58.9 (42.0 – 77.0) | 0.0004 |
| 6MWD (m) | 19 | 480 (322 – 617) | 14 | 333 (192 – 530) | < 0.0001 |

**Echocardiographic results** - Results of the subjective assessment of the right heart are summarized in Table 3. Concentric right ventricular hypertrophy was more frequently observed in WHWTs from group II (75%, N = 12) than from group I (12.5%, N = 3) (P < 0.001). Right ventricle dilatation, septal flattening, and right atrium dilatation were recorded only in some of the CIPF WHWTs, but in any of the controls (Table 3). Echocardiographic data are presented in Table 4. A trend for an increase of MPA/Ao and a decrease of AT:ET and RPAD Index was noted in CIPF WHWTs affected or potentially affected with PH (subgroups IIB and IIC) in comparison with control WHWTs considered non affected with PH (subgroups IA and IB) (Table 4 and Figs *2A – 2C).* A significant difference was found for AT:ET between subgroups IA and IIB (P = 0.002).

Table 3. Characteristics of the study population.

| | Control WHWTs (n=24) (Group I) | | | CIPF WHWTs (n=16) (Group II) | | |
|---|---|---|---|---|---|---|
| | Normal PAP (IA) (n = 3) | Unknown PAP (IB) (n = 18) | PH (IC) (n = 3) | Normal PAP (IIA) (n = 3) | Unknown PAP (IIB) (n = 8) | PH (IIC) (n = 5) |
| RV hypertrophy | 1 | 1 | 1 | 3 | 6 | 3 |
| RV dilatation | 0 | 0 | 0 | 1 | 2 | 0 |
| RA dilatation | 0 | 0 | 0 | 0 | 2 | 0 |
| Septal flattening | 0 | 0 | 0 | 0 | 1 | 2 |

Table 4. Doppler-echocardiographic results.

| | Control WHWTs (n = 24) (Group I) | | | CIPF WHWTs (n = 16) (Group II) | | |
|---|---|---|---|---|---|---|
| | Normal PAP (IA) | Unknown PAP (IB) | PH (IC) | Normal PAP (IIA) | Unknown PAP (IIB) | PH (IIC) |
| AT:ET | 0.517[a] (0.491-0.598) (n = 3) | 0.470 (0.405-0.547) (n = 17) | 0.470 (0.419-0.527) (n = 3) | 0.457 (0.367-0.463) (n = 3) | 0.382[a] (0.272-0.481) (n = 8) | 0.379 (0.334-0.551) (n = 5) |
| MPA/Ao | 0.852 (0.751-0.877) (n = 3) | 0.831 (0.722-1.061) (n = 17) | 0.912 (0.869-0.954) (n = 3) | 0.860 (0.822-0.898) (n = 2) | 0.928 (0.744-1.146) (n = 8) | 1.020 (0.887-1.324) (n = 4) |
| RPAD Index, % | 40.0 (37.8 – 47.0) (n =3) | 41.0 (20.3 – 59.1) (n = 13) | 28.4 (21.5 – 35.2) (n = 2) | 31.2 (30.8 – 31.6) (n = 2) | 29.5 (10.0 – 45.6) (n = 7) | 27.0 (16.7 – 31.5) (n = 3) |

[a] indicates statistical difference between groups with a P-value of 0.002.

Fig. 2: Box plots illustrating MPA/Ao (A), AT:ET (B) and RPAD Index (C) obtained in control WHWTs (group I) and WHWTs affected with CIPF (group II). Subgroups A consisted of dogs with normal VmaxTR (< 2.8 m/s), subgroups B included dogs with no detectable TR, and subgroups C consisted of dogs with VmaxTR suggestive of systolic PH (≥ 2.8 m/s). The box represents the interquartile range, with the median indicated by the horizontal line. The whiskers extend from the minimum to the maximum values. [a] indicates statistical difference between groups with a P-value of 0.002.

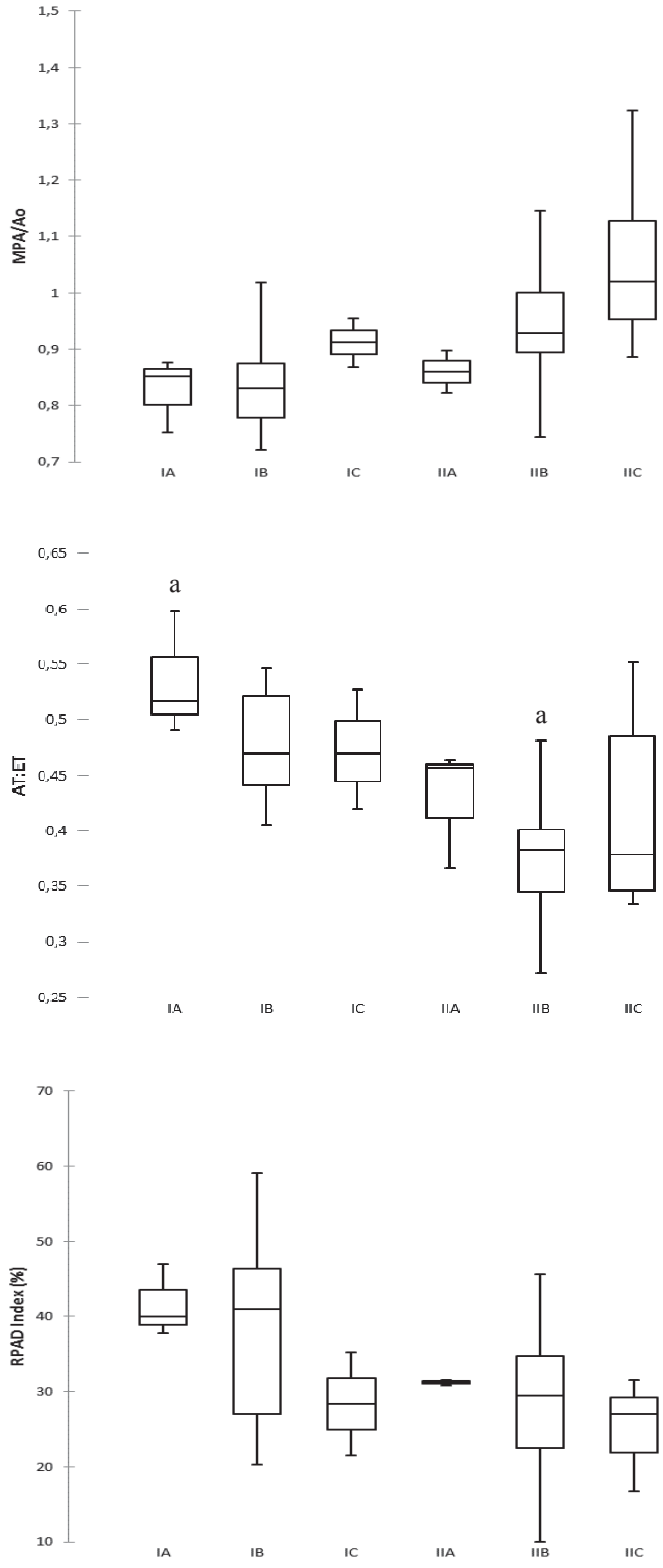

**Pulmonary vein to pulmonary artery ratio-** Echocardiographic images for PV/PA measurements were obtained in all control dogs in both modes, and in all but two CIPF WHWTs in 2D, due to respiratory related artefacts. The PV/PA ratio was significantly decreased in CIPF WHWTs affected with PH (subgroup IIC) in comparison with controls considered non-affected with PH (subgroups IA and IB) in both modes (Table 5 and Fig. 3). This decrease resulted from both an increase in PA diameter and a decrease in PV diameter in CIPF WHWTs affected with PH (Table 5). Correlations between PV/PA in 2D and MM and other Doppler-echocardiographic parameters and clinical parameters of cardiopulmonary function are presented in Table 6. Significant moderate correlations were found between PV/PA measured in both modes and VmaxTR, AT/ET, MPA/Ao, RPAD Index and 6MWD, but not with arterial $pO_2$ values.

**NT-proBNP measurement -** There was no significant difference in serum NT-proBNP concentrations between group I (median 608 pmoL/L, range 250 – 1599) and group II (745 pmoL/L, 250 – 2080) (P = 0.375), neither between the different sub-groups (P = 0.162). There was no correlation between PV/PA and serum NT-proBNP concentration (Table 6).

Table 5: PV/PA results.

| | Control WHWTs (n = 24) (Group I) | | | CIPF WHWTs (n = 16) (Group II) | | |
|---|---|---|---|---|---|---|
| | Normal PAP (IA) (n = 3) | Unknown PAP (IB) (n = 18) | PH (IC) (n = 3) | Normal PAP (IIA) (n = 3) | Unknown PAP (IIB) (n = 8) | PH (IIC) (n = 5) |
| PV (MM) (mm) | 9.1[a] (7.7 – 9.6) | 7.4[b] (4.2 – 10.1) | 6.7 (5.4 – 8.2) | 5.7 (4.4 – 8.1) | 5.6 (3.1 – 8.9) | 3.7[ab] (2.4 – 4.7) |
| PA (MM) (mm) | 8.3 (8.3 – 9.0) | 7.3[cd] (6.3 – 8.5) | 8.4 (6.8 – 9.0) | 8.5 (8.5 – 9.5) | 9.2[c] (7.6 – 9.9) | 9.8[d] (8.2 – 10.3) |
| PV/PA (MM) | 1.012[e] (0.934 - 1.165) | 1.041[fg] (0.636 - 1.296) | 0.800 (0.793 - 0.910) | 0.667 (0.458 - 0.960) | 0.674[f] (0.337 - 0.936) | 0.370[eg] (0.234 - 0.527) |
| PV (2D) (mm) | 7.7[h] (6.2 – 7.8) | 7.0[i] (4.0 – 7.4) | 6.5 (5.3 – 7.2) | 4.7 (4.1 – 5.4) | 4.9 (3.3 – 7.4) | 3.5[hi] (1.8 – 3.6) |
| PA (2D) (mm) | 7.8 (5.9 – 7.9) | 6.9[j] (5.5 – 7.9) | 8.3 (7.0 – 8.9) | 7.9 (7.0 – 8.8) | 8.4 (6.3 – 9.3) | 9.1[j] (8.4 – 9.9) |
| PV/PA (2D) | 0.990[k] (0.983 - 1.060) | 0.948[l] (0.625 - 1.063) | 0.760 (0.737 - 0.871) | 0.618 (0.462 - 0.774) | 0.621 (0.391 - 0.879) | 0.372[kl] (0.187 - 0.428) |

Statistically significant differences are indicated by superscript lowercase letters ($P \leq 0.003$).

Fig. 3: Scatter plots illustrating PV/PA in both MM (A) and 2D (B) obtained in control WHWTs (group I) and WHWTs affected with CIPF (group II). Subgroups A consisted of dogs with normal VmaxTR (< 2.8 m/s), subgroups B included dogs with no detectable TR, and subgroups C consisted of dogs with VmaxTR suggestive of systolic PH (≥ 2.8 m/s).23 Median is indicated by the horizontal line. Statistically significant differences are indicated by superscript lowercase letters (P ≤ 0.003).

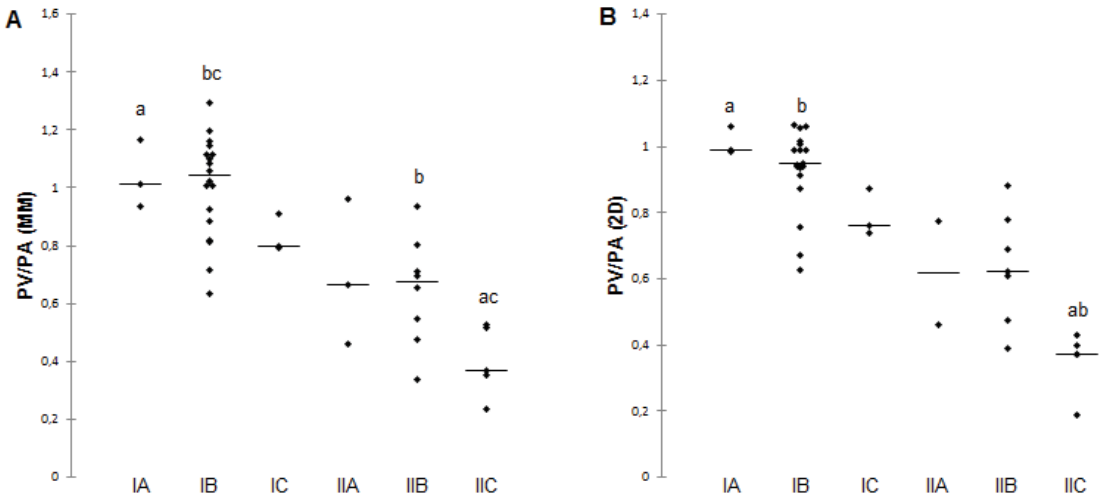


Table 6: Results of correlation analysis.

| | PV/PA (2D) | | | PV/PA (MM) | | |
|---|---|---|---|---|---|---|
| | n | r | *P* | n | r | *P* |
| VmaxTR | 13 | -0.604 | 0.032 | 14 | -0.609 | 0.021 |
| AT:ET | 37 | 0.516 | 0.001 | 39 | 0.524 | 0.001 |
| MPA/Ao | 35 | -0.456 | 0.006 | 37 | -0.493 | 0.002 |
| RPAD Index | 30 | 0.548 | 0.002 | 30 | 0.603 | 0.0004 |
| pO2 | 18 | 0.457 | 0.057 | 20 | 0.391 | 0.088 |
| 6MWD | 31 | 0.605 | 0.0004 | 33 | 0.564 | 0.001 |
| NT-proBNP | 34 | -0.146 | 0.408 | 35 | -0.267 | 0.120 |

### *2.2.6. Discussion*

Assessment of PH is challenging in veterinary medicine. Catheterization of the right heart is not routinely performed and Doppler-estimation of PAP via the measurement of VmaxTR is not always feasible or accurate (Kellihan and Stepien, 2010; Soydan et al., 2015). In the present study, we compared PV/PA values obtained in WHWTs affected with CIPF and age-matched unaffected controls to investigate whether PV/PA could serve as a potential indicator of the presence of pre-capillary PH. We demonstrated that PV/PA ratio was decreased in CIPF WHWTs affected with PH compared with controls non-affected with PH. PV/PA was correlated with VmaxTR, AT/ET, MPA/Ao and RPAD Index, as well as with the 6MWD, which highlights the potential usefulness of this parameter as a non-invasive complementary tool for pre-capillary PH determination in CIPF WHWTs.

Birettoni and collaborators (2010) first described the use of the PV/PA ratio at the 20$^{th}$ ECVIM Congress. They reported a mean PV/PA (MM) of 1 in healthy dogs. This finding has since been confirmed in MM and 2D (Merveille et al., 2015). In this recent study, PV/PA was shown to have good inter-observer reproducibility, to gradually increase with the stage of heart failure and to discriminate dogs in congestive heart failure from asymptomatic dogs suffering from degenerative mitral valve disease. In the present study, a PV/PA value of 1 was again found in healthy dogs and significant lower PV/PA values were found in CIPF WHWTs affected with PH in comparison with controls. The reduced PV/PA was attributable to both an increase in PA diameter and a decrease in PV diameter. Pulmonary artery distension may be explained by an increased pulmonary vascular bed resistance due to the chronic hypoxic vasoconstriction and/or the remodelling of parenchymal lung vessels associated with the underlying progressive fibrotic lung disease (Fulton and Ryerson, 2015). Explanations for the decreased PV diameter can be a reduction of left ventricular preload secondary to increased pulmonary arterial resistance, a compression of the vein by the enlarged adjacent artery or a combination of both. Diuretics administration may also have contributed to decreased preload in some dogs.

Tricuspid regurgitation was found in 50% of WHWTs affected with CIPF. Five (31%) CIPF WHWTs had VmaxTR equal or above 2.8m/s, suggestive of systolic PH. These results are close to previous data published by Schober and Baade (2006), and are in agreement with the human literature where Doppler regurgitation signals adequate for the calculation of systolic PAP were found in only 27% to 48% of people with IPF (Arcasoy et al., 2003; Nathan et al., 2008). Surprisingly, a VmaxTR above 2.8m/s was also found in three (12.5%) controls. Although Doppler measurement of VmaxTR generally tends to underestimate PAP, overestimation is also possible as recently demonstrated by Soydan and associates (2015).

Another explanation for the elevated VmaxTR found in control WHWTs can be that these control dogs were suffering from subclinical early CIPF lesions at the time of echocardiographic examination. The localised GGO observed on thoracic HRCT images of 2 of these control WHWTs may potentially corroborate such a hypothesis or simply reflect ventilation artefacts. Histopathological examination of lung tissue and/or follow-up at regular intervals would be needed to answer this issue, but is out of the scope of the present study.

Doppler-derived systolic time intervals of pulmonary flow, MPA/Ao ratio and RPAD Index have all previously been described as indirect predictors of PH in dogs and were also measured here. Significant decrease of AT/ET was found in CIPF WHWTs from subgroup IIB compared with controls from subgroup IA. This observation tend to confirm results previously obtained in CIPF WHWTs (Schober and Baade, 2006) and in dogs with PH of different aetiologies (mainly left heart disease and various respiratory disorders) (Serres et al., 2007). No difference was found between subgroups for MPA/Ao and RPAD Index probably due to the small sample size and inherent statistical error of type II. A trend for an increase MPA/Ao and a decrease RPAD Index in CIPF-WHWTs from subgroups IIB and IIC compared with controls from subgroups IA and IB was observed, which supports work previously published in the veterinary literature about the use of those indirect echocardiographic parameters of PH.

Significant moderate correlations were found between PV/PA and VmaxTR, AT/ET, MPA/Ao and RPAD Index. Those correlations in addition to the finding that PV/PA was reduced in CIPF WHWTs affected with PH highlighted the potential application of the PV/PA ratio as an indirect non-invasive marker of PH. Significant moderate correlations were also found between PV/PA and 6MWD, while only a trend was observed with arterial $pO_2$ values. These two cardiopulmonary function indices have been shown to be decreased in CIPF WHWTs and to reflect disease cardiopulmonary severity and progression (Lilja-Maula et al., 2014b). In humans, both arterial $pO_2$ and 6MWD were found to be independent predictors of the presence of PH in IPF patients and to serve as complementary tools for PH assessment (Minai et al., 2012; Papakosta et al., 2011). Consequently, the finding that PV/PA was correlated with 6MWD reinforced its potential utility for PH assessment in dogs, despite the absence of correlation with arterial $pO_2$ values more likely due to the small population size.

Serum NT-proBNP concentrations did not differ between groups, and there was no correlation with PV/PA values. In humans, low NT-proBNP concentrations may be used to rule out PH in patients with interstitial lung disease (Andersen et al., 2012b). In dogs, only two papers have been published to date concerning the utility of NT-proBNP in PH assessment. An overlap of data between dogs with or without precapillary PH were found, with NT-proBNP concentrations significantly increased only in dogs with severe PH (Hori et al., 2012; Kellihan

et al., 2011). In our study, the lack of difference between groups could therefore simply reflect the fact that CIPF WHWTs were suffering from mild to moderate, but not severe PH.

The main limitation of the present study was that PAP was not directly measured by right heart catheterization. This technique was not chosen because it is invasive, has inherent risk of complications and would have required a longer duration of general anaesthesia than for thoracic HRCT alone. The second limitation of the present study was that solely a small proportion of dogs included had a measureable TR allowing the estimation of PAP. Finally, 5 WHWTs affected with CIPF were receiving cardiac treatments at the time of echocardiography which could have interfered with the measurements.

In conclusion, results of the present study highlighted the potential usefulness of PV/PA as a non-invasive complementary tool for pre-capillary PH determination in WHWTs affected with CIPF. Further studies are needed to validate this new parameter in larger cohorts of dogs, and to establish reference ranges and cut-off values according to PAP measured by right heart catheterization or estimated by Doppler-echocardiography. It also remains to be determined whether the PV/PA ratio may serve as a monitoring tool of PH therapy in CIPF dogs and may be used for the assessment of precapillary PH of other origins.

## 3. Investigation of biomarkers

Serum and BALF concentrations of CCL2 and CXCL8 chemokines were measured by ELISA in samples obtained from WHWTs affected with CIPF and healthy controls in order to determine if these molecules may serve as markers for the presence of pulmonary fibrosis. Serum CCL2 concentrations were also measured in a series of WHWTs affected with CIPF with available long-term follow-up to determine if concentrations measured at diagnosis may serve as a prognostic factor for CIPF-related survival. Pulmonary expression of genes encoding CCL2, CXCL8, and their respective receptors CCR2 and CXCR2, was assessed by relative qRT-PCR and sources of CCL2 and CXCL8 were localised within the lung by immunohistochemistry to better understand whether those chemokines may act in the pathogenesis of the disease. Finally, with the hypothesis that higher basal blood concentrations of pro-fibrotic molecules may predispose the WHWT breed to develop CIPF, serum concentrations of CCL2, CXCL8, VEGF, and 5-HT were compared between the WHWT breed and 6 other breeds of dogs with variable predisposition for CIPF.

Results of this investigation led to the publication of 2 original articles in *The Veterinary Journal* and in *Research in Veterinary Sciences* (see below pages 126 to 139).

### 3.1. Serum CCL2 and CXCL8 concentrations: CIPF WHWTs vs. healthy controls

Blood samples were obtained in plain tubes from 14 WHWTs affected with CIPF and 18 control WHWTs (Table 1). Thirty minutes after blood collection, tubes were centrifuged at 4 °C for 15 min at 1300 x g. Serum was harvested and transferred into 1.5 mL plastic cryotubes, and samples were stored at -80 °C until analysis.

Table 1: Characteristics of the study population used for serum chemokine dosages.

| Parameters | CIPF WHWTs | Healthy WHWTs |
|---|---|---|
| n | 14 | 18 |
| Gender, M/F | 10/4 | 8/10 |
| Age, years | 11<br>(4.7 – 13.9) | 9.2<br>(2.9 – 16.9) |
| Weight, Kg | 10.6<br>(8.4 – 15.0) | 8.8<br>(7.4 – 12.0) |

Serum CCL2 and CXCL8 measurements were performed using commercial canine ELISA kits (Quantikine ELISA Canine CCL2/MCP-1 Immunoassay and Quantikine ELISA Canine CXCL8/IL8 Immunoassay, R&D Systems) in duplicate, according to the manufacturer's instructions. For CCL2, a first run was performed with samples from 10 WHWTs with CIPF and 10 healthy WHWT controls (Krafft et al., 2013). A second run was performed later on samples from 4 newly diagnosed CIPF cases and 8 additional controls. For CXCL8, all of the samples were analysed together, but analyses were repeated on diluted samples (1:10) in a second run, given that some of the results obtained in the first run were above the highest standard.

Serum CCL2 concentrations were found significantly increased in WHWTs affected with CIPF (median 557.7 pg/mL, range 244.8 - 1446.4) in comparison with controls (256.4 pg/mL, 120.9 – 514.4, P = 0.001) (Fig. 1A). For serum CXCL8 concentrations, no significant difference was observed between WHWTs affected with CIPF (4169.2 pg/mL, 1985.2 – 6874.0) and control WHWTs (3558.4 pg/mL, 2108.0 – 6714.1) (P = 0.608) (Fig. 1B).

Fig. 1: Serum CCL2 concentrations (pg/mL) (A) and CXCL8 concentrations (pg/mL) (B) obtained from WHWTs affected with CIPF and control WHWTs matched for the age. A significant difference (P = 0.001) was observed between the two groups for CCL2 only.

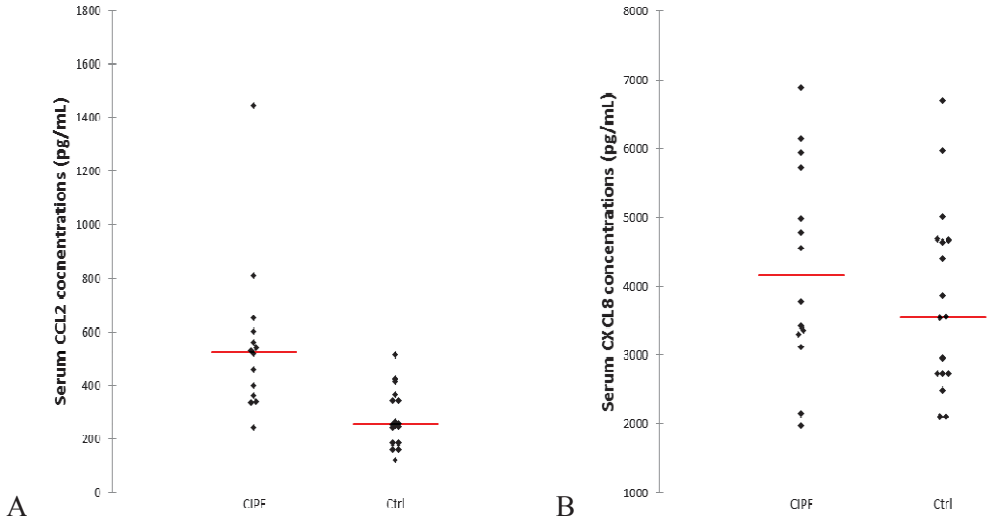


## 3.2. BALF CCL2 and CXCL8 concentrations: CIPF WHWTs vs. healthy controls

BALF samples were collected from 12 WHWTs with CIPF and 8 WHWTs controls (Table 2). The procedure was performed in a standardised manner under general anaesthesia and close monitoring of the cardiopulmonary function (electrocardiogram, pulse-oximetry, Doppler arterial pressure measurement). Bronchoscopy and BAL were performed in a rapid time frame (a few minutes) as followed: two or three (either of 20 mL, or 1 mL/kg each) aliquots

of sterile saline (0.9% NaCl) were instilled into at least two different lung lobes via a flexible fiberoptic bronchoscope (Fujinon EB-530S, Fujifilm) wedged in a bronchus, followed by immediate aspiration of each aliquot by gentle suction. The recovered BALF supernatant was separated from cell pellets by centrifugation at 1300 x *g* for 15 minutes at 5 °C, transferred into 1.5 mL plastic cryotubes and stored at -80 °C until analysis. Concentrations of CCL2 and CXCL8 in BALF were measured with the same commercial canine ELISA kits than those used for serum concentrations determination (R&D Systems) in duplicate and on a single occasion.

Table 2: Characteristics of the study population used for BALF chemokine dosages.

| Parameters | CIPF WHWTs | Healthy WHWTs |
|---|---|---|
| n | 12 | 8 |
| Gender, M/F | 8/4 | 3/5 |
| Age, years | 11.5<br>(5.2 – 14.5) | 9.7<br>(2.9 – 13.8) |
| Weight, Kg | 10.6<br>(8.4 – 15.0) | 8.5<br>(7.5 – 12.0) |

Both CCL2 and CXCL8 concentrations in BALF were significantly higher in WHWTs affected with CIPF compared with healthy controls. BALF concentration of CCL2 (median, range) were 661.54 pg/mL (63.8 – 1400.4) in the CIPF group and 224.5 pg/mL (129.0 – 663.5) in the control group (P = 0.02) (Fig. 2A). BALF concentrations of CXCL8 (median, range) were 137.3 pg/mL (45.5 – 1058.2) in WHWTs affected with CIPF and 8.1 pg/mL (0.7 – 24.3) in controls (P = 0.01) (Fig. 2B).

Fig. 2: BALF CCL2 concentrations (pg/mL) (A) and CXCL8 concentrations (pg/mL) (B) obtained from WHWTs affected with CIPF and control WHWTs matched for the age. A significant difference was observed between the two groups for both CCL2 and CXCL8.

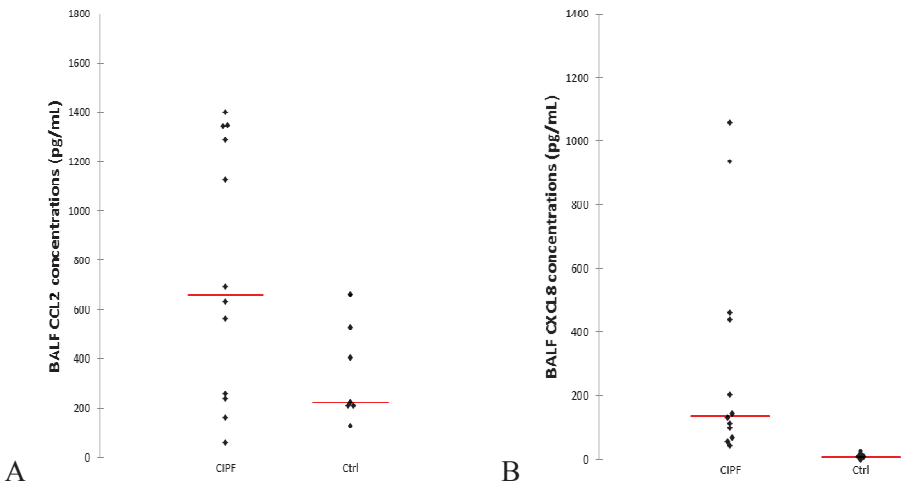

## 3.3. Serum CCL2 concentration in CIPF WHWTs: a survival prognostic marker

As explained in the introduction section, CIPF in WHWTs may have a rapid or a slow progressive phenotype which prevent the establishment of a precise prognosis at the time of diagnosis (Lilja-Maula et al., 2014b). As serum CCL2 concentrations were found to be elevated in WHWTs affected with CIPF compared with controls, we sought to further investigate whether serum CCL2 concentrations measured at diagnosis can be used as an indicator of prognosis. We also aimed to determine whether serum CCL2 concentrations may serve as a surrogate marker of disease severity by calculating correlations with clinical parameters of lung function, namely 6MWD and arterial $pO_2$ values. For this purpose, WHWTs affected with CIPF for which a serum sample at diagnosis was obtained and banked at -80°C, and for which a follow-up was available at the end of the study period (March 2015) were included. Serum CCL2 concentrations were determined using a commercially available canine ELISA kit (Canine CCL2 Quantikine ELISA Kit, R&D systems) in duplicate. For statistical analyses, survival curves were drawn by the Kaplan-Meier method and differences in survival times according to serum CLL2 concentrations at diagnosis were tested with the log-rank test. Spearman analysis was used to assess correlations between serum CCL2 concentrations and lung function parameters.

Sixty WHWTs affected with CIPF (29 male/31 female, median age 11.7 years, median weight 9.8 kg) fulfilled the inclusion criteria. Thirteen of them were examined and sampled at the University of Liège, 35 at the University of Helsinki and the remaining 12 by European veterinary partners of the CIPF project. Forty-three of the CIPF WHWTs had a history of both exercise intolerance and cough, 6 had exercise intolerance alone and 11 dogs exhibited cough alone. The duration of clinical signs at diagnosis ranged from 3 weeks to 3 years with a median of 6 months. Crackles were noticed on lung auscultation in 56 dogs, mild restrictive dyspnoea was present in 21 dogs and cyanosis was observed in 5 dogs. CIPF diagnosis was confirmed by thoracic high resolution computed tomography, lung histopathology, or both examinations in 17, 6 and 27 WHWTs respectively. For the remaining 10 dogs, the diagnosis was suspected based on clinical examination and thoracic X-rays. Among the 60 CIPF WHWTs included, 31 died or were euthanized for CIPF-related reason, 12 died or were euthanized for non-CIPF-related reason and 17 were still alive at the end of the study. The median survival of WHWTs with CIPF-related death or euthanasia was 6.4 months (range 0.4 – 71.9) from diagnosis. Median serum CCL2 concentration in WHWTs affected with CIPF was 488.5 pg/mL (range 163.4 – 1647.7). Serum CCL2 concentrations above 700 pg/mL at diagnosis were significantly associated with a shorter survival time ($P = 0.02$) (Fig. 3). This cut-off value of 700pg/mL was arbitrary chosen based on a visual inspection of the COX regression curve of serum CCL2 and

survival. A weak negative correlation was found between serum CCL2 concentrations and the 6MWD (r = -0,382, P = 0.03, n = 31), while no correlation was observed with arterial pO2 values (r = -0.203, P = 0.162, n = 49).

Fig.3: Kaplan-Meier survival curves for CIPF-specific survival of WHWTs affected with CIPF having a serum CCL2 concentration at diagnosis > 700 pg/mL (green line) or < 700pg/mL (blue line) (P = 0.02). Censored animals (WHWTs alive at study endpoint or died for non-CIPF-related reason) are presented as vertical lines.

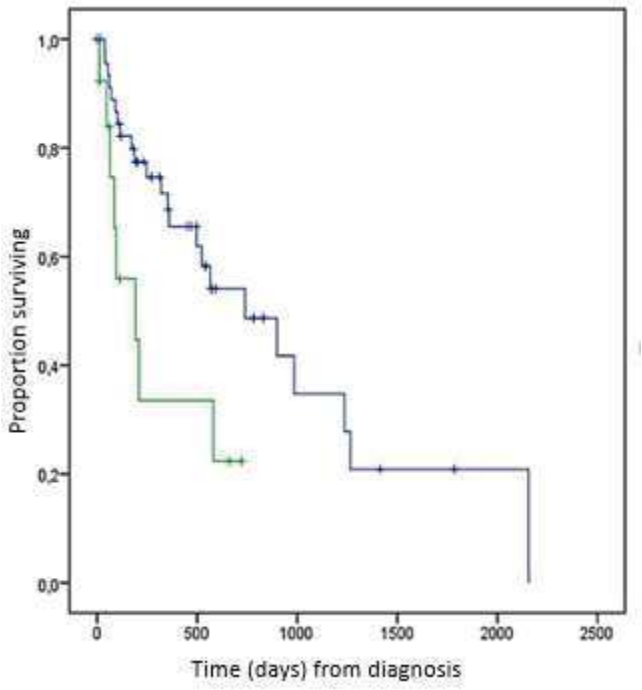


Those results suggest that serum CCL2 concentration measured at diagnosis carries prognostic information in WHWTs suffering from this disease. A weak correlation was found between serum CCL2 concentrations and the 6MWD, while the study failed to demonstrate a correlation with pO2 values. Therefore, further investigations are required to determine the exact value of serum CCL2 concentration as a surrogate marker of CIPF severity in a larger population of dogs.

## 3.4. Lung CCL2/CCR2 and CXCL8/CXCR2 expression assessed by qRT-PCR

Full-thickness lung tissue biopsies were obtained from 18 WHWT with CIPF and from 22 control dogs of various breeds (Table 3). Six of the 22 control dogs provided were from a rescue shelter, euthanized for aggressiveness (2/6) or lack of space (4/6). Causes of euthanasia in the remaining 16 dogs were nasal tumor (3 dogs), old age (3 dogs), testicular tumor, vaginal tumor, buccal osteoma, meningioma, leg osteosarcoma, urinary incontinence, metrorrhagia, perianal fistula, chronic kidney disease and thrombocytopenia. Lung samples were obtained

within 30 minutes after euthanasia and placed in 1.5ml plastic cryotube containing RNAlater (Ambio). Cryotubes were refrigerated at 4 °C for up to 24h and then centrifuged for RNAlater retrieval and frozen at -80 °C until further processing.

Table 3: Characteristics of the study population used for CCL2, CXCL8, CCR2 and CXCR2 qRT-PCR.

| Parameters | CIPF WHWTs | Controls |
|---|---|---|
| n | 18 | 22 |
| Gender, M/F | 9/9 | 10/12 |
| Age, years | 12.0<br>(9.1 – 15.9) | 9.7<br>(3.7 – 16.8) |
| Breed | WHWTs | 6 Jack Russell,<br>5 Beagle,<br>2 Yorkshire,<br>2 mixed breed,<br>1 WHWT,<br>1 Bulldog,<br>1 Newfoundland,<br>1 Leonberg,<br>1 Maltese,<br>1 American Staffordshire,<br>1 Bernese Mountain dog |

Total RNA was extracted from lung tissue samples using the Total RNA isolation Nucleospin® RNA II kit (Macherey-Nagel). Tissue (± 20mg) was added to a 2mL safe-lock microcentrifuge tube (Eppendorf) containing 350µL lysis buffer, 3.5µL β-mercaptoethanol and a 5 mm stainless steel bead (Qiagen). Samples were disrupted using a Tissue Lyser (Qiagen) by shaking the tube at 30 cycles/second for 1 minute. The resulting lysate was centrifuged at 14 000 x g for 3 minutes and the supernatant was processed according to the manufacturer protocol. RNA solutions obtained were stored at -80 °C. For each sample, RNA concentrations were measured with a fluorescence microplate reader after treatment with an intercalating agent (Quant-iTTM RiboGreen RNA Reagent, Invitrogen). RNA quality and integrity were assessed by automated capillary gel electrophoresis (QIAxcel RNA, Qiagen); all samples used for qRT-PCR had a RNA integrity score ≥ 7. After DNase digestion (DNase I RNase-free, Thermo-Scientific), reverse transcriptions were performed with a commercial available kit (RevertAid H Minus First Strand cDNA Synthesis Kit, Thermo Scientific) by using oligo-dT primers in order to amplify only mRNA. cDNA samples obtained were used for qRT-PCR in duplicate with SYBR green (Absolute Blu QPCR SYBR Green ROX Mix, Thermo Scientific) with forward and reverse primers at a final concentration of 1500 µM. qRT-PCR were made in a

384-wells plate in two separate run. A negative control of nuclease free water and five reverse transcriptase negative controls were included in duplicate for each couple of primers. Ribosomal protein L32 (RPL32), ribosomal protein L13A (RPL13A), ribosomal protein S18 (RPS18) and TATA box binding protein (TBP) genes were selected as reference genes for normalization of gene expression. The primer sequences for CCL2, CXCL8, RPL32, RPL13A, RPS18 and TBP were the same as previously described (Peters et al., 2007). The primer sequences for CCR2 (NC_006602.3) and CXCR2 (NM_001003151.1) were designed using Primer3 software from Genbank sequences. Primer sequences are detailed in Table 4. The specificity of the products obtained at the end of the real-time PCR was confirmed by melting curve analysis. Sequencing of the end-PCR product was not performed. SDS 2.4 software (Applied Biosystems) and qbase+ 2.3 software (Biogazelle) were used for data analysis.

Table 4: Primer sequences used for qRT-PCR assays.

| *PCR* | *Primer names* | *Sequences* |
|---|---|---|
| CCL2 | CCL2 (s) | 5'-CACCTGCTGCTATACACTCACC-3' |
| | CCL2 (as) | 5'-GATCACAGCTTCTTTGGGACA-3' |
| CXCL8 | CXCL8 (s) | 5'-CACTCCACACCTTTCCATCC-3' |
| | CXCL8 (as) | 5'-GTCCAGGCACACCTCATTTC-3' |
| CCR2 | CCR2 (s) | 5'-CGTGAAGCTCATTTTCGTGA-3' |
| | CCR2 (as) | 5'-GACTCCTGGAAGGTGCTCAG-3' |
| CXCR2 | CXCR2 (s) | 5'-AGCTGCCTTAATCCCCTCAT-3' |
| | CXCR2 (as) | 5'-CTGAACCTGCTGGGAAACTC-3' |
| RPL32 | RPL32 (s) | 5'-TGGTTACAGGAGCAACAAGAAA-3' |
| | RPL32 (as) | 5'-GCACATCAGCAGCACTTCA-3' |
| RPL13A | RPL13A (s) | 5'-GCCGGAAGGTTGTAGTCGT-3' |
| | RPL13A (as) | 5'-GGAGGAAGGCCAGGTAATTC-3' |
| RPS18 | RPS18 (s) | 5'-TGCTCATGTGGTATTGAGGAA-3' |
| | RPS18 (as) | 5'-TCTTATACTGGCGTGGATTCTG-3' |
| TBP | TBP (s) | 5'-CTATTTCTTGGTGTGCATGAGG-3' |
| | TBP (as) | 5'-CCTCGGCATTCAGTCTTTTC-3' |

Relative CCL2, CXCL8, CCR2 and CXCR2 gene expression was not significantly different between the lungs of WHWT with CIPF and control dogs of various breeds (Fig. 4).

Fig. 4: Box-and-whisker plots illustrating relative gene expression of (A) CCL2, (B) CXCL8, (C) CCR2, and (D) CXCR2 in WHWTs affected with CIPF vs. controls (CTRL). The box represents the interquartile range, with the median indicated by the horizontal line. The whiskers extend from the minimum to the maximum values, excluding outliers that are represented by open circles. There was no difference between groups for any of the gene expression studied.

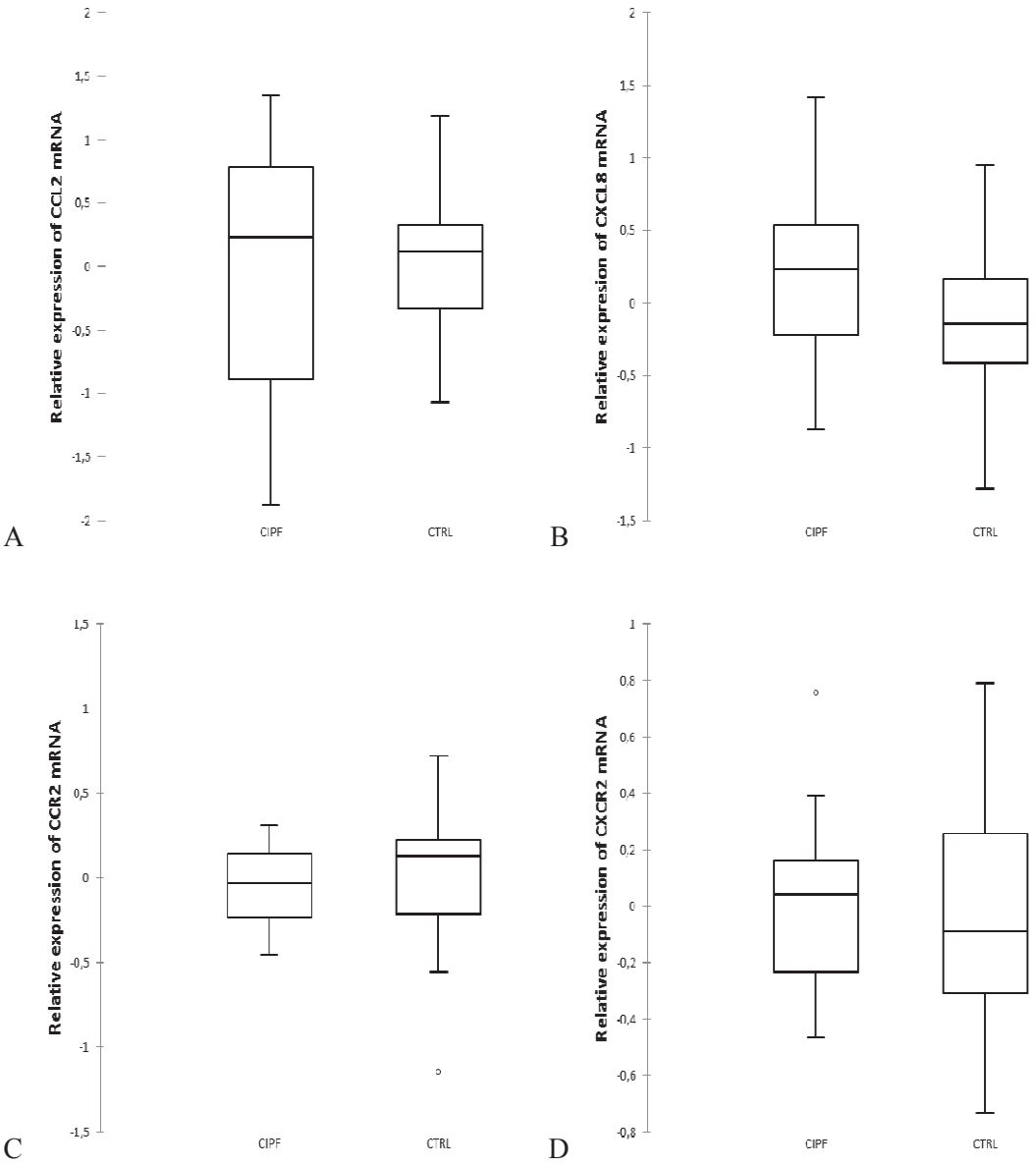


## 3.4. Lung cellular sources of CCL2 and CXCL8 assessed by immunohistochemistry

Lung tissue samples for immunohistochemical analyses were obtained from 4 WHWTs affected by CIPF and 4 control dogs (Table 5). Control dogs were euthanized for thrombocytopenia, buccal osteoma, testicular tumor or urinary incontinence.

Table 5: Characteristics of the study population used immunohistochemical analyses.

| Parameters | CIPF WHWTs | Controls |
|---|---|---|
| n | 4 | 4 |
| Gender, M/F | 3/1 | 4/0 |
| Age, years | 11.7<br>(11.0 – 14.2) | 12.6<br>(11.4 – 15.4) |
| Breed | WHWTs | 1 WHWT,<br>1 Yorkshire,<br>1 Beagle,<br>1 mixed breed |

Lung tissues were sampled within 30 minutes after euthanasia, fixed in 3.5% buffered formalin for 24 to 72 hours, routinely processed, embedded in paraffin and sectioned at 5µm. The sections were deparaffinised with xylene and rehydrated through graded concentrations of ethanol to a final wash in distilled water. Antigens were unmasked by microwaving sections in 10mM citrate buffer, pH 6.0 during 15 minutes. Tissues were incubated with 0.03% hydrogen peroxide containing sodium azide (Peroxidase block, Dako) for 10 minutes to inhibit endogenous peroxidase activity and subsequently washed with saline phosphate-buffered saline (PBS). To reduce background staining, sections were treated with 0.25% casein in PBS (Protein block, Dako) for 10 minutes. Then, sections were incubated in a moist chamber with a goat biotinylated anti-canine CXCL8 antibody (1:10 dilution, R&D Systems) or a goat biotinylated anti-canine CCL2 antibody (1:40 dilution, R&D Systems) overnight at 4 °C. Control sections were treated in parallel but incubated with normal goat serum (Dako) instead of antibody. Sections were then washed with PBS and incubated with horseradish peroxidase conjugated to streptavidin (1:500 dilution, Dako) for 1 hour. After washing with PBS, 3-amino-9-ethylcarbazole (AEC substrate-chromogen, Dako) was applied as the chromogen for 12 minutes. Sections were then washed in distilled water to eliminate the excess chromogen and counterstained with Mayer's haematoxylin for 2.5 minutes. Finally, the slides were washed in water, mounted with commercial mounting medium (Glycergel mounting medium, Dako) and assessed for staining characteristics.

In sections of lung from WHWTs affected with CIPF, an immunostaining for both CCL2 and CXCL8 was observed in bronchial airways epithelial (Figs. 5A, 5B). The staining was strong but localised to only few and sparse epithelial cells. Moreover, in one section, a few hyperplastic epithelial alveolar cells were labelled for CCL2 and CXCL8 in addition to some alveolar macrophages stained for CXCL8 only (Fig. 5C). In sections of lung from control dogs, no staining was observed either for CCL2 or CXCL8 (Fig. 6).

Fig. 5: Immunohistochemical labelling of lung tissue sections obtained from WHWTs affected with CIPF for CCL2 and CXCL8. (A) CCL2 immunoreactivity of bronchial epithelial cells, Bar = 100µm. (B) CXCL8 immunoreactivity of bronchial epithelial cells, Bar = 100µm. (C) CXCL8 immunoreactivity of hyperplastic alveolar epithelial cells and alveolar macrophages (arrows), Bar = 20µm.

A/ 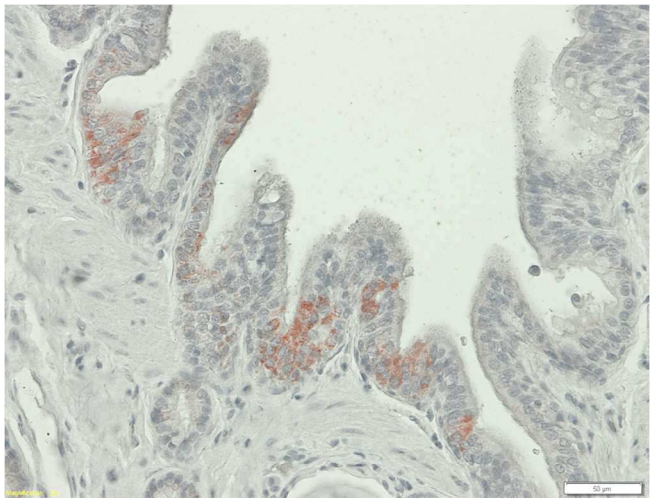

B/ 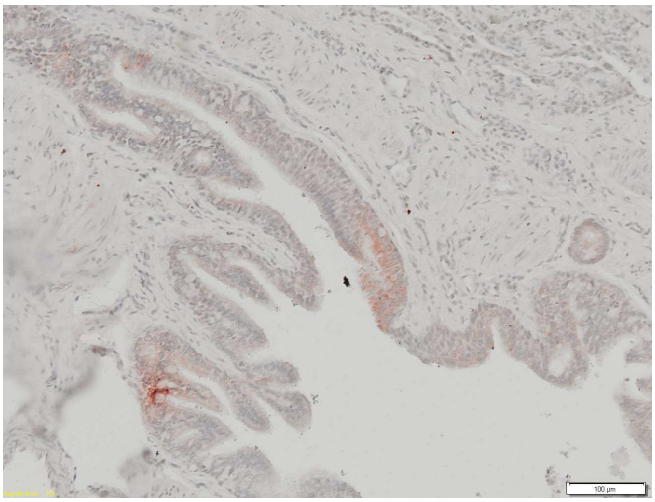

C/ 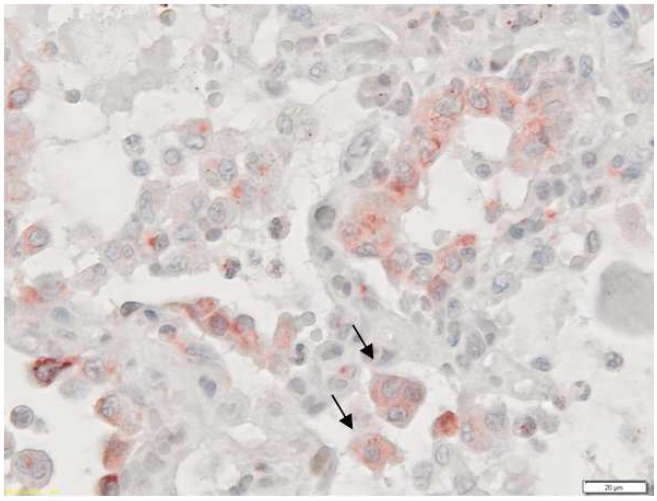

Fig. 6: Immunohistochemical labelling of lung tissue sections obtained from control dogs for CCL2 and CXCL8. (A) No evidence of CCL2 immunoreactivity. Bar = 100 µm. (B,C) No evidence of CXCL8 immunoreactivity. Bar = 100 µm.

A/ 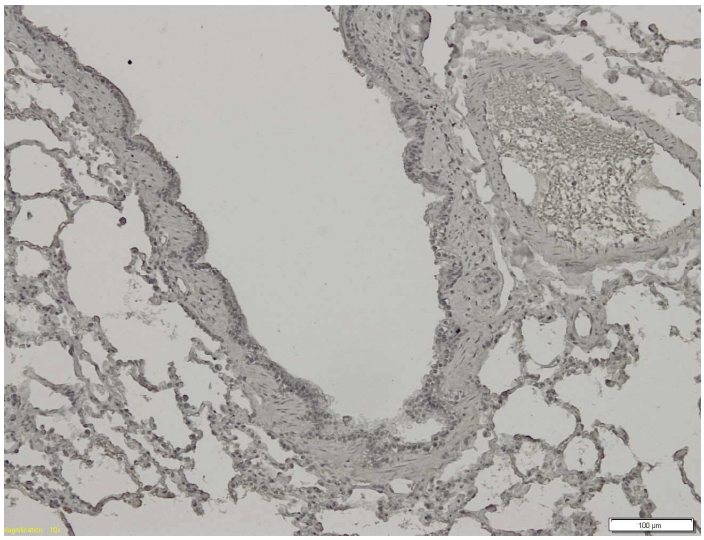

B/ 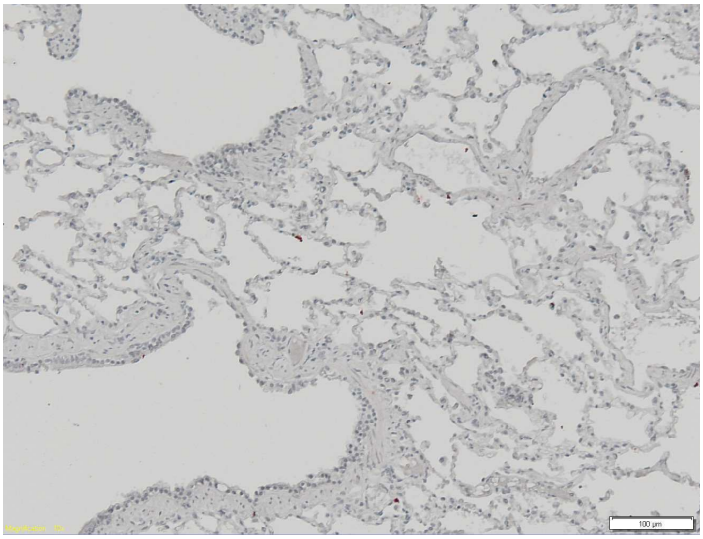

C/ 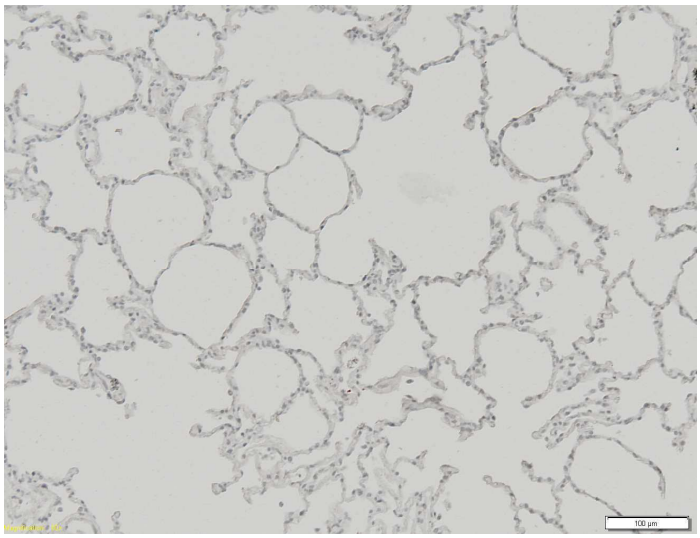

## 3.5. CCL2, CXCL8, VEGF, and 5-HT blood concentrations in healthy dogs from 7 breeds with variable predisposition for CIPF

Blood samples were obtained in plain tubes from 103 healthy dogs from seven different breeds (Table 6). Breeds selected were: WHWT, Scottish terrier (ST), Jack Russell terrier (JRT), Maltese (M), King Charles Spaniel (KCS), Labrador retriever (LR) and Malinois Belgian Shepherd (MBS). Those breeds were considered as highly (WHWT), possibly (ST, JRT) or not (M, KCS, LR, MBS) –CIPF predisposed breeds. ST and JRT were chosen as terrier breeds potentially predisposed to CIPF; in view of the fact that one CIPF case has already been confirmed by histopathology in a dog from the ST breed (Krafft et al., 2011) and that CIPF has been clinically suspected in five JRT, but not histopathologically confirmed (personal observations). Maltese breed was chosen as a non-terrier breed sharing similarities in weight and size with the WHWT breed. KCS breed was chosen as another small size non-terrier breed predisposed for degenerative mitral valve disease, another fibrotic disease (Borgarelli and Buchanan, 2012). LR and MBS breeds were chosen as large breeds definitively not predisposed to fibrotic lung disease.

Table 6: Characteristics of the study population used for CCL2, CXCL8, VEGF and 5-HT dosages.

| Breed | n | Sex, male/female | Age, yr. (median, range) | Weight, kg (median, range) |
|---|---|---|---|---|
| WHWT | 18 | 8/10 | 9.2 (2.9 – 16.9) | 8.7 (7.4 – 12.0) |
| ST | 14 | 3/11 | 5.1 (0.9 – 9.5) | 10.0 (8.5 – 13.6) |
| JRT | 16 | 2/14 | 7.2 (1.0 – 11.8) | 6.9 (5.9 – 12.6) |
| M | 15 | 4/11 | 6.2 (0.9 – 12.6) | 5.3 (4.0 – 9.0) |
| KCS | 14 | 5/9 | 5.8 (0.5 – 10.3) | 8.3 (6.8 – 12.0) |
| LR | 12 | 5/7 | 5.7 (1.6 – 12.2) | 36.4 (23.0 – 42.0) |
| MBS | 14 | 10/4 | 5.5 (1.5 – 7.8) | 31.2 (23.0 – 35.0) |

Thirty minutes after blood collection, tubes were centrifuged at 4 °C for 15 min at 1300 x g. Serum was harvested and transferred into 1.5 mL plastic cryotubes, and samples were stored at -80 °C until analysis. Serum CXCL8, CCL2 and VEGF measurements were performed using commercial canine ELISA kits (Quantikine ELISA Canine CCL2/MCP-1 Immunoassay, Quantikine ELISA Canine CXCL8/IL8 Immunoassay, and Quantikine ELISA Canine VEGF immunoassay, R&D Systems) in duplicate, according to the manufacturer's instructions. Serum 5-HT measurement was performed using a commercial human ELISA kit (Serotonin ELISA, IBL international GmBh) previously validated in dogs (Ljungvall et al., 2013).

Significantly higher serum CXCL8 concentrations were observed in healthy WHWTs in comparison with all other groups of healthy dogs ($P \leq 0.05$) and in M in comparison with KCS and LR ($P \leq 0.008$). Serum CCL2 concentrations were significantly higher in healthy WHWTs and M in comparison with KCS and MBS ($P \leq 0.05$) and in LR in comparison with MBS ($P = 0.04$). Serum 5-HT concentrations obtained in healthy KCS, ST, M and MBS were significantly higher in comparison with those obtained in healthy WHWTs, JRT and LR ($P \leq 0.05$). Results of those ELISA dosages are summarized in Table 7.

Table 7: Results of the CXCL8, CCL2 and 5-HT serum dosages in healthy dogs from 7 breeds with variable predisposition for CIPF. For CXCL8 results, * indicates statistically different from WHWT ($P \leq 0.005$), and † statistically different from M ($P \leq 0.008$). For CCL2 results, * indicates statistically different from WHWT and M ($P \leq 0.01$), and † statistically different from L ($P = 0.04$). For 5-HT results, * indicates statistically different from ST, M, KCS, and MBS ($P \leq 0.05$).

| Breed | n | CXCL8 (pg/mL) | CCL2 (pg/mL) | 5-HT (ng/mL) |
|---|---|---|---|---|
| WHWT | 18 | 3558,4 (2107,9 - 6714,0) | 256.4 (120.9 – 514.4) | 399,4* (192,6 - 583,9) |
| ST | 14 | 2806,1* (669,2 - 4052,3) | 189.8 (142.2 – 569.8) | 655,6 (105,3 - 1105,0) |
| JRT | 16 | 2333,6* (847,4 - 4736,3) | 203.0 (112.3 – 523.7) | 401,7* (41,6 - 770,8) |
| M | 15 | 2619,4* (620,5 - 7923,7) | 255.9 (171.1 – 1265.7) | 537,7 (219,1 - 1002,5) |
| KCS | 14 | 1998,5*† (52,6 - 3887,5) | 188,8* (92,3 - 871,6) | 631,6 (350,8 - 969,6) |
| LR | 12 | 1390,1*† (929,3 - 2881,5) | 178.5 (92.3 – 871.6) | 206,3* (75,4 - 633,8) |
| MBS | 14 | 1338,9* (698,8 - 5203,0) | 115.0*† (76.1 – 190.3) | 530,3 (258,2 - 853,1) |

For serum VEGF concentrations, the majority of samples tested, 92 out of 103 (89.3%), were below the ELISA kit detection limit (39.1 pg/mL) (Fig. 7). By consequence, a quantitative comparison between breeds was not possible. Results above the kit detection limit were found in 3 KCS (21.4%), 3 JRT (18.8%), 3 LR (25.0%), 1 WHWT (5.6%) and 1 ST (7.1%). Frequency of positive results were not different between breed groups (P = 0.147).

Fig. 7: Scatter plot of serum VEGF concentrations (pg/mL) obtained in 7 breeds of dogs with variable predisposition for CIPF. Most of the results were below the detection limit of the ELISA kit precluding the quantitative comparison of blood VEGF concentrations between breeds.

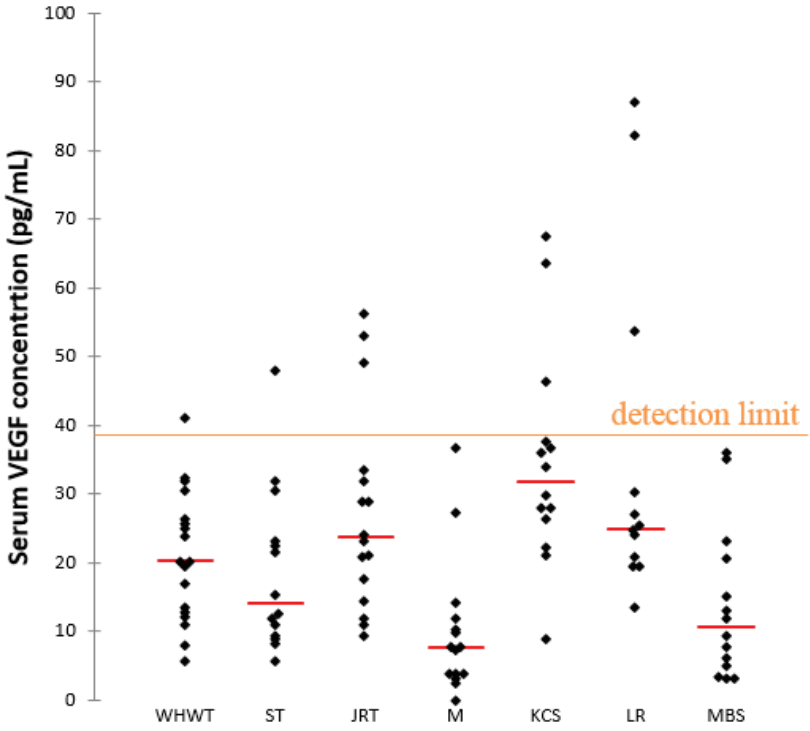

# 4. Search for etiologic agents

## 4.1. Panherpesvirus PCR assay (DPOL gene)

To search for the presence of herpesvirus in samples from WHWTs affected with CIPF we collaborated with Laurent Gillet from our faculty and with Bernhard Ehlers and his team (Robert Koch Institute, Berlin, Germany) who have developed expertise in the discovery of new herpesviruses in diverse range of species (Ehlers et al., 2008).

Results of herpesvirus investigation led to the publication of one publication (short communication) in *The Veterinary Pathology Journal* (see below pages 143 to 145).

Lung samples from 28 WHWTs affected with CIPF and 18 controls of various breeds and blood samples from 19 WHWTs affected with CIPF and 19 control WHWTs previously stored at -80°C were used for DNA extraction. Details about the study population are summarized in Table 1.

Table 1: Characteristics of the study population

| Parameters | CIPF dogs | | Control dogs | |
|---|---|---|---|---|
| | Lung | Blood | Lung | Blood |
| n | 28 | 19 | 18 | 19 |
| Breed | WHWTs | WHWTs | 5 WHWTs<br>6 JRTs<br>1 Maltese<br>1 Bulldog<br>1 Newfoundland<br>1 Beagle<br>1 Am. Staff.<br>2 Mixed breed | WHWTs |
| Gender, M/F | 15/13 | 12/7 | 6/12 | 11/8 |
| Age, yr. | 13.6<br>(9.1 – 16.3) | 13.9<br>(9.1 – 16.0) | 8.5<br>(3.7 – 15.0) | 10.4<br>(5.7 – 15.0) |
| Weight, kg | 9.8<br>(6.3 – 14.8) | 10.3<br>(6.6 – 14.8) | 9.7<br>(2.6 – 47.0) | 8.6<br>(6.6 – 11.0) |

DNA extractions were performed in the laboratory of infectious and parasitic diseases of the Faculty of Veterinary Medicine of Liège using a DNeasy Blood & Tissue kit (QIAGEN Inc.) following the manufacturer's instructions with an overnight incubation in proteinase K at

$56^0$C for lung samples. DNA samples obtained were then send on dry ice to the Robert-Koch Institute for the PCR assay. The panherpesvirus generic DNA polymerase (DPOL) PCR assay was applied to both lung and blood DNA samples with a mixture of degenerate and deoxyinosine-substituted primers in a nested format. The primer sequences are given in Table 2.

Table 2: Primer sequences for pan-herpesvirus PCR assay targeting DPOL gene.
I, deoxyinosine; s, sense; as, antisense

| DPOL PCR | Primer names | Sequences |
|---|---|---|
| First round PCR | DFA (s) | 5'-GAYTTYGC[N/I]AGYYT[N/I]TAYCC-3' |
| | ILK (s) | 5'-TCCTGGACAAGCAGCAR[N/I]YSGC[N/I]MT[N/I]AA-3' |
| | KG1 (as) | 5'-GTCTTGCTCACCAG[N/I]TC[N/I]AC[N/I]CCYTT-3' |
| Second round PCR | TGV (s) | 5'-TGTAACTCGGTGTAYGG[N/I]TTYAC[N/I]GG[N/I]GT-3' |
| | IYG (as) | 5'-CACAGAGTCCGTRTC[N/I]CCRTA[N/I]AT-3' |

The 25µL PCR mixture used to detect the DPOL gene consisted of 1 µL of DNA template (either extracted DNA or primary amplification product), 1 µM of each PCR primer (Metabion, Martinsried, Germany), 200 µM of each deoxynucleoside triphosphate, 2 unit of DNA polymerase AmpliTaq Gold, and 2.5 µL of GeneAmp 10 x PCR buffer (Applied Biosystems GmbH, Darmstadt, Germany) with 5% DMSO (Sigma-Aldrich Chemie GmbH). In first- and second-round PCRs, the reaction mixture was kept for 12 minutes at 95°C for activation of the polymerase and then cycled 45 times with 20 seconds of denaturation at 95°C, 30 seconds of annealing at 46°C, and 30 seconds of strand extension at 72°C, followed by a final extension step at 72°C for 10 minutes. To additionally relax the PCR conditions, the ramp time between the annealing step and the extension step was prolonged 50-fold. In each assay, a DNA of a gammaherpesvirus-positive porcine spleen sample was included as positive control. Water samples were extracted and PCR tested as negative controls. PCR products were electrophoresed through 2% agarose gels and DNA visualized by ethidium bromide staining.

Herpesvirus DPOL PCR analysis of the 46 lung and 38 blood samples issued from WHWTs affected with CIPF and control dogs did not result in amplification of a herpesvirus DPOL sequence (expected product size: approximately 210 bp -230 bp). However, identical

bands of approximately 280 bp and 150 bp length appeared in all lanes (Fig 1); these were of host origin as revealed by exemplary sequence analysis. Furthermore, to demonstrate the potential of the generic PCR method to universally amplify sequences of alpha, beta- and gammaherpesviruses from diverse sample materials, additional herpesvirus-positive control samples were included (Fig. 2). The gammaherpesviruses included were from the Genera Percavirus, Macavirus, Rhadinovirus, and Lymphocryptovirus. The samples were from blood, lung and other organs of diverse animal hosts, including carnivorans.

Fig. 1: Analysis of lung and blood samples collected from WHWTs affected with CIPF with panherpesvirus generic DPOL PCR.

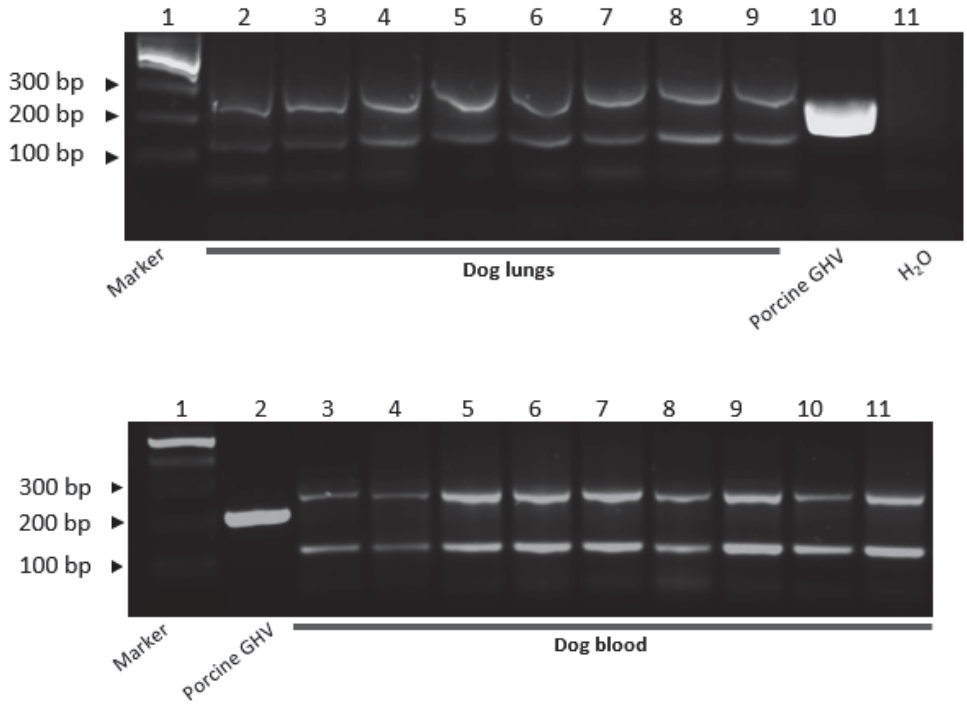


Fig. 2: Additional herpesvirus-positive control samples were included to demonstrate the potential of the generic PCR method to universally amplify sequences of alpha, beta- and gammaherpesviruses from diverse sample materials.

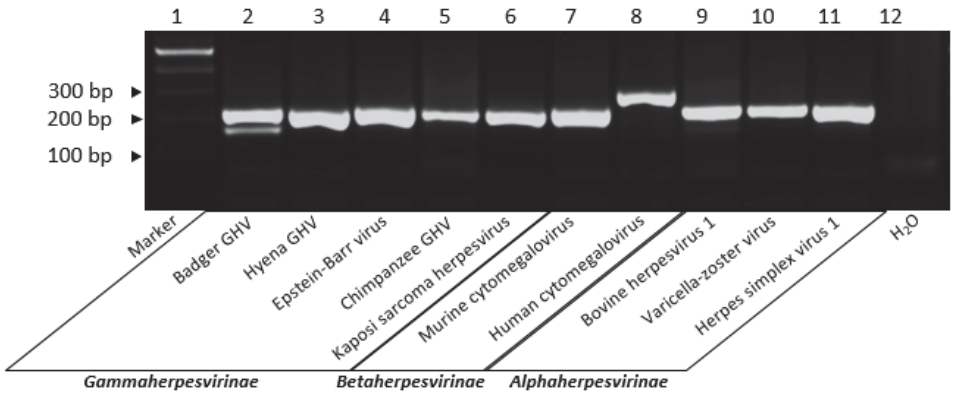

# ARTICLES

Articles submitted, accepted and published in the veterinary literature about the results detailed above are compiled in the following pages.

The Veterinary Journal 206 (2015) 75–82

Contents lists available at ScienceDirect

The Veterinary Journal

journal homepage: www.elsevier.com/locate/tvjl

# Assessment of CCL2 and CXCL8 chemokines in serum, bronchoalveolar lavage fluid and lung tissue samples from dogs affected with canine idiopathic pulmonary fibrosis

Elodie Roels [a,*], Emilie Krafft [a], Frederic Farnir [a], Saila Holopainen [b], Henna P. Laurila [b], Minna M. Rajamäki [b], Michael J. Day [c], Nadine Antoine [a], Dimitri Pirottin [d], Cecile Clercx [a]

[a] Faculty of Veterinary Medicine, University of Liège, Bd de Colonster, Liège, Belgium
[b] Department of Equine and Small Animal Medicine, Faculty of Veterinary Medicine, University of Helsinki, PO Box 57, 00014 Helsinki, Finland
[c] School of Veterinary Sciences, University of Bristol, Langford BS40 5DU, UK
[d] Department of Functional Sciences, Cellular and Molecular Immunology, GIGA-Research, University of Liège, Av de l'Hôpital, Liège, Belgium

ARTICLE INFO

*Article history:*
Accepted 1 June 2015

*Keywords:*
Canine idiopathic pulmonary fibrosis
Chemokine
CCL2
CXCL8

ABSTRACT

Canine idiopathic pulmonary fibrosis (CIPF) is a progressive disease of the lung parenchyma that is more prevalent in dogs of the West Highland white terrier (WHWT) breed. Since the chemokines (C-C motif) ligand 2 (CCL2) and (C-X-C motif) ligand 8 (CXCL8) have been implicated in pulmonary fibrosis in humans, the aim of the present study was to investigate whether these same chemokines are involved in the pathogenesis of CIPF. CCL2 and CXCL8 concentrations were measured by ELISA in serum and bronchoalveolar lavage fluid (BALF) from healthy dogs and WHWTs affected with CIPF. Expression of the genes encoding CCL2 and CXCL8 and their respective receptors, namely (C-C motif) receptor 2 (CCR2) and (C-X-C motif) receptor 2 (CXCR2), was compared in unaffected lung tissue and biopsies from dogs affected with CIPF by quantitative PCR and localisation of CCL2 and CXCL8 proteins were determined by immunohistochemistry.

Significantly greater CCL2 and CXCL8 concentrations were found in the BALF from WHWTs affected with CIPF, compared with healthy dogs. Significantly greater serum concentrations of CCL2, but not CXCL8, were found in CIPF-affected dogs compared with healthy WHWTs. No differences in relative gene expression for CCL2, CXCL8, CCR2 or CXCR2 were observed when comparing lung biopsies from control dogs and those affected with CIPF. In affected lung tissues, immunolabelling for CCL2 and CXCL8 was observed in bronchial airway epithelial cells in dogs affected with CIPF. The study findings suggest that both CCL2 and CXCL8 are involved in the pathogenesis of CIPF. Further studies are required to determine whether these chemokines might have a clinical use as biomarkers of fibrosis or as targets for therapeutic intervention.


## Introduction

Canine idiopathic pulmonary fibrosis (CIPF) is a progressive disease of the lung parenchyma, which mainly affects older dogs of the West Highland white terrier (WHWT) breed (Heikkila-Laurila and Rajamaki, 2014). The aetiology and pathogenesis of CIPF remain to be established, but a genetic basis is strongly suspected due to the breed predisposition (Heikkila-Laurila and Rajamaki, 2014).

CIPF shares several clinical features with human idiopathic pulmonary fibrosis (HIPF) (Corcoran et al., 1999; Lobetti et al., 2001; Heikkila et al., 2011), although there are some histopathological differences between the two syndromes (Syrja et al., 2013). As in HIPF, progression of the disease in dogs can vary considerably, with survival times from onset of clinical signs ranging from around 2 months to 4 years, with a median of 2.7 years (Raghu et al., 2011; Lilja-Maula et al., 2014).

There is no effective therapy available for CIPF at the present time (Heikkila-Laurila and Rajamaki, 2014) and even in HIPF, only two drugs, pirfenidone and nintedanib, have demonstrated a degree of efficacy in slowing progression of the disease (Covvey and Mancl, 2014). In veterinary medicine, the response to specific anti-fibrotic treatment has not yet been determined and few assays are currently available for monitoring progression and, consequently, treatment efficacy for CIPF. Arterial blood gas analysis and the 6-min walking test can be used for evaluation of lung function in dogs affected with CIPF, but these tests may lack sensitivity (Lilja-Maula et al., 2014). There is, therefore, a need for specific biomarkers that could help in determining the severity of lung dysfunction and monitoring disease progression.

Chemokine (C-C motif) ligand 2 (CCL2), also known as monocyte chemoattractant protein (MCP)-1, has been studied extensively in HIPF. Elevated CCL2 concentrations can be detected in bronchoalveolar lavage fluid (BALF) (Capelli et al., 2005; Baran et al.,

* Corresponding author. Tel.: +32 4 366 4243.
*E-mail address:* eroels@ulg.ac.be (E. Roels).

http://dx.doi.org/10.1016/j.tvjl.2015.06.001
1090-0233/

**Table 1**
Details of West Highland white terriers (WHWTs) affected with CIPF included in the study.

| Case number | Signalment | | Diagnostic procedures | | Experimental procedures | | | |
|---|---|---|---|---|---|---|---|---|
| | Age at presentation | Gender | Lung HRCT | Lung histology | Serum ELISA | BALF ELISA | Lung qPCR | Lung IHC |
| 1 | 9 years 10 months | M | + | – | – | + | – | – |
| 2 | 14 years 6 months | M | + | + | – | + | – | – |
| 3 | 10 years 5 months | F | + | – | + | + | – | – |
| 4 | 10 years 6 months | F | + | – | + | + | – | – |
| 5 | 11 years 7 months | M | + | + | + | + | – | – |
| 6 | 12 years 4 months | M | + | – | + | + | – | – |
| 7 | 13 years 11 months | M | + | + | + | + | – | – |
| 8 | 11 years 5 months | M | + | – | + | + | – | – |
| 9 | 10 years 11 months | M | + | – | + | + | – | – |
| 10 | 5 years 2 months | F | + | – | + | + | – | – |
| 11 | 13 years 11 months | M | + | + | + | – | – | – |
| 12 | 10 years 5 months | M | + | – | + | – | – | – |
| 13 | 11 years | M | – | + | + | – | – | + |
| 14 | 11 years 8 months | F | + | + | + | + | + | – |
| 15 | 11 years 7 months | M | + | + | + | + | + | + |
| 16 | 8 years 2 months | M | – | + | + | – | + | – |
| 17 | 14 years 2 months | M | – | + | – | – | + | + |
| 18 | 11 years 5 months | F | – | + | – | – | + | + |
| 19 | 12 years 5 months | F | – | + | – | – | + | – |
| 20 | 12 years 1 months | M | – | + | – | – | + | – |
| 21 | 11 years 9 months | M | + | + | – | – | + | – |
| 22 | 15 years 1 months | F | – | + | – | – | + | – |
| 23 | 8 years 11 months | F | + | + | – | – | + | – |
| 24 | 10 years 9 months | F | + | + | – | – | + | – |
| 25 | 8 years 11 months | M | – | + | – | – | + | – |
| 26 | 11 years 4 months | F | + | + | – | – | + | – |
| 27 | 11 years 8 months | M | + | + | – | – | + | – |
| 28 | 9 years 7 months | F | + | + | – | – | + | – |
| 29 | 12 years 6 months | F | – | + | – | – | + | – |
| 30 | 11 years 4 months | M | – | + | – | – | + | – |
| 31 | 15 years | F | + | + | – | – | + | – |

HRCT, high resolution computed tomography; ELISA, enzyme-linked immunosorbent assay; qPCR, quantitative polymerase chain reaction; IHC, immunohistochemistry.

2007) and blood (Suga et al., 1999; Fujiwara et al., 2012) of patients affected with HIPF and correlate with clinical parameters of lung function (Capelli et al., 2005; Emad and Emad, 2007) and outcome (Shinoda et al., 2009). CCL2 acts via (C-C motif) receptor 2 (CCR2), which is expressed on numerous cell types (Bonecchi et al., 2009). In HIPF, CCL2 acts on pulmonary fibroblasts, leading to synthesis of abundant extracellular matrix, via expression of transforming growth factor (TGF)-β1, a potent pro-fibrotic mediator (Gharaee-Kermani et al., 1996). CCL2 also contributes to lung pathology through recruitment of circulating fibrocytes (Moore et al., 2005), which produce type I collagen (Moore et al., 2005) and which differentiate into fibroblasts and myofibrobasts during the fibroproliferative process observed in HIPF (Phillips et al., 2004). A recent study in a murine model showed that pirfenidone significantly improved lung fibrosis, through attenuation of CCL2 production and reduced fibrocyte recruitment (Inomata et al., 2014), suggesting that CCL2 might be useful as a biomarker of fibrosis as well as a target for therapeutic intervention.

Chemokine (C-X-C motif) ligand 8 (CXCL8), also known as interleukin (IL)-8, is also found in increased concentration in the BALF (Antoniou et al., 2006) and serum (Ziegenhagen et al., 1998b) of patients with HIPF and correlates with lung function (Martina et al., 2009; Vasakova et al., 2009), disease progression (Ziegenhagen et al., 1998a; Totani et al., 2002) and survival (Richards et al., 2012). The role of CXCL8 in the pathogenesis of HIPF is not well understood, but several authors have suggested that CXCL8 might act as a pro-fibrotic factor, via promotion of angiogenesis through chemokine (C-X-C motif) receptor 2 (CXCR2) (Antoniou et al., 2006; Martina et al., 2009; Cui et al., 2010). Furthermore, a single nucleotide polymorphism (rs4073T>A) has been identified in the promoter region of the CXCL8 gene, which has been shown to be significantly associated with increased risk of developing HIPF (Ahn et al., 2011).

Analysis of gene expression in lung samples from CIPF-affected dogs has revealed increased expression of several genes, including those encoding CCL2 and CXCL8 (Krafft et al., 2013). The same study showed that serum CCL2 concentrations were elevated in dogs affected with CIPF, compared with healthy controls of the same breed (Krafft et al., 2013). The aim of the present study was to further evaluate the role of chemokines CCL2 and CXCL8 in the pathogenesis of CIPF, with a view to determining whether these chemokines might have potential as biomarkers of pulmonary fibrosis.

## Materials and methods

### *Study population and samples*

A total of 31 WHWTs affected with CIPF and 41 unaffected control dogs, including 20 WHWTs and 21 dogs of other breeds, were included in the study (Tables 1 and 2). Dogs were recruited at the University of Liège, the University of Helsinki, and by other partners engaged in the European CIPF project.[1] The study was approved by the Committee of Experimental Animals of Western Finland (approval numbers: ESLH-2008-05403, date of approval: 27 June 2008; ESAVI/7383/04.10.07/2013, date of approval: 13 November 2013) and by the equivalent committee of the University of Liège, Belgium (approval number: 1435, date of approval: 14 March 2013). All samples were obtained with informed owner consent.

The diagnostic approach for CIPF has been described elsewhere (Heikkila et al., 2011; Syrja et al., 2013) and the diagnosis was confirmed either by thoracic high-resolution computed tomography (HRCT; $n = 8$), lung histopathology ($n = 10$) or by both methods ($n = 13$). The health status of unaffected WHWTs used as controls for serum and BALF measurements (Table 2A, $n = 18$) was assessed by taking a complete history, performing a physical examination and by performing haematology and serum biochemistry. In nine of these dogs, thoracic HRCT was also performed at the time of sampling, which did not reveal any abnormalities. Lung tissues used as controls for quantitative PCR and immunohistochemistry procedures (Table 2B, $n = 23$) were

[1] See: http://www.caninepulmonaryfibrosis.ulg.ac.be/vet-partners/ (accessed 01.06.15).

**Table 2**
Details of control dogs included in the study.

| | Dog | Signalment | | | Diagnostic procedures | | Experimental procedures | | | |
|---|---|---|---|---|---|---|---|---|---|---|
| | | Age at sampling | Gender | Breed | Lung HRCT | Lung histology | Serum ELISA | BALF ELISA | Lung qPCR | Lung IHC |
| A | 1 | 2 years 11 months | F | WHWT | + | – | + | + | – | – |
| | 2 | 10 years 11 months | F | WHWT | + | + | + | + | – | – |
| | 3 | 10 years 3 months | F | WHWT | + | + | + | + | – | – |
| | 4 | 9 years 3 months | M | WHWT | + | – | + | + | – | – |
| | 5 | 13 years 9 months | M | WHWT | + | + | + | + | – | – |
| | 6 | 7 years 7 months | M | WHWT | + | – | + | + | – | – |
| | 7 | 6 years 6 months | M | WHWT | + | – | + | + | – | – |
| | 8 | 10 years 9 months | F | WHWT | + | – | + | + | – | – |
| | 9 | 13 years 11 months | F | WHWT | – | – | + | – | – | – |
| | 10 | 8 years 6 months | F | WHWT | + | – | + | – | – | – |
| | 11 | 6 years 5 months | F | WHWT | – | – | + | – | – | – |
| | 12 | 12 years 11 months | F | WHWT | – | – | + | – | – | – |
| | 13 | 3 years 7 months | M | WHWT | – | – | + | – | – | – |
| | 14 | 4 years 1 months | M | WHWT | – | – | + | – | – | – |
| | 15 | 10 years 9 months | M | WHWT | – | – | + | – | – | – |
| | 16 | 9 years 7 months | M | WHWT | – | – | + | – | – | – |
| | 17 | 9 years 3 months | M | WHWT | – | – | + | – | – | – |
| | 18 | 6 years | F | WHWT | – | – | + | – | – | – |
| B | 19 | 11 years 5 months | M | WHWT | – | + | – | – | – | + |
| | 20 | 13 years 6 months | M | Beagle | – | + | – | – | + | + |
| | 21 | 15 years 5 months | M | YT | – | + | – | – | + | + |
| | 22 | 11 years 7 months | M | Mixed breed | – | + | – | – | + | + |
| | 23 | 3 years 8 months | F | Bulldog | – | + | – | – | + | – |
| | 24 | 13 years 3 months | M | WHWT | – | + | – | – | + | – |
| | 25 | 10 years 4 months | F | Beagle | – | + | – | – | + | – |
| | 26 | 9 years 5 months | F | Newfoundland | – | + | – | – | + | – |
| | 27 | 9 years 1 months | M | Leonberger | – | + | – | – | + | – |
| | 28 | 4 years 1 months | F | Mixed breed | – | + | – | – | + | – |
| | 29 | 13 years 5 months | F | Beagle | – | + | – | – | + | – |
| | 30 | 11 years 11 months | M | Beagle | – | + | – | – | + | – |
| | 31 | 11 years 6 months | F | Bernese | – | + | – | – | + | – |
| | 32 | 7 years 8 months | M | ASBT | – | + | – | – | + | – |
| | 33 | 13 years 7 months | F | Beagle | – | + | – | – | + | – |
| | 34 | 3 years 11 months | M | JRT | – | + | – | – | + | – |
| | 35 | 7 years | M | JRT | – | + | – | – | + | – |
| | 36 | 10 years | F | JRT | – | + | – | – | + | – |
| | 37 | 5 years 4 months | M | JRT | – | + | – | – | + | – |
| | 38 | 6 years 6 months | M | JRT | – | + | – | – | + | – |
| | 39 | 6 years 11 months | F | Maltese terrier | – | + | – | – | + | – |
| | 40 | 6 years 3 months | F | JRT | – | + | – | – | + | – |
| | 41 | 16 years 9 months | M | YT | – | + | – | – | + | – |

HRCT, high resolution computed tomography; ELISA, enzyme-linked immunosorbent assay; qPCR, quantitative polymerase chain reaction; IHC, immunohistochemistry; WHWT, West Highland white terrier; YT, Yorkshire terrier; ASBT, American Staffordshire bull terrier; JRT, Jack Russell terrier.

obtained from dogs euthanased for reasons unrelated to the study. These dogs had no history or clinical signs of lower respiratory disease at the time of euthanasia and no abnormalities were identified on necropsy and histopathological examination of the lungs.

*Measurement of chemokine concentrations in serum and BALF*

Blood was collected into plain tubes and serum samples stored at –80 °C until analysis. Bronchoscopy and bronchoalveolar lavage were performed as previously described (Heikkila et al., 2011; Krafft et al., 2011). Briefly, two or three (either of 20 mL, or 1 mL/kg each) aliquots of sterile saline (0.9% NaCl) were instilled into at least two different lung lobes via a flexible bronchoscope (Fujinon EB-530S, Fujifilm) under anaesthesia, followed by immediate aspiration by gentle suction. The recovered BALF was centrifuged at 1300 *g* for 15 min at 5 °C and stored at –80 °C until analysis. CCL2 and CXCL8 concentrations were measured in serum and BALF, using commercially available ELISA kits (R&D Systems), tested in duplicate wells, according to the manufacturer's instructions.

*Assessment of CCL2, CXCL8, CCR2 and CXCR2 mRNA expression by quantitative PCR*

Lung biopsies were obtained within 30 min of euthanasia and placed into RNAlater (Ambion). Samples were refrigerated at 4 °C for up to 24 h, then stored at –80 °C until further processing. Total RNA was extracted from lung tissue samples as previously described (Krafft et al., 2013) and stored at –80 °C. RNA concentrations were measured (Quant-iT RiboGreen RNA Reagent, Invitrogen) using a fluorescence microplate reader and RNA quality was assessed by automated capillary gel electrophoresis (QIAxcel RNA, Qiagen). All samples had an RNA integrity score ≥7. After DNase digestion (DNase I RNase-free, Thermo-Scientific), reverse transcription was performed with a commercial kit (RevertAid H Minus First Strand cDNA Synthesis Kit, Thermo Scientific), using an oligo-dT primer. The cDNA samples were assessed by quantitative PCR in duplicate in 384-well plates using SYBR green chemistry (Absolute Blue qPCR SYBR Green ROX Mix, Thermo Scientific), with sense and antisense primers at a final concentration of 150 nM. A negative control of nuclease-free water and non-reverse transcribed (NRT) controls were included in duplicate for each pair of primers.

Ribosomal protein L32 (*RPL32*), ribosomal protein L13A (*RPL13A*), ribosomal protein S18 (*RPS18*) and TATA box binding protein (*TBP*) were selected as reference genes for normalisation of target gene expression. The primer sequences for CCL2, CXCL8, RPL32, RPL13A, RPS18 and TBP are described elsewhere (Peters et al., 2007). The primers for CCR2 (GenBank accession number: NC_006602.3) and CXCR2 (GenBank accession number: NM_001003151.1) were designed using Primer3 software.[2] Primer sequences were: 5′-CGTGAAGCTCATTTTCGTGA-3′ (sense), 5′-GACTCCTGGAAGGTGCTCAG-3′ (antisense) for canine CCR2 and 5′-AGCTGCCTTAATCCCCTCAT-3′ (sense), 5′-CTGAACCTGCTGGGAAACTC-3′ (antisense) for canine CXCR2. The specificity of the products obtained at the end of the PCR was confirmed by melting curve analysis. SDS 2.4 software (Applied Biosystems) and qbase+ 2.3 software (Biogazelle) were used for data acquisition and analysis.

*CCL2 and CXCL8 immunohistochemistry*

Lung tissue biopsies were collected within 30 min of euthanasia, fixed in 3.5% neutral buffered formalin for 24–72 h, embedded in paraffin wax and sectioned at 5 μm. The sections were dewaxed with xylene and rehydrated through graded concentrations of ethanol to distilled water. Antigen retrieval was undertaken by microwaving sections in 10 mM citrate buffer, pH 6.0, for 15 min. Tissues were

[2] See: http://biotools.umassmed.edu/bioapps/primer3_www.cgi (accessed 01.06.15).

incubated with 0.03% hydrogen peroxide containing sodium azide (Peroxidase block, Dako) for 10 min to inhibit endogenous peroxidase activity and subsequently washed with phosphate-buffered saline (PBS). To reduce non-specific staining, sections were blocked with 0.25% casein in PBS (Protein block, Dako) for 10 min. Tissue sections were incubated in a humid chamber with biotinylated goat anti-canine CCL2 antibody (1:40 dilution, R&D Systems) or biotinylated goat anti-canine CXCL8 antibody (1:10 dilution, R&D Systems) overnight at 4 °C. Control sections were treated in parallel, but incubated with normal goat serum (Dako) instead of primary antibody.

Sections were washed with PBS and incubated with horseradish peroxidase conjugated to streptavidin (1:500 dilution, Dako) for 1 h. After washing with PBS, 3-amino-9-ethylcarbazole (AEC substrate-chromogen, Dako) was applied as the chromogen for 12 min. Sections were subsequently washed in distilled water and counterstained with Mayer's haematoxylin for 2.5 min. The slides were washed in water, mounted with commercial mounting medium (Glycergel mounting medium, Dako) and evaluated by light microscopy.

### *Statistical methods*

Serum CCL2 and CXCL8 concentrations were compared between healthy and CIPF-affected WHWTs using a global linear model (SAS software, SAS Institute) integrating the effects of age and gender as covariables. The data are expressed as least squares means ± SE. BALF CCL2 and CXCL8 concentrations were compared between groups using Welch's ANOVA test (SAS software, SAS Institute) as equality of variance was not encountered. The data are expressed as means ± SD. For quantitative PCR results, comparisons between CIPF-affected and control groups were performed using a global linear model (SAS software, SAS Institute) with age and gender as covariables. *P* values <0.05 were considered to be significant.

## Results

### *Chemokine concentrations in serum and BALF*

Serum samples were obtained from 14 WHWTs affected with CIPF (10 males, four females; median age at sampling, 11 years; Table 1) and 18 control WHWTs (eight males, 10 females; median age at sampling, 9.2 years; Table 2A). Significantly greater serum CCL2 concentrations were found in WHWTs affected with CIPF (least squares mean ± SE of 557.7 ± 56.5 pg/mL) compared with control WHWTs (287.1 ± 49.8 pg/mL; $P = 0.001$; Fig. 1A). No significant difference was observed in serum CXCL8 concentrations comparing CIPF-affected (4175.4 ± 361.2 pg/mL) and control WHWTs (3920.1 ± 327.1 pg/mL; $P = 0.608$; Fig. 1B).

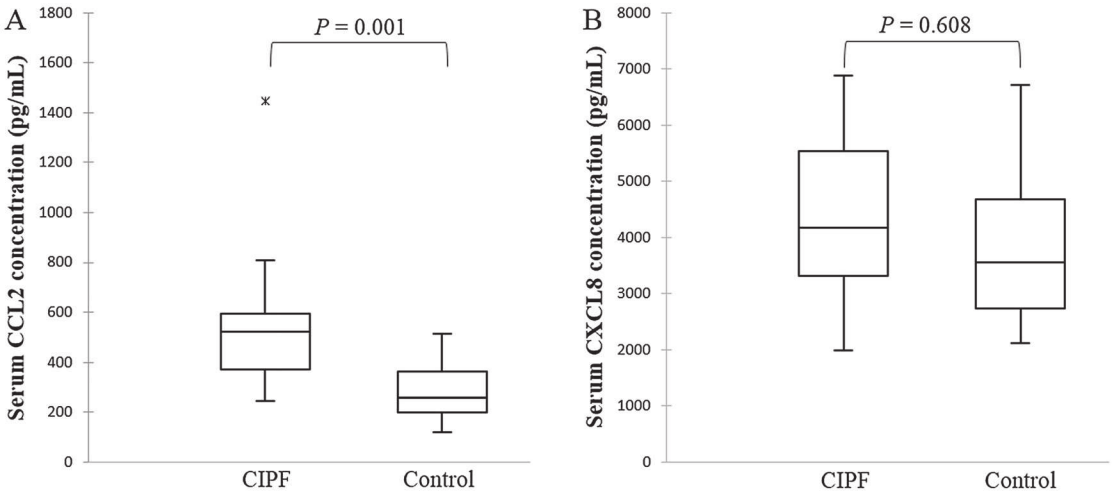


**Fig. 1.** Box-and-whisker plots of (A) CCL2 and (B) CXCL8 measured by ELISA in serum samples from West Highland white terriers (WHWTs) affected with canine idiopathic pulmonary fibrosis (CIPF; $n = 14$) and unaffected WHWTs ($n = 18$). The box represents the interquartile range, with the median indicated by the horizontal line. The whiskers extend from the minimum to the maximum values, excluding extreme outliers that are represented by an asterisk.

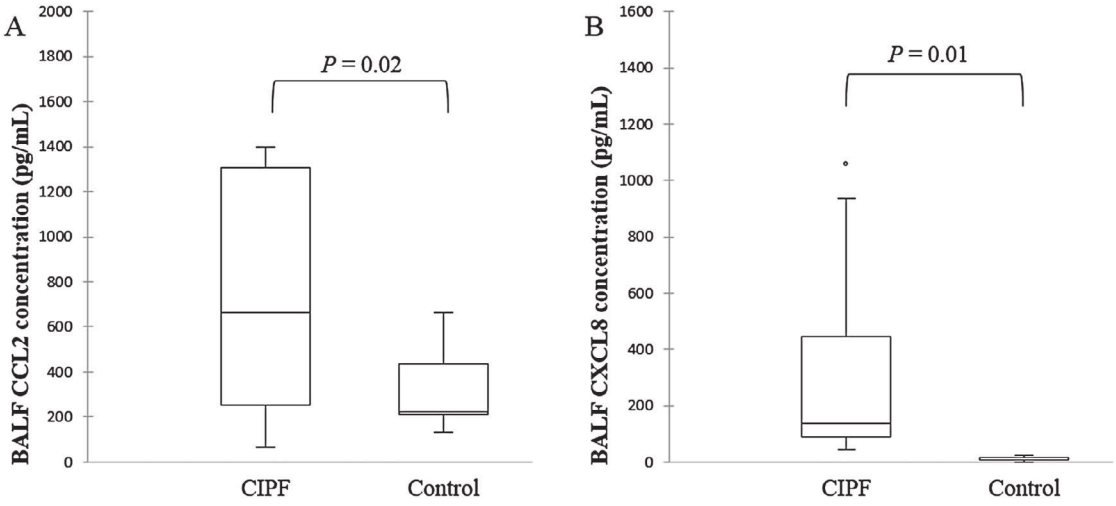


**Fig. 2.** Box-and-whisker plots of (A) CCL2 and (B) CXCL8 measured by ELISA in bronchoalveolar lavage fluid (BALF) from West Highland White terriers (WHWTs) affected with CIPF ($n = 12$) and unaffected WHWTs ($n = 8$). The box represents the interquartile range, with the median indicated by the horizontal line. The whiskers extend from the minimum to the maximum values, excluding outliers that are represented by open circles.

BALF samples were obtained from 12 WHWTs affected with CIPF (eight males, four females; median age 11.5 years; Table 1) and eight unaffected WHWT controls (three males, five females; median age 9.7 years; Table 2A). CCL2 concentrations in the BALF from CIPF-affected dogs (760.6 ± 517.5 pg/mL) were significantly greater than those in the control samples (324.8 ± 187.3 pg/mL; $P = 0.02$; Fig. 2A). The CXCL8 concentrations in BALF from CIPF-affected dogs (313.3 ± 348.9 pg/mL) were also significantly greater than those in the control samples (10.9 ± 7.4 pg/mL; $P = 0.01$; Fig. 2B).

*CCL2, CXCL8, CCR2 and CXCR2 mRNA expression in lung tissues*

Lung biopsies were obtained from 18 WHWTs affected with CIPF (nine males, nine females; median age 12 years; Table 1) and from 22 control dogs of various breeds (10 males, 12 females; median age 9.7 years; Table 2B). Relative expression of CCL2, CXCL8, CCR2 and CXCR2 mRNA was not significantly different comparing the samples from WHWTs affected with CIPF and the control samples (Fig. 3).

*CCL2 and CXCL8 immunoreactivity in lung tissues*

Lung biopsies were obtained from four WHWTs affected with CIPF (three males, one female; median age 11.7 years; Table 1) and four control dogs (four males; median age 12.6 years; Table 2B). In histological sections of lung tissue from CIPF-affected dogs, immunoreactivity for CCL2 (Fig. 4A) and CXCL8 (Fig. 4C) was observed in a proportion of the bronchial airway epithelial cells. In sections of lung from the control dogs, no immunoreactivity was observed for CCL2 (Fig. 4B) or CXCL8 (Fig. 4D). In one section of a CIPF-affected lung, occasional hyperplastic alveolar epithelial cells were labelled for CCL2 and CXCL8 (Fig. 4E) in addition to some alveolar macrophages expressing CXCL8 only (Fig. 4F).

## Discussion

The present study demonstrated that CCL2 chemokine concentrations were greater in both serum and BALF of WHWT dogs affected with CIPF, when compared with similar samples from healthy breed-matched controls. CXCL8 chemokine concentrations were greater in BALF, but not in serum comparing case and control groups. Although there was no difference in mRNA expression for those chemokines or their respective receptors (CCR2 and CXCR2) in homogenised lung tissue of affected vs. unaffected dogs, immunoreactivity for CCL2 and CXCL8 was observed in some of the bronchial airway epithelial cells in lungs from CIPF-affected dogs, but not in controls.

Several studies in patients affected with HIPF and in animal models of pulmonary fibrosis have provided compelling evidence that the chemokine CCL2 plays an important role in the fibroproliferative process (Gharaee-Kermani et al., 2003; Inoshima et al., 2004; Mercer et al., 2009). Involvement of CXCL8 in the pathogenesis of the disease is less well

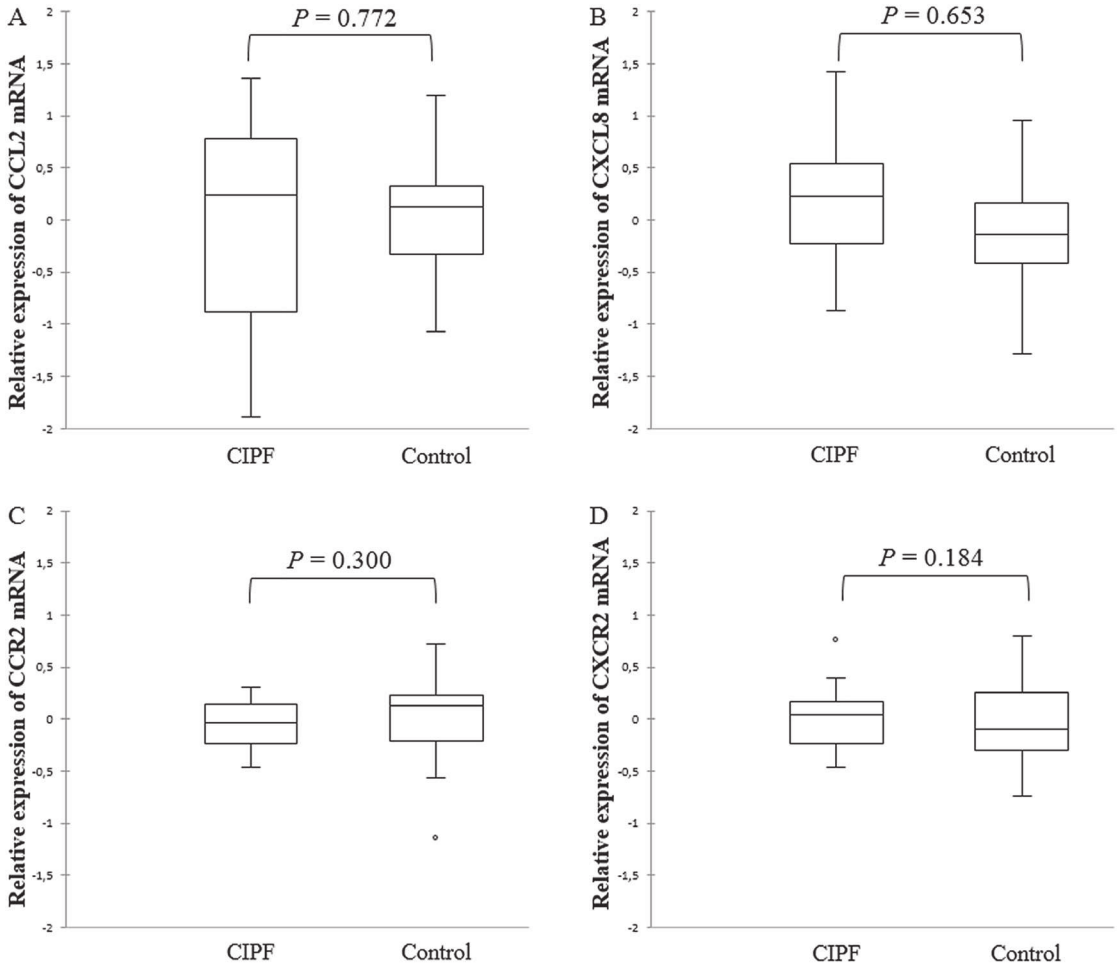


**Fig. 3.** Box-and-whisker plots illustrating relative gene expression of (A) CCL2, (B) CXCL8, (C) CCR2, and (D) CXCR2 in West Highland white terriers (WHWTs) affected with CIPF ($n = 18$) vs. controls ($n = 22$). The box represents the interquartile range, with the median indicated by the horizontal line. The whiskers extend from the minimum to the maximum values, excluding outliers that are represented by open circles.

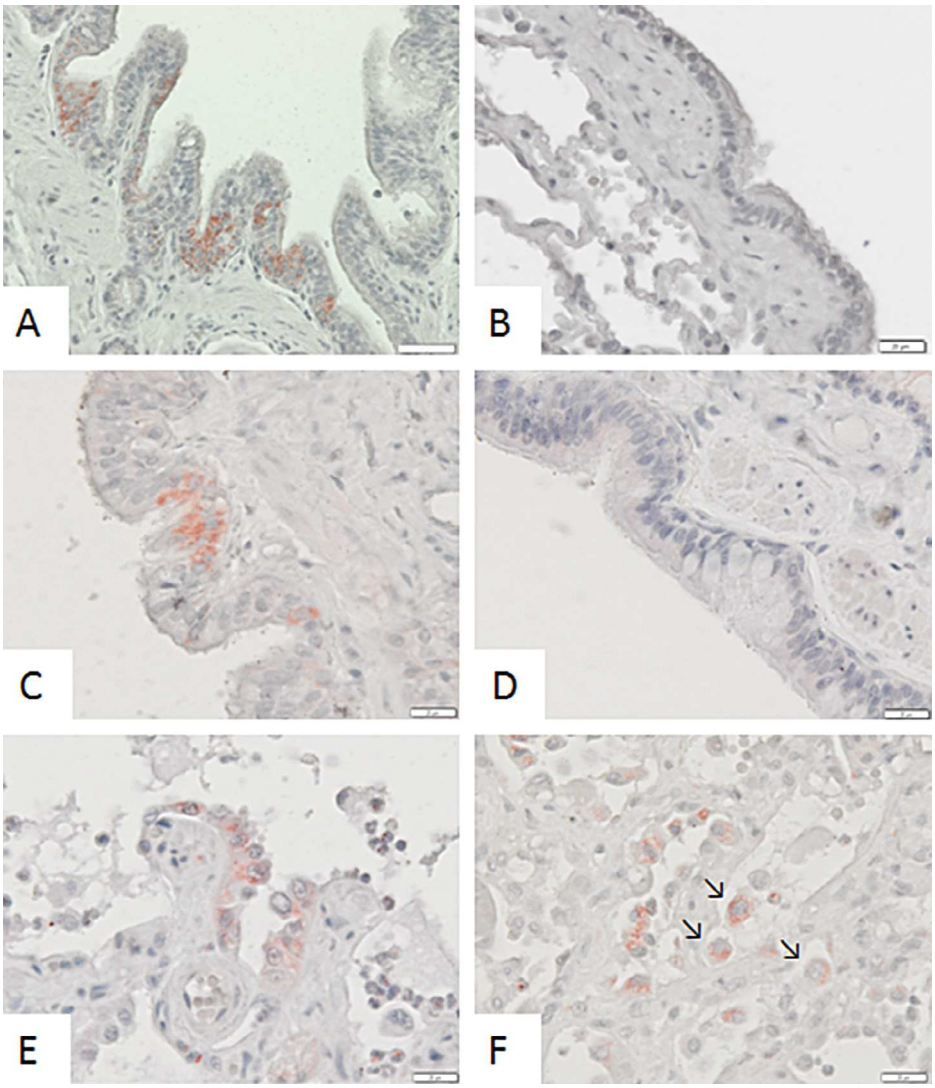


**Fig. 4.** Immunohistochemical labelling of lung tissue sections. (A) CCL2 immunoreactivity of bronchial epithelial cells in lung tissue from a West Highland white terrier (WHWTs) affected with CIPF. Bar = 100 μm. (B) No evidence of CCL2 immunoreactivity in healthy control lung tissue. Bar = 20 μm. (C) CXCL8 immunoreactivity of bronchial epithelial cells in lung tissue from a WHWTs affected with CIPF. Bar = 20 μm. (D) No evidence of CXCL8 immunoreactivity in a healthy control lung. Bar = 20 μm. (E) CXCL8 immunoreactivity of hyperplastic alveolar epithelial cells in lung tissue from a WHWT affected with CIPF. Bar = 20 μm. (F) CXCL8 immunoreactivity of macrophages (arrows) in lung tissue from a WHWT affected with CIPF. Bar = 20 μm.

documented, but several studies have demonstrated its role as a biomarker of disease severity and progression (Keane et al., 1997; Ziegenhagen et al., 1998b; Totani et al., 2002; Vasakova et al., 2009; Richards et al., 2012). The presence of elevated CCL2 concentrations in samples taken from WHWTs affected with CIPF is consistent with similar observations in HIPF patients (Capelli et al., 2005; Emad and Emad, 2007; Fujiwara et al., 2012) and highlights the potential for CCL2 to serve as a biomarker of disease when measured in serum and/or BALF.

Whereas CXCL8 concentrations were found to be elevated in the BALF from WHWTs affected with CIPF, similar to that reported in HIPF (Ziegenhagen et al., 1998a; Antoniou et al., 2006), no difference was observed comparing groups for serum CXCL8, a finding that differs from that reported for HIPF (Ziegenhagen et al., 1998b). Our research findings indicate that CXCL8 might serve as a potential marker of fibrosis in BALF, while its utility in blood samples for this purpose seems less promising. Whether the increase in these chemokines in serum and/or BALF of WHWTs affected with CIPF is a cause or a consequence of the disease has yet to be determined.

No significant differences were seen in the relative expression of CCL2, CXCL8, CCR2 and CXCR2 mRNA comparing lung tissue from WHWTs affected with CIPF and tissue from unaffected dogs. These results contrast with preliminary data that showed upregulation of expression of CCL2 and CXCL8 mRNA in the lungs of dogs affected with CIPF (Krafft et al., 2013). These discrepancies highlight the limitations of quantitative PCR, when applied to tissue biopsies. Histopathologically, CIPF is characterised by diffuse fibrosis with multifocal areas of accentuated subpleural and peribronchiolar fibrosis and profound alveolar epithelial changes (Syrja et al., 2013). The heterogeneous nature of the distribution of fibrosis could potentially explain differences in the outcome of analysis, since a relatively small sample is not necessarily representative of the organ as a whole. Another explanation for the lack of consistency between these two studies might relate to differences in the control populations used. The control group used in the study by Krafft et al. (2013) had a median age of 6.5 years (range 0.2–14 years), whereas the control group used in the present study was older, with a median age of 12.6 years (range 11.4–15.4 years), which was better matched to the case population. Furthermore, neither study used breed-matched tissue samples, which is another limitation of the study design, particularly since

the effect of breed on pulmonary gene expression has not been explored in any great detail. In an ideal situation, the control group would consist of lung tissue from WHWT without any evidence of fibrosis and matched for age and sex, but this is difficult to achieve when undertaking research in a clinical setting.

Immunolabelling for CCL2 and CXCL8 was observed in relatively few bronchial airway epithelial cells in the lungs of dogs affected with CIPF, although there was no evidence of expression in control lung tissue sections. These results may explain why quantitative PCR results failed to show any differences between groups, as it appears that chemokine expression is somewhat sporadic in nature. This observation could also explain the increased chemokine concentrations detected in the BALF of dogs affected with CIPF, as this could be produced locally into the lumen of the airway and not necessarily reach high concentrations in the circulation.

In one lung sample from a dog affected with CIPF, there was additional labelling of hyperplastic alveolar epithelial cells for CCL2 and CXCL8, as well as occasional macrophages expressing CXCL8. The source of CXCL8 in HIPF has been reported to be pulmonary fibroblasts (Keane et al., 1997), while CCL2 is mainly produced by hyperplastic alveolar epithelial cells, bronchial epithelial cells and macrophages (Mercer et al., 2009).

## Conclusions

The results of the present study suggest that both CCL2 and CXCL8 chemokines might be involved in the fibroproliferative process observed in CIPF. Further investigations are required to determine whether these chemokines could have clinical utility as prognostic biomarkers and/or surrogate markers of fibrosis, or as targets for interventional therapy.

## Conflict of interest statement

None of the authors of this paper has a financial or personal relationship with other people or organisations that could inappropriately influence or bias the content of the paper.

## Acknowledgements

This work was supported by a grant from the Fonds De La Recherche Scientifique – FNRS. Preliminary results were presented as an abstract at the 23rd Congress of the European College of Veterinary Internal Medicine – Companion Animals (ECVIM-CA), Liverpool, UK, 12–14 September 2013, and the 18th International Colloquium on Lung and Airway Fibrosis (ICLAF), Mont-Tremblant, Quebec, 20–24 September 2014. We gratefully thank Professor R. Hirt, Dr. E. Bomassi, Dr. D. De Lorenzi, Dr. R. Lavoué and Dr. B. Vanbrugghe for providing materials used in the present study.

## References

Ahn, M.H., Park, B.L., Lee, S.H., Park, S.W., Park, J.S., Kim, D.J., Jang, A.S., Park, J.S., Shin, H.K., Uh, S.T., et al., 2011. A promoter SNP rs4073T>A in the common allele of the interleukin 8 gene is associated with the development of idiopathic pulmonary fibrosis via the IL-8 protein enhancing mode. Respiratory Research 12, 73.

Antoniou, K.M., Tzouvelekis, A., Alexandrakis, M.G., Sfiridaki, K., Tsiligianni, I., Rachiotis, G., Tzanakis, N., Bouros, D., Milic-Emili, J., Siafakas, N.M., 2006. Different angiogenic activity in pulmonary sarcoidosis and idiopathic pulmonary fibrosis. Chest 130, 982–988.

Baran, C.P., Opalek, J.M., McMaken, S., Newland, C.A., O'Brien, J.M., Hunter, M.G., Bringardner, B.D., Monick, M.M., Brigstock, D.R., Stromberg, P.C., et al., 2007. Important roles for macrophages colony-stimulating factor, CC chemokine ligand 2, and mononuclear phagocytes in the pathogenesis of pulmonary fibrosis. American Journal of Respiratory and Critical Care Medicine 176, 78–89.

Bonecchi, R., Galliera, E., Borroni, E.M., Corsi, M.M., Locati, M., Mantovani, A., 2009. Chemokines and chemokine receptors: An overview. Frontiers in Bioscience 14, 540–551.

Capelli, A., Di Stefano, A., Gnemmi, I., Donner, C.F., 2005. CCR5 expression and CC chemokine levels in idiopathic pulmonary fibrosis. The European Respiratory Journal 25, 701–707.

Corcoran, B.M., Cobb, M., Martin, M.W., Dukes-McEwan, J., French, A., Fuentes, V.L., Boswood, A., Rhind, S., 1999. Chronic pulmonary disease in West Highland white terriers. Veterinary Record 144, 611–616.

Covvey, J.R., Mancl, E.E., 2014. Recent evidence for pharmacological treatment of idiopathic pulmonary fibrosis. Annals of Pharmacotherapy 48, 1611–1619.

Cui, A., Anhenn, O., Theegarten, D., Ohshimo, S., Bonella, F., Sixt, S.U., Peters, J., Sarria, R., Guzman, J., Costabel, U., 2010. Angiogenic and angiostatic chemokines in idiopathic pulmonary fibrosis and granulomatous lung disease. Respiration; International Review of Thoracic Diseases 80, 372–378.

Emad, A., Emad, V., 2007. Elevated levels of MCP-1, MIP-alpha and MIP-1 beta in the bronchoalveolar lavage (BAL) fluid of patients with mustard gas-induced pulmonary fibrosis. Toxicology 240, 60–69.

Fujiwara, A., Kobayashi, H., Masuya, M., Maruyama, M., Nakamura, S., Ibata, H., Fujimoto, H., Ohnishi, M., Urawa, M., Naito, M., et al., 2012. Correlation between circulating fibrocytes, and activity and progression of interstitial lung diseases. Respirology (Carlton, Vic.) 17, 693–698.

Gharaee-Kermani, M., Denholm, E.M., Phan, S.H., 1996. Costimulation of fibroblast collagen and transforming growth factor beta1 gene expression by monocyte chemoattractant protein-1 via specific receptors. The Journal of Biological Chemistry 271, 17779–17784.

Gharaee-Kermani, M., McCullumsmith, R.E., Charo, I.F., Kunkel, S.L., Phan, S.H., 2003. CC-chemokine receptor 2 required for bleomycin-induced pulmonary fibrosis. Cytokine 24, 266–276.

Heikkila, H.P., Lappalainen, A.K., Day, M.J., Clercx, C., Rajamaki, M.M., 2011. Clinical, bronchoscopic, histopathologic, diagnostic imaging, and arterial oxygenation findings in West Highland white terriers with idiopathic pulmonary fibrosis. Journal of Veterinary Internal Medicine 25, 433–439.

Heikkila-Laurila, H.P., Rajamaki, M.M., 2014. Idiopathic pulmonary fibrosis in West Highland white terriers. The Veterinary Clinics of North America. Small Animal Practice 44, 129–142.

Inomata, M., Kamio, K., Azuma, A., Matsuda, K., Kokuho, N., Miura, Y., Hayashi, H., Nei, T., Fujita, K., Saito, Y., et al., 2014. Pirfenidone inhibits fibrocyte accumulation in the lungs in bleomycin-induced murine pulmonary fibrosis. Respiratory Research 15, 16.

Inoshima, I., Kuwano, K., Hamada, N., Hagimoto, N., Yoshimi, M., Maeyama, T., Takeshita, A., Kitamoto, S., Egashira, K., Hara, N., 2004. Anti-monocyte chemoattractant protein-1 gene therapy attenuates pulmonary fibrosis in mice. American Journal of Physiology 286, 1038–1044.

Keane, M.P., Arenberg, D.A., Lynch, J.P., 3rd, Whyte, R.I., Iannettoni, M.D., Burdick, M.D., Wilke, C.A., Morris, S.B., Glass, M.C., DiGiovine, B., et al., 1997. The CXC chemokines, IL-8 and IP-10, regulate angiogenic activity in idiopathic pulmonary fibrosis. Journal of Immunology 159, 1437–1443.

Krafft, E., Heikkila, H.P., Jespers, P., Peeters, D., Day, M.J., Rajamaki, M.M., McEntee, K., Clercx, C., 2011. Serum and bronchoalveolar lavage fluid endothelin-1 concentrations as diagnostic biomarkers of canine idiopathic pulmonary fibrosis. Journal of Veterinary Internal Medicine 25, 990–996.

Krafft, E., Laurila, H.P., Peters, I.R., Bureau, F., Peeters, D., Day, M.J., Rajamaki, M.M., Clercx, C., 2013. Analysis of gene expression in canine idiopathic pulmonary fibrosis. The Veterinary Journal 198, 479–486.

Lilja-Maula, L.I., Laurila, H.P., Syrja, P., Lappalainen, A.K., Krafft, E., Clercx, C., Rajamaki, M.M., 2014. Long-term outcome and use of 6-minute walk test in West Highland white terriers with idiopathic pulmonary fibrosis. Journal of Veterinary Internal Medicine 28, 379–385.

Lobetti, R.G., Milner, R., Lane, E., 2001. Chronic idiopathic pulmonary fibrosis in five dogs. Journal of the American Animal Hospital Association 37, 119–127.

Martina, S., Martina, V., Monika, M., Jan, P., Libor, K., Ilja, S., 2009. Angiostatic versus angiogenic chemokines in IPF and EAA. Respiratory Medicine 103, 1651–1656.

Mercer, P.F., Johns, R.H., Scotton, C.J., Krupiczojc, M.A., Konigshoff, M., Howell, D.C., McAnulty, R.J., Das, A., Thorley, A.J., Tetley, T.D., et al., 2009. Pulmonary epithelium is a prominent source of proteinase-activated receptor-1-inducible CCL2 in pulmonary fibrosis. American Journal of Respiratory and Critical Care Medicine 179, 414–425.

Moore, B.B., Kolodsick, J.E., Thannickal, V.J., Cooke, K., Moore, T.A., Hogaboam, C., Wilke, C.A., Toews, G.B., 2005. CCR2-mediated recruitment of fibrocytes to the alveolar space after fibrotic injury. The American Journal of Pathology 166, 675–684.

Peters, I.R., Peeters, D., Helps, C.R., Day, M.J., 2007. Development and application of multiple internal reference (housekeeper) gene assays for accurate normalisation of canine gene expression studies. Veterinary Immunology and Immunopathology 117, 55–966.

Phillips, R.J., Burdick, M.D., Hong, K., Lutz, M.A., Murray, L.A., Xue, Y.Y., Belperio, J.A., Keane, M.P., Strieter, R.M., 2004. Circulating fibrocytes traffic to the lungs in response to CXCL12 and mediate fibrosis. The Journal of Clinical Investigation 114, 438–446.

Raghu, G., Collard, H.R., Egan, J.J., Martinez, F.J., Behr, J., Brown, K.K., Colby, T.V., Cordier, J.F., Flaherty, K.R., Lasky, J.A., et al., 2011. An official ATS/ERS/JRS/ALAT statement: Idiopathic pulmonary fibrosis: Evidence-based guidelines for diagnosis and

management. American Journal of Respiratory and Critical Care Medicine 183, 788–824.
Richards, T.J., Kaminski, N., Baribaud, F., Flavin, S., Brodmerkel, C., Horowitz, D., Li, K., Choi, J., Vuga, L.J., Lindell, K.O., et al., 2012. Peripheral blood proteins predict mortality in idiopathic pulmonary fibrosis. American Journal of Respiratory and Critical Care Medicine 185, 67–76.
Shinoda, H., Tasaka, S., Fujishima, S., Yamasawa, W., Miyamoto, K., Nakano, Y., Kamata, H., Hasegawa, N., Ishizaka, A., 2009. Elevated CC chemokine level in bronchoalveolar lavage fluid is predictive of a poor outcome of idiopathic pulmonary fibrosis. Respiration; International Review of Thoracic Diseases 78, 285–292.
Suga, M., Iyonaga, K., Ichiyasu, H., Saita, N., Yamasaki, H., Ando, M., 1999. Clinical significance of MCP-1 levels in BALF and serum in patients with interstitial lung diseases. The European Respiratory Journal 14, 376–382.
Syrja, P., Heikkila, H.P., Lilja-Maula, L., Krafft, E., Clercx, C., Day, M.J., Ronty, M., Myllarniemi, M., Rajamaki, M.M., 2013. The histopathology of idiopathic pulmonary fibrosis in West Highland white terriers shares features of both non-specific interstitial pneumonia and usual interstitial pneumonia in man. Journal of Comparative Pathology 149, 303–313.
Totani, Y., Saitoh, Y., Sakakibara, H., Miyamori, I., Ishizaki, T., 2002. Clinical characterization of interleukin-8 in patients with idiopathic pulmonary fibrosis. The Journal of the Japanese Respiratory Society 40, 869–874.
Vasakova, M., Sterclova, M., Kolesar, L., Slavcev, A., Pohunek, P., Sulc, J., Skibova, J., Striz, I., 2009. Bronchoalveolar lavage fluid cellular characteristics, functional parameters and cytokine and chemokine levels in interstitial lung diseases. Scandinavian Journal of Immunology 69, 268–274.
Ziegenhagen, M.W., Schrum, S., Zissel, G., Zipfel, P.F., Schlaak, M., Muller-Quernheim, J., 1998a. Increased expression of proinflammatory chemokines in bronchoalveolar lavage cells of patients with progressing idiopathic pulmonary fibrosis and sarcoidosis. Journal of Investigative Medicine 46, 223–231.
Ziegenhagen, M.W., Zabel, P., Zissel, G., Schlaak, M., Muller-Quernheim, J., 1998b. Serum level of interleukin 8 is elevated in idiopathic pulmonary fibrosis and indicates disease activity. American Journal of Respiratory and Critical Care Medicine 157, 762–768.

Research in Veterinary Science 101 (2015) 57–62

Contents lists available at ScienceDirect

Research in Veterinary Science

journal homepage: www.elsevier.com/locate/yrvsc

# Evaluation of chemokines CXCL8 and CCL2, serotonin, and vascular endothelial growth factor serum concentrations in healthy dogs from seven breeds with variable predisposition for canine idiopathic pulmonary fibrosis

E. Roels [a,*], E. Krafft [a], N. Antoine [b], F. Farnir [c], H.P. Laurila [d], S. Holopainen [d], M.M. Rajamäki [d], C. Clercx [a]

[a] Department of Clinical Sciences, Faculty of Veterinary Medicine, University of Liege, Bd de Colonster, Liege, Belgium
[b] Department of Morphology and Pathology, Histology, Faculty of Veterinary Medicine, University of Liege, Bd de Colonster, Liege, Belgium
[c] Department of Animal Productions, Biostatistics and Bioinformatics Applied to Veterinary Sciences, Faculty of Veterinary Medicine, University of Liege, Bd de Colonster, Liege, Belgium
[d] Department of Equine and Small Animal Medicine, Faculty of Veterinary Medicine, PO Box 57, 00014 University of Helsinki, Helsinki, Finland

ARTICLE INFO

*Article history:*
Received 19 February 2015
Accepted 30 May 2015
Available online xxxx

*Keywords:*
Canine idiopathic pulmonary fibrosis
CXCL8
CCL2
Serotonin
VEGF

ABSTRACT

The West Highland white terrier (WHWT) is particularly prone to canine idiopathic pulmonary fibrosis (CIPF). We hypothesized that higher circulating concentrations of chemokines CXCL8, CCL2, serotonin (5-HT), or vascular endothelial growth factor (VEGF) could serve as predisposing factors for CIPF development in the WHWT breed. Serum samples from 103 healthy dogs of seven different breeds variably predisposed to CIPF were collected. Serum CXCL8 concentrations were higher in healthy WHWT compared with each of the other groups of healthy dogs. Serum CCL2 concentrations were higher in healthy WHWT and Maltese compared with King Charles spaniels and Malinois Belgian shepherds. No relevant inter-breed differences were observed for serum 5-HT concentrations regarding CIPF predisposition. VEGF values from 89.3% of samples tested were below the kit detection limit. In conclusion, high CXCL8 blood concentrations and possibly CCL2 concentrations might be related to the breed predisposition of the WHWT for CIPF and warrants further investigations.



## 1. Introduction

Canine idiopathic pulmonary fibrosis (CIPF) is a progressive parenchymal lung disease of unknown origin, which mainly affects older dogs of the West Highland white terrier (WHWT) breed (Heikkilä-Laurila and Rajamäki, 2014). Rare cases have also been described in other terrier breeds such as the Staffordshire terrier (Lobetti et al., 2001) and the Scottish terrier (Krafft et al., 2011). Pathogenesis of CIPF is currently unknown, although a genetic basis is strongly suspected due to the breed predisposition (Heikkilä-Laurila and Rajamäki, 2014). CIPF shares several clinical features with human IPF (Corcoran et al., 1999; Lobetti et al., 2001; Heikkilä et al., 2011); however, there are minor histopathological differences between these entities (Syrjä et al., 2013). In human IPF, chronic alveolar epithelial cell injuries and subsequent dysregulated tissue repair are considered to be the main pathological processes involved in the pathogenesis of this fibroproliferative disease (Coward et al., 2010; Raghu et al., 2011). The mechanisms of repair initiated by a tissue injury are complex and are determined by the presence of biological mediators such as growth factors and chemokines, which coordinate most aspects of the inflammatory and subsequent repair responses. Consequently, we hypothesized that higher circulating concentrations of pro-fibrotic molecules in dogs from the WHWT breed may serve as predisposing factors for CIPF development, by contributing to exacerbated tissue repair after an injury, leading subsequently to the development of fibrosis. This hypothesis is further supported by a recent publication focused on transforming growth factor beta 1 (TGF-β1) demonstrating higher serum TGF-β1 concentrations in healthy dogs from breeds predisposed to CIPF in comparison with breeds not predisposed to the disease (Krafft et al., 2014). Therefore, the aim of the present study was to compare basal circulating blood concentrations of four molecules of interest obtained in healthy dogs from seven breeds differently predisposed to CIPF. Selection of molecules studied was based on their potential implication into the pathogenesis of canine pulmonary fibrosis in view of data from either human or canine literature and were as follows: the chemokine (C-X-C motif) ligand 8 (CXCL8) (Cui et al., 2010; Ahn et al., 2011; Krafft et al., 2013), the chemokine (C-C motif) ligand 2 (CCL2) (Krafft et al., 2013; Moore, 2014), the serotonin (5-HT) (Konigshoff et al., 2010; Krafft et al., 2013), and the vascular endothelial growth factor (VEGF) (Ando et al., 2010; Woodcock et al., 2013).

* Corresponding author at: Faculty of Veterinary Medicine, Small Animal Department, Bd de Colonster 20 B44, 4000 Liege, Belgium. Tel.: +32 4 3664243.
*E-mail address:* roels@ulg.ac.be (E. Roels).

http://dx.doi.org/10.1016/j.rvsc.2015.05.020
0034-5288/

## 2. Materials and methods

### 2.1. Source of samples and ethics statement

A total of 103 healthy dogs from seven different breeds were included in this study. Ninety-three of these dogs were examined and sampled at the University of Liege, Belgium, and the remaining 10 at the University of Helsinki, Finland. Breeds selected were WHWT, Scottish terrier (ST), Jack Russell terrier (JRT), Maltese (M), King Charles spaniel (KCS), Labrador retriever (LR), and Malinois Belgian Shepherd (MBS). Those breeds were considered as highly (WHWT), possibly (ST, JRT), or not (M, KCS, LR, MBS) –CIPF predisposed breeds. ST and JRT were chosen as terrier breeds potentially predisposed to CIPF; given that one CIPF case has already been confirmed by histopathology in a dog from the ST breed (Krafft et al., 2011) and that CIPF has been clinically suspected in five JRT, but not histopathologically confirmed (personal observations). M breed was chosen as a non-terrier breed sharing similarities in weight and size with the WHWT breed. KCS breed was chosen as another small-size non-terrier breed predisposed for degenerative mitral valve disease (DMVD), another fibrotic disease (Borgarelli and Buchanan, 2012). LR and MBS breeds were chosen as large breeds definitively not predisposed to fibrotic lung disease. All dogs included were privately owned, and samples were obtained after acquiring the written consent of the owners. The study protocol was approved by the Committee of Experimental Animals of the University of Liège, Belgium (permit number: 1435, date of approval: 14 March 2013) and by the equivalent committee of Western Finland (permit number: ESLH-2008-05403, date of approval: 27 June 2008; ESAVI/7383/04.10.07/2013, date of approval: 13 November 2013). Detailed features of the study population are summarized in Table 1. Health status was based on complete history and physical examination in all dogs, in addition to routine hematologic and serum biochemical examinations in 87% and 79% of dogs, respectively. A thoracic high-resolution computed tomography (HRCT) was performed in nine out of 18 clinically healthy WHWT and did not reveal any abnormalities. Besides, all included WHWT were followed up at various time intervals after blood sampling. Thirteen of them were still alive at the time of writing, 1.1–6 years after sampling of the blood used in the present study. So far, none of them have developed any respiratory complaint as determined by telephone consultation with the owners. The remaining five dogs were euthanized or died within 6 months to 4.6 years after blood sampling, for reasons unrelated to the respiratory system; lung tissue samples were available in three of these dogs (2.6, 4.4, and 4.6 years after blood sampling, respectively). On lung histopathology, mild interstitial fibrosis was noticed in all three dogs, but none of them ever displayed any signs compatible with CIPF. Given the time interval between blood sampling and lung histopathology and the absence of clinical signs, blood samples from those three dogs were not discarded.

### 2.2. Samples processing

Blood samples were obtained in plain tubes from all dogs. Thirty minutes after blood collection, tubes were centrifuged at 4 °C for 15 min at 1300 × *g*. Serum was harvested and transferred into 1.5 mL plastic cryotubes, and samples were stored at −80 °C until analysis. Serum CXCL8, CCL2, and VEGF measurements were performed using commercial canine ELISA kits (R&D Systems) in duplicate, according to the manufacturer's instructions. Serum 5-HT measurement was performed using a commercial human ELISA kit (IBL international) previously validated in dogs (Ljungvall et al., 2013).

### 2.3. Statistical methods

Descriptive statistics (XLStat software, Addinsoft) was used for clinical (gender, age, and weight), biochemical, and hematologic results; data were reported as median and range. Serum CXCL8, CCL2, and 5-HT concentrations were compared between breeds using a global linear model (SAS software, SAS Institute Inc.) integrating the effects of age and gender as covariables; data were expressed as least square mean ± SE. Proportions were compared using the $Chi^2$ test with the threshold 5%, data were expressed as percentage (XLStat software, Addinsoft). *P*-values ≤ 0.05 were considered as significant.

**Table 1**
Characteristics of the study population.

| Breed | *N* | Sex, male/female | Age, yr (median, range) | Weight, kg (median, range) |
|---|---|---|---|---|
| WHWT | 18 | 8/10 | 9.2 (2.9–16.9) | 8.7 (7.4–12.0) |
| ST | 14 | 3/11 | 5.1 (0.9–9.5) | 10.0 (8.5–13.6) |
| JRT | 16 | 2/14 | 7.2 (1.0–11.8) | 6.9 (5.9–12.6) |
| M | 15 | 4/11 | 6.2 (0.9–12.6) | 5.3 (4.0–9.0) |
| KCS | 14 | 5/9 | 5.8 (0.5–10.3) | 8.3 (6.8–12.0) |
| LR | 12 | 5/7 | 5.7 (1.6–12.2) | 36.4 (23.0–42.0) |
| MBS | 14 | 10/4 | 5.5 (1.5–7.8) | 31.2 (23.0–35.0) |

WHWT, West Highland white terrier. ST, Scottish terrier. JRT, Jack Russell terrier. M, Maltese. KCS, King Charles spaniel. LR, Labrador retriever. MBS, Malinois Belgian Shepherd.

## 3. Results and discussion

### 3.1. Physical, biochemical, and hematologic examination

Physical examination was unremarkable in all dogs included in this study. Dogs did not have any signs or findings indicating disease. Biochemical and hematologic data are summarized in Table 2. Most measured parameters were within laboratory reference ranges or only discreetly increased, except for alkaline phosphatase (ALP) and platelet count. ALP was above the upper limit of reference range in most dogs from WHWT (73%) and ST (75%) breeds; these percentages were high in comparison with those obtained in M (8%), KCS (7%), LR (13%), and MBS (0%) ($P < 0.0001$). These observations are in agreement with previously published data indicating an increased ALP activity in dogs from the WHWT and ST breeds (Gallagher et al., 2006; Nestor et al., 2006; Heikkilä et al., 2011), and possibly attributed in ST to benign subclinical hyperadrenocorticism (Zimmerman et al., 2010). Whether such phenomenon also exists in the WHWT breed has not been investigated. Platelet count was below the lower limit of reference range in most dogs from KCS (54%) breed compared with other breeds: WHWT (0%), ST (7%), JRT (0%), M (0%), LR (29%), and MBS (23%) ($P = 0.002$ vs. WHWT, JRT, and M). In thrombocytopenic KCS, macrothrombocytes were observed on blood smear. This finding can be related to the existence of an autosomal mutation in beta1-tubulin gene in KCS leading to asymptomatic macrothrombocytopenia in this breed (Davis et al., 2008). On the opposite, platelet count was most frequently above the upper limit of reference range in WHWT dogs (39%) compared with other breeds: ST (21%), JRT (17%), M (8%), KCS (15%), LR (0%), and MBS (8%) ($P = 0.147$). Thrombocytosis in apparently healthy WHWT, although not significant in the present study, has already been reported previously (Heikkilä et al., 2011). In human IPF patients, increased platelet reactivity has recently been demonstrated and may participate to the fibroproliferative process observed in the disease by the release of pro-fibrotic mediators such as TGF-β1 (Fernandez and Eickelberg, 2012; Crooks et al., 2014). In dogs, although the reactivity of platelets has not been investigated, a similar hypothesis might explain why breeds with high basal platelet numbers would be more prone to develop lung fibrosis.

### 3.2. CXCL8 and CCL2 concentrations

Serum CXCL8 and CCL2 concentrations (pg/mL) are presented in Figs. 1 and 2, respectively. Significantly higher serum CXCL8 concentrations were observed in healthy WHWT in comparison with all other groups of healthy dogs ($P \leq 0.05$). Significant differences were also

**Table 2**
Biochemical and hematologic data.

| Breed | WHWT | ST | JRT | M | KCS | LR | MBS | References |
|---|---|---|---|---|---|---|---|---|
| TP, (g/L) | 62 (52–74) | 67 (54–87) | 59 (50–73) | 61 (52–70) | 65 (60–75) | 67 (65–72) | 68 (56–71) | 60–80 |
| Creat, (μmol/L) | 79.3 (65.0–115.7) | 81.7 (60.8–93.0) | 89.3 (74.1–106.4) | 90.2 (78.9–101.9) | 73.1 (55.7–97.5) | 112.5 (57.2–144.4) | 80.4 (51.3–122.3) | <133 |
| ALT, (IU/L) | 37 (23–156) | 47 (26–158) | 71 (47–133) | 34 (23–156) | 33 (19–288) | 58 (39–119) | 50 (23–73) | 5–62 |
| ALP, (IU/L) | 191 (40–654) | 176 (32–816) | 64 (24–235) | 40 (9–136) | 63 (29–125) | 56 (23–269) | 54 (21–117) | 12–121 |
| Ht, (%) | 51 (38–59) | 58 (46–67) | 50 (43–59) | 48 (42–54) | 42 (34–47) | 49 (35–56) | 52 (46–58) | 37–55 |
| WBC, ($\times 10^6$ μ/L) | 7820 (4130–11800) | 7925 (4590–22200) | 9160 (6830–11900) | 7340 (4770–14600) | 9040 (6020–15160) | 8070 (4480–18100) | 9000 (5970–13400) | 6000–15000 |
| Plt, ($\times 10^3$ μ/L) | 446 (254–754) | 383 (136–543) | 414 (248–554) | 437 (248–535) | 180 (54–625) | 225 (72.5–340) | 247 (92–560) | 200–500 |

WHWT, West Highland white terrier. ST, Scottish terrier. JRT, Jack Russell terrier. M, Maltese. KCS, King Charles spaniel. LR, Labrador retriever. MBS, Malinois Belgian Shepherd. TP, total protein. Creat, creatinine. ALT, alanine-amino transferase. ALP, alkaline phosphatase. Ht, hematocrit. WBC, white blood cell count. Plt, platelet count. Data are expressed as median and range.

noticed between M and both KCS and LR ($P \leq 0.008$). Serum CCL2 concentrations were significantly higher in healthy WHWT and M in comparison with KCS and MBS ($P \leq 0.05$). A significant difference for serum CCL2 concentrations was also observed between LR and MBS ($P = 0.04$). Effects of age and gender on serum CCL2 and CXCL8 concentrations were not significant.

In humans, both CXCL8 and CCL2 concentrations were found to be increased in blood (Ziegenhagen et al., 1998a; Suga et al., 1999; Fujiwara et al., 2012) and bronchoalveolar lavage fluid (BALF) (Capelli et al., 2005; Antoniou et al., 2006; Baran et al., 2007) of IPF patients compared with healthy volunteers and correlated with lung function (Capelli et al., 2005; Emad and Emad, 2007; Martina et al., 2009; Vasakova et al., 2009), disease progression (Ziegenhagen et al., 1998b; Totani et al., 2002), and outcome (Shinoda et al, 2009; Richards et al., 2012). Furthermore, several studies suggested an involvement of the chemokine CCL2 in the pathogenesis of IPF, notably through its action on resident pulmonary fibroblast and circulating fibrocytes, promoting the generation of abundant extracellular matrix in the lungs (Gharaee-Kermani et al., 1996; Phillips et al., 2004; Moore et al., 2005; Inomata et al., 2014). Such strong evidence involving CXCL8 in the pathogenesis of the disease are lacking, although this chemokine is thought to act as a pro-fibrotic factor in IPF via the promotion of exacerbated

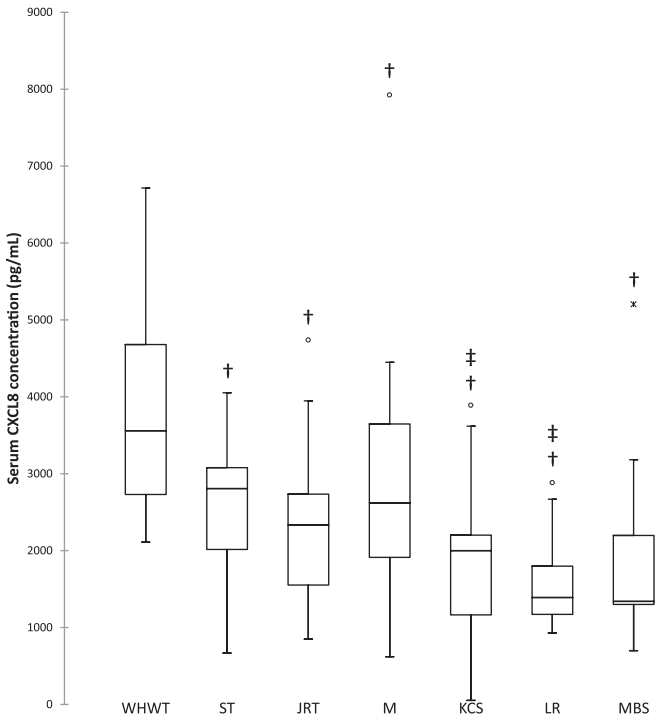


**Fig. 1.** Box plot of serum CXCL8 concentrations (pg/mL) obtained from healthy West Highland white terriers (WHWT, n = 18), Scottish terriers (ST, n = 14), Jack Russell terriers (JRT, n = 16), Maltese (M, n = 15), King Charles spaniels (KCS, n = 14), Labrador retrievers (LR, n = 12), and Malinois Belgian Shepherds (MBS, n = 14). The box represents the interquartile range, with the median indicated by the horizontal line. The whiskers extend from the minimum to the maximum values, excluding outliers that are presented by an open circle or extreme outliers that are presented by asterisks. †Statistically different from WHWT ($P \leq 0.05$). ‡Statistically different from M ($P \leq 0.008$).

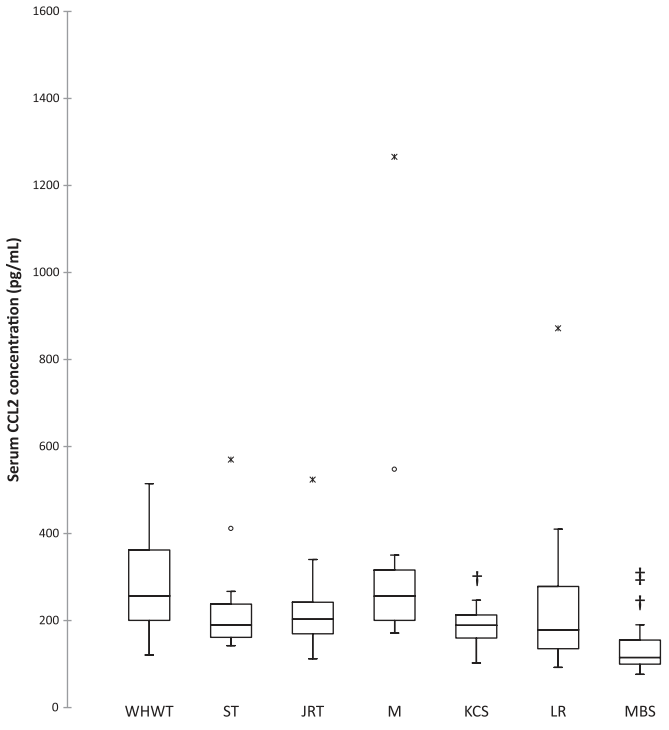


**Fig. 2.** Box plot of serum CCL2 concentrations (pg/mL) obtained from healthy West Highland white terriers (WHWT, n = 18), Scottish terriers (ST, n = 14), Jack Russell terriers (JRT, n = 16), Maltese (M, n = 15), King Charles spaniels (KCS, n = 14), Labrador retrievers (LR, n = 12), and Malinois Belgian Shepherds (MBS, n = 14). The box represents the interquartile range, with the median indicated by the horizontal line. The whiskers extend from the minimum to the maximum values, excluding outliers that are presented by an open circle or extreme outliers that are presented by asterisks. †Statistically different from WHWT and M ($P \leq 0.01$). ‡Statistically different from L ($P = 0.04$).

angiogenesis (Strieter et al., 2002; Rosenkilde and Schwartz, 2004; Antoniou et al., 2006; Martina et al., 2009; Cui et al., 2010).

In dogs, mRNA expression of CXCL8 and CCL2 was found to be increased in CIPF lungs compared with controls (Krafft et al., 2013). Higher CXCL8 concentrations were found in BALF, but not in serum, of WHWT with CIPF in comparison with healthy WHWT, and both BALF and serum CCL2 concentrations were shown to be increased in WHWT with CIPF compared with healthy WHWT (Krafft et al., 2013; personal communications).

In the present study, finding various serum CXCL8 and CCL2 concentrations in healthy dogs from different breeds suggests that such concentrations might be genetically determined in dogs. Although not proven, a cause–effect relationship between the development of CIPF and the high circulating CXCL8 and CCL2 concentrations observed in healthy WHWT might exist. A similar hypothesis was already proposed for serum TGF-β1 concentrations which were also found to be increased in healthy WHWT compared with breeds less predisposed to CIPF (Krafft et al., 2014). However, not all dogs from the WHWT breed develop the disease at an advanced age. Therefore, the high serum TGF-β1, CXCL8, or even CCL2 concentrations found in apparently healthy WHWT might serve as one of the multiple predisposing factors for CIPF development by triggering an inappropriate lung response after an injury, leading subsequently to pulmonary fibrosis. In humans, whether healthy people with increased CXCL8, CCL2, or TGF-β1 blood concentrations are specifically at risk for development of fibrosis has not been studied. Nevertheless, some studies highlighted the fact that IPF patients with a high TGF-β1 producing genotype are incline to have a worse prognosis and a more rapid deterioration in lung function (Arkwright et al., 2000; Alhamad et al., 2013). A single nucleotide polymorphism (rs4073T > A) was also recently found in the promoter of the CXCL8 gene and was significantly associated with higher BALF CXCL8 concentrations and an increased risk of development of IPF in humans (Ahn et al., 2011). Existence of such polymorphism in CIPF dogs has not yet been investigated.

Increased serum CCL2 concentrations observed in healthy M in the present study does not seem to predispose this breed to a fibrotic disease. In human medicine, the chemokine CCL2, while involved in the pathogenesis of IPF, is also involved in a variety of other diseases, ranging from immune-mediated and vascular diseases to cancer (Locati et al, 2005). Whether the high serum CCL2 concentrations observed in healthy M might predispose this breed to specific pathological conditions is unknown.

### 3.3. Serum 5-HT concentrations

Serum 5-HT concentrations (ng/mL) obtained in healthy KCS, ST, M, and MBS were significantly higher in comparison with those obtained in healthy WHWT, JRT, and LR ($P \leq 0.05$). Data are presented in Fig. 3. Effects of age and gender were not significant. These results do not indicate relevant interbreed differences regarding CIPF predisposition and are not in favor of any influence of basal 5-HT concentrations on CIPF development in WHWT. In humans, altered regulation of the serotonin pathway is thought to be associated with the development of pulmonary fibrosis since an increased expression of 5-HT receptors was found in IPF lungs (Fabre and Crestani, 2010; Konigshoff et al., 2010) and anti-serotonin therapy was shown to attenuate induced pulmonary fibrosis in mice (Konigshoff et al., 2010; Skurikhin et al., 2012). In dogs, 5-HT has essentially been studied in the pathogenesis of the DMVD, another fibrotic disease (Oyama and Levy, 2010; Ljungvall et al., 2013; Cremer et al., 2014; Mangklabruks and Surachetpong, 2014). Increased 5-HT blood concentrations were found in healthy KCS in comparison with healthy dogs from other breeds predisposed or not to DMVD (Arndt et al., 2009). In the present study, although KCS displayed the highest serum 5-HT concentration, the difference with other breeds was only significant in comparison with WHWT, JRT, and LR.

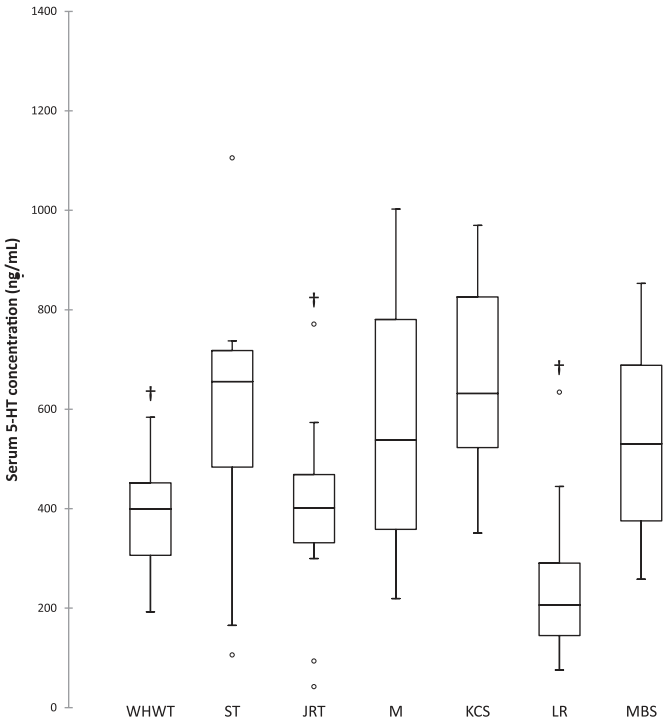


**Fig. 3.** Box plot of serum 5-HT concentrations (ng/mL) obtained from healthy West Highland white terriers (WHWT, n = 18), Scottish terriers (ST, n = 14), Jack Russell terriers (JRT, n = 16), Maltese (M, n = 15), King Charles spaniels (KCS, n = 14), Labrador retrievers (LR, n = 12), and Malinois Belgian Shepherds (MBS, n = 14). The box represents the interquartile range, with the median indicated by the horizontal line. The whiskers extend from the minimum to the maximum values, excluding outliers that are presented by an open circle or extreme outliers that are presented by asterisks. †Statistically different from ST, M, KCS, and MBS ($P \leq 0.05$).

### 3.4. Serum VEGF concentrations

The majority of samples tested for serum VEGF concentrations, 92 out of 103 (89.3%), were below the ELISA kit detection limit (39.1 pg/mL). By consequence, a quantitative comparison between breeds was not possible. Results above the kit detection limit were found in 3 KCS (21.4%), 3 JRT (18.8%), 3 LR (25.0%), 1 WHWT (5.6%), and 1 ST (7.1%). Frequency of positive results was not different between breed groups ($P = 0.147$). In humans, VEGF was found significantly decreased in BALF of IPF patients compared with healthy volunteers (Koyama et al., 2002) and serum concentrations were found to correlate with the disease progression (Ando et al., 2010). Moreover, nintedanib, a tyrosine kinase receptor antagonist which inhibits a number of key receptors including the VEGF receptor, was proven to slow down the progression of the disease and to improve the quality of life in patients with IPF (Woodcock et al., 2013). These observations made in human IPF enhance the interest toward the VEGF molecule in CIPF, although results of the present study were not conclusive due to the assay limitation.

### 3.5. Limitations

Limitations of the present study were that only half of the healthy WHWT underwent a thoracic HRCT and that thoracic X-rays were not available for the healthy other dogs included in this study. Moreover, although CIPF HRCT findings were described in detail (Johnson et al., 2005; Heikkilä et al., 2011), the sensitivity of this imaging technique for detection of early lung lesions has not been established. Therefore, some included WHWT, even the ones that underwent a thoracic HRCT, might already have subclinical CIPF lesions at the time of

sampling, which could have interfered with the results of the present study. This is unlikely, in view of absence of development of respiratory clinical signs in time intervals ranging from 6 months to 6 years after blood sampling. However, the mild interstitial fibrosis noticed on lung histopathology from three included WHWT (2.6–4.6 years after blood sampling), without evidence of CIPF clinical signs, highlights the potential existence of a subclinical CIPF state in dogs from the WHWT breed. Another limitation of the present study could be that some dogs included, no matter from which breed they are belonging, may have suffered from subclinical inflammatory or neoplastic diseases at the time of sampling, that could have influenced serum concentrations.

## 4. Conclusion

The present study demonstrated increased serum CXCL8 concentrations in healthy dogs from the WHWT breed in comparison with other breeds less or not predisposed to CIPF. Serum CCL2 concentrations were increased in healthy WHWT, but also in M, a non CIPF-predisposed breed. No relevant interbreed differences were observed for 5-HT with regard to CIPF predisposition. Breed-related differences in VEGF blood concentrations could not be investigated since most of the results obtained were below the kit detection limit. Increased serum CXCL8 concentrations, and possibly CCL2 concentrations, found in healthy WHWT might be related to the breed predisposition of the WHWT for CIPF and possibly serve as predisposing factor for disease development. Further investigations are warranted to explore how those chemokines systemically and locally participate to pulmonary fibrosis mechanisms.

## Acknowledgements

This work was supported by a grant from the 'Fonds de la Recherche Scientifique (FNRS)'. Preliminary results were presented as an abstract at the 18th International Colloquium on Lung and Airway Fibrosis (ICLAF), Mont-Tremblant, Quebec, 20–24 September 2014. We gratefully thank Joëlle Piret from the Department of Morphology and Pathology of the University of Liège for her technical assistance.

## References

Ahn, M.H., Park, B.L., Lee, S.H., Park, S.W., Park, J.S., Kim, D.J., Jang, A.S., Park, J.S., Shin, H.K., Uh, S.T., Kim, Y.K., Kim, Y.W., Han, S.K., Jung, K.S., Lee, K.Y., Jeong, S.H., Park, J.W., Choi, B.W., Park, I.W., Chung, M.P., Shin, H.D., Song, J.W., Kim, D.S., Park, C.S., Shim, Y.S., 2011. A promoter SNP rs4073T > A in the common allele of the interleukin 8 gene is associated with the development of idiopathic pulmonary fibrosis via the IL-8 protein enhancing mode. Respiratory Research 12, 73.

Alhamad, E.H., Cal, J.G., Shakoor, Z., Almogren, A., Alboukai, A.A., 2013. Cytokine gene polymorphisms and serum cytokine levels in patients with idiopathic pulmonary fibrosis. BMC Medical Genetics 14, 66.

Ando, M., Miyazaki, E., Ito, T., Hiroshige, S., Nureki, S.I., Ueno, T., Takenaka, R., Fukami, T., Kumamoto, T., 2010. Significance of serum vascular endothelial growth factor level in patients with idiopathic pulmonary fibrosis. Lung 188, 247–252.

Antoniou, K.M., Tzouvelekis, A., Alexandrakis, M.G., Sfiridaki, K., Tsiligianni, I., Rachiotis, G., Tzanakis, N., Bouros, D., Milic-Emili, J., Siafakas, N.M., 2006. Different angiogenic activity in pulmonary sarcoidosis and idiopathic pulmonary fibrosis. Chest 130, 982–988.

Arkwright, P.D., Laurie, S., Super, M., Pravica, V., Schwarz, M., Webb, A.K., Hutchinson, I.V., 2000. TGF-β1 genotype and accelerated decline in lung function of patients with cystic fibrosis. Thorax 55, 459–462.

Arndt, J.W., Reynolds, C.A., Singletary, G.E., Connolly, J.M., Levy, R.J., Oyama, M.A., 2009. Serum serotonin concentrations in dogs with degenerative mitral valve disease. Journal of Veterinary Internal Medicine 23, 1208–1213.

Baran, C.P., Opalek, J.M., McMaken, S., Newland, C.A., O'Brien Jr., J.M., Hunter, M.G., Bringardner, B.D., Monick, M.M., Brigstock, D.R., Stromberg, P.C., Hunninghake, G.W., Marsh, C.B., 2007. Important roles for macrophage colony-stimulating factor, CC chemokine ligand 2, and mononuclear phagocytes in the pathogenesis of pulmonary fibrosis. American Journal of Respiratory and Critical Care Medicine 176, 78–89.

Borgarelli, M., Buchanan, J.W., 2012. Historical review, epidemiology and natural history of degenerative mitral valve disease. Journal of Veterinary Cardiology 14, 93–101.

Capelli, A., Di Stefano, A., Gnemmi, I., Donner, C.F., 2005. CCR5 expression and CC chemokine levels in idiopathic pulmonary fibrosis. The European Respiratory Journal 25, 701–707.

Corcoran, B.M., Cobb, M., Martin, M.W., Dukes-McEwan, J., French, A., Fuentes, V.L., Boswood, A., Rhind, S., 1999. Chronic pulmonary disease in West Highland white terriers. The Veterinary Record 144, 611–616.

Coward, W.R., Saini, G., Jenkins, G., 2010. The pathogenesis of idiopathic pulmonary fibrosis. Therapeutic Advances in Respiratory Disease 4, 367–388.

Cremer, S.E., Singletary, G.E., Olsen, L.H., Wallace, K., Haggstrom, J., Ljungvall, I., Hoglund, K., Reynolds, C.A., Pizzinat, N., Oyama, M.A., 2014. Serotonin concentrations in platelets, plasma, mitral valve leaflet, and left ventricular myocardial tissue in dogs with myxomatous mitral valve disease. Journal of Veterinary Internal Medicine 28, 1534–1540.

Crooks, M.G., Fahim, A., Nassem, K.M., Morice, A.H., Hart, S.P., 2014. Increased platelet reactivity in idiopathic pulmonary fibrosis is mediated by a plasma factor. Plos One 9, e111347.

Cui, A., Anhenn, O., Theegarten, D., Ohshimo, S., Bonella, F., Sixt, S.U., Peters, J., Sarria, R., Guzman, J., Costabel, U., 2010. Angiogenic and angiostatic chemokines in idiopathic pulmonary fibrosis and granulomatous lung disease. Respiration 80, 372–378.

Davis, B., Toivio-Kinnucan, M., Schuller, S., Boudreaux, M.K., 2008. Mutation in β1-tubulin correlates with macrothrombocytopenia in Cavalier King Charles Spaniels. Journal of Veterinary Internal Medicine 22, 540–545.

Emad, A., Emad, V., 2007. Increased levels of MCP-1, MIP-alpha and MIP-1 beta in the bronchoalveolar lavage (BAL) fluid of patients with mustard gas-induced pulmonary fibrosis. Toxicology 240, 60–69.

Fabre, A., Crestani, B., 2010. Serotonin: a new start for an old friend. Thorax 65, 946–947.

Fernandez, I.E., Eickelberg, O., 2012. The impact of TGF-β on lung fibrosis, from targeting to biomarkers. Proceedings of the American Thoracic Society 9, 111–116.

Fujiwara, A., Kobayashi, H., Masuya, M., Maruyama, M., Nakamura, S., Ibata, H., Fujimoto, H., Ohnishi, M., Urawa, M., Naito, M., Takagi, T., Kobayashi, T., Gabazza, E.C., Takei, Y., Taguchi, O., 2012. Correlation between circulating fibrocytes, and activity and progression of interstitial lung diseases. Respirology 17, 693–698.

Gallagher, A.E., Panciera, D.L., Panciera, R.J., 2006. Hyperphosphatasemia in scottish terriers: 7 cases. Journal of Veterinary Internal Medicine 20, 418–421.

Gharaee-Kermani, M., Denholm, E.M., Phan, S.H., 1996. Costimulation of fibroblast collagen and transforming growth factor beta1 gene expression by monocyte chemoattractant protein-1 via specific receptors. The Journal of Biological Chemistry 271, 17779–17784.

Heikkilä, H.P., Lappalainen, A.K., Day, M.J., Clercx, C., Rajamäki, M.M., 2011. Clinical, bronchoscopic, histopathologic, diagnostic imaging, and arterial oxygenation findings in West Highland White Terriers with idiopathic pulmonary fibrosis. Journal of Veterinary Internal Medicine 25, 433–439.

Heikkilä-Laurila, H.P., Rajamäki, M.M., 2014. Idiopathic pulmonary fibrosis in West Highland white terriers. The Veterinary Clinics of North America. Small Animal Practice 44, 129–142.

Inomata, M., Kamio, K., Azuma, A., Matsuda, K., Kokuho, N., Miura, Y., Hayashi, H., Nei, T., Fujita, K., Saito, Y., Gemma, A., 2014. Pirfenidone inhibits fibrocyte accumulation in the lungs in bleomycin-induced murine pulmonary fibrosis. Respiratory Research 15, 16.

Johnson, V.S., Corcoran, B.M., Wotton, P.R., Schwarz, T., Sullivan, M., 2005. Thoracic high-resolution computed tomographic findings in dogs with canine idiopathic pulmonary fibrosis. The Journal of Small Animal Practice 46, 381–388.

Konigshoff, M., Dumitrascu, R., Udalov, S., Amarie, O.V., Reiter, R., Grimminger, F., Seeger, W., Schermuly, R.T., Eickelberg, O., 2010. Increased expression of 5-hydroxytryptamine2A/B receptors in idiopathic pulmonary fibrosis: a rationale for therapeutic intervention. Thorax 65, 949–955.

Koyama, S., Sato, E., Haniuda, M., Numanami, H., Nagai, S., Izumi, T., 2002. Decreased level of vascular endothelial growth factor in bronchoalveolar lavage fluid of normal smokers and patients with pulmonary fibrosis. American Journal of Respiratory and Critical Care Medicine 166, 382–385.

Krafft, E., Heikkilä, H.P., Jespers, P., Peeters, D., Day, M.J., Rajamäki, M.M., Mc Entee, K., Clercx, C., 2011. Serum and bronchoalveolar lavage fluid endothelin-1 concentrations as diagnostic biomarkers of canine idiopathic pulmonary fibrosis. Journal of Veterinary Internal Medicine 25, 990–996.

Krafft, E., Laurila, H.P., Peters, I.R., Bureau, F., Peeters, D., Day, M.J., Rajamäki, M.M., Clercx, C., 2013. Analysis of gene expression in canine idiopathic pulmonary fibrosis. Veterinary Journal 198, 479–486.

Krafft, E., Lybaert, P., Roels, E., Laurila, H.P., Rajamäki, M.M., Farnir, F., Myllarniemi, M., Day, M.J., Mc Entee, K., Clercx, C., 2014. Transforming growth factor beta 1 activation, storage, and signaling pathways in idiopathic pulmonary fibrosis in dogs. Journal of Veterinary Internal Medicine 28, 1666–1675.

Ljungvall, I., Hoglund, K., Lilliehook, I., Oyama, M.A., Tidholm, A., Tvedten, H., Haggstrom, J., 2013. Serum serotonin concentration is associated with severity of myxomatous mitral valve disease in dogs. Journal of Veterinary Internal Medicine 27, 1105–1112.

Lobetti, R.G., Milner, R., Lane, E., 2001. Chronic idiopathic pulmonary fibrosis in five dogs. Journal of the American Animal Hospital Association 37, 119–127.

Locati, M., Bonecchi, R., Corsi, M.M., 2005. Chemokines and their receptors. American Journal of Clinical Pathology 123, S82–S85.

Mangklabruks, T., Surachetpong, S.D., 2014. Plasma and platelet serotonin concentrations in healthy dogs and dogs with myxomatous mitral valve disease. Journal of Veterinary Cardiology 16, 155–162.

Martina, S., Martina, V., Monika, M., Jan, P., Libor, K., Ilja, S., 2009. Angiostatic versus angiogenic chemokines in IPF and EAA. Respiratory Medicine 103, 1651–1656.

Moore, B.B., 2014. Following the path of CCL2 from prostaglandins to periostin in lung fibrosis. American Journal of Respiratory Cell and Molecular Biology 50, 848–852.

Moore, B.B., Kolodsick, J.E., Thannickal, V.J., Cooke, K., Moore, T.A., Hogaboam, C., Wilke, C.A., Toews, G.B., 2005. CCR2-mediated recruitment of fibrocytes to the alveolar space after fibrotic injury. The American Journal of Pathology 166, 675–684.

Nestor, D.D., Holan, K.M., Johnson, C.A., Schall, W., Kaneene, J.B., 2006. Serum alkaline phosphatase activity in Scottish Terriers versus dogs of other breeds. Journal of the American Veterinary Medical Association 228, 222–224.

Oyama, M.A., Levy, R.J., 2010. Insights into serotonin signaling mechanisms associated with canine degenerative mitral valve disease. Journal of Veterinary Internal Medicine 24, 27–36.

Phillips, R.J., Burdick, M.D., Hong, K., Lutz, M.A., Murray, L.A., Xue, Y.Y., Belperio, J.A., Keane, M.P., Strieter, R.M., 2004. Circulating fibrocytes traffic to the lungs in response to CXCL12 and mediate fibrosis. The Journal of Clinical Investigation 114, 438–446.

Raghu, G., Collard, H.R., Egan, J.J., Martinez, F.J., Behr, J., Brown, K.K., Colby, T.V., Cordier, J.F., Flaherty, K.R., Lasky, J.A., Lynch, D.A., Ryu, J.H., Swigris, J.J., Wells, A.U., Ancochea, J., Bouros, D., Carvalho, C., Costabel, U., Ebina, M., Hansell, D.M., Johkoh, T., Kim, D.S., King Jr., T.E., Kondoh, Y., Myers, J., Muller, N.L., Nicholson, A.G., Richeldi, L., Selman, M., Dudden, R.F., Griss, B.S., Protzko, S.L., Schunemann, H.J., 2011. An official ATS/ERS/JRS/ALAT statement: idiopathic pulmonary fibrosis: evidence-based guidelines for diagnosis and management. American Journal of Respiratory and Critical Care Medicine 183, 788–824.

Richards, T.J., Kaminski, N., Baribaud, F., Flavin, S., Brodmerkel, C., Horowitz, D., Li, K., Choi, J., Vuga, L.J., Lindell, K.O., Klesen, M., Zhang, Y., Gibson, K.F., 2012. Peripheral blood proteins predict mortality in idiopathic pulmonary fibrosis. American Journal of Respiratory and Critical Care Medicine 185, 67–76.

Rosenkilde, M.M., Schwartz, T.W., 2004. The chemokine system – a major regulator of angiogenesis in health and disease. Acta Pathologica, Microbiologica et Immunologica Scandinavica 112, 481–495.

Shinoda, H., Tasaka, S., Fujishima, S., Yamasawa, W., Miyamoto, K., Nakano, Y., Kamata, H., Hasegawa, N., Ishizaka, A., 2009. Increased CC chemokine level in bronchoalveolar lavage fluids is predictive of a poor outcome in idiopathic pulmonary fibrosis. Respiration 78, 285–292.

Skurikhin, E.G., Andreeva, T.V., Khmelevskaya, E.S., Ermolaeva, L.A., Pershina, O.V., Krupin, V.A., Ermakova, N.N., Reztsova, A.M., Stepanova, I.E., Gol'dberg, V.E., Dygai, A.M., 2012. Effect of antiserotonin drug on the development of lung fibrosis and blood system reactions after intratracheal administration of bleomycin. Bulletin of Experimental Biology and Medicine 152, 519–523.

Strieter, R.M., Belperio, J.A., Keane, M.P., 2002. CXC chemokines in angiogenesis related to pulmonary fibrosis. Chest 122, 298S–301S.

Suga, M., Iyonaga, K., Ichiyasu, H., Saita, N., Yamasaki, H., Ando, M., 1999. Clinical significance of MCP-1 levels in BALF and serum in patients with interstitial lung diseases. The European Respiratory Journal 14, 376–382.

Syrjä, P., Heikkilä, H.P., Lilja-Maula, L., Krafft, E., Clercx, C., Day, M.J., Ronty, M., Myllarniemi, M., Rajamäki, M.M., 2013. The histopathology of idiopathic pulmonary fibrosis in west highland white terriers shares features of both non-specific interstitial pneumonia and usual interstitial pneumonia in man. Journal of Comparative Pathology 149, 303–313.

Totani, Y., Saitoh, Y., Sakakibara, H., Miyamori, I., Ishizaki, T., 2002. Clinical characterization of interleukin-8 in patients with idiopathic pulmonary fibrosis. The Journal of the Japanese Respiratory Society 40, 869–874.

Vasakova, M., Sterclova, M., Kolesar, L., Slavcev, A., Pohunek, P., Sulc, J., Skibova, J., Striz, I., 2009. Bronchoalveolar lavage fluid cellular characteristics, functional parameters and cytokine and chemokine levels in interstitial lung diseases. Scandinavian Journal of Immunology 69, 268–274.

Woodcock, H.V., Molyneaux, P.L., Maher, T.M., 2013. Reducing lung function decline in patients with idiopathic pulmonary fibrosis: potential of nintedanib. Journal of Drug Design Development and Therapy 7, 503–510.

Ziegenhagen, M.W., Schrum, S., Zissel, G., Zipfel, P.F., Schlaak, M., Muller-Quernheim, J., 1998a. Increased expression of proinflammatory chemokines in bronchoalveolar lavage cells of patients with progressing idiopathic pulmonary fibrosis and sarcoidosis. Journal of Investigative Medicine 46, 223–231.

Ziegenhagen, M.W., Zabel, P., Zissel, G., Schlaak, M., Muller-Quernheim, J., 1998b. Serum level of interleukin 8 is increased in idiopathic pulmonary fibrosis and indicates disease activity. American Journal of Respiratory and Critical Care Medicine 157, 762–768.

Zimmerman, K.L., Panciera, D.L., Panciera, R.J., Oliver, J.W., Hoffmann, W.E., Binder, E.M., Randall, D.C., Kinnarney, J.H., 2010. Hyperphosphatasemia and concurrent adrenal gland dysfunction in apparently healthy Scottish terriers. Journal of the American Veterinary Medical Association 237, 178–186.

Veterinary Pathology OnlineFirst, published on April 22, 2016 as doi:10.1177/0300985816641991

Brief Communication

Veterinary Pathology
1-3

DOI: 10.1177/0300985816641991
vet.sagepub.com

# No Evidence of Herpesvirus Infection in West Highland White Terriers With Canine Idiopathic Pulmonary Fibrosis

**E. Roels[1], M. Dourcy[2], S. Holopainen[3], M. M. Rajamäki[3], L. Gillet[2], B. Ehlers[4], and C. Clercx[1]**

## Abstract

In humans, horses, and rodents, an association between pulmonary fibrotic disorders and gammaherpesvirus infection has been suggested. In dogs, canine idiopathic pulmonary fibrosis (CIPF), a progressive fibrotic lung disease of unknown origin and poorly understood pathophysiology, has been reported to occur in West Highland white terriers (WHWTs). The present study investigated the potential association between CIPF and herpesvirus infection. A PCR assay, using a mixture of degenerate and deoxyinosine-substituted primers targeting highly conserved regions of the DNA polymerase gene (DPOL) of herpesviruses, was applied on both lung and blood samples from WHWTs affected with CIPF and controls. Herpesvirus DPOL sequence could not be amplified from any of 46 lung samples (28 affected WHWTs and 18 control dogs of various breeds) and 38 blood samples (19 CIPF WHWTs and 19 control age-matched WHWTs) included. An association between CIPF and herpesvirus infection is therefore unlikely. Investigation of other causes of the disease is warranted.

## Keywords

dogs, lung, respiratory, idiopathic pulmonary fibrosis, gammaherpesviruses

Canine idiopathic pulmonary fibrosis (CIPF) is a progressive fibrotic lung disease which is most commonly reported in aged dogs of the West Highland white terrier (WHWT) breed.[6] Clinical signs in WHWTs affected with CIPF include progressive dyspnea, exercise intolerance and cough.[6] In addition, inspiratory Velcro-like crackles are commonly noticed on lung auscultation.[6] The cause and pathogenesis of CIPF are currently unknown, but a genetic basis is strongly suspected due to the breed predisposition.[6] Not all dogs from the WHWT breed develop CIPF at an advanced age, which suggests the involvement of triggering events in the development of the disease. CIPF shares several clinical features with human IPF, although histopathological differences have been described.[11] In human IPF, repetitive alveolar epithelial cell injuries and subsequent disordered tissue repair are considered to be the main pathological process involved in this fibro-proliferative disease.[3] Several studies have implicated viral infections, particularly Epstein Barr virus (EBV) infection, as a cause of epithelial injury and therefore as an important factor in the pathogenesis of IPF.[10] Indeed, EBV has been frequently detected in the lungs of IPF patients compared with control patients across several studies.[10] In horses, a fibrotic pulmonary disease called equine multinodular pulmonary fibrosis was proven to be associated with gammaherpesvirus infection. Equine herpesvirus 5 has been consistently isolated from lung tissue of affected horses, while none of the control horses were found positive.[13] Compelling evidence for gammaherpesvirus involvement has also been observed in experimental murine models of pulmonary fibrosis.[8,9] Based on these results obtained in humans, horses and rodents, and in view of the fact that a causative agent for CIPF has not yet been identified, we investigated the potential association between herpesvirus infection and CIPF in WHWTs.

For this purpose, a generic PCR assay[5] targeting highly conserved regions of the DNA polymerase gene (DPOL) of alpha-, beta- and gammaherpesviruses was applied to lung and blood samples collected from WHWTs affected with CIPF and from control unaffected dogs. Lung tissue samples collected from 15 male and 13 female WHWTs affected with CIPF (age: 9.1 to 16.3 years, median 13.6 years), and 18 control dogs (6

[1]Department of Clinical Sciences, FARAH, Faculty of Veterinary Medicine, University of Liège, Liège, Belgium
[2]Department of Infectious and Parasitic Diseases, FARAH, Faculty of Veterinary Medicine, University of Liège, Liège, Belgium
[3]Department of Equine and Small Animal Medicine, Faculty of Veterinary Medicine, University of Helsinki, Helsinki, Finland
[4]Robert Koch-Institute, Berlin, Germany

**Corresponding Author:**
E. Roels, Department of Clinical Sciences, Faculty of Veterinary Medicine, Quartier Vallée 2, Avenue de Cureghem 3, Building B44, 4000 Liège, Belgium.
Email: eroels@ulg.ac.be

male and 12 female) of various breeds (5 WHWTs, 6 Jack Russell terriers, 2 Mixed breed, 1 Beagle, 1 Bulldog, 1 Newfoundland, 1 Maltese, 1 American Staffordshire) (age: 3.7 to 15.0 years, median 8.6 years) were included in the study. From 19 of the above mentioned WHWTs with CIPF, EDTA blood samples were also collected and included in the study. EDTA blood samples from 11 male and 8 female unaffected WHWTs, aged from 5.7 to 15.0 years (median 10.4 years) were included for control. The CIPF diagnosis was achieved according to a previously published approach and was confirmed by lung histopathology in all dogs.[6] Health status of the control WHWTs was assessed by taking a complete history and by performing a physical examination, hematology, serum biochemistry, echocardiography and thoracic high-resolution computed tomography, which did not reveal any abnormalities. Lung tissues used as controls were obtained from dogs euthanized for reasons unrelated to the study. These dogs had no history or clinical signs of lower respiratory disease at the time of euthanasia and no abnormalities were identified on necropsy and histopathological examination of their lungs. Lung biopsies were obtained within 30 minutes after euthanasia, snap-frozen in liquid nitrogen and stored at –80°C until further processing. Blood was collected from the jugular vein into EDTA tubes, aliquoted in 1.5 mL plastic cryotubes and stored at –80°C until analysis. DNA was extracted from both lung and blood samples with a commercially available kit following manufacturer instructions (DNeasy Blood & Tissue kit, QIAGEN GmbH, Hilden, Germany), with an overnight incubation in proteinase K at 56°C for lung samples. DNA samples were stored at –80°C until analysis. The panherpesvirus generic DPOL PCR was performed with a mixture of degenerate and deoxyinosine-substituted primers in a nested format as described previously.[5]

PCR analysis of the 46 lung and 38 blood samples from WHWTs affected with CIPF and control dogs did not result in any amplification of a herpesvirus DPOL sequence (expected product size: approximately 210 bp–230 bp). However, identical bands of approximately 280 bp and 150 bp length appeared in all lanes (Figs. 1 and 2); these were of host origin as revealed by exemplary sequence analysis. In contrast, samples (spleen, lymph node, blood and other matrices) of human and animal origin (including carnivorans) that had previously tested positive for members of the herpesvirus subfamilies *Alpha-*, *Beta-*, and *Gammaherpesvirinae*, and were analyzed here for control, gave rise to the expected DPOL amplification products (Fig. 3). Although the generic PCR employed here may not detect all vertebrate herpesviruses with equal sensitivity, this molecular technique has previously been shown to successfully identify a plethora of novel alpha-, beta- and gammaherpesviruses in a wide range of host species including carnivorans.[4,5] We are therefore confident that the negative results obtained here were due to the absence of herpesvirus DNA in the dog samples (at least in clinically relevant numbers) rather than to a limitation of the method. However, based on the present results, a herpesvirus contribution to the pathogenesis of CIPF cannot completely be excluded, as "hit and run" mechanism[1] may be at work or a very low load of latent or persistent herpesvirus may exist that can be missed with the methodology employed here. So far, few reports have suggested the existence of an EBV-like virus in dogs, associated with lymphoma and oro-nasal tumor based on serological and molecular data.[2,7] However, contrasting negative results were reported in a very recent study using degenerate PCR assays on 112 canine tissue samples.[12] Consequently, these conflicting published results together with the results presented here do not sufficiently support the existence of

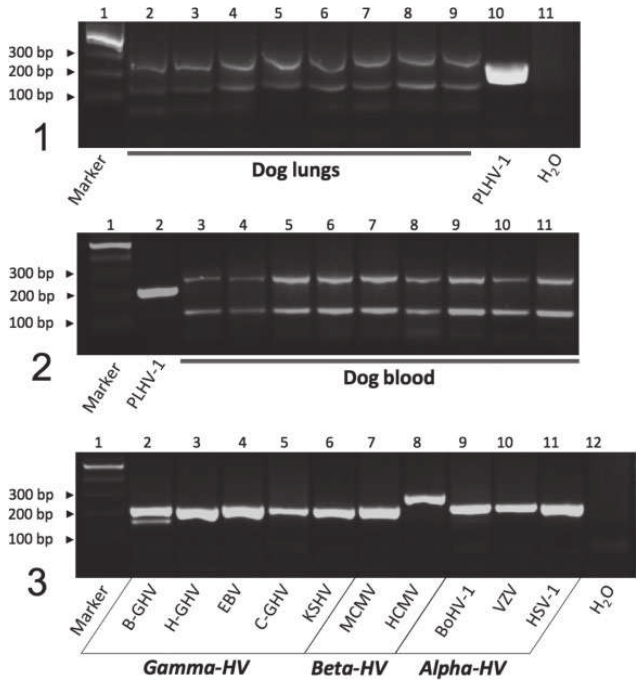


**Figures 1–2.** Analysis of lung (Fig. 1) and blood (Fig. 2) samples collected from West Highland White Terrier (WHWT) dogs affected with CIPF with panherpesvirus generic DPOL PCR. **Figure 1.** Lane 1: 100 bp ladder (Marker); lanes 2–9: lung samples of CIPF-affected WHWTs; lane 10: porcine lymphotropic gammaherpesvirus 1 (PLHV-1) (genus *Macavirus*; positive control; sample origin: spleen); lane 11: PCR-grade water. **Figure 2.** Lane 1: 100 bp ladder (Marker); lane 2: positive control as in Fig. 1; lanes 3–11: blood samples of CIPF-affected WHWTs. **Figure 3.** Additional herpesvirus-positive control samples were included to demonstrate the potential of the generic PCR method to universally amplify sequences of alpha, beta- and gammaherpesviruses from diverse sample materials. Lane 1: 100 bp ladder (Marker); lane 2: gammaherpesvirus of badger (B-GHV) (genus *Percavirus*; sample origin: blood); lane 3: gammaherpesvirus of hyena (H-GHV) (genus *Rhadinovirus*; sample origin: lung); lane 4: Epstein-Barr virus (EBV) (human; genus *Lymphocryptovirus*; sample origin: adenocarcinoma); lane 5: gammaherpesvirus of chimpanzee (C-GHV) (genus *Lymphocryptovirus*; sample origin: lymph node); lane 6: Kaposi sarcoma herpesvirus (KSHV) (human; genus *Rhadinovirus*; sample origin: blood); lane 7: murine cytomegalovirus (MCMV) (genus *Muromegalovirus*; sample origin: lung); lane 8: human cytomegalovirus (HCMV) (genus *Cytomegalovirus*; sample origin: urine); lane 9: bovine herpesvirus 1 (BoHV-1) (genus *Varicellovirus*; sample origin: vaginal swab); lane 10: varicella-zoster virus (VZV) (genus *Varicellovirus*; sample origin: skin swab); lane 11: herpes simplex virus type 1 (HSV-1) (human; genus *Simplexvirus*; sample origin: spleen); lane 12: PCR-grade water. GHV; gammaherpesvirus.

gammaherpesviruses in dogs and encourage further research in this field.

In conclusion, the results of the present study suggest that an association between herpesvirus infection and CIPF is unlikely. Investigation of other causative agents potentially associated with CIPF is warranted.

## Acknowledgements

The authors thank Cornelia Walter for excellent technical assistance.

## Declaration of Conflicting Interests

The author(s) declared no potential conflicts of interest with respect to the research, authorship, and/or publication of this article.

## Funding

The author(s) received no financial support for the research, authorship, and/or publication of this article.

## References

1. Ambinder RF. Gammaherpesviruses and "hit-and-run" oncogenesis. *Am J Pathol*. 2000;**156**:1–3.
2. Chiu HC, Chow KC, Fan YH, et al. Expression of EBV-encoded oncogenes and EBV-like virions in multiple canine tumors. *Vet Microbiol*. 2013;**163**(1–2): 79–89.
3. Coward WR, Saini G, Jenkins G. The pathogenesis of idiopathic pulmonary fibrosis. *Ther Adv Respir Dis*. 2010;**4**(6):367–388.
4. Ehlers B, Dural G, Yasmum N, et al. Novel mammalian herpesviruses and lineages within the Gammaherpesvirinae: cospeciation and interspecies transfer. *J Virol*. 2008;**82**(7):3509–3516.
5. Ehlers B, Kuchler J, Yasmum N, et al. Identification of novel rodent herpesviruses, including the first gammaherpesvirus of Mus musculus. *J Virol*. 2007; **81**(15):8091–8100.
6. Heikkila-Laurila HP, Rajamaki MM. Idiopathic pulmonary fibrosis in West Highland white terriers. *Vet Clin North Am Small Anim Pract*. 2014;**44**(1): 129–142.
7. Huang SH, Kozak PJ, Kim J, et al. Evidence of an oncogenic gammaherpesvirus in domestic dogs. *Virology*. 2012;**427**(2):107–117.
8. Lok SS, Haider Y, Howell D, et al. Murine gammaherpes virus as a cofactor in the development of pulmonary fibrosis in bleomycin resistant mice. *Eur Respir J*. 2002;**20**:1228–1232.
9. McMillan TR, Moore BB, Weinberg JB, et al. Exacerbation of established pulmonary fibrosis in a murine model by gammaherpesvirus. *Am J Respir Crit Care Med*. 2008;**177**:771–780.
10. Molyneaux PL, Maher TM. The role of infection in the pathogenesis of idiopathic pulmonary fibrosis. *Eur Respir Rev*. 2013;**22**(129):376–381.
11. Syrja P, Heikkila HP, Lilja-Maula L, et al. The histopathology of idiopathic pulmonary fibrosis in West Highland white terriers shares features of both nonspecific interstitial pneumonia and usual interstitial pneumonia in man. *J Comp Pathol*. 2013;**149**(2–3):303–313.
12. Waugh EM, Gallagher A, McAulay K, et al. Gammaherpesviruses and canine lymphoma: no evidence for direct involvement in commonly occurring lymphomas. *J Gen Virol*. 2015;**96**(Pt7):1863–1872.
13. Williams KJ, Maes R, Del Piero F, et al. Equine multinodular pulmonary fibrosis: a newly recognized herpesvirus-associated fibrotic lung disease. *Vet Pathol*. 2007;**44**:849–862.

# DISCUSSION

Objectives of the present work were to improve the phenotype characterization of CIPF using HRCT and echocardiography, and to search for biomarkers and for etiologic agents.

Our first aim was to investigate whether HRCT images of the lungs obtained under sedation can be used for the diagnosis of CIPF. Being able to rely on images obtained under sedation would be helpful for the diagnosis but also for follow-up investigations since general anaesthesia is often at risk in cardiopulmonary diseased patients. Furthermore, the possibility to safely, easily, and rapidly repeat T-HRCT examination in WHWTs affected with CIPF may be useful for improving our knowledge about the natural history of the disease, as well as for assessing the effect of potential novel treatments in the future. We compared T-HRCT images obtained under sedation and general anaesthesia in WHWTs affected with CIPF and controls for the identification and gradation of specific CIPF features using the glossary of terms of the Fleischner Society (Hansell et al., 2008) and a scoring system. We found that T-HRCT images obtained under sedation were more frequently impacted by motion artefacts than images obtained under general anaesthesia, but were of sufficient quality to permit the identification of specific pulmonary features of CIPF in the majority of cases, allowing the confirmation of the CIPF diagnosis. However, differences were found between sedation and general anaesthesia in the identification of consolidations and in the gradation of GGO and mosaic attenuation pattern extent, suggesting that sedation and general anaesthesia cannot be used interchangeably with the same confidence for comparison of repeated examinations over time. Explanations for the differences observed between sedation and general anaesthesia for the identification and gradation of those specific lesions are more likely related to the different respiratory pattern of the dogs under both conditions. Indeed, during sedation, dogs were allowed to breathe by themselves and images were obtained either during inspiratory or expiratory phase (or a mix of both), while during general anaesthesia, an end-expiratory pause was artificially induced. Mosaic attenuation pattern, GGO or consolidations may all be influenced by the breathing pattern and the amount of air present in the alveoli. Consequently, standardized anaesthesia and ventilation protocols should be advised to obtain comparable and reliable images for prospective long-term follow-up studies in the future. Otherwise sedation seems to be a good alternative for HRCT diagnosis of CIPF when general anaesthesia is not recommended. Honeycombing, the major feature of IPF in humans, was not observed in our population of WHWTs affected with CIPF, which suggests a different pathophysiology or disease severity between CIPF in dogs and IPF in humans; this is an important issue which requires further investigations in the future.

Our second objective was to investigate whether the recently described echocardiographic index PV/PA (Merveille et al., 2015), can be used for the non-invasive diagnosis of precapillary PH in WHWTs affected with CIPF. As explained in the introduction section, the diagnosis of PH in veterinary medicine is challenging as right heart catheterization is not performed in practice, and given that the non-invasive echocardiographic diagnosis of PH requires the presence of a tricuspid regurgitant jet which is not always the case (Schober and Baade, 2006; Soydan et al., 2015). Our study demonstrated that the PV/PA ratio was significantly decreased in WHWTs affected with CIPF and concomitant PH (confirmed by the presence of a VmaxTR above 2.8 m/s) in comparison with unaffected controls without PH (VmaxTR below 2.8 m/s) or presumed to be free of PH (absence of TR allowing an estimation of PAP). PV/PA was also correlated with other echocardiographic indices that have been shown to be useful in the diagnosis of PH: Vmax TR, AT:ET, MPA/Ao and RPAD Index, and with the 6MWD, while there was no correlation with arterial pO2 values and with serum NT-proBNP concentrations.

Only 50% of WHWTs affected with CIPF included in our study had a measurable TR, with a TR maximal velocity compatible with the presence of PH in 31% of the CIPF dogs. This result is comparable with the one found by Schober and collaborators (2006) who described a TR in 58% of their included CIPF WHWTs, 44% having a VmaxTR above 3.1m/s. This finding is also in agreement with the human literature where Doppler regurgitation signals adequate for the calculation of systolic PAP were found in only 27% to 48% of people affected with IPF depending on studies (Arcasoy et al., 2003; Nathan et al., 2008). Furthermore, in dogs with a measurable TR, underestimation or overestimation of PAP based on VmaxTR value may occur such as recently described by Soydan and collaborators (2015). Indeed, these authors showed that using peak TR velocity as surrogate for invasive PAP measurements is prone to inaccuracy as the correlation between the 2 methods was moderate with wide confidence intervals. Similar discrepancies between echocardiography and RHC have also been described in human medicine with moderate correlation between the two methods (Attaran et al., 2009; Rich et al., 2011). In the specific context of IPF, echocardiography was found accurate for reflecting PAP measured by RHC in only 40% of cases (Nathan et al., 2008). Another study in IPF patients confirmed that PAP estimated by echocardiography is not reliably accurate as the mean bias between the 2 methods was 7.75 mmHg with limits of agreements ranging from -35 to 20 mmHg (Swanson et al., 2008). In our study, 3 WHWTs affected with CIPF had VmaxTR below 2.8 m/s suggesting the absence of PH. However, according to their PV/PA values in 2D ranging from 0.462 to 0.774 with a median of 0.618 (range in control dogs without PH = 0.983 – 1.060), those dogs may potentially suffer from PH, their Vmax TR being possibly underestimated. On the contrary, 3 control WHWTs had VmaxTR values compatible with PH, while they were

clinically healthy and had biochemical and haematological results within normal limits. While overestimation of VmaxTR is possible for those dogs, they also might have suffered from subclinical early CIPF lesion and secondary PH at the time of echocardiography; their PV/PA values slightly decreased (median 0.760, range 0.737-0.871) being compatible with this hypothesis. Ideally, control dogs need to be followed at regular intervals, but practically such a repetitive follow-up is difficult to achieve, particularly in apparently healthy individuals.

Decreased PV/PA in CPIF WHWTs with PH was attributable to both an increase in PA diameter and a decrease in PV diameter. PA distension may appear as a consequence of an increased pulmonary vascular bed resistance due to the remodelling of parenchymal lung vessels associated with the underlying progressive fibrotic lung disease and chronic hypoxic vasoconstriction (Fulton and Ryerson, 2015). In IPF patients suffering from PH, structural alterations in pulmonary arteries include proliferative intimal lesions, media thickening and adventitial fibrosis, and range from isolated thickening to complete occlusion of the vessels by scar tissue (Farkas et al., 2011). The decreased PV diameter could be explained by a reduction of left ventricular preload secondary to increased pulmonary arterial resistance, a compression of the vein by the enlarged adjacent artery or a combination of both. Administration of diuretics may also have contributed to decreased preload in some dogs. An invasive measure of the central venous pressure could potentially help us to better understand the mechanism leading to a reduction in the diameter of the pulmonary vein, but was not performed in our study.

In addition to PV/PA, we investigated other echocardiographic indices that have been showed to be useful in the diagnosis of PH. A trend for an increased MPA/Ao and for a decreased AT:ET and RPAD Index was observed for CIPF WHWTs with PH compared with healthy WHWTs without PH but the difference between groups was not significant, more likely explained by the small numbers of dogs in each category. Reduced AT:ET values observed in CIPF WHWTs in our study tends to confirm results previously obtained by Schober and collaborators (2006) who demonstrated that this index may predict PH (> 45mmHg) at a cut-off value of ≤ 0.31 with a sensitivity and specificity of 73 and 87% respectively. Serres and collaborators (2007) later confirmed the use of AT:ET for the diagnosis of PH (> 30 mmHg) in dogs with PH of different aetiologies (mainly left heart disease and various respiratory disorders) at a cut-off value of ≤ 0.44 (Se 71%, Sp 71%). In our study, 10 CIPF WHWTs had AT:ET values below 0.38 (only 1 CIPF dog below 0.31), while control dogs were all above 0.4, which tends to corroborate that the decrease of AT:ET may reflect the presence of PH. Similar decrease in AT:ET has also been reported in the human literature related to patients suffering from PH secondary to chronic interstitial lung disease (Nowak et al., 2008). Higher MPA/Ao values were found in CIPF WHWTs with PH which supports the work made by Serres and

associates (2007) who demonstrated that MPA/Ao was correlated with PAP estimated by TR ($r = 701$, $P < 0.001$) and can be used for the diagnosis of PH (PAP > 30 mmHg) at a cut-off value of 0.98 with a moderate sensitivity and specificity (73 and 76% respectively). A trend for a decreased RPAD Index was observed CIPF WHWTs with PH compared with controls, suggesting a reduced compliance of pulmonary arteries in CIPF. The recent publication by Venco and associates (2014) indicated that, in heartworm-infected dogs, RPAD Index values lower than 35%, 27% or 22% were indicative of mild, moderate or severe PH respectively. Another recent work about the RPDA Index was done by Visser and collaborators (2016) and corroborated the finding that a RPAD Index below 29% may predict PH (> 50mmHg). In the present study, a RPAD Index value below 35% were found in 10 (83%) out of 12 WHWTs affected with CIPF, including 4 dogs (33%) with values below 29%. A RPAD Index value below 35% was also found in 6 out of 18 (33%) controls (5 of those 6 dogs having values below 29%). This finding of low RPAD Index value in control dogs may support the likelihood that some of them were suffering from PH due to subclinical CIPF lesions. Another explanation may reside in the different study population characteristics (our study population being older than studies from Visser and Venco), pulmonary arterial compliance having been shown to decrease in old dogs (Mercier et al., 2010).

Finally, significant moderate correlations were found between PV/PA and VmaxTR, AT:ET, MPA/Ao and RPAD Index. Those correlations in addition to the finding that PV/PA was reduced in CIPF WHWTs with PH highlighted the potential application of the PV/PA ratio as an indirect non-invasive marker for PH assessment in WHWTs affected with CIPF. Significant moderate correlations were also found between PV/PA and the 6MWD, but not between PV/PA and arterial pO2 values or serum NT-proBNP concentrations. In humans, 6MWD was found to be an independent predictor of the presence of PH in IPF patients, increasing PAP being associated with statistically significant decline in 6MWD (Minai et al., 2012). IPF patients with PH were also shown to have significant lower arterial pO2 at rest in comparison with IPF patients without PH, but solely a moderate correlation was found between PAP and arterial pO2 ($r = -0.331$, $P = 0.01$, $n = 139$) (Papakosta et al., 2011). In our study, the absence of correlation between PV/PA and arterial pO2 could therefore be explained by the small study population size or simply by the poor sensitivity of this test to reflect ventilation/perfusion mismatch and reduced diffusion capacity caused by pulmonary vasculopathy and the extent of fibrosis. Serum NT-proBNP concentrations did not differ between CIPF WHWTs and controls, and there was no correlation with PV/PA values. These results do not favour a diagnostic utility for NT-proBNP measurement in dogs with PH secondary to chronic pulmonary disease, and contrast with the human literature where NT-proBNP concentrations below 95 ng/L may be used to rule out PH in patients with interstitial

lung disease (Andersen et al., 2012b). In dogs, only two papers have been published to date concerning the utility of NT-proBNP in PH assessment. These studies found an overlap of data between dogs with or without precapillary PH, with NT-proBNP concentrations significantly increased only in dogs with severe PH (Hori et al., 2012; Kellihan et al., 2011). In our study, the lack of difference between groups, could therefore be due to the fact that WHWTs affected with CIPF were most frequently suffering from mild PH.

Our third objective was to investigate whether chemokines CCL2 and CXCL8 are potentially involved in the fibroproliferative mechanism in CIPF and may serve as biomarkers of the disease. We also aimed to determine whether higher basal concentrations in those chemokines and in VEGF and 5-HT in apparently healthy WHWTs may be considered as potential predisposing factors for CIPF. In human IPF, chronic alveolar epithelial cell injury and subsequent dysregulated tissue repair are considered to be the main pathological processes involved in this fibroproliferative disease (Coward et al., 2010; Raghu et al., 2011). The mechanisms of repair initiated by a tissue injury are complex and are determined by the presence of biological mediators such as cytokines, growth factors and chemokines, which coordinate most aspects of the inflammatory and subsequent repair responses. Consequently, altered regulation of those molecules after injury may contribute to dysregulated repair and the development of fibrosis. Several studies have provided compelling evidence that the chemokine CCL2 plays an important role in the fibroproliferative process observed in human IPF (Antoniades et al., 1992; Gharaee-Kermani et al., 2003; Inoshima et al., 2004; Mercer et al., 2009; Moore et al., 2001; Zhang et al., 1994), while implication of CXCL8 in the pathogenesis of the disease is less well documented (Keane et al., 1997; Richards et al., 2012; Totani et al., 2002; Vasakova et al., 2009; Ziegenhagen et al., 1998). Our study has shown that both serum and BALF concentrations of CCL2 were significantly increased in WHWTs with CIPF compared with healthy control WHWTs, and that serum CCL2 concentration carry prognostic information in WHWTs affected with CIPF. These findings are in agreement with observations made in human IPF (Baran et al., 2007; Capelli et al., 2005; Car et al., 1994; Emad and Emad, 2007; Fujiwara et al., 2012; Suga et al., 1999) and highlight the potential role of the CCL2 chemokine as a marker of CIPF disease. CXCL8 was significantly increased in the BALF of WHWTs with CIPF compared with that from healthy dogs, in accordance with observations made in human IPF (Antoniou et al., 2006; Ziegenhagen et al., 1998a), but no difference was observed between groups for serum CXCL8 concentrations, a finding that differs from the human literature (Ziegenhagen et al., 1998b). However, significant higher CXCL8 concentrations were found in healthy dogs from the WHWT breed in comparison with 6 other breeds less or not predisposed to CIPF, which suggests that CXCL8 might be related to the breed predisposition of the WHWT for CIPF and possibly serve as predisposing factor for

disease development; based on the hypothesis that higher circulating concentrations of pro-fibrotic molecules may contributing to exacerbated tissue repair after an injury leading subsequently to the development of fibrosis. Similar finding was also observed for CCL2 serum concentrations which were found elevated in healthy WHWTs in comparison with less predisposed breeds (King Charles spaniel and Malinois Belgian Shepherd), while increased CCL2 concentration were also present in healthy Maltese, a non-CIPF predisposed breed. No relevant interbreed differences were observed for 5-HT with regard to CIPF predisposition, and we could not investigate breed related differences in VEGF blood concentrations since most of the results obtained were below the ELISA kit detection limit. Note that we compared CCL2 and CXCL8 between healthy WHWTs and WHWTs affected with CIPF and that we did not include dogs with other chronic respiratory diseases. The reason is that other respiratory diseases such as eosinophilic bronchopneumopathy (EBP) and chronic bronchitis (CB) are essentially found in dogs from breeds other than the WHWT breed, while CIPF is found in WHWTs but rarely in other breeds. Therefore comparing the chemokine concentration between the different diseases (CIPF vs. EBP vs. CB) is not meaningful, given the presence of a breed effect on both CCL2 and CXCL8 chemokine basal concentration. Finally, the analysis of serum and BALF chemokines dosage in combination with clinical, physiological or radiological data has not been evaluated in the present study, but could have been interesting given that such multivariate models are increasingly developed in human medicine to stage IPF severity and help predict survival (Sgalla et al., 2015).

By qRT-PCR, we found no statistically significant difference in relative lung expression of CCL2, CXCL8, CCR2 and CXCR2 genes between WHWTs with CIPF and control dogs of various breeds. These results did not confirm preliminary data that showed an increased expression of CCL2 and CXCL8 chemokine genes in the lungs of dogs with CIPF compared with controls (Krafft et al., 2013). These discrepancies highlight limitations of the qRT-PCR technique in the context of CIPF. Indeed, the heterogeneous distribution of fibrosis in CIPF lungs could potentially explain an absence of difference between groups, if samples used in qRT-PCR assays had been taken from less affected regions of the fibrotic lungs (Syrja et al., 2013). Another explanation for the discrepancies observed between these studies may relate to the different control populations used. In comparison to the control group used in the previous study (median age, 6.5 years, range 0.2 - 14), the control group used in the our study was older (median age 12.6 years, range 11.4 – 15.4) in order to better match with the CIPF group, and this age parameter could possibly have influenced the results. Moreover, in our study, an intercalating dye, SYBR green, was used for real-time PCR while TaqMan probes, known to be more specific, were used in the previous study. However, the specificity of the PCR products obtained in the present study was confirmed by a melting curve analysis at the end of the

reaction and the SYBR green and TaqMan technologies have been shown to perform equally well in quantification assays (Buh Gasparic et al., 2010). Finally, both previous and present studies are limited by the fact that dogs from the control group are not WHWTs, but are of various breeds that may or may not be predisposed to CIPF. Influence of breed on pulmonary gene expression in healthy dogs has not been explored. Ideally, the control group should be composed only of WHWTs without fibrosis and matched for the age but, practically, we were unable to obtain such samples in a sufficient number.

By immunohistochemistry, labelling for CCL2 and CXCL8 was observed in only a few bronchial airway epithelial cells in the lungs of dogs with CIPF, while there was no labelling in control lung sections. These results may help to understand why qRT-PCR results were not different between groups as only few cells were labelled. This observation can also explain, at least partially, the increased chemokines concentrations observed in the BALF of dogs with CIPF compared with controls without difference in qRT-PCR results between groups. Moreover, it is important to remind that mRNA levels do not always correlate with protein levels given the existence of post-transcriptional and post-translational modifications. Furthermore, in one lung from a dog with CIPF, there was labelling of some hyperplastic alveolar epithelial cells for both CCL2 and CXCL8 and of a few macrophages for CXCL8. In the human literature, the cellular source of CXCL8 in IPF is reported to be the pulmonary fibroblasts (Keane et al., 1997), while CCL2 is mainly produced by hyperplastic alveolar epithelial cells, bronchial epithelial cells and macrophages (Mercer et al., 2009). Note that a limitation of the immunohistochemical method employed in our study was that we did not have access to positive control tissues. Instead, we decided to employ a negative control by incubating sections in parallel with normal goat serum instead of the primary antibody.

Finally, the last aim of the present work was to search for etiologic agent and particularly for herpesviruses, given that an association between pulmonary fibrotic disorders and gammaherpesvirus infection has been suggested in humans, horses and experimental murine model of fibrosis (Williams, 2014), and since the existence of an EBV-like virus has been proposed in dogs in association with neoplasm (Chiou et al., 2005; Chiu et al., 2013; Huang et al., 2012). Unfortunately, the pan-herpes PCR assay employed in our study did not allow us to detect herpesviral DNA sequence in any of the samples included. This PCR assay is considered to be the methodology of choice for broad detection of herpesvirus in association with diseases. Indeed, this molecular technique is sensitive and allowed the discovery of more than 100 alpha-, beta- and gammaherpesviruses by Bernhard Ehlers and his team. In particular, sequences of novel members belonging to all 4 gammaherpesvirus genera have been amplified: lymphocryptoviruses (Ehlers et al., 2003; Ehlers et al., 2010; Prepens et al., 2007),

rhadinoviruses (Benson et al., 2006; Ehlers et al., 2008; Ehlers and Lowden, 2004; Prepens et al., 2007), macaviruses (Chmielewicz et al., 2001; Chmielewicz et al., 2003; Ehlers and Lowden, 2004; Ehlers et al., 1999) and Percavirus (Ehlers et al., 2008). In addition, other research groups have applied comparable PCR protocols using the same primer binding sites for identification of herpesviruses (Lacoste et al., 2001; Lacoste et al., 2000; VanDevanter et al., 1996). This included also gammaherpesviruses of carnivorans (Cabello et al., 2013; Ehlers et al., 2008). To further unequivocally demonstrate the generic power of the method employed in our study, we included alpha-, beta-, and gammaherpesvirus-positive samples as positive controls. The gammaherpesviruses were from the Genera Percavirus, Macavirus, Rhadinovirus, and Lymphocryptovirus. The samples were from blood, lung and other organs of diverse animal hosts, including carnivorans. Using supplementary methodologies such as next-generation sequencing in a larger number of dogs would potentially have increased to strength of our study and allow us to detect other categories of viruses such as retrovirus which have been involved in pulmonary interstitial diseases in other species and in humans.

# LIMITATIONS, PERSPECTIVES AND CONCLUSIONS

Limitations of the present work are multiple. The major limitation consists in the difficulty to correctly standardize the diagnostic and sampling procedures performed on each dog included. Indeed, as stated in the introduction section, CIPF is a rare disease for which the diagnosis requires the exclusion of other cardiorespiratory diseases through several examinations including thoracic HRCT; histopathological examination of pulmonary tissue being not indicated in the diagnostic approach due to a risk-benefice imbalance (surgical procedure with increased anaesthetic risk for an incurable disease). At Liège University, we were able to acquire only 4 new CIPF cases per year despite the huge communication around the CIPF project (website, discussion with breeders, proposal of free clinical examination and follow-up). Consequently, to obtain a sufficient number of cases for studies, collaborations with the veterinary Finnish team from the University of Helsinki and with European veterinary collaborators was needed. However, the diagnostic approach is not strictly identical between investigators and institutions and may have influence clinical data recording and samples procedure collection. To limit this bias, a website was created at the beginning of the present work (http://www.caninepulmonaryfibrosis.ulg.ac.be), in order to allow access to standardized clinical and sampling procedure sheets, to harmonize the recruitment of data and to facilitate the transfer of samples to Liège faculty. Special boxes containing all the material needed for blood, BALF and lung sampling were designed and are sent on request to veterinarians who wants to participate in the collection of cases. Despite this, thoracic HRCT or histopathological confirmation of the CIPF diagnosis could not be obtained for each case included, even the ones who were examined at the faculty of Liège, either due to owner's decision (not incline to anesthetize their dog or to allow lung sampling after death) or simply to technical limitation (lack of imaging devices in veterinary private practice). Furthermore, impact of the travelling on the samples obtained by partners is not negligible as protein or RNA stability may be impacted by variation in temperature and conditions of storage. Besides, the different methodologies of samples collection between the different institutions may potentially have interfered with subsequent analysis. For example, for BALF collection, the method used at Liège University consists in instilling a fixed amount of sterile saline in the lung, while the method employed at the University of Helsinki is based on a body weight adjusted amount of instilled sterile saline (2mL/kg). Consequently, the proportion of epithelial lining fluid (ELF) obtained with the BAL may vary depending on the method employed due to a variation in the degree of dilution. To encounter this issue, several techniques have been developed in order to determine the fraction of ELF recovered from the BALF. Those techniques are based on the presence of endogen molecules such as urea or albumin for which the concentrations in the BALF are compared with those in the plasma, or on the addition of exogenous molecules such

as methylene blue or inulin for which the concentrations in the BALF are compared with those initially introduced (Kirschvink et al., 2001; Mills and Litster, 2005; Rennard et al., 1986). However, we chosen not to employ such techniques of normalisation given that a recent publication made by Melamies and associates (2011) demonstrated that there was no difference between the fixed or weigh-adjusted BALF methodologies for the proportion recovery of ELF in healthy experimental beagle dogs. Note that the difference between the two techniques in pathological situations has not been investigated and may potentially yield different conclusions, particularly if severe bronchial remodelling are present and prevent an optimal collection of the liquid after instillation.

Another limitation of our work resides in the selection of the control population. Whenever possible, we tried to recruit control dogs matched for the age and for the breed with the CIPF population to limit the impact of physiological variants on the interpretation of the data. However, with such strict criteria, obtaining lung samples was extremely difficult. Therefore we had to select lungs of dogs from other breeds, who died or were euthanatized for reasons unrelated to the cardiorespiratory system. This is not ideal as it is presently unknown whether a breed effect exists on lung gene expression. Furthermore, to ensure the control status of WHWTs included, a complete history, physical examination and blood work were performed at minimum. Despite this, some controls may be suffering from subclinical early CIPF lesions (such as hypothesized by the presence of localized GGO on T-HRCT images in some controls) that could impact the results of our investigations. Similarly, some controls were possibly suffering from other subclinical pathologies not obvious at the time of sampling but enough to impact the results (e.g.: CCL2 and CXCL8 have been proved to be involved in a diversity of pathological mechanisms and in carcinogenesis) (Bonecchi et al., 2009; Locati et al., 2005). The same is true for the CIPF population given that the disease affects aged dogs which may suffer from other concomitant diseases. Those diagnostic constraints seriously jeopardize the establishment of well-designed and phenotyped cohorts of dogs, but are inherent to the research in clinic, particularly in old individuals.

Finally, a more global limitation about the clinical research in dogs is the lack of specifically-developed materials (reagents, tools, etc.) for this species. Indeed, in the majority of cases, validation of human dedicated products (antibodies, ELISA kits) is needed for the research in dog. Specific canine products may lack sensitivity, such as it was the case for the VEGF canine ELISA kit for which the majority of the samples tested were below the kit detection limit.

To encounter those limitations related with the diagnostic constraints and continue to improve our understanding about the disease, a longitudinal prospective study allowing to

follow a cohort of apparently healthy WHWTs at various time points until the development of the disease would be ideal, although difficult to implement in practice due to the poor compliance of dog's owners and the presumed rarity of the disease. Such a study design would allow to identify early CIPF markers that would have the capacity to reflect the presence and the progression of the disease and to indicate the prognosis. Such sensitive markers of the disease, alone or in combination, would be ideal in the future to test the effect of a potential targeted anti-fibrotic treatment. Furthermore, recruitment of well-phenotyped CIPF cases and controls has to be pursued over the next few years in order to increase the population size for future studies and to build adequate validation cohort for validation of biomarkers.

Given that CIPF is still an incurable disease of unknown origin, search for causative agents that could potentially be targeted is of importance. Thanks to the development of new technologies such as next-generation sequencing, investigation of microbial alteration in the lung environment might be of interest. Indeed, differences in the composition and diversity of the respiratory microbiota has been shown in human IPF (Molyneaux et al., 2014), and interpretation of those data in dogs might reveal clinically informative, especially in the framework of the development of novel therapeutic options in the future. Another field of research may target the investigation of the coagulation profile of CIPF dogs, given that an imbalance between thrombosis and fibrinolysis has been demonstrated in human IPF patients favouring a local and systemic pro-thrombotic state (Crooks and Hart, 2015), while unfortunately current treatments options failed to demonstrate any benefit in this field (Noth et al., 2012). Search for microaspiration secondary to gastro-oesophageal reflux may also be interesting in dogs, given the increased attention about the use of anti-acid treatment in IPF patients (Ghebre and Raghu, 2016). Furthermore, in human medicine, several clinical trials have already been done or are actually under progress to target specific mediators of fibrosis (see: https://clinicaltrials.gov/), whereas most of the studies already performed had provided negative or conflicting results, except for nintedanib and pirfenidone. Whether those therapeutic options may be transposed to the dog species and help in the management of the disease require investigations after exploration of the implication of those targets in CIPF. We also hope that the genome wide association study (GWAS) actually under progress at the University of Helsinki will bring interesting results. Indeed, identification of canine individuals at risk to develop the disease would allow to adapt breeding's programs in order to limit the spreading of CIPF across generation. However, GWAS reside on the basic principle to compare large cohorts of both diseased and matched unaffected control dogs. Given that CIPF is a disease of the old dog, it is impossible to predict if the apparently controls included would not develop the disease within the couple of years that follow blood sampling; this issue seriously complicates the interpretation of a GWAS results at the moment.

Thanks to the several years of research on CIPF and to the results of the present work, we can conclude that CIPF is a complex and still poorly understood disease which continues to require more investigations to understand why it affects a particular dog breed, to identify predisposing factors or inciting agents involved, and develop effective treatments. Advances made on the HRCT and echocardiographic findings in the present work would allow us to improve our phenotypic classification of dogs for further studies and to efficiently select and treat patients according to their comorbidities. Our hope for the future would be to have the opportunity to offer novel therapeutic solutions to cure these dogs or prolonge their life expectancy with preservation of their quality of life. In such therapeutic trials, discovery made about biomarkers, particularly CCL2 and CXCL8, would have their importance to allow the assessment of treatment effectiveness.

# REFERENCES

Ahn, M.H., Park, B.L., Lee, L.H., et al., 2011. A promoter SNP rs4073T>A in the common allele of the interleukin 8 gene is associated with the development of idiopathic pulmonary fibrosis via the IL-8 protein enhancing mode. Respiratory research 12, 73.

Andersen, C.U., Mellemkjaer, S., Hilberg, O., et al., 2012a. Pulmonary hypertension in interstitial lung disease: prevalence, prognosis and 6 min walk test. Respiratory medicine 106, 875-882.

Andersen, C.U., Mellemkjaer, S., Nielsen-Kudsk, J.E., et al., 2012b. Diagnostic and prognostic role of biomarkers for pulmonary hypertension in interstitial lung disease. Respiratory medicine 106, 1749-1755.

Ando, M., Miyazaki, E., Ito, T., et al., 2010. Significance of serum vascular endothelial growth factor level in patients with idiopathic pulmonary fibrosis. Lung 188, 247-252.

Antoniades, H.N., Neville-Golden, J., Galanopoulos, T., et al., 1992. Expression of monocyte chemoattractant protein 1 mRNA in human idiopathic pulmonary fibrosis. Proceedings of the national academy of sciences of the United States of America 89, 5371-5375.

Antoniou, K.M., Tzouvelekis, A., Alexandrakis, M.G., et al., 2006. Different angiogenic activity in pulmonary sarcoidosis and idiopathic pulmonary fibrosis. Chest 130, 982-988.

Antoniou, K.M., Margaritopoulos, G.A., Tomassetti, S., et al., 2014. Interstitial lung disease. European respiratory review 23, 40-54.

Arcasoy, S.M., Christie, J.D., Ferrari, V.A., et al., 2003. Echocardiographic assessment of pulmonary hypertension in patients with advanced lung disease. American journal of respiratory and critical care medicine 167, 735-740.

ATS/ERS, 2002. American Thoracic Society/European Respiratory Society International Multidisciplinary Consensus Classification of the Idiopathic Interstitial Pneumonias. American journal of respiratory and critical care medicine 165, 277-304.

Attaran, R.R., Ramaraj, R., Sorrell, V.L., et al., 2009. Poor correlation of estimated pulmonary artery systolic pressure between echocardiography and right heart catheterization in patients awaiting cardiac transplantation: results from the clinical arena. Transplantation proceedings 41, 3827-3830.

Aubry, M.C., Myers, J.L., Douglas, W.W., et al., 2002. Primary pulmonary carcinoma in patients with idiopathic pulmonary fibrosis. Mayo Clinic proceedings 77, 763-770.

Bach, J.F., Rozanski, E.A., MacGregor, J., et al., 2006. Retrospective evaluation of sildenafil citrate as a therapy for pulmonary hypertension in dogs. Journal of veterinary internal medicine 20, 1132-1135.

Back, H., Kendall, A., Grandon, R., et al., 2012. Equine multinodular pulmonary fibrosis in association with asinine herpesvirus type 5 and equine herpesvirus type 5: a case report. Acta veterinaria scandinavica 54, 57.

Bagnato, G., Harari, S., 2015. Cellular interactions in the pathogenesis of interstitial lung diseases. European respiratory review 24, 102-114.

Balakrishnan, A., King, L.G., 2014. Updates on pulmonary function testing in small animals. The veterinary clinics of North America small animal practice 44, 1-18.

Baran, C.P., Opalek, J.M., McMaken, S., et al. 2007. Important roles for macrophage colony-stimulating factor, CC chemokine ligand 2, and mononuclear phagocytes in the pathogenesis of pulmonary fibrosis. American journal of respiratory and critical care medicine 176, 78-89.

Barkauskas, C.E., Noble, P.W., 2014. Cellular mechanisms of tissue fibrosis. New insights into the cellular mechanisms of pulmonary fibrosis. American journal of physiology Cell physiology 306, C987-996.

Barratt, S., Millar, A., 2014. Vascular remodelling in the pathogenesis of idiopathic pulmonary fibrosis. QJM 107, 515-519.

Baumwart, R.D., Meurs, K.M., Bonagura, J.D., 2005. Tei index of myocardial performance applied to the right ventricle in normal dogs. Journal of veterinary internal medicine 19, 828-832.

Benson, K.A.S., Manire, C.A., Ewing, R.Y., et al., 2006. Identification of novel alpha-and gammaherpesviruses from cutaneous and mucosal lesions of dolphins and whales. Journal of virological methods 136, 261-266.

Birettoni, F., Caivano, D., Giorgi, M.E., et al., 2010. A novel echocardiographic index in the dog: pulmonary vein:pulmonary artery diameter. The 20th annual European colloquium of veterinary internal medicine (ECVIM) congress proceedings, Toulouse, France.

Bonagura, J.D., Twedt, D.C., 2014. Kirk's Current Veterinary Therapy XV. Saunders Elsevier. 1413 p.

Bonecchi, R., Galliera, E., Borroni, E.M., et al., 2009. Chemokines and chemokine receptors: an overview. Frontiers in bioscience 14, 540-551.

Bonella, F., Stowasser, S., Wollin, L., 2015. Idiopathic pulmonary fibrosis: current treatment options and critical appraisal of nintedanib. Journal of drug, design development and therapy 9, 6407-6419.

Borensztajn, K., Crestani, B., Kolb, M., 2013. Idiopathic pulmonary fibrosis: from epithelial injury to biomarkers--insights from the bench side. Respiration 86, 441-452.

Borgarelli, M., Buchanan, J.W., 2012. Historical review, epidemiology and natural history of degenerative mitral valve disease. Journal of veterinary cardiology 14, 93-101.

Buh Gasparic, M., Tengs, T., La Paz, J.L., et al., 2010. Comparison of nine different real-time PCR chemistries for qualitative and quantitative applications in GMO detection. Analitycal and bioanalytical chemistry 396, 2023-2029.

Cabello, J., Esperón, F., Napolitano, C., et al., 2013. Molecular identification of a novel gammaherpesvirus in the endangered Darwin's fox (Lycalopex fulvipes). Journal of general virology 94, 2745-2749.

Camelo, A., Dunmore, R., Sleeman, M.A., et al., 2014. The epithelium in idiopathic pulmonary fibrosis: breaking the barrier. Frontiers in pharmacology 4, 173.

Caminati, A., Madotto, F., Cesana, G., et al., 2015. Epidemiological studies in idiopathic pulmonary fibrosis: pitfalls in methodologies and data interpretation. European respiratory review 24, 436-444.

Capelli, A., Di Stefano, A., Gnemmi, I., et al., 2005. CCR5 expression and CC chemokine levels in idiopathic pulmonary fibrosis. The European respiratory journal 25, 701-707.

Car, B.D., Meloni, F., Luisetti, M., et al., 1994. Elevated IL-8 and MCP-1 in the bronchoalveolar lavage fluid of patients with idiopathic pulmonary fibrosis and pulmonary sarcoidosis. American journal of respiratory and critical care medicine 149, 655-659.

Chambers, R.C., Mercer, P.F., 2015. Mechanisms of alveolar epithelial injury, repair, and fibrosis. Annals of the American thoracic society 12, S16-20.

Chiou, S.H., Chow, K.C., Yang, C.H., et al., 2005. Discovery of Epstein-Barr virus (EBV)-encoded RNA signal and EBV nuclear antigen leader protein DNA sequence in pet dogs. Journal of general virology 86, 899-905.

Chiu, H.C., Chow, K.C., Fan, Y.H., et al., 2013. Expression of EBV-encoded oncogenes and EBV-like virions in multiple canine tumors. Veterinary microbiology 163, 79-89.

Chmielewicz, B., Goltz, M., Ehlers, B., 2001. Detection and multigenic characterization of a novel gammaherpesvirus in goats. Virus research 75, 87-94.

Chmielewicz, B., Goltz, M., Franz, T., et al., 2003. A novel porcine gammaherpesvirus. Virology 308, 317-329.

Ciccarese, F., Attina, D., Zompatori, M., 2016. Combined pulmonary fibrosis and emphysema (CPFE): what radiologist should know. Riologica medica [Epub ahead of print].

Cohn, L.A., Norris, C.R., Hawkins, E.C., et al., 2004. Identification and characterization of an idiopathic pulmonary fibrosis-like condition in cats. Journal of veterinary internal medicine 18, 632-641.

Collard, H.R., Anstrom, K.J., Schwarz, M.I., et al., 2007. Sildenafil improves walk distance in idiopathic pulmonary fibrosis. Chest 131, 897-899.

Corcoran, B.M., Cobb, M., Martin, M.W., et al., 1999a. Chronic pulmonary disease in West Highland white terriers. The veterinary record 144, 611-616.

Corcoran, B.M., Dukes-McEwan, J., Rhind, S., et al., 1999b. Idiopathic pulmonary fibrosis in a Staffordshire bull terrier with hypothyroidism. The Journal of small animal practice 40, 185-188.

Corcoran, B.M., King, L.G., Schwarz, T., et al., 2011. Further characterisation of the clinical features of chronic pulmonary disease in West Highland white terriers. The veterinary record 168, 355.

Coward, W.R., Saini, G., Jenkins, G., 2010. The pathogenesis of idiopathic pulmonary fibrosis. Therapeutic advances in respiratory disease 4, 367-388.

Crooks, M.G., Hart, S.P., 2015. Coagulation and anticoagulation in idiopathic pulmonary fibrosis. European respiratory review 24, 392-399.

Currie, P.J., Seward, J.B., Chan, K.L., et al., 1985. Continuous wave Doppler determination of right ventricular pressure: a simultaneous Doppler-catheterization study in 127 patients. Journal of the American college of cardiology 6, 750-756.

Datta, A., Scotton, C.J., Chambers, R.C., 2011. Novel therapeutic approaches for pulmonary fibrosis. British journal of pharmacology 163, 141-172.

Demir, R., Kucukoglu, M.S., 2015. Six-minute walk test in pulmonary arterial hypertension. The Anatolian journal of cardiology 15, 249-254.

Devine, M.S., Garcia, C.K., 2012. Genetic interstitial lung disease. Clinics in chest medicine 33, 95-110.

Douglas, W.W., Ryu, J.H., Schroeder, D.R., 2000. Idiopathic pulmonary fibrosis: Impact of oxygen and colchicine, prednisone, or no therapy on survival. American journal of respiratory and critical care medicine 161, 1172-1178.

Dunowska, M., Hardcastle, M.R., Tonkin, F.B., 2014. Identification of the first New Zealand case of equine multinodular pulmonary fibrosis. New Zealand veterinary journal 62, 226-231.

Ebina, M., Shimizukawa, M., Shibata, N., et al., 2004. Heterogeneous increase in CD34-positive alveolar capillaries in idiopathic pulmonary fibrosis. American journal of respiratory and critical care medicine 169, 1203-1208.

Egan, J.J., 2011. Follow-up and nonpharmacological management of the idiopathic pulmonary fibrosis patient. European respiratory review 20, 114-117.

Ehlers, B., Ulrich, S., Goltz, M., 1999. Detection of two novel porcine herpesviruses with high similarity to gammaherpesviruses. Journal of general virology 80, 971-978.

Ehlers, B., Ochs, A., Leendertz, F., et al., 2003. Novel simian homologues of Epstein-Barr virus. Journal of virology 77, 10695-10699.

Ehlers, B., Lowden, S., 2004. Novel herpesviruses of Suidae: indicators for a second genogroup of artiodactyl gammaherpesviruses. Journal of general virology 85, 857-862.

Ehlers, B., Dural, G., Yasmum, N., et al., 2008. Novel mammalian herpesviruses and lineages within the Gammaherpesvirinae: cospeciation and interspecies transfer. Journal of virology 82, 3509-3516.

Ehlers, B., Spieß, K., Leendertz, F., et al., 2010. Lymphocryptovirus phylogeny and the origins of Epstein–Barr virus. Journal of general virology 91, 630-642.

El-Sherief, A.H., Gilman, M.D., Healey, T.T., et al., 2014. Clear vision through the haze: a practical approach to ground-glass opacity. Current problems in diagnostic radiology 43, 140-158.

Emad, A., Emad, V., 2007. Elevated levels of MCP-1, MIP-alpha and MIP-1 beta in the bronchoalveolar lavage (BAL) fluid of patients with mustard gas-induced pulmonary fibrosis. Toxicology 240, 60-69.

Eriksson, M., von Euler, H., Ekman, E., et al., 2009. Surfactant protein C in canine pulmonary fibrosis. Journal of veterinary internal medicine 23, 1170-1174.

Evola, M.G., Edmondson, E.F., Reichle, J.K., et al., 2014. Radiographic and histopathologic characteristics of pulmonary fibrosis in nine cats. Veterinary radiology & ultrasound 55, 133-140.

Fabre, A., Marchal-Somme, J., Marchand-Adam, S., et al., 2008. Modulation of bleomycin-induced lung fibrosis by serotonin receptor antagonists in mice. The European respiratory journal 32, 426-436.

Fabre, A., Crestani, B., 2010. Serotonin: a new start for an old friend? Thorax 65, 946-947.

Farkas, L., Gauldie, J., Voelkel, N.F., et al., 2011. Pulmonary hypertension and idiopathic pulmonary fibrosis: a tale of angiogenesis, apoptosis, and growth factors. American journal of respiratory cell and molecular biology 45, 1-15.

Fernandez, I.E., Eickelberg, O., 2012. New cellular and molecular mechanisms of lung injury and fibrosis in idiopathic pulmonary fibrosis. Lancet 380, 680-688.

Fidalgo, S., Ivanov, D.K., Wood, S.H., 2013. Serotonin: from top to bottom. Biogerontology 14, 21-45.

Fingerlin, T.E., Muprhy, E., Zhang, W., et al., 2013. Genome-wide association study identifies multiple susceptibility loci for pulmonary fibrosis. Nature genetics 45, 613-620.

Frishman, W.H., Grewall, P., 2000. Serotonin and the heart. Annals of medicine 32, 195-209.

Fulton, B.G., Ryerson, C.J., 2015. Managing comorbidities in idiopathic pulmonary fibrosis. International journal of general medicine 8, 309-318.

Gallagher, A.E., Panciera, D.L., Panciera, R.J., 2006. Hyperphosphatasemia in Scottish terriers: 7 cases. Journal of veterinary internal medicine 20, 418-421.

Gharaee-Kermani, M., McCullumsmith, R.E., Charo, I.F., et al., 2003. CC-chemokine receptor 2 required for bleomycin-induced pulmonary fibrosis. Cytokine 24, 266-276.

Ghebre, Y.T., Raghu, G., 2016. Idiopathic Pulmonary Fibrosis: Novel Concepts of Proton Pump Inhibitors as Antifibrotic Drug. American journal of respiratory and critical care medicine [Epub ahead of print].

Glaser, S., Obst, A., Koch, B., et al., 2013. Pulmonary hypertension in patients with idiopathic pulmonary fibrosis - the predictive value of exercise capacity and gas exchange efficiency. PLoS One 8, e65643.

Glaspole, I., Goh, N.S., 2010. Differentiating between IPF and NSIP. Chronic respiratory disease 7, 187-195.

Han, M.K., Bach, D.S., Hagan, P.G., et al., 2013. Sildenafil preserves exercise capacity in patients with idiopathic pulmonary fibrosis and right-sided ventricular dysfunction. Chest 143, 1699-1708.

Hansell, D.M., Bankier, A.A., MacMahon, H., et al., 2008. Fleischner Society: glossary of terms for thoracic imaging. Radiology 246, 697-722.

Hansell, D.M., Goldin, J.G., King, T.E., et al., 2015. CT staging and monitoring of fibrotic interstitial lung diseases in clinical practice and treatment trials: a position paper from the Fleischner Society. The Lancet respiratory medicine 3, 483-496.

Heikkila, H.P., Lappalainen, A.K., Day, M.J., et al., 2011. Clinical, bronchoscopic, histopathologic, diagnostic imaging, and arterial oxygenation findings in West Highland White Terriers with idiopathic pulmonary fibrosis. Journal of veterinary internal medicine 25, 433-439.

Heikkila, H.P., Krafft, E., Jespers, P., et al., 2012. Procollagen type III amino terminal propeptide concentrations in dogs with idiopathic pulmonary fibrosis compared with chronic bronchitis and eosinophilic bronchopneumopathy. Veterinary journal 196, 52-56.

Heikkila-Laurila, H.P., Rajamaki, M.M., 2014. Idiopathic pulmonary fibrosis in West Highland white terriers. The veterinary clinics of North America small animal practice 44, 129-142.

Hodnett, P.A., Naidich, D.P., 2013. Fibrosing interstitial lung disease. A practical high-resolution computed tomography-based approach to diagnosis and management and a review of the literature. American journal of respiratory and critical care medicine 188, 141-149.

Hori, Y., Uchide, T., Saitoh, R., et al., 2012. Diagnostic utility of NT-proBNP and ANP in a canine model of chronic embolic pulmonary hypertension. Veterinary journal 194, 215-221.

Huang, S.H., Kozak, P.J., Kim, J., et al., 2012. Evidence of an oncogenic gammaherpesvirus in domestic dogs. Virology 427, 107-117.

Hyldgaard, C., Hilberg, O., Bendstrup, E., 2014. How does comorbidity influence survival in idiopathic pulmonary fibrosis? Respiratory medicine 108, 647-653.

Inomata, M., Kamio, K., Azuma, A., et al., 2014. Pirfenidone inhibits fibrocyte accumulation in the lungs in bleomycin-induced murine pulmonary fibrosis. Respiratory research 15, 16.

Inomata, M., Nishioka, Y., Azuma, A., 2015. Nintedanib: evidence for its therapeutic potential in idiopathic pulmonary fibrosis. Journal of core evidence 10, 89-98.

Inoshima, I., Kuwano, K., Hamada, N., et al., 2004. Anti-monocyte chemoattractant protein-1 gene therapy attenuates pulmonary fibrosis in mice. American journal of physiology 286, L1038-1044.

Jackson, R.M., Glassberg, M.K., Ramos, C.F., et al., 2010. Sildenafil therapy and exercise tolerance in idiopathic pulmonary fibrosis. Lung 188, 115-123.

Jacob, J., Hansell, D.M., 2015. HRCT of fibrosing lung disease. Respirology 20, 859-872.

Jeong, Y.J., Lee, K.S., Chung, M.P., et al., 2014. Chronic hypersensitivity pneumonitis and pulmonary sarcoidosis: differentiation from usual interstitial pneumonia using high-resolution computed tomography. Seminars in ultrasound, CT and IMR 35, 47-58.

Johnson, V.S., Corcoran, B.M., Wotton, P.R., et al., 2005. Thoracic high-resolution computed tomographic findings in dogs with canine idiopathic pulmonary fibrosis. The journal of small animal practice 46, 381-388.

Kadoch, M.A., Cham, M.D., Beasley, M.B., et al., 2015. Idiopathic interstitial pneumonias: a radiology-pathology correlation based on the revised 2013 American Thoracic Society-European Respiratory Society classification system. Current problems in diagnostic radiology 44, 15-25.

Kage, H., Borok, Z., 2012. EMT and interstitial lung disease: a mysterious relationship. Current opinion in pulmonary medicine 18, 517-523.

Katzenstein, A.L., Mukhopadhyay, S., Myers, J.L., 2008. Diagnosis of usual interstitial pneumonia and distinction from other fibrosing interstitial lung diseases. Human pathology 39, 1275-1294.

Kaunisto, J., Salomaa, E.R., Hodgson, U., et al., 2013. Idiopathic pulmonary fibrosis--a systematic review on methodology for the collection of epidemiological data. BMC pulmonary medicine 13, 53.

Keane, M.P., Arenberg, D.A., Lynch, J.P.,et al., 1997. The CXC chemokines, IL-8 and IP-10, regulate angiogenic activity in idiopathic pulmonary fibrosis. Journal of immunology 159, 1437-1443.

Kellihan, H.B., Stepien, R.L., 2010. Pulmonary hypertension in dogs: diagnosis and therapy. The veterinary clinics of North America small animal practice 40, 623-641.

Kellihan, H.B., Mackie, B.A., Stepien, R.L., 2011. NT-proBNP, NT-proANP and cTnI concentrations in dogs with pre-capillary pulmonary hypertension. Journal of veterinary cardiology 13, 171-182.

Kellihan, H.B., Waller, K.R., Pinkos, A., et al., 2015. Acute resolution of pulmonary alveolar infiltrates in 10 dogs with pulmonary hypertension treated with sildenafil citrate: 2005-2014. Journal of veterinary cardiology 17, 182-191.

Kellum, H.B., Stepien, R.L., 2007. Sildenafil citrate therapy in 22 dogs with pulmonary hypertension. Journal of veterinary internal medicine 21, 1258-1264.

Kendall, R.T., Feghali-Bostwick, C.A., 2014. Fibroblasts in fibrosis: novel roles and mediators. Frontiers in pharmacology 5, 123.

Kenn, K., Gloeckl, R., Behr, J., 2013. Pulmonary rehabilitation in patients with idiopathic pulmonary fibrosis--a review. Respiration 86, 89-99.

Kim, H.J., Perlman, D., Tomic, R., 2015. Natural history of idiopathic pulmonary fibrosis. Respiratory medicine 109, 661-670.

King, T.E., Jr., Behr, J., Brown, K.K., et al., 2008. BUILD-1: a randomized placebo-controlled trial of bosentan in idiopathic pulmonary fibrosis. American journal of respiratory and critical care medicine 177, 75-81.

King, T.E., Jr., Brown, K.K., Raghu, G., et al., 2011a. BUILD-3: a randomized, controlled trial of bosentan in idiopathic pulmonary fibrosis. American journal of respiratory and critical care medicine 184, 92-99.

King, T.E., Jr., Pardo, A., Selman, M., 2011b. Idiopathic pulmonary fibrosis. Lancet 378, 1949-1961.

Kirschvink, N., Fievez, L., Dogne, S., et al., 2001. Comparison of inulin with urea as dilutional markers of bronchoalveolar lavage in healthy and heaves-affected horses. Veterinary research 32, 145-154.

Kishaba, T., 2015. Practical management of idiopathic pulmonary fibrosis. Sarcoidosis, vasculitis and diffuse lung diseases 32, 90-98.

Kleiboeker, S.B., Schommer, S.K., Johnson, P.J., et al., 2002. Association of two newly recognized herpesviruses with interstitial pneumonia in donkeys (Equus asinus). Journal of veterinary diagnostic investigation 14, 273-280.

Kligerman, S.J., Henry, T., Lin, C.T., et al., 2015. Mosaic Attenuation: Etiology, Methods of Differentiation, and Pitfalls. Radiographics 35, 1360-1380.

Konigshoff, M., Dumitrascu, R., Udalov, S., et al., 2010. Increased expression of 5-hydroxytryptamine2A/B receptors in idiopathic pulmonary fibrosis: a rationale for therapeutic intervention. Thorax 65, 949-955.

Koyama, S., Sato, E., Haniuda, M., et al., 2002. Decreased level of vascular endothelial growth factor in bronchoalveolar lavage fluid of normal smokers and patients with pulmonary fibrosis. American journal of respiratory and critical care medicine 166, 382-385.

Krafft, E., Heikkila, H.P., Jespers, P., et al., 2011. Serum and bronchoalveolar lavage fluid endothelin-1 concentrations as diagnostic biomarkers of canine idiopathic pulmonary fibrosis. Journal of veterinary internal medicine 25, 990-996.

Krafft, E., Laurila, H.P., Peters, I.R., et al., 2013. Analysis of gene expression in canine idiopathic pulmonary fibrosis. Veterinary journal 198, 479-486.

Krafft, E., Lybaert, P., Roels, E., et al., 2014a. Transforming growth factor beta 1 activation, storage, and signaling pathways in idiopathic pulmonary fibrosis in dogs. Journal of veterinary internal medicine 28, 1666-1675.

Krafft, E., Roels, E., Laurila, H.P., et al., 2014b. Is 5-hydrocytryptamine (serotonin) involved in the pathogenesis of canine idiopathic pulmonary fibrosis?. The 18th international colloquium on lung and airway fibrosis (ICLAF) proceedings, Mont-tremblant, Quebec, Canada.

Krafft, E. 2015. Canine idiopathic pulmonary fibrosis: transcriptome analysis, investigation of TGF beta 1 patwhays and search for biomarkers (PhD thesis). University of Liège, 176p.

Kreuter, M., Bonella, F., Wijsenbeek, M., et al., 2015. Pharmacological treatment of idiopathic pulmonary fibrosis: current approaches, unsolved issues, and future perspectives. Biomed research international 2015, 329481.

Lacasse, Y., Girard, M., Cormier, Y., 2012. Recent advances in hypersensitivity pneumonitis. Chest 142, 208-217.

Lacoste, V., Mauclre, P., Dubreuil, G., et al., 2000. Virology: KSHV-like herpesviruses in chimps and gorillas. Nature 407, 151-152.

Lacoste, V., Mauclère, P., Dubreuil, G., et al., 2001. A novel γ2-herpesvirus of the rhadinovirus 2 lineage in chimpanzees. Genome research 11, 1511-1519.

Lamas, D.J., Kawut, S.M., Bagiella, E., et al., 2011. Delayed access and survival in idiopathic pulmonary fibrosis: a cohort study. American journal of respiratory and critical care medicine 184, 842-847.

Larruskain, A., Jugo, B.M., 2013. Retroviral infections in sheep and goats: small ruminant lentiviruses and host interaction. Viruses 5, 2043-2061.

Leonard, C.D., Johnson, L.R., Bonadio, C.M., et al., 2009. Changes in tracheal dimensions during inspiration and expiration in healthy dogs as detected via computed tomography. American journal of veterinary research 70, 986-991.

Ley, B., Brown, K.K., Collard, H.R., 2014. Molecular biomarkers in idiopathic pulmonary fibrosis. American journal of physiology. Lung cellular and molecular physiology 307, 681-691.

Lilja-Maula, L., Palviainen, M.J., Heikkila, H.P., et al., 2013. Proteomic analysis of bronchoalveolar lavage fluid samples obtained from West Highland White Terriers with idiopathic pulmonary fibrosis, dogs with chronic bronchitis, and healthy dogs. American journal of veterinary research 74, 148-154.

Lilja-Maula, L., Syrja, P., Laurila, H.P., et al., 2014a. Comparative study of transforming growth factor-beta signalling and regulatory molecules in human and canine idiopathic pulmonary fibrosis. Journal of comparative pathology 150, 399-407.

Lilja-Maula, L., Laurila, H.P., Syrja, P., et al., 2014b. Long-term outcome and use of 6-minute walk test in West Highland white terriers with idiopathic pulmonary fibrosis. Journal of veterinary internal medicine 28, 379-385.

Lilja-Maula, L., Syrja, P., Laurila, H.P., et al., 2015. Upregulation of alveolar levels of activin B, but not activin A, in lungs of west highland white terriers with idiopathic pulmonary fibrosis and diffuse alveolar damage. Journal of comparative pathology 152, 192-200.

Ljungvall, I., Hoglund, K., Lilliehook, I., et al., 2013. Serum serotonin concentration is associated with severity of myxomatous mitral valve disease in dogs. Journal of veterinary internal medicine 27, 1105-1112.

Lobetti, R.G., Milner, R., Lane, E., 2001. Chronic idiopathic pulmonary fibrosis in five dogs. Journal of the American animal hospital association 37, 119-127.

Locati, M., Bonecchi, R., Corsi, M.M., 2005. Chemokines and their receptors: roles in specific clinical conditions and measurement in the clinical laboratory. American journal of clinical pathology 123 Suppl, S82-95.

Manens, J., Ricci, R., Damoiseaux, C., et al., 2014. Effect of body weight loss on cardiopulmonary function assessed by 6-minute walk test and arterial blood gas analysis in obese dogs. Journal of veterinary internal medicine 28, 371-378.

Marenzoni, M.L., Passamonti, F., Lepri, E., et al., 2011. Quantification of Equid herpesvirus 5 DNA in clinical and necropsy specimens collected from a horse with equine multinodular pulmonary fibrosis.Journal of veterinary diagnostic investigation 23, 802-806.

Martina, S., Martina, V., Monika, M., et al., 2009. Angiostatic versus angiogenic chemokines in IPF and EAA. Respiratory medicine 103, 1651-1656.

Matsuse, T., Ikegami, A., Ohga, E., et al., 1996. Expression of immunoreactive activin A protein in remodeling lesions associated with interstitial pulmonary fibrosis. The American journal of pathology 148, 707-713.

Mayer, K., Buchbinder, A., Morty, R.E., 2012. Activin A: a mediator governing inflammation, immunity, and repair. American journal of respiratory and critical care medicine 185, 350-352.

McGoon, M.D., Kane, G.C., 2009. Pulmonary hypertension: diagnosis and management. Mayo clinic proceedings 84, 191-207.

Melamies, M.A., Jarvinen, A.K., Seppala, K.M., et al., 2011. Comparison of results for weight-adjusted and fixed-amount bronchoalveolar lavage techniques in healthy Beagles. American journal of veterinary research 72, 694-698.

Mercer, P.F., Johns, R.H., Scotton, C.J., et al., 2009. Pulmonary epithelium is a prominent source of proteinase-activated receptor-1-inducible CCL2 in pulmonary fibrosis. American journal of respiratory and critical care medicine 179, 414-425.

Mercier, E., Mathieu, M., Sandersen, C.F., et al., 2010. Evaluation of the influence of age on pulmonary arterial pressure by use of right ventricular catheterization, pulsed-wave Doppler echocardiography, and pulsed-wave tissue Doppler imaging in healthy Beagles. American journal of veterinary research 71, 891-897.

Mercier, E., Bolognin, M., Hoffmann, A.C., et al., 2011. Influence of age on bronchoscopic findings in healthy beagle dogs. Veterinary journal 187, 225-228.

Merveille, A.C., Bolen, G., Krafft, E., et al., 2015. Pulmonary vein-to-pulmonary artery ratio is an echocardiographic index of congestive heart failure in dogs with degenerative mitral valve disease. Journal of veterinary internal medicine 29, 1502-1509.

Meyer, K.C., Cardoni, A., Xiang, Z.Z., 2000. Vascular endothelial growth factor in bronchoalveolar lavage from normal subjects and patients with diffuse parenchymal lung disease. Journal of laboratory and clinical medicine 135, 332-338.

Meyer, K.C., 2014. Diagnosis and management of interstitial lung disease. Translational respiratory medicine 2, 4.

Meyer, K.C., Danoff, S.K., Lancaster, L.H., et al., 2015. Management of idiopathic pulmonary fibrosis in the elderly patient: addressing key questions. Chest 148, 242-252.

Miele, A., Dhaliwal, K., Du Toit, N., et al., 2014. Chronic pleuropulmonary fibrosis and elastosis of aged donkeys: similarities to human pleuroparenchymal fibroelastosis. Chest 145, 1325-1332.

Mills, P.C., Litster, A.L., 2005. Using urea dilution to standardise components of pleural and bronchoalveolar lavage fluids in the dog. New Zealand veterinary journal 53, 423-428.

Milman, G., Smith, K.C., Erles, K., 2011. Serological detection of Epstein-Barr virus infection in dogs and cats. Veterinary microbiology 150, 15-20.

Minai, O.A., Santacruz, J.F., Alster, J.M., et al., 2012. Impact of pulmonary hemodynamics on 6-min walk test in idiopathic pulmonary fibrosis. Respiratory medicine 106, 1613-1621.

Minnis, P., Henry, K., Keane, M.P., 2016. Reflux in idiopathic pulmonary fibrosis. QJM 109, 7-10.

Molyneaux, P.L., Maher, T.M., 2013. The role of infection in the pathogenesis of idiopathic pulmonary fibrosis. European respiratory review 22, 376-381.

Molyneaux, P.L., Cox, M.J., Willis-Owen, S.A., et al., 2014. The role of bacteria in the pathogenesis and progression of idiopathic pulmonary fibrosis. American journal of respiratory and critical care medicine 190, 906-913.

Moore, B.B., Paine, R., 3rd, Christensen, P.J., et al., 2001. Protection from pulmonary fibrosis in the absence of CCR2 signaling. Journal of immunology 167, 4368-4377.

Moore, B.B., Kolodsick, J.E., Thannickal, V.J., et al., 2005. CCR2-mediated recruitment of fibrocytes to the alveolar space after fibrotic injury. The American journal of pathology 166, 675-684.

Morrow, L.D., Smith, K.C., Piercy, R.J., et al., 2011. Retrospective analysis of post-mortem findings in 1,444 aged donkeys. Journal of comparative pathology 144, 145-156.

Nathan, S.D., Shlobin, O.A., Barnett, S.D., et al., 2008. Right ventricular systolic pressure by echocardiography as a predictor of pulmonary hypertension in idiopathic pulmonary fibrosis. Respiratory medicine 102, 1305-1310.

Nathan, S.D., Albera, C., Bradford, W.Z., et al., 2016. Effect of continued treatment with pirfenidone following clinically meaningful declines in forced vital capacity: analysis of data from three phase 3 trials in patients with idiopathic pulmonary fibrosis. Thorax 71, 429-435.

Nelson, R.W., Couto, C.G., Davidson, A.P., et al., 2014. Diagnostic tests for the lower respiratory tract, In: Small animal internal medicine, 5th ed. Mosby Elsevier, pp. 263-298.

Nestor, D.D., Holan, K.M., Johnson, C.A., et al., 2006. Serum alkaline phosphatase activity in Scottish Terriers versus dogs of other breeds. Journal of the American veterinary medical association 228, 222-224.

Neufeld, G., Cohen, T., Gengrinovitch, S., et al., 1999. Vascular endothelial growth factor (VEGF) and its receptors. FASEB journal 13, 9-22.

Neurohr, C., Behr, J., 2015. Changes in the current classification of IIP: A critical review. Respirology 20, 699-704.

Niedermaier, G., Poth, T., Gehlen, H., 2010. Clinical aspects of multinodular pulmonary fibrosis in two warmblood horses. The Veterinary record 166, 426-430.

Norris, A.J., Naydan, D.K., Wilson, D.W., 2005. Interstitial lung disease in West Highland White Terriers. Veterinary pathology 42, 35-41.

Norris, C.R., Griffey, S.M., Walsh, P., 2002. Use of keyhole lung biopsy for diagnosis of interstitial lung diseases in dogs and cats: 13 cases (1998-2001). Journal of the American veterinary medical association 221, 1453-1459.

Noth, I., Anstrom, K.J., Calvert, S.B., et al., 2012. A placebo-controlled randomized trial of warfarin in idiopathic pulmonary fibrosis. American journal of respiratory and critical care medicine 186, 88-95.

Nowak, J., Jastrzebski, D., Streb, W., et al., 2008. Right ventricular function in patients with severe interstitial lung disease: a Tissue Doppler imaging study. Journal of physiology and pharmacology 59 Suppl 6, 531-538.

Olivier, B., 2015. Serotonin: a never-ending story. European journal of pharmacology 753, 2-18.

Olson, A.L., Swigris, J.J., 2012. Idiopathic pulmonary fibrosis: diagnosis and epidemiology. Clinics in chest medicine 33, 41-50.

Ou, X.M., Li, W.C., Liu, D.S., et al., 2009. VEGFR-2 antagonist SU5416 attenuates bleomycin-induced pulmonary fibrosis in mice. International immunopharmacology 9, 70-79.

Papakosta, D., Pitsiou, G., Daniil, Z., et al., 2011. Prevalence of pulmonary hypertension in patients with idiopathic pulmonary fibrosis: correlation with physiological parameters. Lung 189, 391-399.

Paradies, P., Spagnolo, P.P., Amato, M.E., et al., 2014. Doppler echocardiographic evidence of pulmonary hypertension in dogs: a retrospective clinical investigation. Veterinary research communications 38, 63-71.

Pariaut, R., Saelinger, C., Strickland, K.N., et al., 2012. Tricuspid annular plane systolic excursion (TAPSE) in dogs: reference values and impact of pulmonary hypertension. Journal of veterinary internal medicine 26, 1148-1154.

Patel, N.M., Lederer, D.J., Borczuk, A.C., et al., 2007. Pulmonary hypertension in idiopathic pulmonary fibrosis. Chest 132, 998-1006.

Pearson, E.G., 1984. Diagnosis of causes of respiratory diseases in cattle. Modern veterinary practice 65, 204-209.

Peters, I.R., Peeters, D., Helps, C.R., et al., 2007. Development and application of multiple internal reference (housekeeper) gene assays for accurate normalisation of canine gene expression studies. Veterinary immunology and immunopathology 117, 55-66.

Poletti, V., Ravaglia, C., Gurioli, C., et al., 2016. Invasive diagnostic techniques in idiopathic interstitial pneumonias. Respirology 21, 44-50.

Popper, H.H., 2013. Interstitial lung diseases-can pathologists arrive at an etiology-based diagnosis? A critical update. Virchows archives 462, 1-26.

Prasad, R., Gupta, N., Singh, A., et al., 2015. Diagnosis of idiopathic pulmonary fibrosis: Current issues. Intractable & rare disease research 4, 65-69.

Prepens, S., Kreuzer, K.-A., Leendertz, F., et al., 2007. Discovery of herpesviruses in multi-infected primates using locked nucleic acids (LNA) and a bigenic PCR approach. Virology journal 4, 1-15.

Prockop, D.J., Kivirikko, K.I., Tuderman, L., et al., 1979. The biosynthesis of collagen and its disorders. The New England journal of medecine 301, 13-23.

Puglisi, S., Torrisi, S.E., Vindigni, V., et al., 2016. New perspectives on management of idiopathic pulmonary fibrosis. Therapeutic advances in chronic disease 7, 108-120.

Raghu, G., Collard, H.R., Egan, J.J., et al., 2011. An official ATS/ERS/JRS/ALAT statement: idiopathic pulmonary fibrosis: evidence-based guidelines for diagnosis and management. American journal of respiratory and critical care medicine 183, 788-824.

Raghu, G., Anstrom, K.J., King, T.E., Jr., et al., 2012. Prednisone, azathioprine, and N-acetylcysteine for pulmonary fibrosis. The New England journal of medecine 366, 1968-1977.

Raghu, G., Behr, J., Brown, K.K., et al., 2013a. Treatment of idiopathic pulmonary fibrosis with ambrisentan: a parallel, randomized trial. Annales of internal medicine 158, 641-649.

Raghu, G., Million-Rousseau, R., Morganti, A., et al., 2013b. Macitentan for the treatment of idiopathic pulmonary fibrosis: the randomised controlled MUSIC trial. The European respiratory journal 42, 1622-1632.

Reinero, C.R., Cohn, L.A., 2007. Interstitial lung diseases. The veterinary clinics of North America small animal practice 37, 937-947.

Rennard, S.I., Basset, G., Lecossier, D., et al., 1986. Estimation of volume of epithelial lining fluid recovered by lavage using urea as marker of dilution. Journal of applied physiology 60, 532-538.

Renzoni, E., Srihari, V., Sestini, P., 2014. Pathogenesis of idiopathic pulmonary fibrosis: review of recent findings. F1000Prime Rep 6, 69.

Rich, J.D., Shah, S.J., Swamy, R.S., et al., 2011. Inaccuracy of Doppler echocardiographic estimates of pulmonary artery pressures in patients with pulmonary hypertension: implications for clinical practice. Chest 139, 988-993.

Richards, T.J., Kaminski, N., Baribaud, F., et al., 2012. Peripheral blood proteins predict mortality in idiopathic pulmonary fibrosis. American journal of respiratory and critical care medicine 185, 67-76.

Richeldi, L., Cottin, V., du Bois, R.M., et al., 2016. Nintedanib in patients with idiopathic pulmonary fibrosis: Combined evidence from the TOMORROW and INPULSIS trials. Respiratory medicine 113, 74-79.

Ridge, C.A., Bankier, A.A., Eisenberg, R.L., 2011. Mosaic attenuation. Amercian journal of roentgenology 197, W970-977.

Roels, E., Clercx, C., 2015. Exercice intolerance and chronic cough in a geriatric dog. Clinician's brief december 2015, 25-28.

Roels, E., Gommeren, K., Farnir, F., et al., 2016. Comparison of 4 point-of-care blood gas analyzers for arterial blood gas analysis in healthy dogs and dogs with cardiopulmonary disease. Journal of veterinary emergency and critical care doi: 10.1111/vec.12469

Rose, C.E., Jr., Sung, S.S., Fu, S.M., 2003. Significant involvement of CCL2 (MCP-1) in inflammatory disorders of the lung. Microcirculation 10, 273-288.

Ross, B., D'Orleans-Juste, P., Giaid, A., 2010. Potential role of endothelin-1 in pulmonary fibrosis: from the bench to the clinic. American journal of respiratory cell and molecular biology 42, 16-20.

Russo, R.C., Guabiraba, R., Garcia, C.C., et al., 2009. Role of the chemokine receptor CXCR2 in bleomycin-induced pulmonary inflammation and fibrosis. American journal of respiratory cell and molecular biology 40, 410-421.

Schober, K.E., Baade, H., 2006. Doppler echocardiographic prediction of pulmonary hypertension in West Highland white terriers with chronic pulmonary disease. Journal of veterinary internal medicine 20, 912-920.

Selman, M., Buendia-Roldan, I., 2012. Immunopathology, diagnosis, and management of hypersensitivity pneumonitis. Seminars in respiratory and critical care medicine 33, 543-554.

Selman, M., Pardo, A., King, T.E., Jr., 2012. Hypersensitivity pneumonitis: insights in diagnosis and pathobiology. American journal of respiratory and critical care medicine 186, 314-324.

Serres, F.J., Chetboul, V., Tissier, R., et al., 2006. Doppler echocardiography-derived evidence of pulmonary arterial hypertension in dogs with degenerative mitral valve disease: 86 cases (2001-2005). Journal of the American veterinary medical association 229, 1772-1778.

Serres, F., Chetboul, V., Gouni, V., et al., 2007. Diagnostic value of echo-Doppler and tissue Doppler imaging in dogs with pulmonary arterial hypertension. Journal of veterinary internal medicine 21, 1280-1289.

Sgalla, G., Biffi, A., Richeldi, L., 2015. Idiopathic pulmonary fibrosis: Diagnosis, epidemiology and natural history. Respirology 21, 427-437.

Shinoda, H., Tasaka, S., Fujishima, S., et al., 2009. Elevated CC chemokine level in bronchoalveolar lavage fluid is predictive of a poor outcome of idiopathic pulmonary fibrosis. Respiration 78, 285-292.

Silva, C.I., Muller, N.L., Lynch, D.A., et al., 2008. Chronic hypersensitivity pneumonitis: differentiation from idiopathic pulmonary fibrosis and nonspecific interstitial pneumonia by using thin-section CT. Radiology 246, 288-297.

Singh, I., Ma, K.C., Berlin, D.A., 2015. Pathophysiology of pulmonary hypertension in chronic parenchymal lung disease. American journal of medicine 129, 366-371.

Smith, J.S., Gorbett, D., Mueller, J., et al., 2013a. Pulmonary hypertension and idiopathic pulmonary fibrosis: a dastardly duo. American journal of medican sciences 346, 221-225.

Smith, M., Dalurzo, M., Panse, P., et al., 2013b. Usual interstitial pneumonia-pattern fibrosis in surgical lung biopsies. Clinical, radiological and histopathological clues to aetiology. Journal of clinical pathology 66, 896-903.

Soare, T., Leeming, G., Morgan, R., et al., 2011. Equine multinodular pulmonary fibrosis in horses in the UK. The Veterinary record 169, 313.

Soydan, L.C., Kellihan, H.B., Bates, M.L., et al., 2015. Accuracy of Doppler echocardiographic estimates of pulmonary artery pressures in a canine model of pulmonary hypertension. Journal of veterinary cardiology 17, 13-24.

Spagnolo, P., Rossi, G., Cavazza, A., et al., 2015. Hypersensitivity Pneumonitis: A Comprehensive Review. Journal of investigational allergology and clinical immunology 25, 237-250.

Spelta, C.W., Axon, J.E., Begg, A., et al., 2013. Equine multinodular pulmonary fibrosis in three horses in Australia. Australian veterinary journal 91, 274-280.

Sperandeo, M., Varriale, A., Sperandeao, G., et al., 2009. Transthoracic ultrasound in the evaluation of pulmonary fibrosis: our experience. Ultrasound in medicine and biology 35, 723-729.

Straub, OC., 2004. Maedi – visna virus infection in sheep. History and present knowledge. Comparative immunology, microbiology and infectious diseases 27, 1-5.

Suga, M., Iyonaga, K., Ichiyasu, H., et al., 1999. Clinical significance of MCP-1 levels in BALF and serum in patients with interstitial lung diseases. The European respiratory journal 14, 376-382.

Sun, L., Louie, M.C., Vannella, K.M., et al., 2011. New concepts of IL-10-induced lung fibrosis: fibrocyte recruitment and M2 activation in a CCL2/CCR2 axis. American journal of physiology. Lung cellular and molecular physiology 300, 341-353.

Sverzellati, N., Lynch, D.A., Hansell, D.M., et al., 2015. American Thoracic Society-European Respiratory Society Classification of the Idiopathic Interstitial Pneumonias: Advances in Knowledge since 2002. Radiographics 35, 1849-1871.

Swanson, K.L., Utz, J.P., Krowka, M.J., 2008. Doppler echocardiography-right heart catheterization relationships in patients with idiopathic pulmonary fibrosis and suspected pulmonary hypertension. Mecial sciences monitor 14, 177-182.

Swigris, J.J., Brown, K.K., 2010. The role of endothelin-1 in the pathogenesis of idiopathic pulmonary fibrosis. BioDrugs 24, 49-54.

Syrja, P., Heikkila, H.P., Lilja-Maula, L., et al., 2013. The histopathology of idiopathic pulmonary fibrosis in West Highland White terriers shares features of both non-specific interstitial pneumonia and usual interstitial pneumonia in man. Journal of comparative pathology 149, 303-313.

Thannickal, V.J., Horowitz, J.C., 2006. Evolving concepts of apoptosis in idiopathic pulmonary fibrosis. Proceedings of the American thoracic society 3, 350-356.

Thomas, S., Bonchev, D., 2010. A survey of current software for network analysis in molecular biology. Human genomics 4, 353-360.

Tomassetti, S., Piciucchi, S., Tantalocco, P., et al., 2015. The multidisciplinary approach in the diagnosis of idiopathic pulmonary fibrosis: a patient case-based review. European respiratory review 24, 69-77.

Totani, Y., Saitoh, Y., Sakakibara, H., et al., 2002. Clinical characterization of interleukin-8 in patients with idiopathic pulmonary fibrosis. The journal of the Japanese respiratory society 40, 869-874.

Travis, W.D., Hunninghake, G., King, T.E., Jr., et al., 2008. Idiopathic nonspecific interstitial pneumonia: report of an American Thoracic Society project. American journal of respiratory and critical care medicine 177, 1338-1347.

Travis, W.D., Costabel, U., Hansell, D.M., et al., 2013. An official American Thoracic Society/European Respiratory Society statement: Update of the international multidisciplinary classification of the idiopathic interstitial pneumonias. American journal of respiratory and critical care medicine 188, 733-748.

VanDevanter, D.R., Warrener, P., Bennett, L., et al., 1996. Detection and analysis of diverse herpesviral species by consensus primer PCR. Journal of clinical microbiology 34, 1666-1671.

Vasakova, M., Sterclova, M., Kolesar, L., et al., 2009. Bronchoalveolar lavage fluid cellular characteristics, functional parameters and cytokine and chemokine levels in interstitial lung diseases. Scandinavian journal of immunology 69, 268-274.

Venco, L., Mihaylova, L., Boon, J.A., 2014. Right Pulmonary Artery Distensibility Index (RPAD Index). A field study of an echocardiographic method to detect early development of pulmonary hypertension and its severity even in the absence of regurgitant jets for Doppler evaluation in heartworm-infected dogs. Veterinary parasitology 206, 60-66.

Ventetuolo, C.E., Kawut, S.M., Lederer, D.J., 2012. Plasma endothelin-1 and vascular endothelial growth factor levels and their relationship to hemodynamics in idiopathic pulmonary fibrosis. Respiration 84, 299-305.

Visser, L.C., Scansen, B.A., Schober, K.E., et al., 2014. Echocardiographic assessment of right ventricular systolic function in conscious healthy dogs: Repeatability and reference intervals. Journal of veterinary cardiology 17, 83-96.

Visser, L.C., Im, M.K., Johnson, L.R., et al., 2016. Diagnostic value of right pulmonary artery distensibility index in dogs with pulmonary hypertension: comparison with Doppler echocardiographic estimates of pulmonary arterial pressure. Journal of veterinary internal medicine 30, 543-552.

Wallaert, B., Wemeau-Stervinou, L., Salleron, J., et al., 2012. Do we need exercise tests to detect gas exchange impairment in fibrotic idiopathic interstitial pneumonias? Pulmonary medicine 2012, 657180.

Wallis, A., Spinks, K., 2015. The diagnosis and management of interstitial lung diseases. BMJ 350, 2072.

Waugh, E.M., Gallagher, A., McAulay, K., et al., 2015. Gammaherpesviruses and canine lymphoma: no evidence for direct involvement in commonly occurring lymphomas. Journal of general virology 96, 1863-1872.

Webb, J.A., Armstrong, J., 2002. Chronic idiopathic pulmonary fibrosis in a West Highland white terrier. The Canadian veterinary journal 43, 703-705.

Williams, K., Malarkey, D., Cohn, L., et al., 2004. Identification of spontaneous feline idiopathic pulmonary fibrosis: morphology and ultrastructural evidence for a type II pneumocyte defect. Chest 125, 2278-2288.

Williams, K.J., Maes, R., Del Piero, F., et al., 2007. Equine multinodular pulmonary fibrosis: a newly recognized herpesvirus-associated fibrotic lung disease. Veterinary pathology 44, 849-862.

Williams, K.J., 2014. Gammaherpesviruses and pulmonary fibrosis: evidence from humans, horses, and rodents. Veterinary pathology 51, 372-384.

Yan, Z., Kui, Z., Ping, Z., 2014. Reviews and prospectives of signaling pathway analysis in idiopathic pulmonary fibrosis. Autoimmunity reviews 13, 1020-1025.

Yang, I.V., Fingerlin, T.E., Evans, C.M., et al., 2015. MUC5B and Idiopathic Pulmonary Fibrosis. Annals of the American thoracic society 12, 193-199.

Zhang, K., Gharaee-Kermani, M., Jones, M.L., et al., 1994. Lung monocyte chemoattractant protein-1 gene expression in bleomycin-induced pulmonary fibrosis. Journal of immunology 153, 4733-4741.

Zhou, W., Wang, Y., 2016. Candidate genes of idiopathic pulmonary fibrosis: current evidence and research. Journal of the application of clinical genetics 9, 5-13.

Ziegenhagen, M.W., Zabel, P., Zissel, G., et al., 1998. Serum level of interleukin 8 is elevated in idiopathic pulmonary fibrosis and indicates disease activity. American journal of respiratory and critical care medicine 157, 762-768.

Zimmerman, K.L., Panciera, D.L., Panciera, R.J., et al., 2010. Hyperphosphatasemia and concurrent adrenal gland dysfunction in apparently healthy Scottish Terriers. Journal of the American veterinary medical association 237, 178-186.

Zimmermann, G.S., von Wulffen, W., Huppmann, P., et al., 2014. Haemodynamic changes in pulmonary hypertension in patients with interstitial lung disease treated with PDE-5 inhibitors. Respirology 19, 700-706.

Zisman, D.A., Schwarz, M., Anstrom, K.J., et al., 2010. A controlled trial of sildenafil in advanced idiopathic pulmonary fibrosis. The New England journal of medecine 363, 620-628.